Physical processes and biogeochemistry of particle fluxes over the Beaufort slope and in Canada Basin

by

Mary C. O'Brien
B.Sc., University of Alberta, 1972

A Thesis Submitted in Partial Fulfillment
of the Requirements for the Degree of

MASTER OF SCIENCE

in the School of Earth and Ocean Sciences

Supervisory Committee

Physical processes and biogeochemistry of particle fluxes over the Beaufort slope and in Canada Basin

by

Mary C. O'Brien
B.Sc., University of Alberta, 1972

Supervisory Committee

Dr. Thomas F. Pedersen (Dean of Science, University of Victoria)
Co-Supervisor

Dr. Robie W. Macdonald (Research Scientist, Institute of Ocean Sciences, Department of Fisheries and Oceans, Canada.)
Co-Supervisor

Dr. Jay T. Cullen (Associate Professor, School of Earth and Ocean Sciences, University of Victoria)
Departmental Member

Abstract

Supervisory Committee
Dr. Thomas F. Pedersen, Dean of Science, University of Victoria
Co-Supervisor
Dr. Robie W. Macdonald, Research Scientist, Institute of Ocean Sciences, Department of Fisheries and Oceans, Canada
Co-Supervisor
Dr. Jay T. Cullen, Associate Professor, School of Earth and Ocean Sciences, University of Victoria
Departmental Member

Sedimentation rates and compositions of sinking particles were investigated at three sites on the Beaufort slope and one in Canada Basin during the period 1990-1994 using moored sequential sediment traps. A method was developed to identify the terrigenous and biogenic components of the fluxes. The physical context including ice cover, ocean currents, river inputs, winds, air temperature, incident light, and nutrient availability provide essential information to the interpretation of the particle fluxes and to the understanding of shelf-basin sediment transport in this area. Eddies, internal waves, upwelling and downwelling, and the state of the ice cover all played important and overlapping roles in the pattern of observed fluxes. A peak in the flux of highly terrigenous material under complete ice cover in mid-winter to the northwest of Mackenzie Trough was associated with predominantly downwelling conditions and the passage of a series of eddies and internal waves. A prolonged spring diatom bloom occurred in the mid-slope area and was clearly associated with an early opening of the ice on the east side of the shelf. Higher fluxes at the Canada Basin site were associated with a large eddy clearly identifiable from the current-T-S record and also from the composition

of the suspended material carried with it. At the base of the slope (2700 m), the composition was highly terrigenous and remarkably consistent. Higher up the slope (700 m), biogenic peaks in the summer diluted the terrigenous material briefly, but it appears that there is a constant background of highly terrigenous material. There was a high degree of variability between sites and over the slope there was not enough data to asses the inter-annual variability. In Canada Basin, the inter-annual variability was closely linked to the extent of open water in the summer period. At all sites, lateral transport is clearly indicated by the increase in flux with depth. The data robustly demonstrate the need for detailed knowledge of physical processes for informed interpretation of particle fluxes and sediment transport in this area.

Table of Contents

List of Tables

List of Figures

List of Appendices

Acknowledgments

The data set gathered for this thesis is the result of the hard work of numerous colleagues in the field and in the lab. Many, many thanks to the "NOGAP TEAM"!! You know who you are; I won't list the names for fear of leaving someone out; this thesis was not possible without you! The work was done under the umbrellas of the Northern Oil and Gas Action Program (NOGAP) and the Northern Contaminants Program (NCP) and in collaboration with the Pacific Marine Environmental Lab (PMEL) in Seattle. Very special thanks to the Canadian Coast Guard and the officers and crews of the icebreakers from which most of this work was done, and also to the Polar Continental Shelf Base Project (PCSBP) in Tuktoyaktuk for which the spring sampling programs depended on for accommodation and logistics. I owe a large debt of gratitude to Dr. Robie Macdonald who provided the inspiration, the insight, the encouragement, and the tenacity to initiate and most importantly, to see this work through to completion. Without Dr. Macdonald's support and faith in me, this thesis would not have been possible. Special thanks to Dr. Kazuo Iseki who initiated the early Arctic sediment trap program and to Doug Sieberg who patiently, competently, and cheerfully solved all the many logistical problems inherent in deploying and recovering moorings under extreme conditions both from ships and through the ice. It has been a great honour to work with Dr. Tom Pedersen whose suggestions have enriched this thesis and broadened my thinking; his time and attention was generously given and greatly appreciated. Many thanks to Dr. Humfrey Melling who was exceedingly generous in sharing his expertise and his time with regards to a wide variety of physical oceanography issues; in addition, his contributions of data have significantly enriched this thesis. I very much appreciate the contributions of Dr. Jay Cullen and Dr. Roger Francois whose suggestions have greatly improved the final version. Finally, I would like to thank family and friends who lovingly encouraged and supported me in this endeavour!!

Dedication

This thesis and MSc degree is dedicated to my beautiful sons Tim and Aaron.

Chapter 1 Introduction

The Arctic is currently undergoing dramatic changes and the determination of the character, direction, and magnitude of these changes is critical to predicting future impacts on both local and global scales (Macdonald et al., 2005). Variations in freshwater delivery and sea ice coverage will likely have profound physical and biological consequences that are expected to be manifested most clearly on the pan-Arctic shelves and shelf breaks (Carmack et al., 2006). Although much has improved since the Canadian Arctic Expedition (1913 to 1918) with its mixture of success and tragedy, the harsh environment and high cost of access still limit research in the region compared to other more accessible areas of the world oceans, and much remains to be known about biogeochemical cycles in this high latitude environment.

Sedimentation rates and compositions of sinking particles seaward of the Beaufort Sea shelf break are studied in this thesis, and provide insights on the transition in biogeochemical and physical processes from the shelf to the deep basin. Processes that drive shelf-basin exchanges like those that influence sinking particle fluxes in the Beaufort region need to be studied as a function of time if we are to assess the relative importance of variability in such processes. Moreover, focused studies of this nature are critical to refining model based predictions of future impacts due to climate change. It is widely predicted, for example, that Arctic shelves will more frequently be ice-free and for increasingly extended periods each year (see for example, Stroeve et al., 2007; Serreze et al., 2007; Comiso et al., 2008). The ice edge position relative to the shelf break has been shown to moderate the efficiency of exchange of both water and suspended particles between the shelves and deep basins (Carmack and Chapman, 2003). An intensification of such exchanges has the potential to change radically nutrient and carbon balances in these regions. In this context, this thesis will focus on several important questions, for which existing answers are sparse: 1) What processes and ranges of material fluxes are presently occurring between the shelf and the deep basin; 2) What changes can be expected at this transition zone with fluctuations in ice cover; 3) What physical parameters are most influential in driving the system in a particular direction;

and 4) What is the relationship between particle fluxes and compositions to specific biological and physical processes? These four questions shape five objectives of the thesis: 1) examination of the magnitude, timing, composition, and variability of particle fluxes beyond the shelf break of this highly estuarine, highly river impacted area; 2) determination of the source and transport pathways of the settling particles and understanding of the linkages between particle fluxes on the shelf edge and those in Canada Basin; 3) estimation of the delivery of carbon to the ocean bottom and offshore under the particular conditions present during the sediment trap collections; 4) relating the magnitudes and compositions of particle fluxes to, and determining the relative importance of controlling physical factors in the system such as ice cover, river input, wind, current, stratification, nutrient levels, and light availability; and 5) suggesting methodologies and approaches that will assist future investigations.

Field work for the present study was conducted during the period 1990 to 1994 under the joint umbrellas of the Northern Oil and Gas Project (NOGAP; http://www.ainc-inac.gc.ca/oil/index_e.html) and the Northern Contaminants Program (NCP; http://www.itk.ca/environment/contaminants-ncp.php). As part of a major interdisciplinary study of the Northern Oil and Gas Action Program (NOGAP B.6), the Northern Contaminants Program (NCP), and in cooperation with scientific personnel from PMEL (Pacific Marine Environmental Laboratory) in Seattle, three moorings were placed in the Canada Basin. This was part of an Arctic climate study designed to gather information to assist in understanding the role of the Arctic in global climate change. Background information was derived from data collected during the Beaufort Sea Project (BSP) in the seventies and the Northern Oil and Gas Project in the eighties. Ongoing programs such as the Canadian Arctic Shelf Exchange Study (CASES; http://www.quebec-ocean.ulaval.ca/cases/network.asp), the Western Arctic Shelf-Basin Interaction Project (SBI; http://sbi.utk.edu/), and the International Polar Year (IPY; http://www.ipycanada.ca/) are now rapidly advancing our knowledge of how arctic shelves function and communicate with deep arctic basins. The work presented here complements these far-reaching efforts.

This study in particular focuses on the timing, magnitude, and composition of particle fluxes at two sites on the Mackenzie Shelf slope (SS-5 and AM1-92), one site at

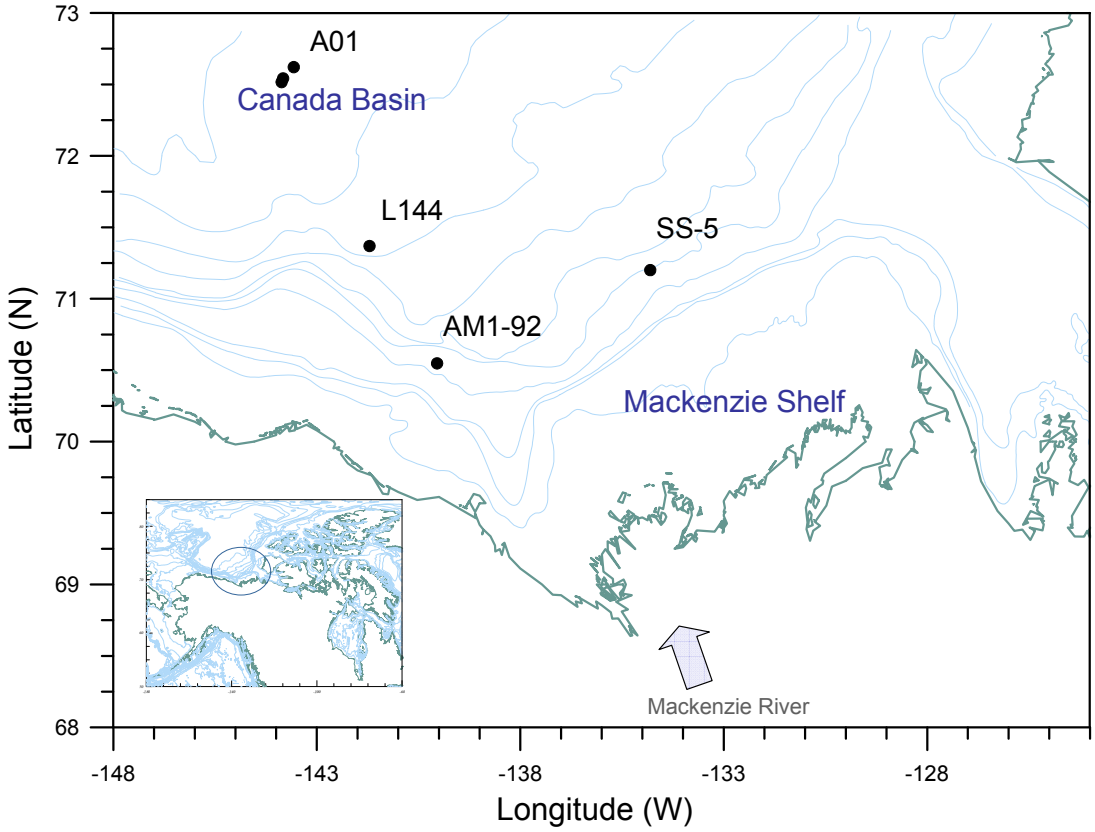

Figure 1-1 Location of study area and mooring sites (A01, L144, AM1-92, and SS-5).

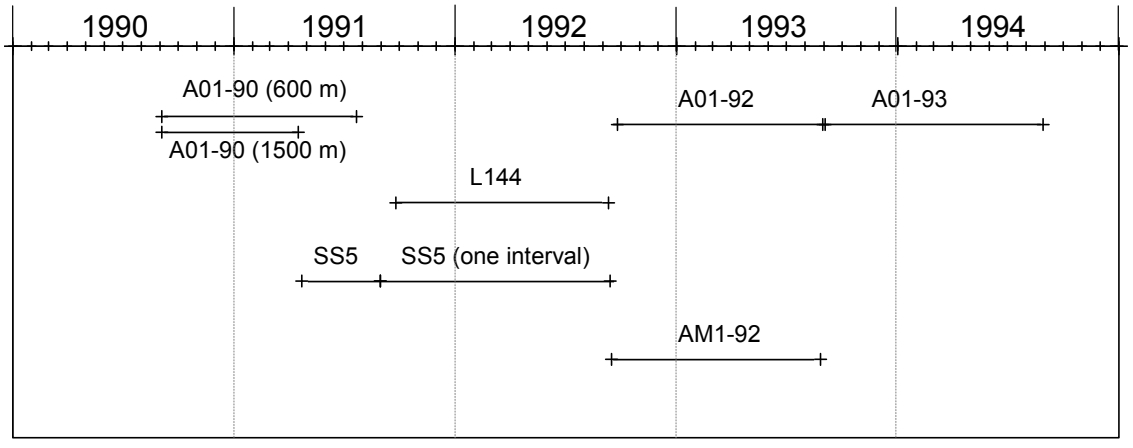

Figure 1-2 Deployment period of moorings. Note that there were 3 deployments of the site A01 mooring in Canada Basin (A01-90 with traps at 600 and 1500 m, A01-92 with a trap at 600 m, and A01-93 with a trap at 568 m). Station L144 had sediment traps at two depths (412 and 1311 m). There were three sediment traps on each of the moorings SS-5 (at 199, 349, and 499 m) and AM1-92 (140, 290, and 490 m).

the base of the Mackenzie Shelf slope (L144), and one site in the Canada Basin (A01). Station locations are shown in Figure 1.1, and the sediment trap sampling periods are shown in Figure 1.2. This work extends previous research conducted on the inner shelf and at the Canadian Beaufort Shelf edge in 1987-1988 (O'Brien et al., 2006).

The remainder of the thesis is divided into 6 chapters. Chapter 2 offers a general overview of the physical and biological setting of the Beaufort Shelf and Canada Basin and includes specific information on ice coverage and river inputs for the study period (1990 to 1994). Chapter 3 summarizes the methodologies employed in the collection and analysis of the sediment trap samples, details additional data sources, and presents the data from the sediment traps at the shelf slope sites (SS-5, AM1-92, and L144). Chapter 4 covers the findings from the sediment traps in Canada Basin (A01). Chapter 5 examines and compares the annual and seasonal fluxes and outlines the methodology for the discrimination of particle fluxes into terrigenous (allochthonous) and biogenic (autochthonous) contributions to the total fluxes. Chapter 6 presents and discusses the terrigenous and biogenic fluxes at each of the four mooring sites in the context of the physical forcing. The impact of winds, ice dynamics, and river inputs are considered, and the current, temperature-salinity (T-S), and Upward Looking Sonar (ULS) records from the moorings are utilized to shed light on processes relevant to sediment transport. Finally, Chapter 7 summarizes and discusses the findings. In the context of disappearing Arctic ice cover, possible effects on particle fluxes and sediment transport are explored. In addition, a sampling scheme designed to improve the understanding of biogeochemical cycling and transport of biogenic and terrigenous particles on the shelf, over the slope and in the deep basins of the Beaufort Sea and Canada Basin is proposed. A number of appendices document data tables and additional information as outlined in the Table of Contents and referred to in the text.

Chapter 2 Physical and biological setting

The geographical setting and the physical and biological characteristics of the Beaufort Sea and Canada Basin provide a background to factors important to understanding the flux of particles over the Beaufort Shelf slope and to shelf-basin exchanges of freshwater, ice, and sediments. Although the following discussions include the Beaufort Sea as a whole, the emphasis is on the Mackenzie Shelf portion of the Beaufort Sea as the Mackenzie River freshwater and sediment inputs tend to be dominant.

2.1 Geography

The Beaufort Sea and Canada Basin lie within the Arctic Ocean which has two major sub-basins (the Eurasian and Amerasian basins) surrounded by shallow seas (Figure 2.1). The Arctic Ocean has a significantly larger percent of total area covered by continental shelves, ~ 53 %, than the other world oceans (Jakobsson, 2002). These shelves are the locale of most of the primary and secondary production in the Arctic (Grebmeier, 1998), and they exert a strong influence on both its thermohaline structure (Aagaard et al., 1985) and the maintenance of ice cover (Aagaard and Carmack, 1989). The Beaufort Sea comprises only ~ 3.5 % of the continental shelf area of the Arctic Ocean (Jakobsson, 2002), and is a relatively narrow region compared to the broad shelves on the Eurasian side that rim the Arctic Ocean from the Chukchi to the Barents seas (Figure 2.1). The Beaufort Sea has three distinct shelves demarcated by Barrow Canyon, Mackenzie Trough, and the entrances to Amundsen Gulf and McClure Strait (Figure 2.2).

Two of the principal geomorphic areas of the Beaufort Sea—the Alaska Shelf (~70 km wide and ~650 km long) and the Banks Island Shelf (~60-100 km by ~150-250 km)—are fed by arctic rivers that run over permafrost and have negligible winter flows (Dunton et al., 2006). In contrast, the Mackenzie Shelf of the Beaufort Sea (~120 km wide and ~450 km long) is broader than the Alaskan shelf, and is heavily impacted by massive Mackenzie River inflows of freshwater (3.3×10^{11} m^3 a^{-1}; Macdonald et al., 1998) and suspended sediments (estimates of 62 to 85 Mt a^{-1} delivered offshore; Carson, 1998, 1999). The Mackenzie River drainage basin is vast (1.8×106 km^2) and includes

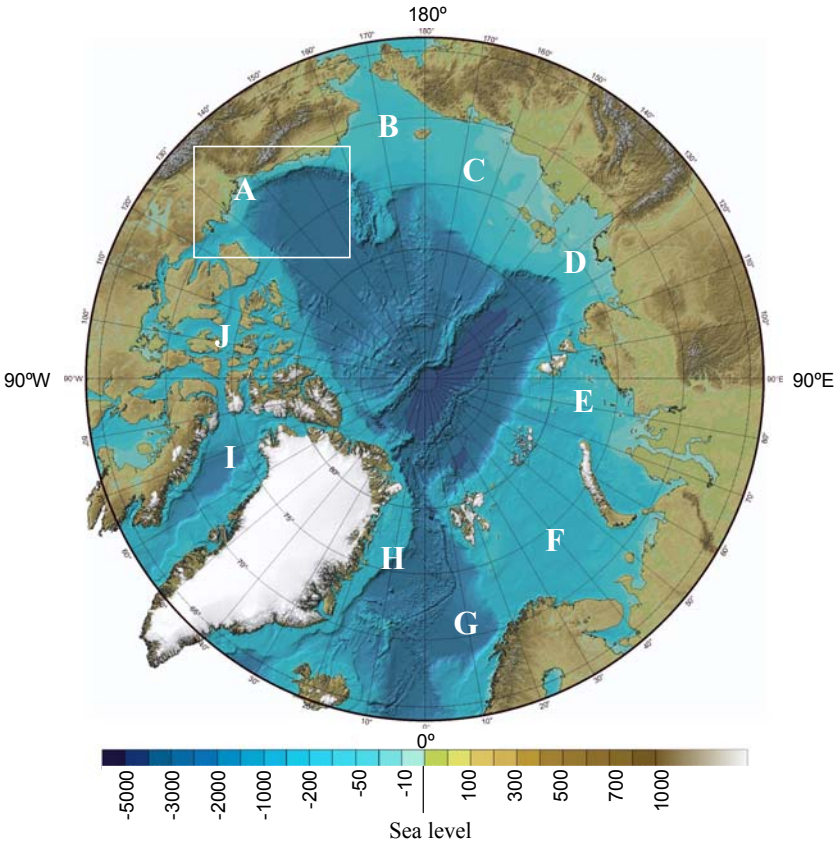

Key to marginal seas:

A. Beaufort Sea
B. Chukchi Sea
C. East Siberian Sea
D. Laptev Sea
E. Kara Sea
F. Barents Sea
G. Norwegian Sea
H. Greenland Sea
I. Baffin Bay
J. Canadian Archipelago

Figure 2-1 Overview of the Arctic Ocean and its marginal seas (see key above). The study area, the Beaufort Sea and Canada Basin is highlighted by the white rectangle, see Figure 2.2 for blow-up of study area. Adapted from map on the International Bathymetric Chart of the Arctic Ocean (IBCAO) website (http://www.ngdc.noaa.gov/mgg/bathymetry/arctic/arctic.html).

both arctic and temperate environments (Reeder et al., 1972; Macdonald and Yu, 2006). The Mackenzie Shelf begins at the eastern edge of Mackenzie Trough, and borders the north shore of the Yukon, the Mackenzie River Delta, the Tuktoyaktuk Peninsula, and the mouth of Amundsen Gulf. The massive delivery of freshwater makes this shelf the most estuarine of all the panarctic shelves (Dunton et al., 2006; Macdonald et al., 2000;

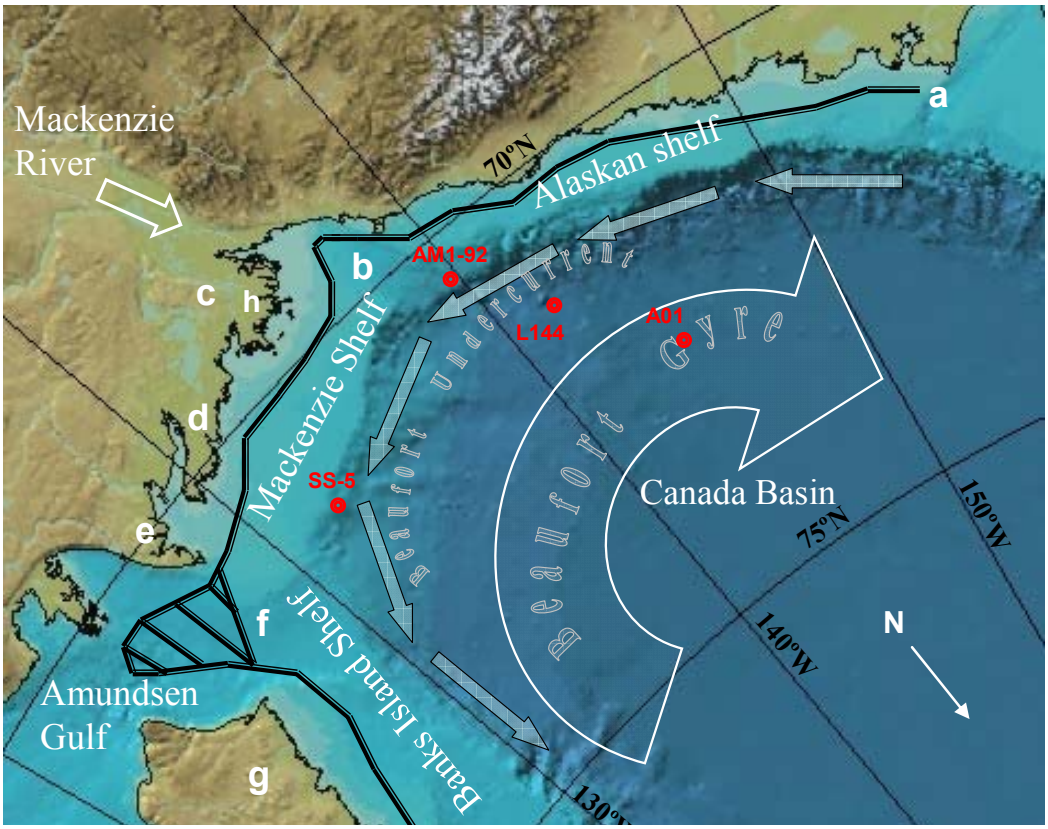

Key to place names:

a. Barrow Canyon
b. Mackenzie Trough
c. Mackenzie River Delta
d. Tuktoyaktuk Peninsula
e. Bathurst Peninsula
f. Mouth of Amundsen Gulf
g. Banks Island
h. Richards Island

Figure 2-2 Mooring locations (red dots), large scale currents (the Beaufort Undercurrent, the Beaufort Gyre), the three shelf areas of the Beaufort Sea (Alaskan, Mackenzie, and Banks Island shelves), the flaw/lead/polynya system at approximately the 20 m isobath (black line), and place names designated by letters a to h (see key at the bottom of the map).

Macdonald et al., 1987), and the Mackenzie River provides an annual outflow that constitutes a 6.2 m layer of freshwater over the Mackenzie Shelf (Macdonald et al., 1987).

2.2 Interplay of freshwater, saltwater, and ice

The Beaufort Sea shelves are ice covered for much of the year and there is considerable inter-annual variation in the ice cover in the summer months (Melling et al., 2005). Differences in ice coverage between the years 1990 to 1994, the period of this

study, exemplify this variability (Figure 2.3; data derived from the National Snow and Ice Data Center (NSIDC)). In 1991 ice persisted on the shelf over the spring and summer whereas in 1993, there was relatively little ice on the shelf from early spring to late fall. The ice cover has a profound impact on many shelf processes. It affects the way freshwater spreads on the shelf (Macdonald et al., 1995), alters atmospheric exchanges with the water column (Semiletov et al., 2006), and changes the transfer of energy to the water column via surface winds (Carmack and Chapman, 2003). In addition, it acts as a source of freshwater to the surface during melting and serves as a sink for freshwater during freezing (Macdonald, 2000).

A flaw/lead/polynya system at about the 20 m isobath links the Beaufort Sea shelves in the winter, and landfast ice extends from the shore out to the edge of the flaw lead (Macdonald and Carmack, 1991[b]; Stirling and Cleator, 1981). There are a few persistent polynyas such as one at the mouth of Amundsen Gulf (Stirling and Cleator, 1981) and another over Mackenzie Trough such as the one that occurred in the winter of 1987 to 1988 (O'Brien et al., 2006). The seaward edge of the landfast ice, the stamukhi zone, crumples into heavily ridged hummocks and deep ice keels resulting from wind driven collisions and shear stresses between the pack ice and the landfast ice edge.

This flaw/lead system is extremely important during the winter for the formation and export of ice from the shelf and for the creation of brine plumes resulting from the rejection of salt during the formation of new ice (Macdonald, 2000; Melling and Riedel, 1996). Downward convection resulting from these brine plumes increases the depth of the mixed layer and with sufficient strength, these flows can move along the bottom and flow into the deep waters of Canada Basin either to be incorporated into the halocline over Canada Basin or into deeper waters of the basin (Cavalieri and Martin, 1994; Melling and Moore, 1995). This brine-driven convection can have a profound effect on the freshwater balance of the shelf and basin, and in addition, may be an important mechanism for transporting suspended particles from the shelf to the deep basin.

The Mackenzie Shelf acts as a positive estuary in the summer due to plume spreading and a negative estuary in the winter when brine rejection resulting from ice formation causes permanent separation between freshwater and saltwater (Macdonald, 2000). The source of the water available for freezing in the lead can affect the amount of

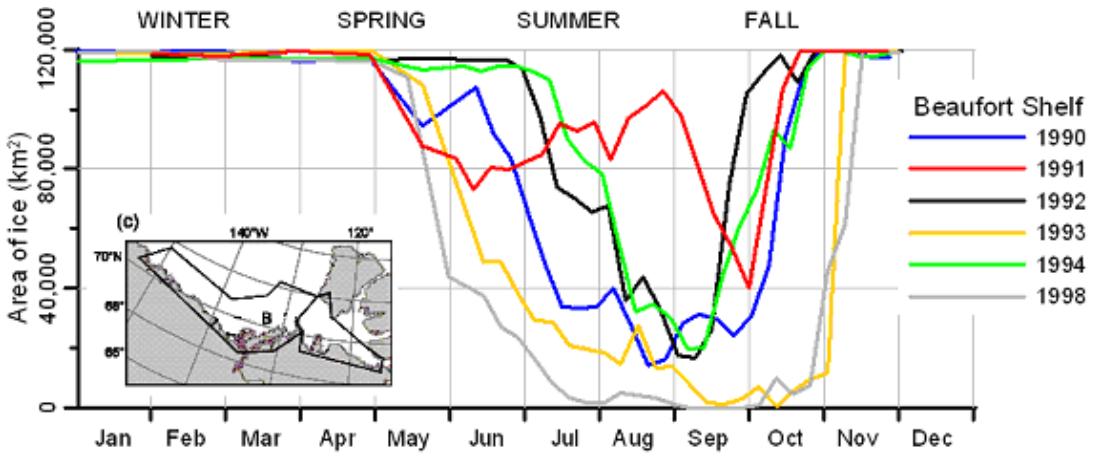

Figure 2-3 Ice coverage (km^2) on the Beaufort shelf (see area marked B on inset map) for the years 1990 to 1994 and 1998. Ice coverage data is from the National Snow and Ice Data Center (NSIDC).

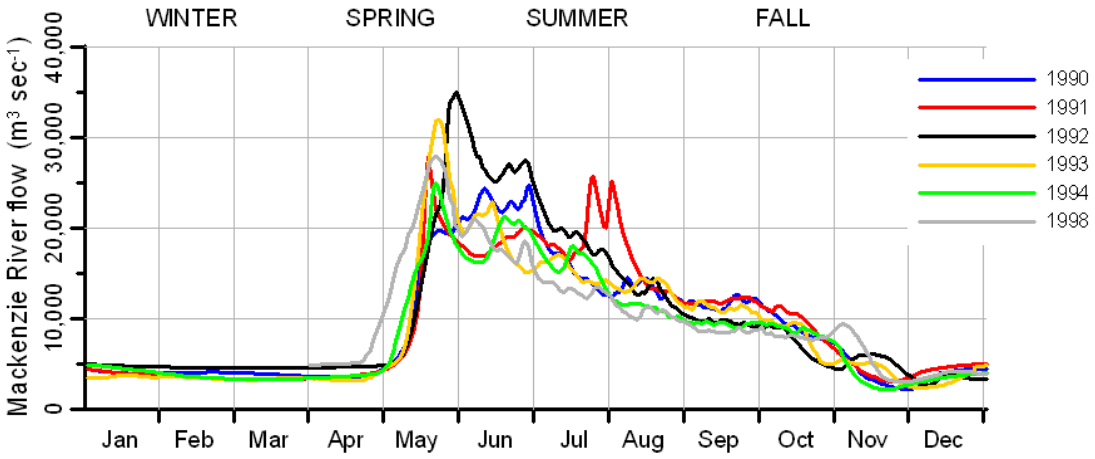

Figure 2-4 River flows (m^3 sec^{-1}) measured at Arctic Red River. Data is from the Water Survey of Canada (HYDAT CD-ROM version 96 - 1.04).

brine drainage that can take place. The Mackenzie Shelf is a known exporter of ice (Melling and Riedel, 1996) and has a short residence time for freshwater (Macdonald, 2000). Stratification on the shelf depends on river input, ice melt, and convection due to brine rejection. Surface winds affect river plume distribution and there is interannual variation in stratification and freshwater distribution (Giovando and Herlinveaux, 1981).

The Mackenzie River has the fourth largest watershed and the fourth highest discharge rate of rivers into the Arctic Ocean (Dittmar and Katner, 2003), and it discharges massive amounts of freshwater and suspended sediments onto the shelf largely in a pulse during the spring freshet. The timing and magnitude of freshwater influxes from the Mackenzie River onto the shelf show wide inter-annual variability, an observation that applies to the four years of this study (1990 to 1994) (Figure 2.4, data from the Water Survey of Canada, HYDAT). For example, in 1992, the peak spring inflows were considerably higher and occurred later than in the other years. In 1991, there were peaks inflows in late July and early August not present in other years. The narrowness of the Mackenzie Shelf as compared to the broad Eurasian shelves implies that this shelf will be especially important for the export of freshwater and sediments to the deep ocean basins.

2.3 Sources, sinks, transport, and transformation of sediment

The prime sources of sediment input to the ocean are rivers and coastal erosion and thus, the morphologies and dynamics of watersheds and coastlines play pivotal roles in sedimentation on and beyond continental shelves. The sediment load of the Mackenzie River is about 128 Mt a^{-1} (Carson et al., 1998) but the delta traps about half of this amount, and the remainder (estimates ranging from 64 to 85 M t a^{-1}; Carson et al., 1998, 1999) spreads over the Mackenzie Shelf. Estimates of the fluvial sediment input to the Mackenzie Shelf are about ten times the contribution from coastal erosion in that area (Rachold et al., 2000).

Suspended sediments supplied to the shelf by the Mackenzie River are composed mostly of clays (35-55%) and silts (40-60%) with only minor amounts of fine sand (Hill et al., 1991), and more than 90% of this suspended material arrives in the months June, July, and August (Macdonald et al., 1998). The balance between sediment inputs from rivers and from coastal erosion varies considerably from one Arctic region to another.

The Mackenzie Shelf area differs markedly from the Laptev Sea in that for the former, the sediment input has an overwhelmingly riverine source whereas for the latter, sediments are derived overwhelmingly from coastal erosion. By way of contrast, the combined riverine and coastal erosion inputs from the Laptev Sea exceed the combined inputs for the Mackenzie Shelf area (Rachold et al., 2000). In addition to the large terrestrial inputs to the Mackenzie Shelf from rivers and coastal erosion, smaller amounts of sediment originate from biological activity and ice rafting.

Over the Holocene, the Mackenzie Delta functioned (and functions) as a large sink for riverine sediments, and on the adjacent shelf, sediment deposition has been greatest across the front of the delta and in depressions such as Mackenzie and Kugmallit Troughs (Hill et al., 1991). On a small scale, depressions created by ice keel gouging on the shelf create environments conducive to sediment deposition (Macdonald and Thomas, 1991). More broadly, over the Holocene, sediment accumulation rates range between 5200 and 10400 g m^{-2} a^{-1} in areas of high deposition to less than 900 g m^{-2} a^{-1} on the eastern side of the shelf and out to about the 100 m isobath (Hill et al., 1991; Macdonald et al., 1998). Estimations of accumulation rates derive from the depth of sediment accumulation above an unconformity interpreted as delineating the Holocene transgression. Note that sediment accumulation rates vary considerably over time with recent rates generally less than past rates.

Due to extreme seasonality in both river inputs and ice cover, the Beaufort shelf is a very dynamic area for sediment dispersal (Fissel and Birch, 1984). In addition to simple gravitational settling, Beaufort Shelf sediments are carried within wind-driven buoyant river plumes, move along in large- and small-scale current regimes, and are actively resuspended during storm activity. Sea-bottom gouging by ice keels reworks and re-introduces sediments into the water column, and ice formation traps and subsequently exports sediments. In addition, mid- and bottom nepheloid layers play an important but poorly understood role in sediment transport in the area (O'Brien et al., 2006).

In winter, the stamukhi zone acts as a dam to confine the settling of suspended particles, at least partially, to the nearshore zone (Macdonald et al., 1987). There may be a close coupling between the sedimentation of biogenic and terrigenous particles due to the large terrigenous supply (Hedges et al., 1997; Armstrong et al., 2002; Passow, 2004).

Macdonald et al. (1998) estimated that 12-13% of the total Mackenzie River sediment load is exported off the shelf by ice rafting, turbidity flows, surface plumes, and likely other mechanisms. If only the sediment input onto the shelf (after the river transits the delta where it deposits about half its sediment load) is considered, about 75% of the sediment deposits locally and 25% (amounting to about 16.4 Mt a^{-1}) exports beyond the shelf break (Macdonald et al., 1998). These estimates are made from sediment accumulation data and remain very uncertain.

As the sediment-laden river waters flow onto the shelf, increasing salinity promotes the flocculation of particles and a consequent increase in sediment deposition rates (Droppo et al., 1998). However, constant reworking of the deposits by resuspension, bioturbation, and ice keel gouging all affect their geochemistry, the extent of re-mineralization, and the particle size distribution. The character of sediments transported beyond the shelf edge is therefore likely the product of a combination of these processes.

2.4 Carbon sources and sinks

The Mackenzie Shelf is highly impacted by fluvial inputs of terrestrial carbon. Given the current intense interest in constructing carbon budgets on continental shelves worldwide (de Haas et al., 2002), determination of the long-term fate of such material on the Mackenzie Shelf is an important objective. Box model budgets constructed to account for the two principal organic carbon sources on the shelf—terrestrial input and *in situ* aquatic primary production—provide preliminary estimates (Macdonald et al., 1998). This work has shown that although marine primary production (PP) provides the largest source of carbon to the shelf (3.0 Mt a^{-1}), very little of it appears to be sequestered in the shelf sediments (only ~2%). This implies that over 98% of the marine PP re-mineralizes and/or exports off the shelf. Of the terrestrial carbon delivered to the shelf from riverine and coastal erosion sources (total of ~1.29 Mt a^{-1}), it is estimated that about 40% is sequestered on the shelf, ~50% is exported from the shelf, and only ~10% is re-mineralized (Macdonald et al., 1998). The estimates for the relative proportions contributed by terrigenous and biogenic carbon sources and sequestered by sinks are far more uncertain than the estimates for bulk sediment. Thus, it is very important to develop tools to distinguish between the terrigenous and biogenic contributions to sediments and material suspended in the water column.

Proxies used in the Arctic to distinguish between terrestrial and marine sources of carbon include molar ratios of organic carbon and nitrogen, stable carbon and nitrogen isotopic compositions, ratios of organic carbon to aluminum in the surface sediments of the shelf (O'Brien et al., 2006), and biomarker assays such as n-alkane determinations (Stein and Macdonald, 2004; section 7.2.3, pp. 178-186). This study uses the approach outlined in O'Brien et al. (2006) to partition the trapped particles into terrigenous and biogenic contributions (see Section 5.4 for further details). In addition, combinations of biogeochemical proxies (organic carbon content, biogenic silica, and stable isotopes of carbon and nitrogen) assist in the interpretation of the sediment trap data.

In the interior of the Arctic Ocean, applications of combinations of proxies have aided in the discrimination between periods of high terrigenous input, glacial-interglacial cycles, and intervals in which marine productivity dominated (Schubert and Stein, 1996). For example, cores from Amundsen and Makarov basins and the Lomonosov Ridge exhibit periods of high terrigenous inputs characterized by high percent organic carbon and periods of high marine productivity characterized by low organic carbon contents, high hydrogen indices, low carbon to nitrogen ratios, high opal contents, and high contents of n-alkanes (C17 to C19) typically found in algae (Schubert and Stein, 1996).

2.4 Currents, eddies and upwelling

Topography, tides, wind, ice cover, ice formation, ice melt, and river inflow all influence ocean currents in the Arctic Ocean. The main large-scale current systems in the Beaufort Sea/Canada Basin region are the Beaufort Gyre (Macdonald et al., 1999; Proshutinsky et al., 2002; Plueddemann et al., 1998) and the Beaufort Undercurrent (Aagaard, 1984; Carmack, 1990). Sea-ice and basin waters circulate in the Beaufort Gyre in a clockwise direction around Canada Basin (Figure 2.2). This circulation is wind driven and associated with a high-pressure system located over the Central Arctic. The currents within the Beaufort Gyre appear to alternate between anticyclonic and cyclonic modes along with atmospheric regime shifts of 5 to 7 years duration that result from changes in the intensity and locations of the Icelandic low and the Siberian high (Proshutinsky and Johnson, 1997; Proshutinsky et al., 1999). The Canada Basin forms a vast trap for freshwater from runoff and ice melt as a direct result of the circulation of the Beaufort Gyre. Thus, the gyre may play a significant role in regulating Arctic climate

variability by accumulating freshwater during anticyclonic regimes and releasing freshwater during cyclonic regimes (Proshutinsky et al., 2002).

The Beaufort Undercurrent is a subsurface, bathymetrically steered flow that starts beyond the 50 m isobath of the Beaufort Sea shelves and extends to the base of the slope (Aagaard, 1984). The mean flow is to the east but there are frequent reversals to the west that are often associated with upwelling onto the outer shelf (Aagaard, 1989). Along the Alaskan shelf break, the current presents as a narrow jet with a mean easterly direction (Pickart, 2004) whereas along the Mackenzie shelf break, the flows are highly variable (Kulikov et al., 1988; Kulikov, 2004). Off the shelf, the Beaufort Undercurrent is not subject to wind forcing but rather is part of a large basin-scale circulation subject to ocean forcing such as shelf waves and eddies (Aagaard, 1989). The portion of the current overlying the outer part of the shelf may be subject to local forcing such as winds and freshwater inflows. To the west, a temperature maximum originating from the mixing of Bering Sea and Alaskan coastal waters identifies the Beaufort Undercurrent (Aagaard, 1984). A variety of other hydrographic parameters and current measurements also trace the progress of the Beaufort Undercurrent as it travels eastward. By this means, nutrient-rich waters of Pacific and Atlantic origin move eastward where they episodically move onto the shelf during wind generated upwelling events (Macdonald et al., 1987). In addition, this current may be important in the transport of suspended materials along and beyond the shelf break. Cross-shelf flows capable of transporting material between the inner and outer shelves occur near the inshore edge of the Beaufort Undercurrent (Aagaard, 1984). In addition, the Beaufort Shelf Undercurrent may be an important source of eddies that have been observed in the in the Beaufort Sea and Canada Basin (Pickart, 2004, Mathis, 2007). Exchanges across the shelf break occur because of upwelling due to surface stresses from wind and ice motion. In the Mackenzie Trough, large upwelling events capable of bringing nutrient rich water onto the shelf are associated with wind events in the short ice-free summer season and with ice motion in the winter (Williams et al., 2006). Such upwelling episodes occur in association with northeasterly winds (Carmack and Kulikov, 1998). For the Mackenzie Shelf, upwelling is sensitive to the position of the ice edge relative to the shelf break (Carmack and Chapman, 2003). On the inner shelf, currents are wind driven with the effect most

pronounced in summer in open water conditions (Aagaard, 1984; MacNeill, 1975; Giovando and Helinveaux, 1981).

2.5 Primary productivity, light, and nutrients

The Arctic Ocean has historically been thought of as the least productive on an aerial basis of all oceans largely due to the presence of permanent ice cover over the deep basins and the strong stratification that limits advective supply of nutrients and ultimately new production in the surface ocean. The shelves are therefore very important, as noted in the recent review by Sakshaug (2004) which highlighted the Arctic shelves as key sites for both primary and secondary production in the region.

Primary production on the Beaufort shelves ranges from 30 to 70 g C m^{-2} y^{-1} (Carmack et al., 2006; Sakshaug, 2004; Macdonald et al., 1987). Ice-edge blooms are very important in this region and stratification frequently limits available nutrients (Sakshaug, 2004). In years with a lot of ice on the shelf, the depth of the mixed layer is shallower and access to nutrients for new production is more restricted (Macdonald et al., 1987). However, upwelling of nutrients onto the shelf occurs frequently in the Mackenzie Trough region (Macdonald et al., 1987; Williams et al., 2006) and plays a major role in supporting new production.

Early assessments of primary production over the deep Arctic basins were very low, typically <1 g C m^{-2} y^{-1}. However, recent estimates exceed 11 g C m^{-2} y^{-1} due to the inclusion of ice-algal production in multiyear ice as well as production in open leads within the pack ice (Gosselin et al., 1997). Other estimates range even higher, to >15 g C m^{-2} y^{-1} in Canada Basin (Cota et al., 1996) when DOC is included, for example. Studies of oxygen drawdown and in-growth of nitrate in deep water suggest the mean value should be doubled to ~30 g C m^{-2} y^{-1} (Macdonald and Carmack, 1991[a]; Macdonald et al., 1993). This is consistent with an Arctic Ocean-wide assessment based on oxygen distributions that yielded modern average rates of primary productivity in the range 19-38 g C m^{-2} y^{-1} (Pomeroy, 1997).

Multiple factors affect the triggering of a phytoplankton bloom in the Beaufort region. These include the presence and thickness of ice and/or snow, the degree of shading by ice algae, the stability of the water column, presence of the river plume, and availability of nutrients. The timing and the magnitude of the primary production in the

Arctic are controlled primarily by light and nutrient availability, both of which are highly seasonal in nature (Sakshaug, 2004). Light availability is particularly germane. In winter, the sun stays below the horizon, and in the long days of the summer, low solar elevation and low surface irradiance due to cloud cover and fog reduce the incident light. Ice cover limits the penetration of light to varying degrees depending on snow cover, ice thickness, presence of melt ponds, and the concentrations of rafted sediments and ice algae associated with the ice. A layer of ice algae at the bottom of the ice or a high concentration of phytoplankton in the water column or at the pycnocline can result in a limiting of light by shading. Deep vertical mixing can limit photosynthesis by carrying phytoplankton to depths with insufficient light, whereas when the water column is strongly stratified, and as long as sufficient nutrients are available, there is a better chance of a light regime suitable for growth. In addition, high concentrations of suspended material or yellow matter can severely limit the penetration of light into the water column, and the depth of the photosynthetic limit (1 % of the surface light) varies from 66 m in pre-bloom Arctic waters to < 3.5 m during extreme blooms (Sakshaug, 2004 and references therein).

Early spring (pre-bloom) concentrations of nutrients in the surface layer depend on the degree of vertical mixing and upwelling that took place over the winter, and ice edges are often areas where both light and the surface-layer nutrients are tapped for phytoplankton growth. Ratios (mol:mol) of the major nutrients exhibit geographical variations, however. Si:N molar ratios vary in different areas of the Arctic (Codispoti, 1979; Anderson and Dyrssen, 1981; Harrison and Cota, 1991) ranging from about 2.36 in the Chukchi Sea to 1.87 in the Mackenzie shelf area. In Eurasian waters, the Si:N ratios are typically 0.31. N:P ratios in the Arctic range between 11 and 16 and it is likely that ratios of <16 in general indicate nitrogen limiting conditions. In coastal waters of lower salinity, however, it is likely that phosphate limitation occurs, because Arctic Rivers are generally rich in available nitrogen and silicate but poor in phosphate (Macdonald et al., 1987; Gordeev et al., 1996). Following the spring bloom, nutrients in the mixed layer are commonly undetectable (Sakshaug, 2004) and productivity subsequently declines.

2.6 Sediment trap studies in the Arctic

Production in the Arctic is episodic and exhibits a mosaic pattern (Sakshaug, 2004) with highly variable vertical export (Wassmann et al., 2004, Honjo, 1990). Much remains unknown in the relationship between primary production and export production in the region. Sediment trap data sets are few in number, represent widely disparate areas, vary in water column depths, and often span short durations (see summary in Wassmann., 2004). Moreover, estimates of annual vertical fluxes of organic carbon from the existing trap studies vary widely. Below the thick ice of the Canadian Ice Island the estimates are very low (< 0.2 g C m^{-2} y^{-1}, Hargrave et al., 1989, 1994), whereas in shallow, highly productive areas in the Northern Bering Sea, they are much higher (39 g C m^{-2} y^{-1}, Fukuchi et al., 1993).

There are two published sediment-trap data sets in the Mackenzie shelf area of the Beaufort Sea that offer information on the settling fluxes of carbon. O'Brien et al (2006) demonstrated that at the shelf break (200 m isobath), organic carbon fluxes at 50 m above the bottom, varied between 5.8 g C m^{-2} y^{-1} over the Mackenzie Trough and 1.6 g C m^{-2} y^{-1} at the center of the shelf edge north of Kugmallit Bay. These measurements represent a year in which there was very little ice on the shelf in summer (1987). In the second study, organic carbon fluxes measured at 200 m were 1.0 to 1.7 g C m^{-2} y^{-1} on the slope (at the 300 and 500 m isobaths) north of Kugmallit Bay (Forest et al., 2006). Additional measurements made in the Cape Bathurst Polynya but as yet unpublished (See Table 2 in Forest et al., 2006; data from Sampei et al. in prep.) yielded organic carbon fluxes of 2.8 to 12.8 g C m^{-2} y^{-1}.

Chapter 3 Particle fluxes on the shelf slope

3.1 Overview of data presentation

This chapter presents sediment trap data from three moorings deployed seaward of the Beaufort Shelf edge, two (SS-5 and AM1-92) at the 700 metre isobath on the Beaufort Shelf slope and the other (L144) at the 2700 metre isobath on the shelf rise (Figures 1.1 and 2.1b; Appendix 1). The moorings at SS-5 and AM1-92 were each fitted with three sequential sediment traps and the mooring at L144 with two. Additional instrumentation was fitted to acquire continuous records of current direction, current speed, temperature, salinity, pressure, ice presence, and ice draft. See Appendix 1 for detailed station information, mooring configurations, instrumentation, and sediment trap schedules.

Trapped particulates were analyzed for organic carbon (POC), total nitrogen (TN), biogenic silica (BIOSI), chlorophyll *a* (CHLA) , phaeophytins (PHAEO), and stable isotopes of carbon and nitrogen ($\delta^{13}C$ and $\delta^{15}N$). In addition, elemental analysis was done for a suite of major and minor elements of which only aluminum (Al) is included here. Section 3 provides an overview of the data and includes information on the moorings and sediment traps, outlines the sampling protocols and analytical techniques, and provides information on additional data sources. Sections 3.2 to 3.4 present the biogeochemical data from stations SS-5, AM1-92, and L144 respectively, Section 3.5 gives an overview of the stable isotope data, Section 3.6 discusses patterns exhibited by elemental and weight ratios of the biogenic components, and finally, Section 3.7 presents scanning electron microscope (SEM) evidence from the trap samples. Mackenzie River flows are included on some plots to add seasonal context and reflect the importance of the river impact on the timing, magnitude and composition of the particulate material in the water column beyond the shelf edge.

3.1.1 Information on moorings and sediment traps

Two types of sequential sediment traps were used, the Parflux Mark 6-13 trap (Honjo and Doherty, 1988) and the Baker/Milburn trap (Baker and Milburn, 1983; Baker et al., 1988). The sequential traps were set up with delay periods long enough to allow the

mooring to be deployed and settled in place before the carousel rotated to the first sampling position. At all sites, collection intervals were synchronized between traps at different depths on the same mooring, and intervals varied from 13 days to 35 days depending on the program objectives and field logistics.

The Baker/Milburn trap is a 1 metre long, 220 cm ID PVC tube that houses an asymmetrical polyethylene funnel (Baker and Milburn, 1983). The gravitationally settling particles in the water column are collected *via* the funnel into one of ten 200 mL acrylic sample tubes. The collection area of the Baker trap is 0.032 m^2. The bottles were rotated into position at time-intervals determined by switch settings on the timer electronics board.

The Parflux Mark 6-13 trap consists of a large funnel lined with fibreglass or polyethylene, a rotator/timer assembly, a stepping motor in a housing containing silicone 200 CS 20, a compensating bladder (to equalize the pressure in the motor housing), and a carousel assembly with a fixed plate and a rotating plate accommodating 13 sample containers. The timer schedule setup and data retrieval were accomplished using an Epson computer. The collection area of the Parflux Mark 6-13 trap is 0.509 m^2 and the funnel concentrates gravitationally settling particles into the receiving bottles on the carousel. Teflon face seals between the fixed and rotating plates ensure a minimum of exchange between the contents of the sample containers and the surrounding water.

Station SS-5 was located north of Richards Island about midway along the Canadian Beaufort slope which runs roughly northeast/southwest parallel to Tuktoyaktuk Peninsula and offshore of Kugmallit Trough. The SS-5 mooring was placed in 714 m of water and instrumentation consisted of three Baker/Milburn sequential sediment traps (199, 349, and 499 m) and three current meters (99, 206, and 506 m fitted with temperature (99, 206, and 506 m), conductivity (99, 206, and 512 m), and a pressure sensor (99 m) (see Appendix 1 for more detail). Samples were collected at 13 day intervals starting on April 22, 1991 and ending on August 30, 1991. At SS-5, the traps were fitted with an additional cup in the start/end position that allowed for the successful collection of one long interval from August 30, 1991 to September 12, 1992. This long interval included the initial delay time of 1.66 days at the beginning of the deployment so that the total time period for this interval is 381 days. The material collected in the short

delay period is insignificant compared to the total interval. Even though this sample cup was in the open position, there was a very high degree of confidence that no disturbance of the sample occurred during the mooring recovery.

The second station, AM1-92 was located on the western edge of the Mackenzie Shelf on the west side of Mackenzie Trough at the eastern edge of the Alaskan portion of the Beaufort shelf slope. The mooring was deployed in 710 m of water and was fitted with three Baker/Milburn sequential sediment traps (140, 290, and 490 m), current meters (59, 161, and 512 m), Seacats (60 and 162 m), and an Upward Looking Sonar (55 m) (see Appendix 1 for more detail). Continuous temperature (59, 60, 161, and 162 m), salinity (59, 60, 162, and 512 m), and pressure (59, 60, and 162 m) records were obtained over the deployment period (see Appendix 1 for more detail). Samples were collected at 35 day intervals starting on September 15, 1992 and ending on August 26, 1993. The trap at 140 m collected only one sample before malfunctioning, the 290 m trap collected a complete set of samples, and the 490 m trap malfunctioned on the tenth interval and the tenth sample was lost on recovery.

The third site L144 was located in 2700 m at the base of the shelf slope northwest of Mackenzie Trough and on the north eastern corner of the Alaskan Beaufort shelf. The mooring was deployed in 2715 m of water. Instrumentation included two Parflux Mark 6-13 sequential sediment traps (412 and 1311 m), four current meters (87, 106, 161, and 419 m), one SEACATS (at 98 m), and an Upward Looking Sonar (78 m) (see Appendix 1 for more detail). Continuous temperature (87, 98, 106, 161, and 419 m), salinity (98 m), and pressure (87 and 98 m) records were obtained (see Appendix 1 for more detail). Samples were collected at 35 day intervals starting on September 25, 1991 and ending on September 10, 1992. There was a complete collection of 13 samples at both depths for this site.

3.1.2 Sampling protocols and analytical techniques

The sediment trap cups were acid cleaned (10% hydrochloric acid (HCl)) for a minimum of 24 hours, and prior to deployment, the cups were filled with a solution of filtered seawater, mercuric chloride (1-2 g L^{-1}) as a preservative, and NaCl (8-10 g L^{-1}) to create a density gradient. The seawater was obtained from the intended depth of the trap and filtered through a 0.2 µm Nuclepore filter. On recovery, samples were kept cool in

the dark to allow the trapped particles to settle and to prevent alterations to the pigment contents. Samples were sieved through an acid cleaned 500 micron NITEX sieve, the supernatant was sampled and analyzed for nitrate, silicate and phosphate, and the >500 μm fractions were preserved for future zooplankton identification. The <500 μm samples were split using a MacLean rotary splitter and sub-samples were prepared for analysis of particulate organic carbon (POC), total nitrogen (TN), biogenic silica (BIOSI), chlorophyll *a* (CHLA), phaeophytins (PHAEO), stable isotopes of carbon and nitrogen ($\delta^{13}C$ and $\delta^{15}N$), elemental analysis of major and minor elements (only aluminum (Al) is reported here), and examination by scanning electron microscopy (SEM). Throughout all the analysis, duplicates were run in order to assess analytical precision.

Sub-samples for the elemental analysis, the BIOSI, and SEM were filtered onto 0.45 μm Nuclepore filters, rinsed three times with DMQ, dried in an oven at 50 ^{o}C, cooled in a desiccator chamber, and weighed to a constant weight. The sum of the weights on these Nuclepore filters divided by the fraction that the sum represented of the total sample was used to calculate the total weight in each cup. The total dry weight (TDW) flux (mg m^{-2} d^{-1}) for each interval was calculated by dividing the total weight in mg in each cup by the collection area of the trap and the collection period in days.

The samples for the analysis of POC and TN were filtered onto 21 mm quartz filters (for the samples from stations SS-5, AM1-92, L144, A01-92, and A01-93), and onto 25 mm silver filters (25 mm) for the samples from station A01-90. The samples were stored in Petri dishes and the inorganic carbon was removed by the addition of 100 to 300 μL of 0.5 N HCl which was left on the sample for ½ hour. The sample was then dried at 50 ºC for 12 hours to remove the inorganic carbon. The samples plus filters were tamped into a pre-combusted nickel sleeve and analyzed on a Leeman CE440 Elemental Analyzer. The instrument was standardized frequently with acetanalide and instrument blanks were run throughout the analysis to ensure instrument stability. Filter blanks were run and the averages of these blanks were used to correct for contributions from the filters. Reference sediments were used to track the accuracy of the results. One of the standard reference sediment (BCSS-1) was purchased from a supplier, and two other reference sediments (MT-1 and MT-2) were prepared in the lab (homogenized sediments from Beaufort Sea multi-trap sediment trap samples described in O'Brien et al., 2006).

No corrections were made for dissolution of POC and TN in the supernatant during the period of deployment and during sample handling so the results reported for POC and TN must be considered as minimum values. There were 56 samples run in duplicate and the pooled standard deviation (S_p) was calculated for the POC analysis (Sp=0.25 %; range of results from 2.57 to 12.64 %) and the TN analysis (S_p=0.045%; range of results from 0.34 to 2.39).

Biogenic silica (BIOSI) was determined by extracting amorphous silica from the sample with 2M Na_2CO_3 and then measuring the dissolved silicon concentration in the extract by molybdate-blue spectrophotometry based on the method by Mortlock and Froelich (1989). The pooled standard deviation is based on the replicates and is S_p=1.95 ug Si/mg (n=9) for the range 6.3 to 306.9 ug Si/mg. Using this method, there is no correction done for leaching of silica from aluminosilicates or for incomplete dissolution of radiolarians but Mortlock and Froelich (1989) demonstrated that systematic errors due to these effects are small compared to the range of opal contents encountered. Given the high clay content of sediments on the Beaufort shelves and in Mackenzie River suspended particulates, it is recommended that future analysis in this area be done by methods that account for any interference by lithogenic silica (Ragueneau and Tréguer, 1994; Conley, 1998; Ragueneau et al., 2005). At site L144, there were a large number of radiolarians observed in the SEM photographs and it is possible but not certain that they may have contributed significantly to the BIOSI for some samples.

Chlorophyll a (CHLA) and phaeophytin (PHAEO) were analyzed using a Turner Design fluorometer calibrated with pure chlorophyll *a* following the method outlined in Parsons et al., 1984. Care was taken to keep the samples cold and in the dark before analysis.

Aluminum concentrations were determined by inductively coupled plasma with optical emission spectrometry (ICP-OES) analysis of acid solutions produced by the dissolution of glasses prepared by fusion with lithium metaborate following the protocols at the Department for Earth and Ocean Sciences at the University of British Columbia, Vancouver, B.C., Canada. Reference standards and duplicates of samples were run throughout the analysis.

Carbon and nitrogen isotope analysis was performed at the Department for Earth and Ocean Sciences at the University of British Columbia, Vancouver, B.C., Canada. Stable carbon isotope ($\delta^{13}C_{organic}$) composition of organic carbon was determined on de-carbonated (using 10% HCl) sub-samples using a VG PRISM isotope ratio mass spectrometer with a Carlo Erba CHN analyzer fitted in-line as the gas preparation device (Calvert et al., 1995). The isotopic data for organic carbon ($\delta^{13}C_{organic}$) were measured relative to the PDB (Pee Dee Belemnite) standard and reported in the conventional δ-notation (Equation 3.1). The isotopic composition for total nitrogen ($\delta^{15}N_{total}$) was determined on a second set of untreated sub-samples using the same CHN-PRISM set-up and reported referenced to air N_2 (Equation 3.2) (Waser et al., 1998[1]; Waser et al., 1998[2]).

$$\delta^{13}C_{organic} = \{((^{13}C/^{12}C)_{sample}/(^{13}C/^{12}C)_{standard})-1\} \times 10^3 \text{ ‰} \quad \text{(Equation 3.1)}$$

$$\delta^{15}N_{total} = \{((^{15}N/^{14}N)_{sample}/(^{15}N/^{14}N)_{standard})-1\} \times 10^3 \text{ ‰} \quad \text{(Equation 3.2)}$$

3.1.3 Information on additional data sources

Supporting physical and chemical data come from a variety of sources. Nutrient (nitrate, silicate, and phosphate) data were analyzed according to the protocols in Barwell-Clarke and Whitney, 1996, and obtained from Dr. Humfrey Melling (for the spring period) at the Institute of Ocean Sciences (IOS), Sidney, B.C. and from the IOS Data Archive (for all other periods). CTD casts for the spring period were also obtained from Dr. Melling and all others were from the IOS Data Archive. Continuous profiles of transmissivity and Chlorophyll *a* were obtained from the IOS Data Archive. Instrumentation on the moorings (see Appendix 1) included: 1) AANDERAA RCM4, RCM5, and RCM7 current meters equipped variously with temperature, conductivity, and pressure sensors, 2) SEABIRD SEACATS with temperature, conductivity, and pressure sensors, and 3) Upward Looking Sonars (ULS) at the tops of all the moorings except SS-5. Mackenzie River discharges were obtained from the Water Survey of Canada (HYDAT CD-ROM). Wind velocity at a 10-m elevation (at 6 hour intervals) was obtained from the National Centers for Environmental Prediction (NCEP).

3.2 Station SS-5

The mooring at station SS-5 (71.200 ºN /134.8067 ºW) was fitted with Baker/Milburn sediment traps (Baker and Milburn, 1983) at 199, 349, and 499 metres. See Appendix 1 for detailed mooring information and trap schedules. The trap collection consisted of a 130-day spring/summer period with ten 13-day sampling intervals (April 22 to August 30, 1991) plus a single 381-day interval (August 30, 1991 to September 12, 1992). All the biogeochemical data discussed are for material < 500 μm unless otherwise stated. The sediment trap data at site SS-5 naturally divide into four periods based on a large peak in flux (see Figure 3.1), and this subdivision facilitates later discussion of biological and physical factors. The four divisions are referred to in the text as the pre-export period (intervals 1-3), the export period (intervals 4-7), the post-export period (intervals 8-10) and finally, a long 381-day period (interval 11). The Baker/Milburn sediment traps usually collect ten samples but in this case, an additional cup in the zero position provided one long integrated sample.

3.2.1 Total dry weight (TDW) fluxes and aluminum content at station SS-5

The TDW fluxes at the SS-5 traps ranged from 6 to 622 mg m^{-2} d^{-1} during spring and summer 1991 (Figure 3.1, Table 3.1 and Appendix 2). The pre-export phase (April 22 to May 31) was a period of relatively low TDW flux at all three depths. In contrast, most the material was collected in the 52-day export period (May 31 to July 22), and constitutes 89%, 73%, and 75% of the total weight collected over the full 130-day spring/summer period at the 199, 349 and 499 m traps respectively.

Dramatic increases in TDW (by factors of 5.5, 11.1, and 4.0) occur in the top, middle, and bottom traps respectively from the third to the fourth collection interval (May 31 to June 13; Figure 3.1). The peak TDW flux at all the depths occurs in interval 6 (June 26 to July 9), reaching the maximum flux of 622 mg m^{-2} d^{-1} in the 499 m trap. Fluxes decrease to much lower levels in the post-export period (intervals 8 to 10; July 22-August 30), with the most pronounced decline in the shallowest trap. Interestingly, the 499 m trap flux declines continuously over the post-export period whereas the 349 m trap shows a peak in flux for the last two intervals of the summer. Over the full 130-day collection

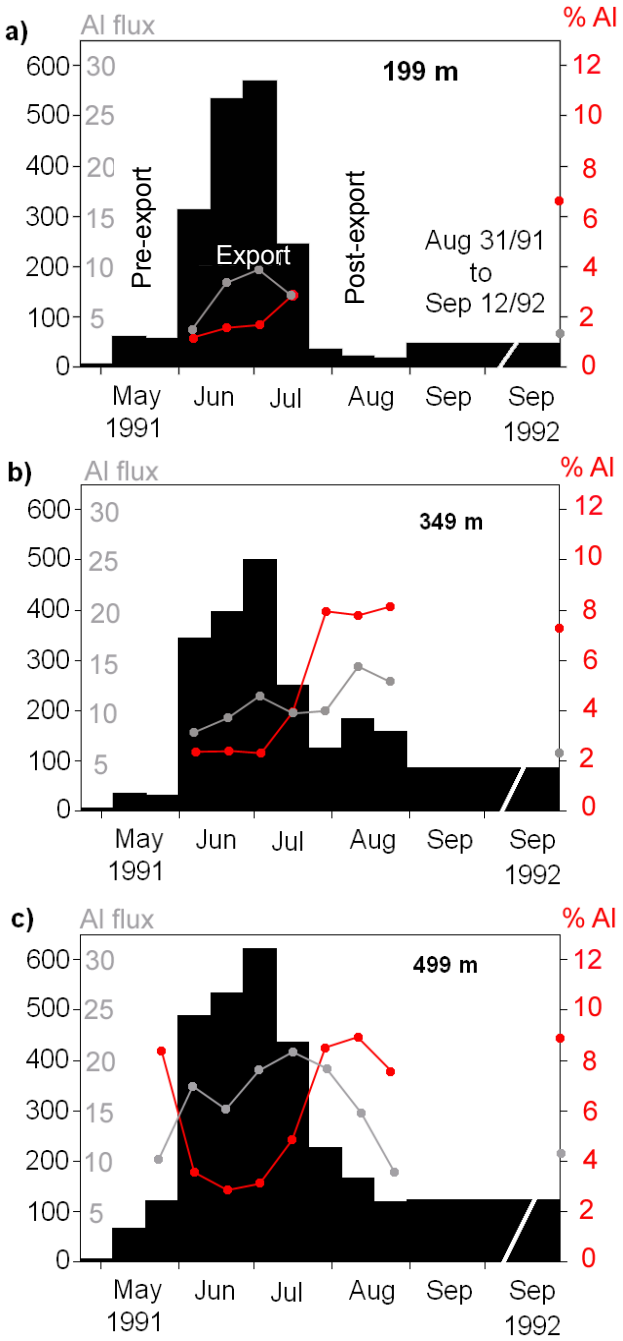

Figure 3-1 Total dry weight (TDW) fluxes (black bar plot; black axis), percent aluminum content (%Al; red line; red axis), and aluminum flux (grey line; grey axis) at station SS-5 for traps at depths: a) 199 metres, b) 349 metres, and c) 499 metres. The first 10 intervals are 13 days in duration (April 22, 1991 to August 30, 1991). The last interval is 381 days long (Aug 30, 1991 to September 12, 1992) as represented by the shortened time scale on the plot. The %Al and Al flux data for the 381-day interval are plotted on the right y-axis (see the red and grey dots). Units for TDW and aluminum fluxes are mg mg^{-2} d^{-1}. In the text, the fluxes are discussed in 4 periods: pre-export (intervals 1-3), export (intervals 4-7), post-export (intervals 8-10), and the fall 1991 to fall 1992 period where the sample was collected in one cup for 381 days (interval 11).

Table 3-1 Data summary of fluxes and percent compositions for sediment trap samples from sites SS-5, AM1-92, and L144. Table includes particulate organic carbon (POC), total nitrogen (TN), molar ratio of particulate organic carbon to total nitrogen (CNmolar ratio), biogenic silica (BIOSI), chlorophyll a (CHLA), and phaeopigments (PHAEO).

Station	Trap Depth		TDW flux	POC	POC flux	TN	TN flux	CN Ratio	BIOSI	BIOSI flux	CHLA flux	PHAEO flux
	m		mg m^{-2} d^{-1}	%	mg m^{-2} d^{-1}	%	mg m^{-2} d^{-1}	molar	%	mg m^{-2} d^{-1}	µg m^{-2} d^{-1}	µg m^{-2} d^{-1}
SS-5	199	average	186.2	8.2	14.1	1.1	1.6	8.9	14.3	50.3	29.9	840.3
		std dev	218.2	1.9	16.3	0.5	1.8	1.5	12.3	63.9	38.6	1046.2
		n	10	10	10	10	10	10	10	10	10	10
		median	59.5	7.7	4.3	1.1	0.6	8.8	14.5	8.3	17.2	327.8
		max	568.7	12.3	43.7	2.4	4.9	10.8	30.7	149.6	99.8	2585.3
		min	6.8	4.9	0.8	0.7	0.2	6.0	0.6	0.2	0.8	8.0
SS-5	349	average	203.3	7.7	13.6	1.2	1.6	8.8	12.5	42.4	28.0	618.0
		std dev	167.5	2.4	11.2	0.7	1.1	2.2	10.6	48.4	30.4	755.5
		n	10	10	10	10	10	10	10	10	10	10
		median	171.1	7.0	9.0	0.8	1.1	9.3	8.0	10.1	7.4	90.8
		max	499.8	11.7	33.1	2.4	3.7	11.5	25.5	125.4	79.3	1913.2
		min	5.5	5.0	0.6	0.6	0.1	5.2	0.8	0.2	2.6	11.7
SS-5	499	average	278.9	5.8	16.6	0.7	1.9	9.4	11.8	53.6	30.6	692.2
		std dev	220.1	1.1	14.5	0.2	1.5	1.4	9.3	59.0	31.7	796.9
		n	10	10	10	10	10	10	10	10	10	10
		median	196.7	5.3	9.8	0.7	1.2	9.7	6.5	14.8	10.8	140.9
		max	621.8	8.0	38.9	1.3	4.2	11.0	23.6	144.5	73.7	1771.9
		min	6.0	4.5	0.5	0.5	0.1	7.0	2.6	1.7	1.1	9.5
L144	412	average	66.8	5.1	2.9	0.8	0.4	7.9	4.7	3.4	0.8	15.8
		std dev	70.7	1.1	2.6	0.3	0.3	1.2	1.8	3.5	1.0	17.7
		n	13	13	13	13	13	13	13	13	13	13
		median	41.5	4.9	2.3	0.7	0.3	8.0	4.3	1.8	0.2	7.0
		max	260.5	7.9	8.8	1.5	1.3	10.5	8.1	11.1	2.9	54.2
		min	6.0	3.4	0.5	0.5	0.1	6.2	2.9	0.3	0.0	0.6
	1311	average	148.0	3.1	4.6	0.4	0.6	8.9	4.4	6.6	0.6	11.8
		std dev	86.4	0.3	2.8	0.0	0.3	0.6	0.5	4.3	0.5	7.3
		n	13	13	13	13	13	13	13	13	13	13
		median	123.3	3.0	3.7	0.4	0.5	8.8	4.2	5.0	0.5	7.9
		max	406.9	4.0	12.5	0.5	1.5	9.8	5.5	19.1	2.0	26.0
		min	76.7	2.7	2.3	0.4	0.3	7.5	3.6	3.3	0.3	5.3
AM1-92	140	average	43.5	10.2	4.5	1.7	0.7	7.2	3.3	1.4	1.3	25.6
		std dev	n/a	n/a	n/a	n/a	n/a	n/a	n/a	n/a	n/a	n/a
		n	1	1	1	1	1	1	1	1	1	1
		median	43.5	10.2	4.5	1.7	0.7	7.2	3.3	1.4	1.3	25.6
		max	43.5	10.2	4.5	1.7	0.7	7.2	3.3	1.4	1.3	25.6
		min	43.5	10.2	4.5	1.7	0.7	7.2	3.3	1.4	1.3	25.6
	290	average	189.5	6.5	10.5	0.7	1.1	11.0	3.7	5.7	5.6	58.7
		std dev	106.3	5.0	8.3	0.2	0.3	6.9	2.7	3.2	8.9	65.2
		n	10	10	10	10	10	10	10	10	10	10
		median	154.6	4.7	8.2	0.7	1.1	8.2	2.4	5.3	1.1	29.3
		max	400.8	19.2	33.3	0.9	1.5	29.9	9.3	12.5	25.5	215.1
		min	67.3	2.5	5.6	0.4	0.5	7.8	1.2	1.9	0.5	14.0
	490	average	321.3	4.2	15.6	0.6	1.9	8.7	4.1	19.9	29.4	234.0
		std dev	269.6	1.6	21.5	0.2	2.3	1.3	3.6	38.4	72.1	493.5
		n	9	9	9	9	9	9	9	9	9	9
		median	195.3	3.9	7.1	0.6	1.2	8.2	2.9	6.0	1.0	31.0
		max	952.6	7.5	71.8	0.8	7.8	10.8	12.7	120.8	218.4	1503.6
		min	100.9	2.5	4.5	0.4	0.6	7.1	1.6	2.9	0.7	10.9

Table 3-2 Correlation tables for biogenic components and TDW for stations: a) SS-5, b) AM1-92, and c) L144. Table includes correlations for total dry weight (TDW) flux, particulate organic carbon (POC) flux, total nitrogen (TN) flux, molar ratio of organic carbon to total nitrogen (CNmolar) ratio, biogenic silica (BIOSI) flux, chlorophyll a (CHLA) flux, phaeophytin (PHAEO) flux, %POC, %TN, and %BIOSI. Color-coding is as follows: bold red denotes r > 0.9; plain red denotes 0.7 < r < 0.9; plain black denotes 0.7 < r < -0.7; and blue denotes r < - 0.7.

a) Station SS-5 (all data; n=33)

	TDW flux	POC flux	TN flux	CN_{molar} ratio	BIOSI flux	CHLA flux	PHAEO flux	%POC	%TN	%BIOSI
TDW flux	1									
POC flux	**0.98**	1								
Tot N flux	**0.97**	**1.00**	1							
CN_{molar} ratio	0.82	0.79	0.77	1						
BIOSI flux	**0.96**	**0.97**	**0.96**	0.78	1					
CHLA flux	**0.93**	**0.94**	**0.93**	0.72	**0.96**	1				
PHAEO flux	**0.91**	**0.93**	**0.91**	0.75	**0.98**	**0.95**	1			
%POC	-0.24	-0.12	-0.11	-0.45	0.06	0.00	-0.01	1		
%TN	-0.48	-0.40	-0.38	-0.76	-0.27	-0.28	-0.31	**0.90**	1	
%BIOSI	0.88	**0.91**	**0.90**	0.83	**0.93**	0.88	**0.94**	0.15	-0.25	1

b) Station AM1-92 (all data; n=20)

	TDW flux	POC flux	TN flux	CN_{molar} ratio	BIOSI flux	CHLA flux	PHAEO flux	%POC	%TN	%BIOSI
TDW flux	1									
POC flux	0.81	1								
Tot N flux	**0.91**	**0.94**	1							
CN_{molar} ratio	-0.03	0.40	0.06	1						
BIOSI flux	0.85	**0.93**	**0.98**	0.09	1					
CHLA flux	0.80	**0.92**	**0.96**	0.09	**0.99**	1				
PHAEO flux	0.80	**0.91**	**0.96**	0.10	**0.99**	**1.00**	1			
%POC	-0.15	0.39	0.08	0.87	0.13	0.16	0.16	1		
%TN	-0.27	0.08	0.04	0.08	0.09	0.14	0.14	0.57	1	
%BIOSI	0.45	0.73	0.69	0.31	0.76	0.81	0.82	0.44	0.34	1

c) Station L144 (all data; n=26)

	TDW flux	POC flux	TN flux	CN_{molar} ratio	BIOSI flux	CHLA flux	PHAEO flux	%POC	%TN	%BIOSI
TDW flux	1									
POC flux	**0.96**	1								
Tot N flux	**0.95**	**0.99**	1							
CN_{molar} ratio	0.59	0.60	0.50	1						
BIOSI flux	**0.95**	**0.96**	**0.91**	0.69	1					
CHLA flux	0.70	0.81	0.82	0.50	0.75	1				
PHAEO flux	0.63	0.76	0.78	0.44	0.66	**0.94**	1			
%POC	-0.54	-0.39	-0.39	-0.55	-0.47	-0.20	-0.17	1		
%TN	-0.58	-0.48	-0.45	-0.74	-0.55	-0.32	-0.29	**0.96**	1	
%BIOSI	0.11	0.22	0.17	0.46	0.38	0.38	0.33	-0.02	-0.16	1

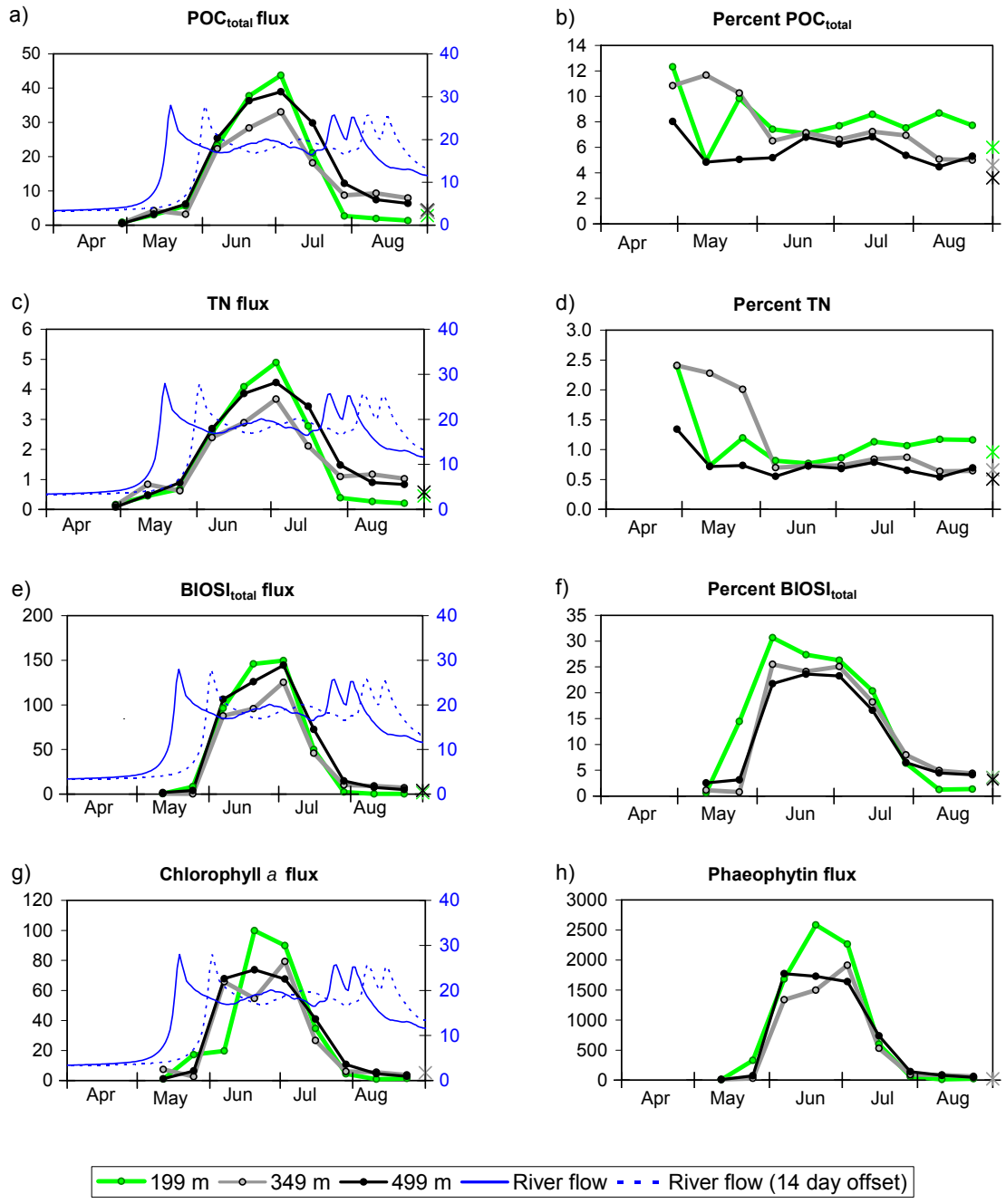

Figure 3-2 Biogenic components (<500 µm portion) at station SS-5 for the three trap depths (199, 349 and 499 m) are plotted at the mid-point of each 13-day interval (April 22 to August 30, 1991). Parameters plotted are: a) total particulate organic carbon flux (POC flux; mg m^{-2} d^{-1}), b) percent POC, c) total nitrogen flux (TN flux; mg m-2 d^{-1}), d) percent TN, e) total biogenic silica flux (BIOSI flux; mg m^{-2} d^{-1}), f) percent BIOSI, g) chlorophyll a flux (CHLA flux; µg m^{-2} d^{-1}), and h) phaeophytin flux (PHAEO flux; µg m^{-2} d^{-1}). The Mackenzie River flows as measured at Arctic Red River (see Figure 2.2) are shown (solid blue line; m^3 sec^{-1} x 10^3) along with a 14-day offset (dashed blue line; as a rough estimate of the time taken to transit from Arctic Red to the shelf edge). The x symbols shown on the right y-axis indicate the data for the 381-day collection (August 31, 1991 to September 12, 1992) at 199 (green x), 349 (grey x), and 499 m (black x) respectively.

period at SS-5 (Apr 22 to Aug 30), the total sample weights collected at the 199, 349, and 499 m traps increase with depth (775, 846, and 1160 mg respectively) yielding respective fluxes of 186, 203, and 279 mg m^{-2} d^{-1}.

As observed for the spring/summer 1991 collection, the total material collected over the 381 day interval also increased with depth (571, 1066, and 1507 mg for the 199, 349, and 499 m traps respectively) as did the respective fluxes (46.8, 87.4, and 123.7 mg m^{-2} d^{-1}). The fluxes from the fall of 1991 to the fall of 1992 are much smaller than would be expected when compared to the corresponding depths in the spring/summer period of 1991 suggesting that very different conditions prevailed between the years 1991 and 1992, especially in the spring/summer seasons.

The aluminum (Al) content at SS-5 (Figure 3.1) ranged from 1.16% to 8.98% with the lowest values (1.16 to 3.35%) occurring in the first three intervals of the export period. Fluxes ranged from 3.6 to 20.9 mg m^{-2} d^{-1} for the 1991 spring/summer period with higher fluxes generally correlating with lower absolute Al concentrations. With the exception of the last interval in late summer of 1991, %Al and Al fluxes increase with trap depth at each collection interval, and at all three depths marked increases in concentration occurred right after the TDW flux peak at interval 6.

3.2.2 Biogenic fluxes at station SS-5

Spring/summer fluxes of POC, TN, and BIOSI for the <500 μm material at SS-5 in 1991 are high throughout the 52 day export period (Figures 3.2a, 3.2c, 3.2e, and 3.2g), and correlate strongly with each other and with TDW flux ($r \geq 0.96$) (Table 3.2). The TDW flux also correlates well with %BIOSI ($r = 0.88$; Table 3.2a) but poorly and negatively with %POC ($r = -0.24$) and %TN ($r = -0.48$). In addition, %POC and %TN correlate strongly with each other ($r = 0.90$) but poorly with %BIOSI ($r = 0.15$ and 0.25 respectively) (Table 3.2).

POC content ranges between 4.5% and 12.3% of the TDW over all three depths and is consistently lowest at 499 m (Figure 3.2b). Indeed, the average %POC over the ten 13-day intervals decreases with depth (8.2%, 7.7%, and 5.8% at 199, 349, and 499 m respectively.

POC fluxes range from <1 to 44 mg m^{-2} d^{-1} for the 130-day spring/summer period in 1991. All three depths show a steady rise in POC flux over intervals 4-6 of the export

period, and a peak in POC flux at interval 6. In the post-export period (intervals 8-10), the POC fluxes drop to <3 mg m^{-2} d^{-1} in the 199 m trap and to 6-12 mg m^{-2} d^{-1} in the 349 and 499 traps. The flux patterns of TN and POC are very similar, and as with %POC, the lowest %TN values are consistently at the 499 m depth.

BIOSI content (Figure 3.2f) ranges overall between 0.6 and 30% of the TDW with a slightly higher average (for intervals 1-10) at 199 m (14.5%) than at 349 and 499 m (12.4 and 12.1% respectively). Corresponding fluxes (Figure 3.2e) range from <1 to 150 mg m^{-2} d^{-1} and show coincident peaks with POC, TN, and TDW fluxes in July at all depths.

CHLA and PHAEO fluxes (Figure 3.2g and 3.2h) correlate strongly with TDW, POC, TN, and BIOSI fluxes ($r > 0.9$) in the May to mid-July period, and fall to very low levels by July 22. The close correspondence with fluxes of the other biological components implies a near-constant stoichiometry within the settling particulate matter over the course of the bloom period.

3.3 Station AM1-92

The mooring at station AM1-92 (70.548ºN /140.045ºW; 710 m bottom depth) was deployed in mid-September of 1992 and recovered at the end of August 1993 before the tenth cup had closed. The material in the 10th cup (July 25 to August 26) was recovered intact at the 290 m trap but was lost in recovery in the 490 m trap. The top trap malfunctioned and only the first sample was recovered. The trapping interval for AM1-92 was 35 days (except for 10th interval, which was 30 days) so the resolution of the timing of events is poor as compared to SS-5, where the interval was 13 days. All the biogeochemical data discussed are for material < 500 µm unless otherwise stated, and are listed in Table 3.1 (data summary), Table 3.2b (correlation tables), and Appendix 2 (data tables).

3.3.1 Total dry weight (TDW) fluxes and aluminum content at station AM1-92

Over the full deployment period, the TDW fluxes at AM1-92 range from 44 to 953 mg m^{-2} d^{-1} (Figure 3.3). The sediment trap record is discussed in two periods: 1) the fall/winter/early spring from September 15, 1992 to May 16, 1993 covering intervals 1-7;

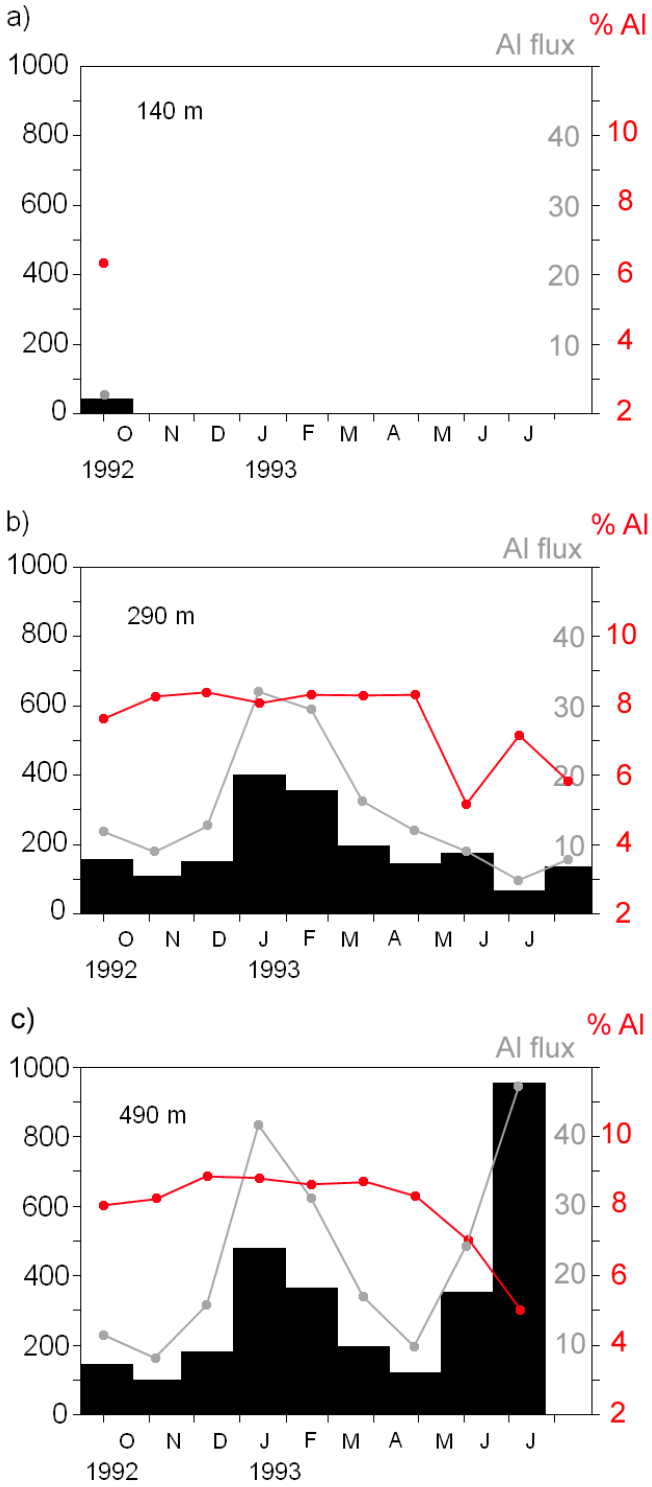

Figure 3-3 Total dry weight (TDW) fluxes (black bar plot; black axis on the left), percent aluminum (%Al; red line; red axis on the right), and aluminum flux (Al flux; grey line, grey axis on the right) at station AM1-92 for traps at depths: a) 140 metres, b) 290 metres, and c) 490 metres. The intervals are 35 days in duration (September 13, 1992 to August 26, 1993). Units for TDW flux and aluminum flux are mg mg^{-2} d^{-1}. The trap at 140 m only collected one sample before a malfunction occurred and the last sample of the 490 m trap was lost during recovery.

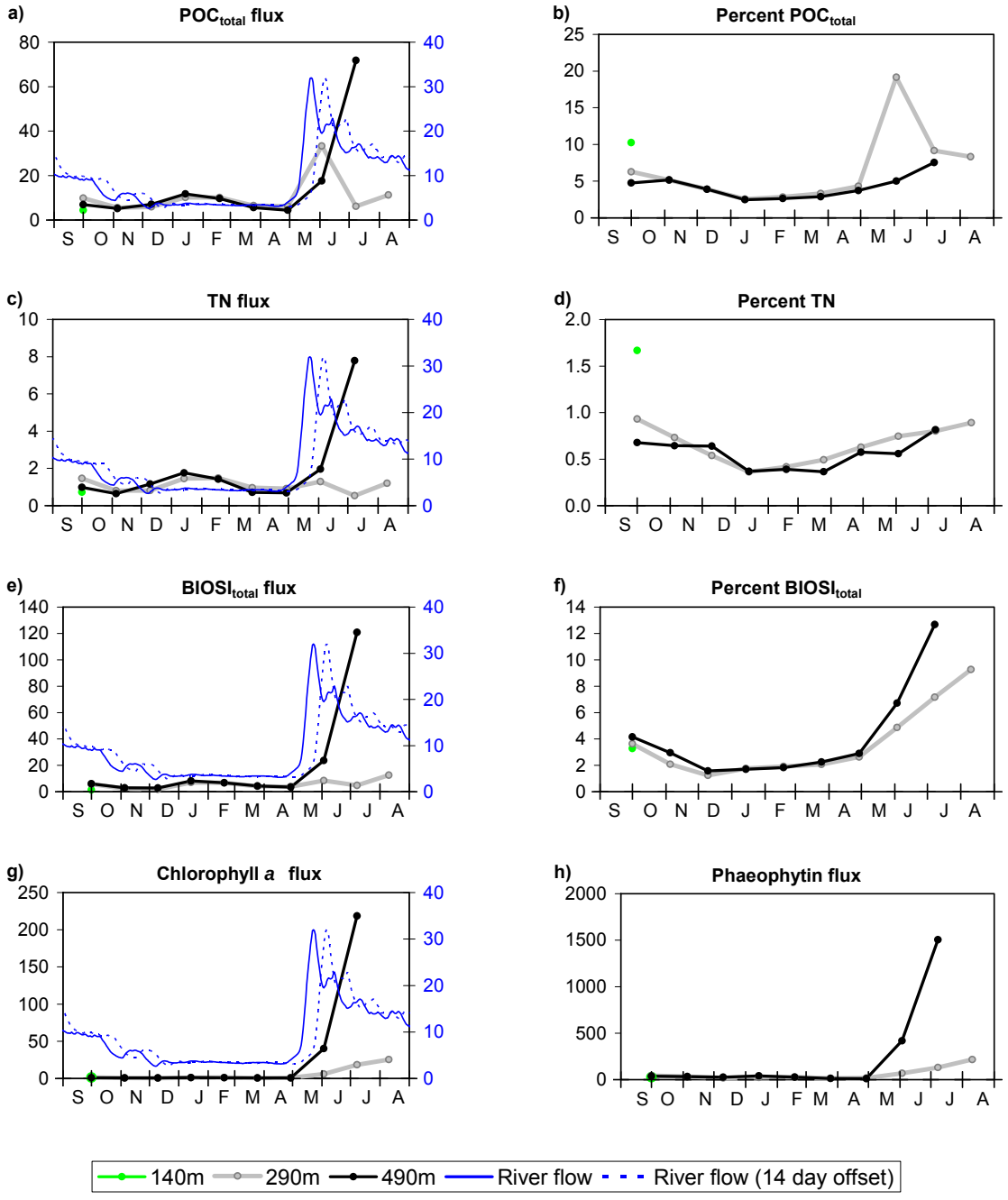

Figure 3-4 Biogenic components (<500 µm portion) for station AM1-92 plotted at the mid-point of each 35-day interval (September 13, 1992 to August 26, 1993): a) total particulate organic carbon flux (POC flux; mg m^{-2} d^{-1}), b) percent POC, c) total nitrogen flux (TN flux; mg m^{-2} d^{-1}), d) percent TN, e) total biogenic silica flux (BIOSI flux; mg m^{-2} d^{-1}), f) percent BIOSI, g) chlorophyll a flux (CHLA flux; µg m^{-2} d^{-1}), and h) phaeophytin flux (PHAEO flux; µg m^{-2} d^{-1}). The Mackenzie River flows as measured at Arctic Red River (see Figure 2.2) are shown (solid blue line; m^3 sec^{-1} x 10^3) along with a 14-day offset (dashed blue line; rough estimate of time for river water to transit from Arctic Red River to the shelf edge). Note that the 140 m trap only sampled one interval before malfunctioning, and there are only 9 intervals for the trap at 490 m since the tenth sample was lost during retrieval.

and 2) the spring/summer period from May 16, 1993 to August 26, 1993 covering intervals 8-10.

A notable feature is a strong winter peak in January-February at both 290 and 490 m depth (Figure 3.3; intervals 4 and 5). This peak represents 40% of the total mass of material collected at 290 m (over intervals 1-10) and 29% of the total at 490 m (over intervals 1-9).

The pattern differed in spring/summer (May 16 to August 26, intervals 8-10), when sedimentation in the 490 m trap was pronounced with no equivalent accumulation 200 m higher in the water column (Figure 3.3). The maximum flux of 953 mg m^{-2} d^{-1} observed in late June-July at AM1-92 stands out; indeed, it exceeds the peak TDW flux measured at site SS-5.

Aluminum concentrations at station AM1-92 ranged overall from 5.0 to 8.8% of TDW, and were slightly higher in the fall to early spring period (intervals 1-7; Figure 3.3). Throughout the winter months (December to March), both the aluminum fluxes and contents were lower in the mid-depth trap than at 490 m. The mid-winter peak in aluminum flux at both 290 and 490 m was surprising since the site was under continuous ice cover during the sampling period. The strongest peak in aluminum flux occurs at 490 m in June/July coincident with a decrease in aluminum content (due to dilution by the increase in the biogenic fluxes), this peak is absent at the 290 m.

3.3.2 Biogenic fluxes at station AM1-92

TDW, POC, TN, and BIOSI fluxes over the fall, winter and early spring (September 15, 1992 to May 16, 1993, intervals 1-7) all exhibit similar patterns (Figures 3.4a, 3.4c, and 3.4e). While fluxes of POC, TN, and BIOSI strongly correlate with each other ($0.93 \leq r \leq 0.98$) and with the TDW flux ($0.81 \leq r \leq 0.91$), %POC and %TN ($r = -0.15$ and -0.27 respectively) are only weakly correlated with TDW, and moderately correlated with %BIOSI ($r = 0.45$). The correlations between %POC, %TN, and %BIOSI are all in the low positive range ($0.34 \leq r \leq 0.57$; Table 3.2b).

POC contents (Figure 3.4b) range between 2.4 % and 19.2 % and tend to be lowest in the deepest trap. The highest %POC concentrations occurred in the May-June interval (19.1 wt. %) at 290 m depth before sharply declining in July (Fig. 3.4b).

The fall to early spring POC fluxes (Figure 3.4a) range between 4.5 and 11.8 mg $m^{-2}d^{-1}$ and show a small mid-winter peak at both depths. The spring/summer POC flux pattern markedly differs from the concentration profiles (compare Figs. 3.4a and b) with the maximum POC flux being recorded at 490 m (71.8 mg $m^{-2}d^{-1}$ between June 20 and July 25, 1993).

Neither % TN nor %BIOSI show the high increase seen in organic carbon content in June (Figure 3.4d). Moreover, while the BIOSC content increases fourfold between early June and late July, the TN content only marginally increases.

CHLA and PHAEO fluxes at AM1-92 (Figures 3.4g and 3.4h) correlate strongly with fluxes of TDW (r = 0.80), POC (r = 0.92 and 0.91), TN (r = 0.96), and BIOSI (r = 0.99), and like the other biogenic components, show maxima at 490 m depth in mid summer.

3.4 Station L144

Two Parflux Mark 6-13 sediment traps (Honjo and Doherty, 1988) at 412 and 1311 m depth collected samples at station L144 (71.37ºN 141.71ºW) from September 25, 1991 to September 10, 1992. The collection comprises 13 samples of 27 days duration each at both depths. All the biogeochemical data discussed here are for material that passed a 500 μm mesh, unless otherwise stated. Data are listed in Table 3.1 (summary); Table 3.2c (correlation tables); and Appendix 2 (data tables)).

3.3.1 Total dry weight (TDW) fluxes and aluminum content at station L144

The TDW fluxes at L144 range from 6 to 407 mg m^{-2} d^{-1} with the highest flux occurring in August/September at 1311 m. Fluxes at 1311 m are quite variable, and with the exception of the first interval in the fall, are higher than at 412 m. Fluxes at 412 m are higher in the fall, and drop down to low values by mid-November, and then increase slowly beginning in early May.

The range of aluminum content at L144 (Figure 3.5) is much greater at 412 m (6.2 to 8.2%) than at 1311 m (7.5 to 8.2%). Al fluxes range from 0.4 to 33.0 mg m^{-2} d^{-1}, and the highest peak has a high Al content (>8%) and coincides with the late summer peak in TDW flux at 1311 m (Figure 3.5). At both depths, the patterns of Al and TDW fluxes are remarkably similar (Figure 3.5).

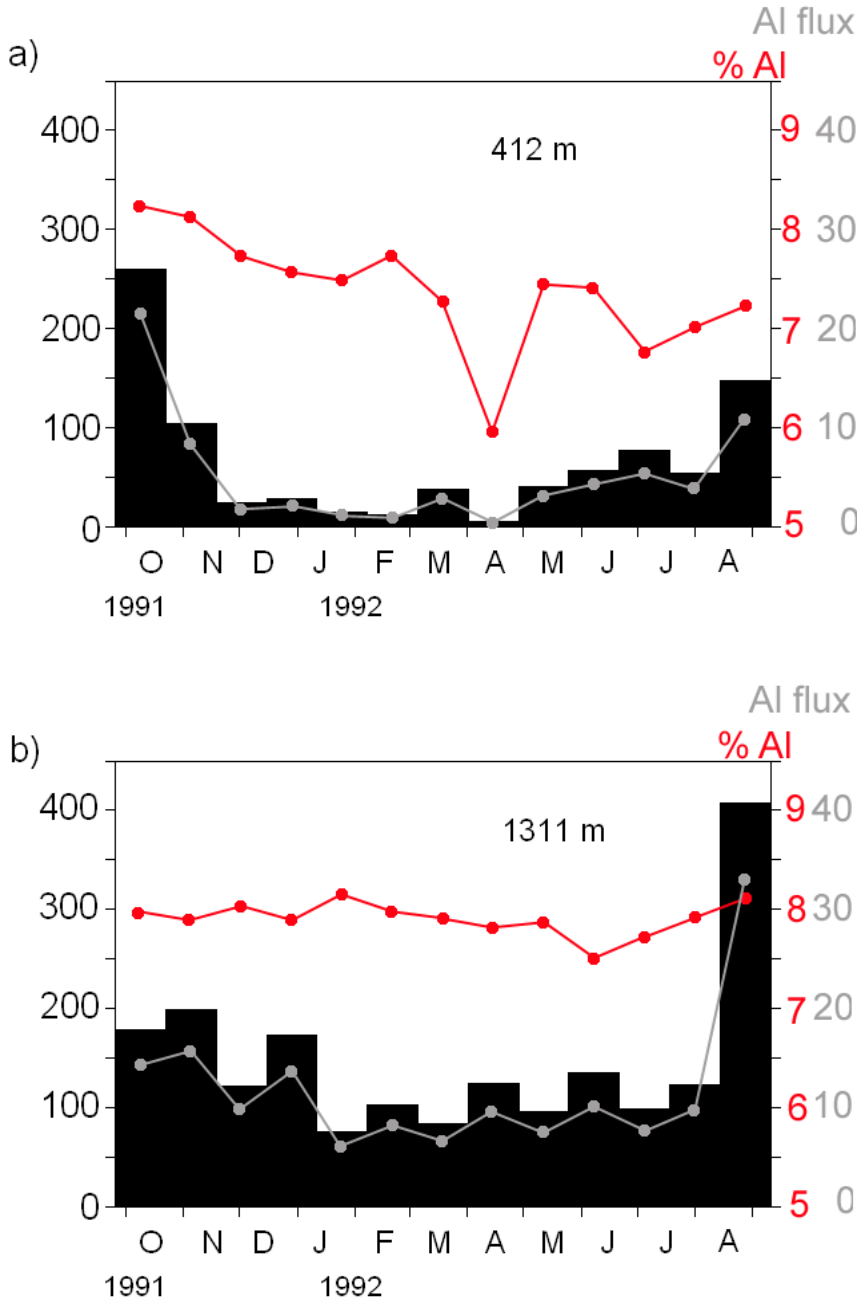

Figure 3-5 Total dry weight (TDW) fluxes (black bar plot; black axis), percent aluminum (%Al; red line; red axis), and aluminum flux (Al flux; grey line; grey axis) for station L144 at trap depths: a) 412 metres and b) 1311 metres. The intervals are 27 days in duration (September 25, 1991 to October 9, 1992). Units for TDW and aluminum fluxes are mg mg^{-2} d^{-1}. The bottom depth was 2700 m.

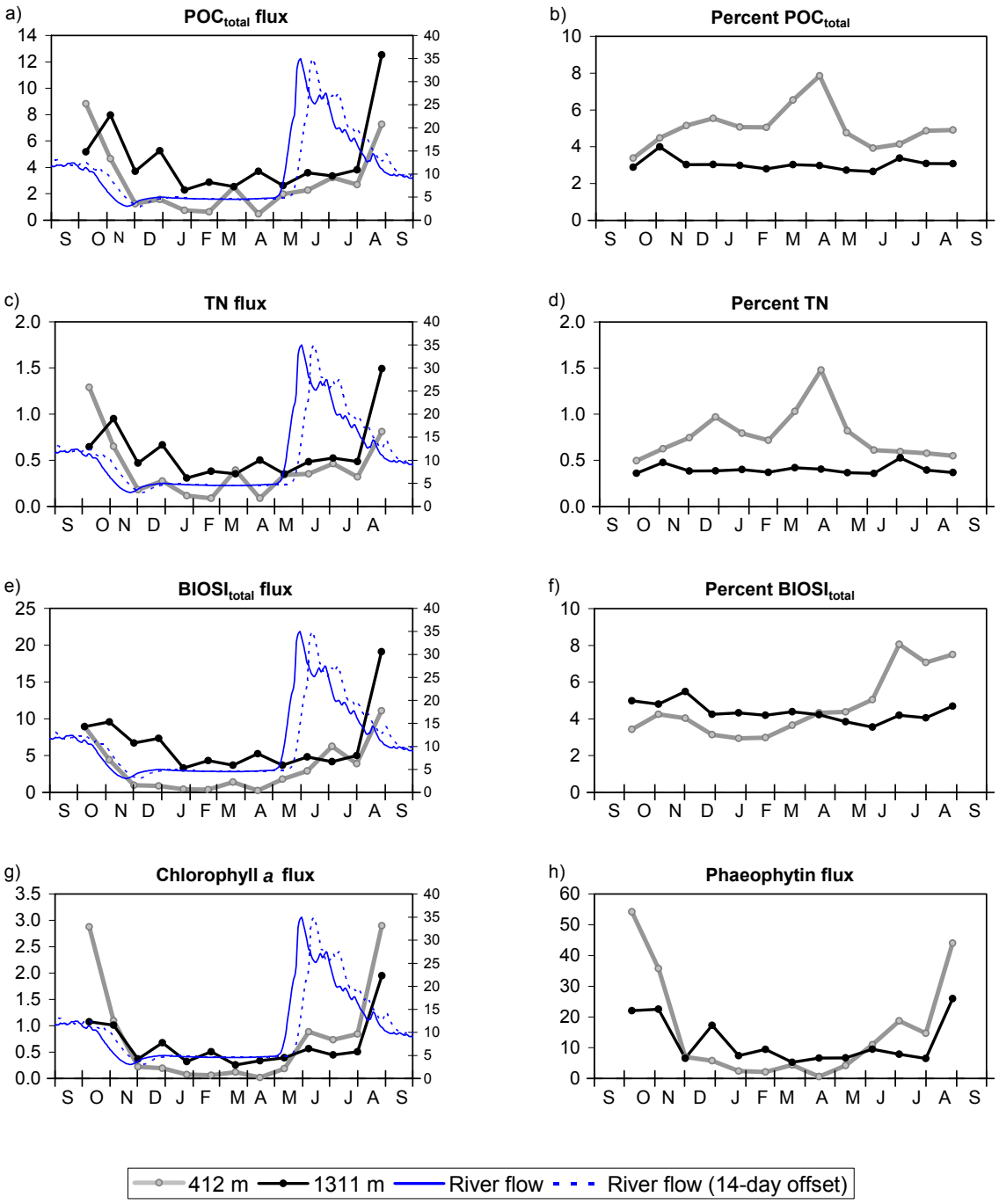

Figure 3-6 Biogenic components (<500 µm portion) for station L144 at the two trap depths (412 and 1311 m) plotted at the mid-point of each 27-day interval (September 25, 1991 to September 9, 1992). Parameters plotted are: a) total particulate organic carbon flux (POC flux; mg m-2 d-1), b) percent POC, c) total nitrogen flux (TN flux; mg m-2 d-1), d) percent TN, e) total biogenic silica flux (BIOSI flux; mg m-2 d-1), f) percent BIOSI, g) chlorophyll a flux (CHLA flux; µg m-2 d-1), and h) phaeophytin flux (PHAEO flux; µg m-2 d-1). The Mackenzie River flows as measured at Arctic Red River (see Figure 2.2) are also shown (solid blue line; m3 sec-1 x 103) and with a 14-day offset (dashed blue line; rough estimate of the time taken to transit from Arctic Red to the shelf edge).

3.3.2 Biogenic fluxes at station L144

At site L144, the TDW flux shows good correlations with the fluxes of POC, TN, and BIOSI (r = 0.96, 0.95, and 0.89 respectively). POC flux correlates very strongly with TN flux (r = 0.99), and BIOSI shows good correlation with the fluxes of POC (r = 0.89) and TN (r = 0.85). In addition, %POC shows a strong correlation with %TN (r = 0.96). The fluxes of POC, TN, and BIOSI show similar patterns to the TDW flux with higher fluxes in the fall/late summer and lower fluxes in the winter/early spring (Figures 3.6a, 3.6c, and 3.6e). In general, the POC, TN, and BIOSI fluxes are higher at 1311 m than at 412 m with only a few exceptions. See Table 3.2c for correlation coefficients for the biogenic components at station L144.

The POC and TN contents (ranges of 3.4 to 7.9% and 0.4 to 1.5% respectively) at L144 are consistently lower in the deep trap (Figures 3.6b and 3.6d). For these constituents, content varies little at 1311 m but is quite variable at 412 m, where there is a general pattern of increasing content from the fall to early spring and a decrease thereafter. The highest POC and TN contents occur at 412 m in April when the TDW flux is low (Figures 3.5, 3.6b, and 3.6d). Fluxes of POC (range 0.5 to 12.5 mg m^{-2} d^{-1}) and TN (range 0.1 to 1.5 mg m^{-2} d^{-1}) are highest in late-summer/early-fall (Figures 3.6a and 3.6c).

In the fall through to early spring, the BIOSI content is greater at 1311 m than at 412 m whereas from early spring to late summer, it is greatest at 412 m (Figure 3.6f). BIOSI contents range from 2.9 to 8.1% with the highest content occurring in June at 412 m. There is relatively little variation in BIOSI content in the deep trap. BIOSI fluxes range from 0.3 to 11.1 mg m^{-2} d^{-1} with the maximum fluxes occurring in August (Figure 3.6e). For most intervals, the BIOSI flux is greatest in the deep trap.

CHLA and PHAEO fluxes at L144 are highest in late summer and early fall (Figure 3.6g and 3.6h). Throughout the winter and into early spring, the fluxes are lower at 412 m than at 1311 m, and from spring to early fall, fluxes are higher at 412 m. CHLA fluxes range from 0.0 to 2.9 ug m^{-2} d^{-1} and the PHAEO fluxes range from 0.6 to 54.2 ug m^{-2} d^{-1}. The deep trap shows considerable variability in pigment fluxes throughout the winter months.

3.5 Stable isotopes of carbon ($\delta^{13}C$) and nitrogen ($\delta^{15}N$)

At site SS-5, the stable carbon isotopic ratios ($\delta^{13}C$) range between -22.9 and -24.8 ‰. The highest ("heaviest) values are at the beginning and the lowest ("lightest") values at the end of the export peak, and values are similar at all three intermediate-water depths (Figure 3.7a; Appendix 2). Insufficient sample precluded analyses for the pre-export period (intervals 1-3) at 199 and 349 m, for the first interval at 499 m, and for the late summer samples (intervals 8-10) at 199 m. The range in $\delta^{13}C$ at station SS-5 is much smaller than at sites AM1-92 and L144 (Figure 3.7a).

At AM1-92, the $\delta^{13}C$ exhibits the remarkably wide range of -12.2 to -26.4 ‰ (Figure 3.7a; Appendix 2). There is an increasing trend in $\delta^{13}C$ from the fall to early spring reaching a maximum in interval 8 (May 18 to June 22) followed by a sharp decrease to low values coincident with high Mackenzie River inputs (Figure 3.7a). Although it appears unusual, there is a high level of confidence in the very high $\delta^{13}C$ value (-12.2) at interval 8 at 290 m as it was repeated in a duplicate analysis. From late fall to mid-winter, $\delta^{13}C$ is almost identical at 290 and 490 m, but there after, the values at 290 m exceed those at 490 m. Broadly similar distributions are seen at site L144 with lighter $\delta^{13}C$ values (~ -23 to -24) occurring in fall and winter and slightly heavier values (~ -22 to -23) in the spring and the bloom period (particularly in the March through early July interval). This is followed by a decrease in the late summer possibly associated with river inputs (Figure 3.7a; Appendix 2). At site L144, the increasing trend in $\delta^{13}C$ over the winter followed by a decrease in spring/summer occurs at both 412 and 1311 m but with different timing. At L144, the $\delta^{13}C$ values are lower at 412 m than at 1311 m except for the early spring period.

Across the entire data set, $\delta^{15}N$ values range from 5.61 to 11.81 ‰ and exhibit a temporal pattern similar to that of $\delta^{13}C$ (Figure 3.7b; Appendix 2). At SS-5, (499 m), $\delta^{15}N$ decreases (~9.9 to ~6.5 ‰) over the pre-export and export periods and then increases over the post-export period (to ~7.9 ‰). At both L144 and AM1-92, an increasing trend in $\delta^{15}N$ over winter is followed by a sharp decrease in spring/summer. Overall, site L144 (412 m) shows the greatest range in $\delta^{15}N$ with a maximum of 11.8 in early spring and minimums in spring/summer coincident with peak river inputs. At L144, $\delta^{15}N$ increases markedly from ~ 7 ‰ in late fall 1991 to nearly 12 ‰ in the early spring

a)

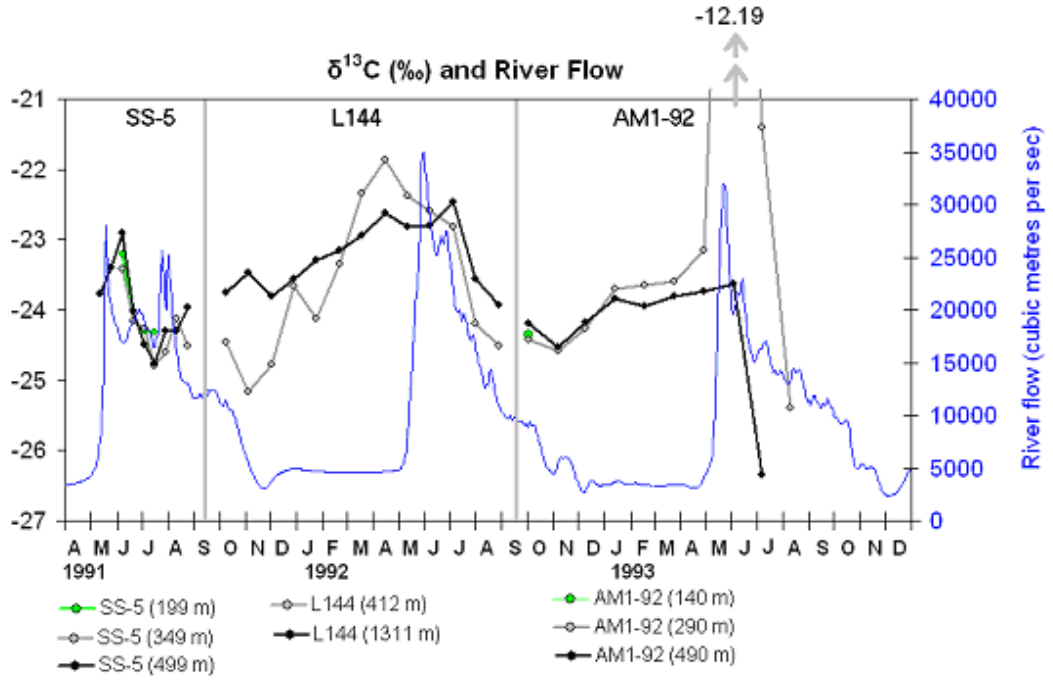

b)

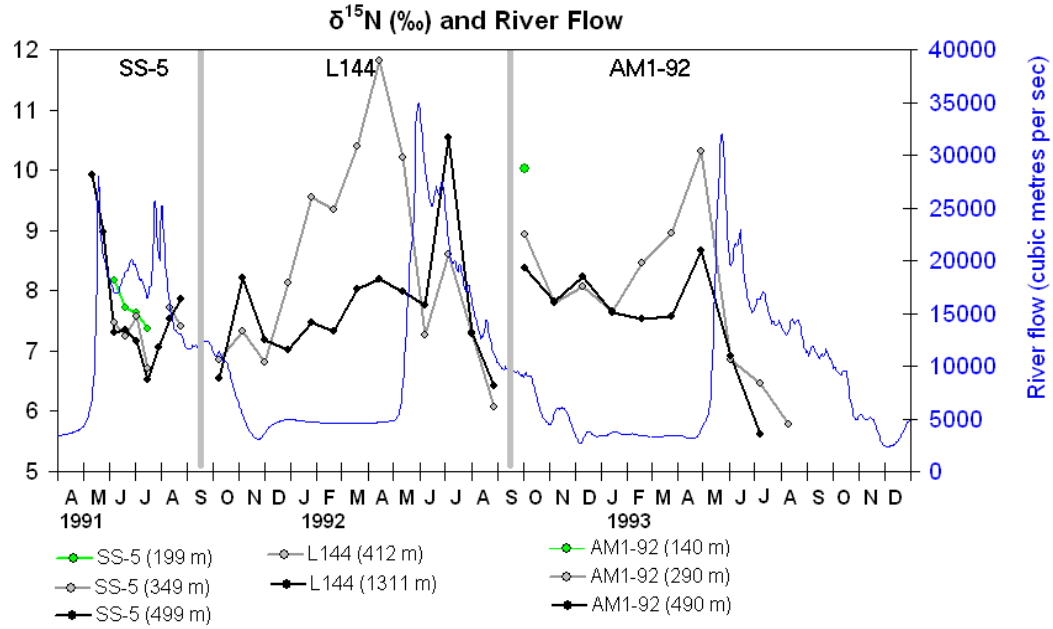

Figure 3-7 a) Stable carbon isotope ratios ($\delta^{13}C$) and b) Stable nitrogen isotope ratios ($\delta^{15}N$) for the sediment trap samples from sites SS-5, L144, and AM1-92. Mackenzie River flows at Arctic Red River (m^3 sec^{-1}) are plotted in blue. Note one very high value (-12.19) that is off the scale and shown above the plot for interval 8 at station AM1-92 (290 m).

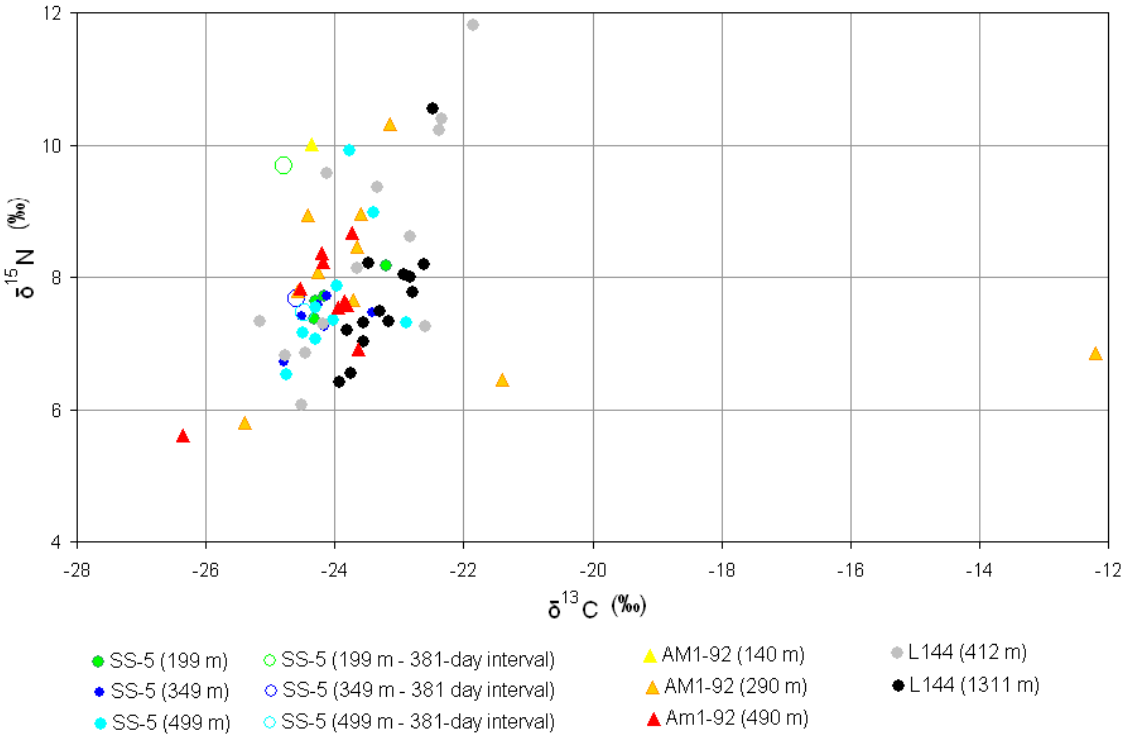

Figure 3-8 Stable isotope ratio of nitrogen ($\delta^{15}N$) versus stable isotope ratio for carbon ($\delta^{13}C$) for stations SS-5, AM1-92 and L144. Units are ‰.

at 412 m before declining to <6.5 ‰ in the summer; values at 1311 m are lighter than at 412 m over the winter and generally heavier in the fall and summer (Figure 3.7b). At AM1-92, $\delta^{15}N$ values are very similar at both depths (290 and 490 m) throughout the fall/early winter and then generally higher at 290 m from mid-winter into summer.

There are definite and similar temporal patterns in $\delta^{13}C$ and $\delta^{15}N$ at all three of the sites. If the one high value of -12.2 (AM1-92, 290 m, interval 8) is excluded, there is a significant correlation between these isotopic signatures (r=0.64) with heavier $\delta^{13}C$ and heavier $\delta^{15}N$ tending to occur together; with no data excluded, the correlation is poor. At least three distinct source materials can be roughly assigned as follows: A) low $\delta^{13}C$ (< -25) and low $\delta^{15}N$ (< 6), B) high $\delta^{13}C$ (> -22) along with a $\delta^{15}N$ of <7, and C) $\delta^{13}C$ of around >-24 with high $\delta^{15}N$ (>10). This is a simplistic view considering the seasonal extremes of river input and ice cover and the range of possible biogeochemical processes occurring throughout the water column. The significance of $\delta^{13}C$ and $\delta^{15}N$ signatures will

be further discussed in relation to seasons, sources, and other constituents in Chapter 5 and in the context of physical forcing in Chapter 6.

3.6 Ratios

3.6.1 CN_{molar} ratio

In general, the CN_{molar} ratios at sites SS-5, AM1-92, and L144 (range of 5.2 to 11.5 plus one high value of 29.9) exhibit increases in the spring and are on average higher than the Redfield ratio (Figure 3.9a, Table 3.1). At SS-5, the CN_{molar} ratios (range 5.2 to 11.5) show moderate correlations ($0.72 < r < 0.83$) with TDW, POC, TN, BIOSI, CHLA, and PHAEO fluxes as well as with %BIOSI whereas correlations with %TN and %POC are poor and negative (Figure 3.9a; Tables 3.1 and 3.2). The ratios at SS-5 are lowest in the early spring, increase during the export period and decrease in the late summer. In contrast to SS-5, CN_{molar} ratios at site AM1-92 (range 7.1 to 29.9) show poor correlations with the fluxes ($r < 0.4$) (Figure 3.9a). In addition, at AM1-92, the ratios show poor correlations with %BIOSI and %TN but a good correlation with %POC ($r = 0.87$; this may be misleading as the high values of %POC and CN_{molar} ratio at interval 8 at 290 m skew the results). The fall to early spring period at AM1-92 exhibit a narrow range of ratios (7.1 to 9.4) while in the spring/period the range is much greater (10.5 to 29.9). The sample with the high ratio of 29.9 (AM1-92, interval 8, 290 m) is unique in having high %POC (19%) and high $\delta^{13}C$ (-12.2) signatures. At L144, the CN_{molar} ratios (range 6.2 to 10.5) exhibit only moderate to low correlations with the fluxes ($0.44 < r < 0.69$), negative correlation with %POC and %TN, and low correlation with %BIOSI ($r = 0.46$)(Figure 3.9a). Over the fall and winter at L144, the ratios are higher at the deepest trap and over the spring/summer, there is an increasing trend and the ratios are slighltly higher at 412 m.

3.6.6 BIOSI/POC and BIOSI/TN ratios (mol/mol)

The temporal patterns of BIOSI/POC and BIOSI/TN ratios are very similar at all three sites (Figures 3.9e and 3.9f). Site SS-5 exhibits the highest range in values (see Table 3-1 for data summary) but all the sites show increases in the ratios beginning in early spring (Figures 3.9e and 3.9f). From the fall to early spring, the ratios tend to be

a)

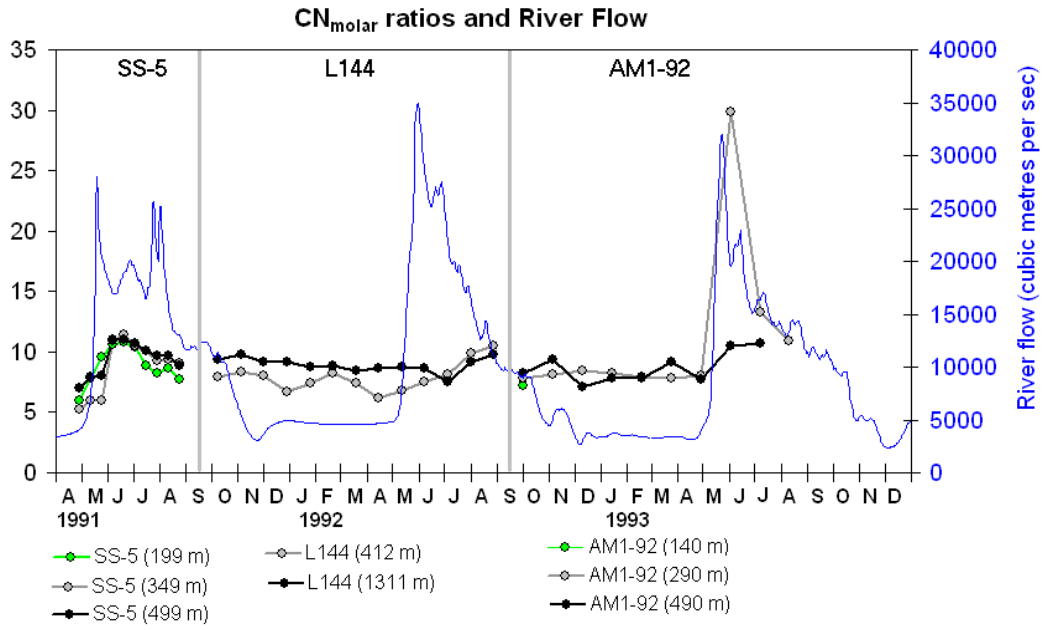

b)

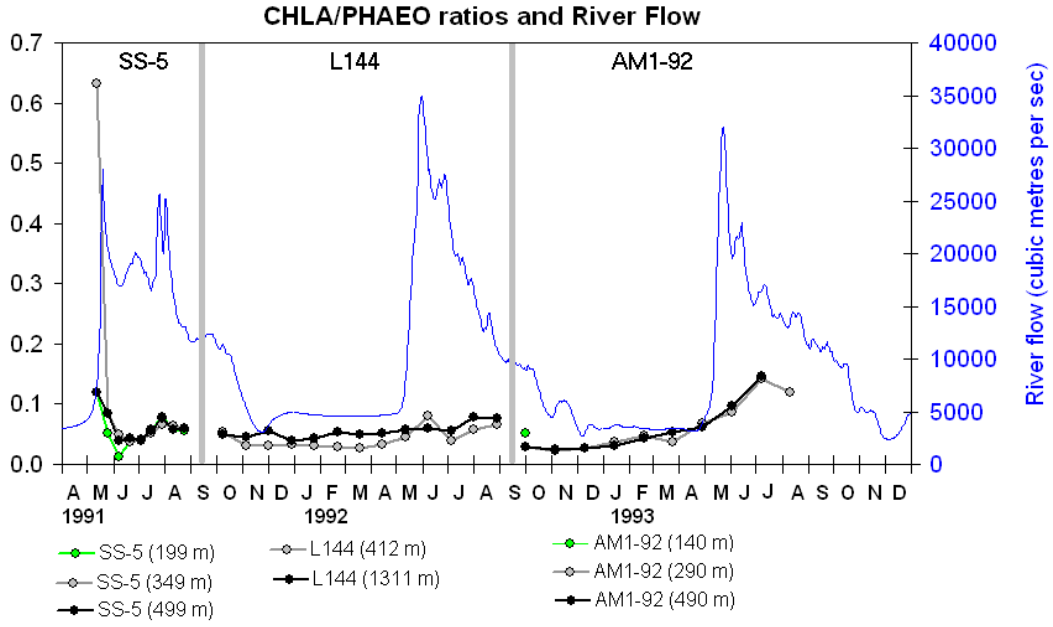

Figure 3-9 Elemental ratios plotted for stations SS-5 (199, 349, and 499 m), AM1-92 (140, 290, and 490 m), and L144 (412 and 1311 m) as follows: a) $CN_{molar\ ratios}$ (mol/mol), b) CHLA/PHAEO (µg/µg), c) CHLA/BIOSI (µg/mg), d) CHLA/POC (µg/mg), e) BIOSI/POC (mol/mol), and f) BIOSI/TN (mol/mol). Figure 3-9 continues for the following 2 pages

c)

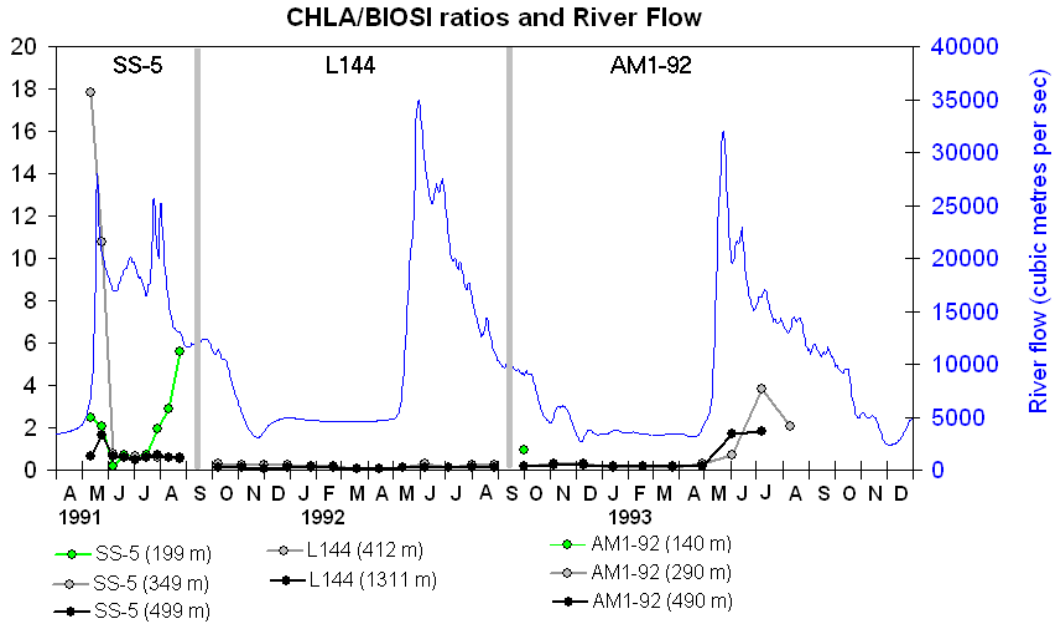

d)

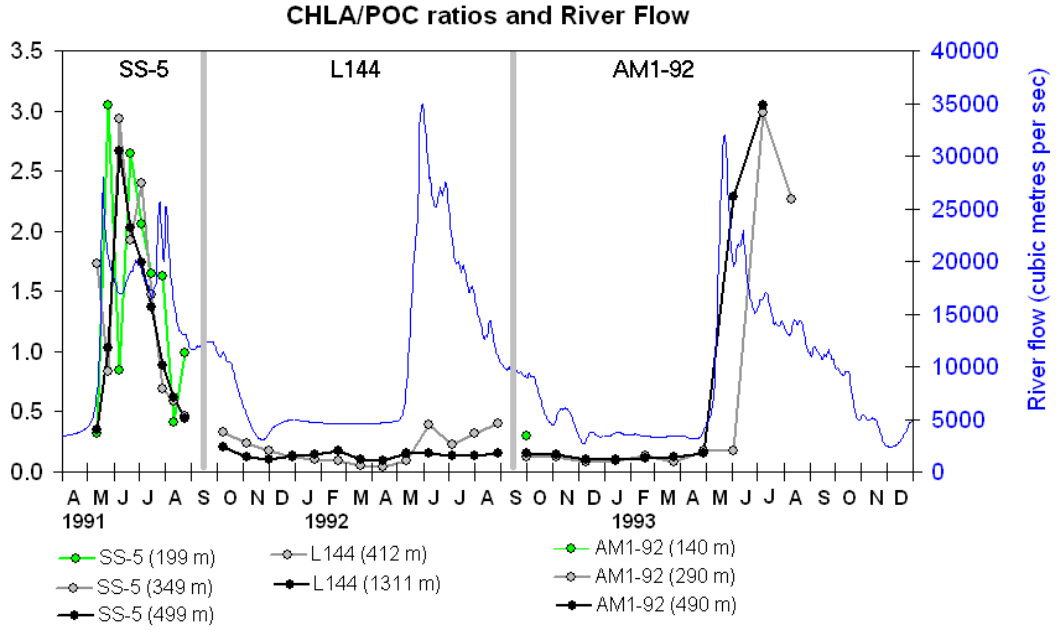

Continuation of Figure 3.9

e)

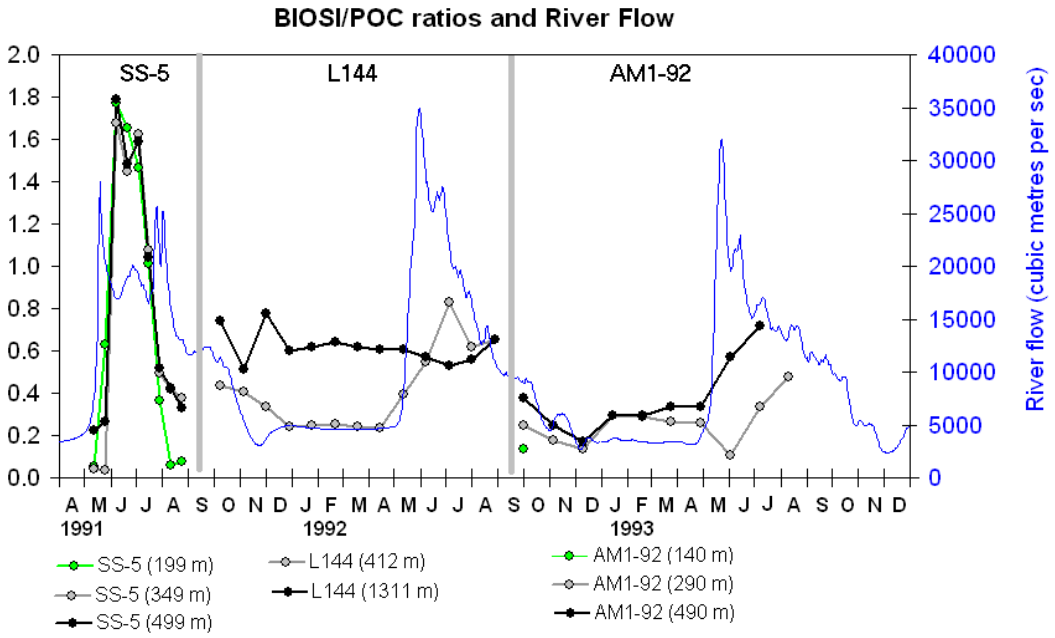

f)

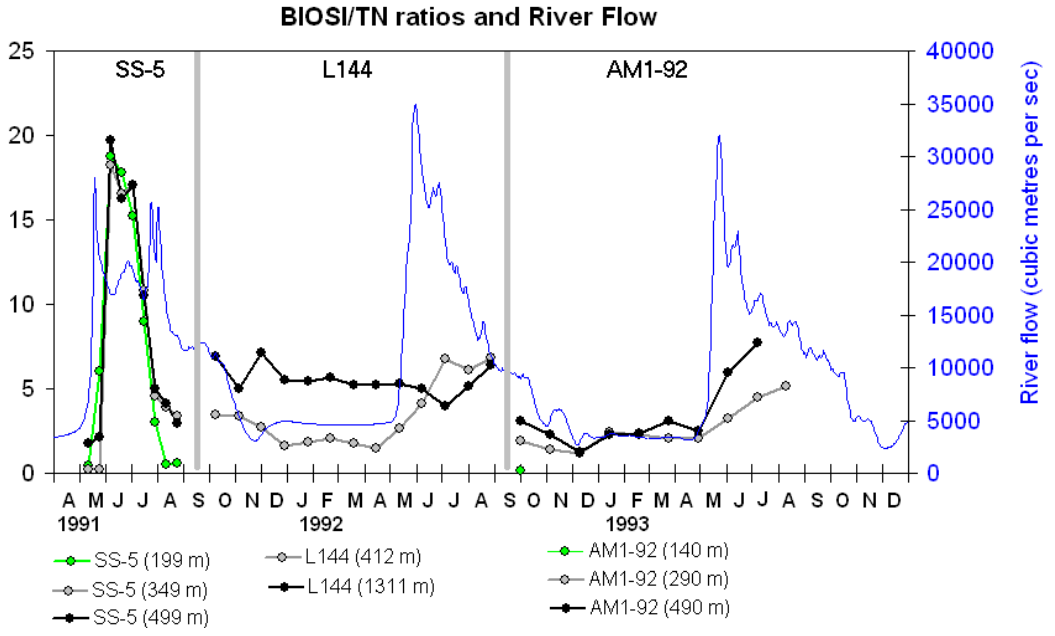

Continuation of Figure 3.9

higher at the deepest trap especially at site L144. At site AM1-92, the ratios are virtually equal at intervals 4 and 5 coincident with the high mid-winter TDW flux peak.

3.6.7 Ratios with pigments (CHLA/PHAEO, CHLA/POC, CHLA/BIOSI)

The ratio of CHLA/PHAEO (ug/ug) is used as an indicator of the degree to which exported material has been grazed by zooplankton, with lower ratios indicating a higher degree of grazing. Over the three sites, (with only one exception), the CHLA/PHAEO ratio was less than 0.2 (Figure 3.9b). At SS-5, the CHLA/PHAEO ratio (range0.01 to 0.63) had a median value of 0.057 and the ratios were lowest during the export period. The ratios at AM1-92 (range ~0.02 to 0.15) showed a gradual increase from fall to the following summer and the ratios were quite similar at the two depths over the whole collection period. At L144, the CHLA/PHAEO ratios exhibit the smallest range of the three stations (0.03 to 0.08), and at most intervals, the ratio is slightly lower at 412 m than at 1311. It is interesting to note that whereas at site SS-5, the CHLA/PHAEO ratios show a decrease during the strong export period, at site AM1-92, the ratios increase during the main export peak.

Ratios of CHLA/BIOSI (ug/mg) and CHLA/POC (ug/mg) provide important information on the timing and composition of the diatom bloom. At station SS-5, this ratio (range 0.2 to 17.8) has a median value of 0.64 and a very steady value of ~ 0.6 during the export- and post-export periods at 349 and 499 m. The increased ratio at the end of the summer at 199 m is most likely due to the decrease in BIOSI rather than an increase in CHLA. Levels of both CHLA and BIOSI at SS-5 are higher at the two lower depths in late summer. Site AM1-92 exhibits only a small range of CHLA/BIOSI ratios (0.1 to 3.8) with ratios of <0.3 for the fall and winter and higher values in the spring/summer period (Figure 3.9c). At station L144 the CHLA/BIOSI ratios remain very low (<0.32) at both trap depths in all seasons (Figure 3.9c).

At station SS-5, the CHLA/POC ratios (ug/mg) vary from 0.3 to 3.0 with a median value of 1.4 (Figure 3.9d). The highest CHLA/POC ratio occurs in interval 3 at 199 m just prior to the export period and is followed by an abrupt decrease at the beginning of the export period (interval 4). At 349 and 499 m, the ratios are highest at the beginning of the export period (interval 4) and there is a steady decline thereafter. There is a marked difference between 199 m and 499 m in the pattern of CHLA/POC at the

beginning of the export period (interval 4). Since the pattern for the PHAEO/POC ratio at 199 m does not show the decrease exhibited at 199 m for the CHLA/POC ratio at the beginning of the export period, it is possible that the first pulse into the traps at this depth may be due to a release of ice associated diatoms (particularly *Melosira arctica*) containing considerable levels of degraded pigments but very little CHLA. This may be consistent with the over-wintering of a growth ice associated algae in the fall.

At AM1-92, the CHLA/POC ratio (range 0.1 to 3.0) exhibits very low ratios (<0.2) from fall to early spring and increases thereafter to a maximum of ~ 3 in the spring/summer (Figure 3.9d). Notably, at interval 8, the ratio increased abruptly at 490 m but stayed low at 290 m (note that this sample at 290 m stands out with regards to other parameters as well). Station L144 exhibits very low CHLA/POC ratios and exhibits a small increase at the 412 m depth in spring and summer (Figure 3.9d). From mid-winter to early spring, the ratio at 412 m is less than at 1311 m, whereas in the fall, spring and summer, the ratios are higher at 412 m. The greatest increases in the ratios are at 290 m from June to the end of August.

3.7 Scanning electron microscope (SEM) evidence

An in-depth treatment of the sediment trap data on a species abundance basis is beyond the scope of this study but scanning electron microscope (SEM) photographs provide useful qualitative descriptions of the sediment trap samples. A selection of these photographs is included here.

At SS-5, the pre-export material appears to consist mainly of terrigenous material and biogenic detritus such as small fragments of diatom tests (Figure 3.10, see interval 2). At the beginning of the export period, there is an abrupt transition to large numbers of diatom tests in the samples (Figure 3.10, see interval 4) including an abundance of Melosira arctica, an ice-associated diatom known to settle in mats in the Arctic spring. An assortment of pennate and centric diatoms occurs along with the *M. arctica* in the material from the export period (Figure 3.10, see intervals 4 and 6). Post-export-period material (Figure 3.10, interval 10) consists mainly of terrigenous material, small fragments of diatom tests, a few radiolarians, a few coccolithophorids and a few fecal pellets.

At 490 m at AM1-92, winter material (intervals 4 and 5) is composed mainly of fine-grained terrigenous material while diatoms dominate in spring/summer (intervals 8 to 10). A large number of the ice algae *Nitzschia frigida*, likely released from melting of the underside of the sea ice, occurs in the 290 m sample in early summer (Figure 3.11, interval 8).

At L144, a large number of radiolarians, tintinnids, and silicoflagellates were present in the samples at both 412 and 1311 m and over the whole deployment period (Figure 3.12). On a strictly qualitative basis, it appears that radiolarians and siliconflagellates contribute substantially to the biogenic silica at L144, and are very much more abundant at this site than at SS-5 and AM1-92.

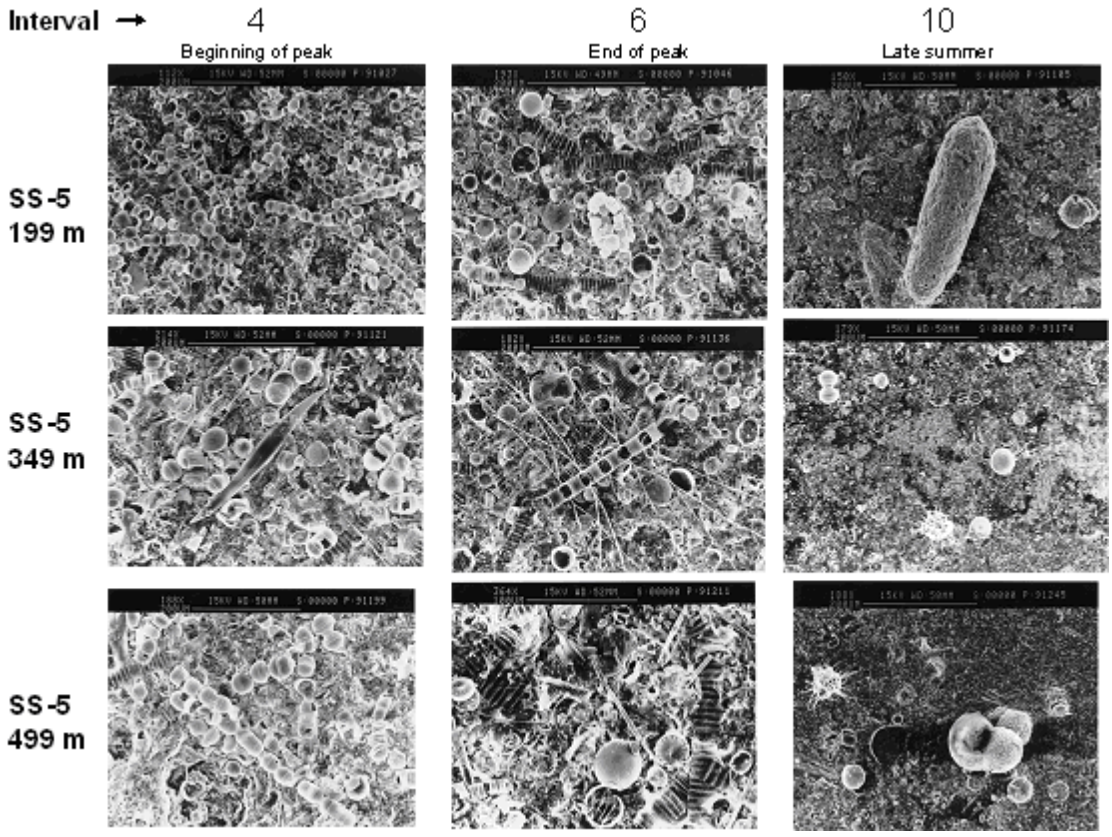

Figure 3-10 Scanning electron microscope photographs of sediment trap samples at station SS-5 at the 3 depths 199, 349, and 499 m for interval 2 (in the pre-export period), intervals 4 and 6 (in the export period), and interval 10 (in the post-export period).

a)

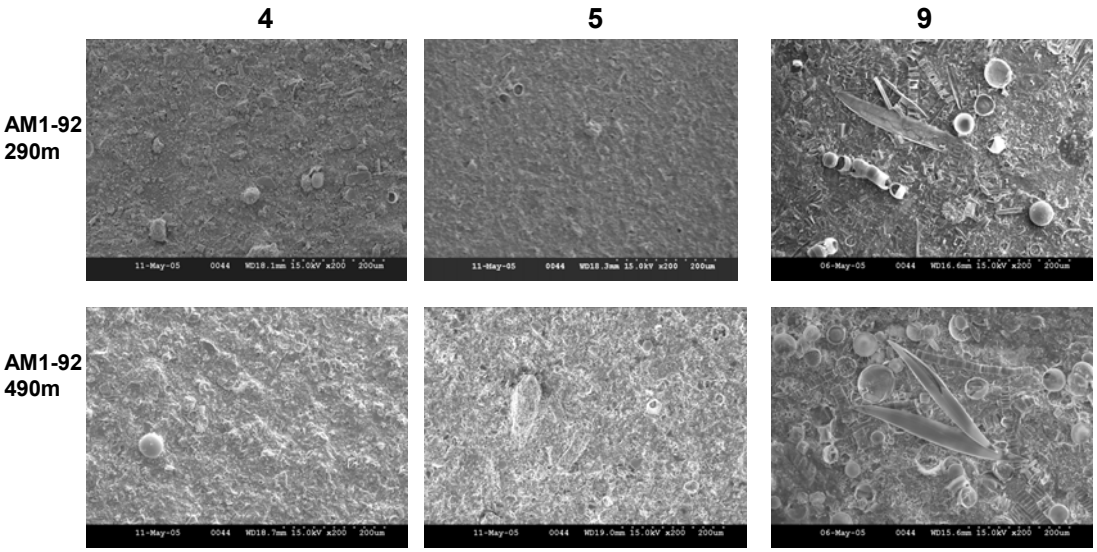

b)

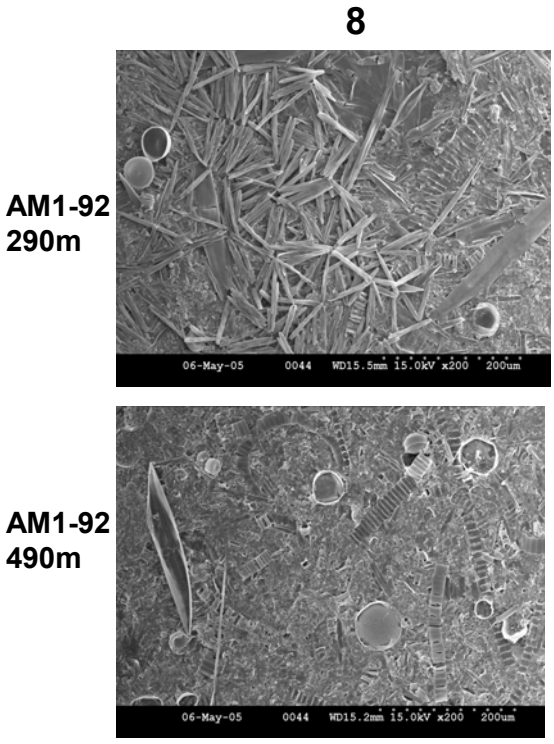

Figure 3-11 Scanning electron microscope (SEM) photographs of the material trapped at station AM1-92 at 290 and 490 m at a) intervals 4 (start of winter peak), 5 (end of winter peak) and 9 (high summer peak June/July 1993); b) interval 8 shows ice algae at 290 m and distinct difference in biological material between 290 and 490 m in May/June 1994.

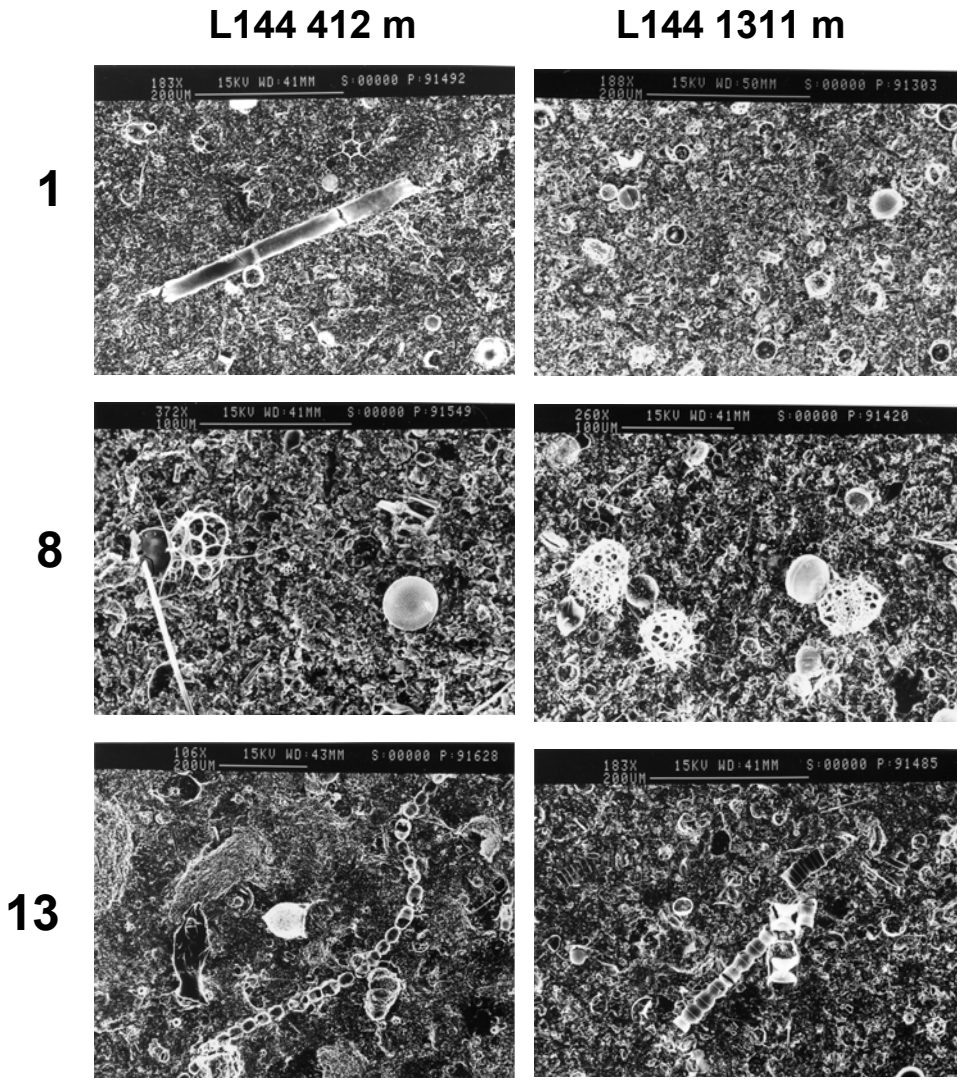

Figure 3-12 Scanning electron microscope (SEM) photographs of the material at station L144 for intervals 1, 8, and 13 at 412 and 1311 m.

Chapter 4 Particle fluxes in Canada Basin

To collect and analyze a time series of the vertical flux of particles in Canada Basin, moorings were established at stations A01-90, A01-92, and A01-93 (see Figures 1.1 and 2.2). Water depths at these sites exceeded 3000 m. Station L144 (described in Chapter 3) was originally intended to be part of the Canada Basin series but due to extreme ice conditions it was instead established in 2700 m of water on the abyssal plain at the base of the continental slope. Data for L144 are included for comparative purposes here (Figures 4.1 to 4.8). Details of the moorings and sequential trap schedules at each the three Canada Basin sites are outlined in Appendix 1, analytical methods are detailed in Chapter 3, and data tables can be found in Appendix 2.

4.1 Overview of moorings at climate station A01

Station A01-90 (72.621 ºN 143.568 ºW) was established in 3339 m of water in September of 1990 and recovered through the ice in the spring of 1992. Two Baker/Milburn-type sequential sediment traps were placed at 615 and 1515 metres below surface and set to sample at 32-day intervals. Nine complete intervals were retrieved by the shallower trap, and only six intervals at 1515 m, the result of trap malfunction. Additional instrumentation on the mooring included an Upward Looking Sonar (ULS; at 59 m), seven Recording Current Meters (AANDERAA types RCM4 and RCM5; at 65, 85, 135, 190, 315, 617, and 1517 m), one transmissometer (at 85 m), and two SEACATS (at 66 and 191 m). Details are provided in Appendices 1 and 2.

The mooring at A01-92 (72.542 ºN 143.830 ºW) was deployed in 3375 m of water in September of 1992 and recovered in August of 1993. Two sediment traps were installed on the mooring, at 600 m (Parflux Mark 6-13 type) for which a full set of 13 samples was recovered, and at 1510 m from which no samples were retrieved due to trap malfunction. The sampling interval for the 600 m trap was 27 days. Additional instrumentation on the mooring included an upward looking sonar (ULS; 59 metres), seven current meters (AANDERAA types RCM4 and RCM5; at depths 64, 80, 127, 181, 305, 610, and 1512 metres), 2 SEACATS (at 65 and 183 metres), and one transmissometer (at 80 metres).

Two traps were installed on the mooring at station A01-93 (72.517 ºN 143.866 ºW; 3370 m water depth) which was deployed in September of 1993 and recovered in August of 1995. Twelve of thirteen samples, each of which collected for 30 days, were retrieved from the shallowest trap (a Parflux Mark 6-13 type) (installed 568 m below surface. The second trap at 1482 metres malfunctioned and no samples were collected. Additional instrumentation on the mooring included an upward looking sonar (ULS; 52 metres), seven current meters (AANDERAA type RCM4; at depths 58, 77, 81, 137, 263,570, and 1484 metres), 2 SEACATS (at 60 and 139 metres), and one transmissometer (at 77 metres).

4.2 Results

Sample analyses included total dry weight (TDW), particulate organic carbon (POC), total nitrogen (TN), biogenic silica (BIOSI), chlorophyll *a* (CHLA), and phaeophytins (PHAEO). Analysis of the trap samples was limited by sample size and not all analyses were performed on all stations. The samples at station A01-90 were particularly small as the Baker/Milburn trap has a much smaller collection area and thus very few measurements of BIOSI, CHLA, and PHAEO were possible. No aluminum or stable isotope measurements were performed on the station A01 samples.

4.2.1 Total dry weight (TDW) fluxes

The TDW fluxes at the A01 stations (Figure 4.1) ranged from 0.4 to 65.1 mg m^{-2} d^{-1} over the three deployments. For A01-90 and A01-92, the fall/winter TDW fluxes in the 615 and 600 m traps were low (<6.6 mg m^{-2} d^{-1}) while at A01-93, at approximately the same depth (568 m), the fluxes were significantly higher and quite erratic, ranging up to the highest value observed, ~65 mg m^{-2} d^{-1} in February, 1994. The deep trap (1515 m) at A01-90 exhibited a distinct winter peak of 42 mg m^{-2} d^{-1} from mid-January to mid-February, 1991.

TDW fluxes at A01 increased over the spring and peaked in the summer in both 1990 and 1992 (Figure 4.1), while at A01-93 fluxes were generally higher and much more erratic. It is notable that the peak TDW flux in February at A01-93 exceeded the 1992 winter TDW fluxes at station L144 at 412 m, which was much closer to the shelf edge and presumably more subject to shelf edge processes. Overall, particle fluxes in the

Canada Basin showed considerable inter-annual variability in the early 1990s, and exhibited episodic mid-winter events of variable magnitude and duration as well as marked variability between stations in the timing and magnitude of the spring peak.

Table 4-1 Simple linear correlation coefficients for the sediment trap fluxes and percent compositions for stations A01-90 (615 and 1515 m), A01-92 (600 m), and A01-93 (568 m). Coefficients greater than 0.7 are highlighted in red.

	TDW flux	%POC	POC flux	%TN	TN flux	CN Ratio	%BIOSI	BIOSI flux	CHLA flux	PHAEO flux
TDW flux	1									
%POC	-0.335	1								
POC flux	0.737	0.139	1							
%TN	-0.335	**0.975**	0.058	1						
TN flux	0.717	0.185	**0.974**	0.134	1					
CN Ratio	0.098	-0.409	0.039	-0.545	-0.084	1				
%BIOSI	0.179	-0.575	0.013	-0.639	-0.084	0.502	1			
BIOSI flux	**0.884**	-0.502	0.568	-0.531	0.506	0.439	0.482	1		
CHLA	0.424	-0.183	0.381	-0.242	0.236	0.578	0.231	0.505		
CHLA flux	0.431	-0.190	0.387	-0.248	0.244	0.580	0.210	0.489	1	
PHAEO	0.457	-0.255	0.384	-0.303	0.238	0.536	0.314	0.568	0.955	
PHAEO flux	0.454	-0.255	0.384	-0.303	0.239	0.538	0.290	0.544	**0.962**	1

4.2.2 Biogenic fluxes

Percent POC and TN are strongly correlated (r = 0.98; Table 4.1) and both are negatively correlated with %BIOSI (r = -0.575 and -0.639 respectively). Accordingly, fluxes of POC and TN correlate strongly with each other (r = 0.97) but only moderately with TDW flux (r = 0.74 and 0.72 respectively). In contrast, the biogenic silica (BIOSI) flux correlates well with TDW flux (r = 0.88) but poorly with POC and TN fluxes (r = 0.56 and 0.51 respectively) (Table 4.1).

Highest POC fluxes over the three A01 deployments (Figure 4.2) at ~600 m water depth occurred in June 1994, and reached ~5.6 mg m^{-2} d^{-1}. Fall and winter fluxes at A01-90 and A01-92 were very low (<0.5 mg m^{-2} d^{-1}) and comparatively high at A01-93 (0.93 to 3.03 mg m^{-2} d^{-1}) with peaks in mid-September and mid-February, roughly comparable to those observed at 412 m at L144.

All three A01 deployments exhibited a peak in POC flux at ~600 m in spring/summer but with variable timing: late-June/early-July of 1991 at A01-90, late July/early August of 1993 at A01-92, and early to late June of 1994 at A01-93. At the

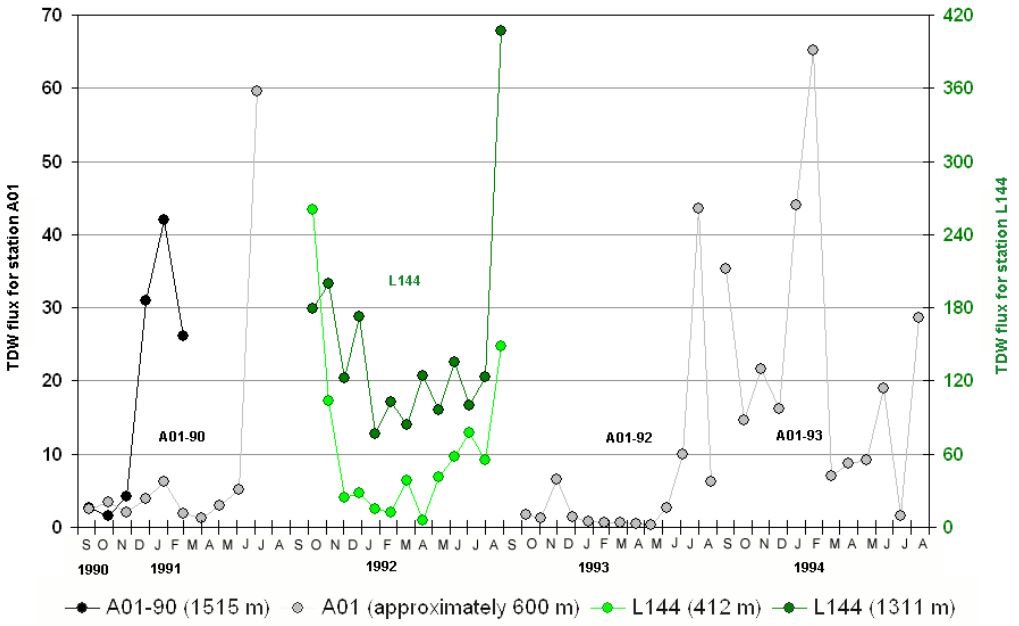

Figure 4-1 Total dry weight (TDW) flux data for sediment trap material from stations A01-90 (615 and 1515 m), A01-92 (600m), A01-93 (568 m), and L144 (412 and 1311 m). Note that the y-axis for the station L144 data (on the right in green) is a factor of six greater than the y-axis for the A01 data (on the left). The units for TDW flux are mg m^{-2} d^{-1}.

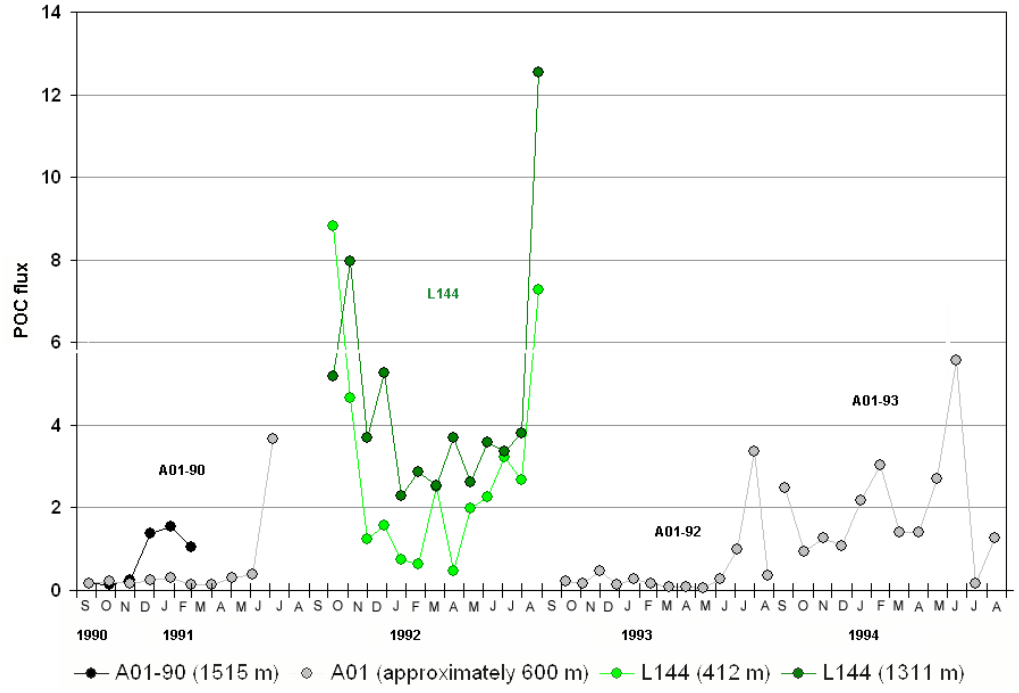

Figure 4-2 Particulate organic carbon (POC) flux data for sediment trap material from stations A01-90 (615 and 1515 m), A01-92 (600m), A01-93 (568 m), and L144. The units for POC flux are mg m^{-2} d^{-1}.

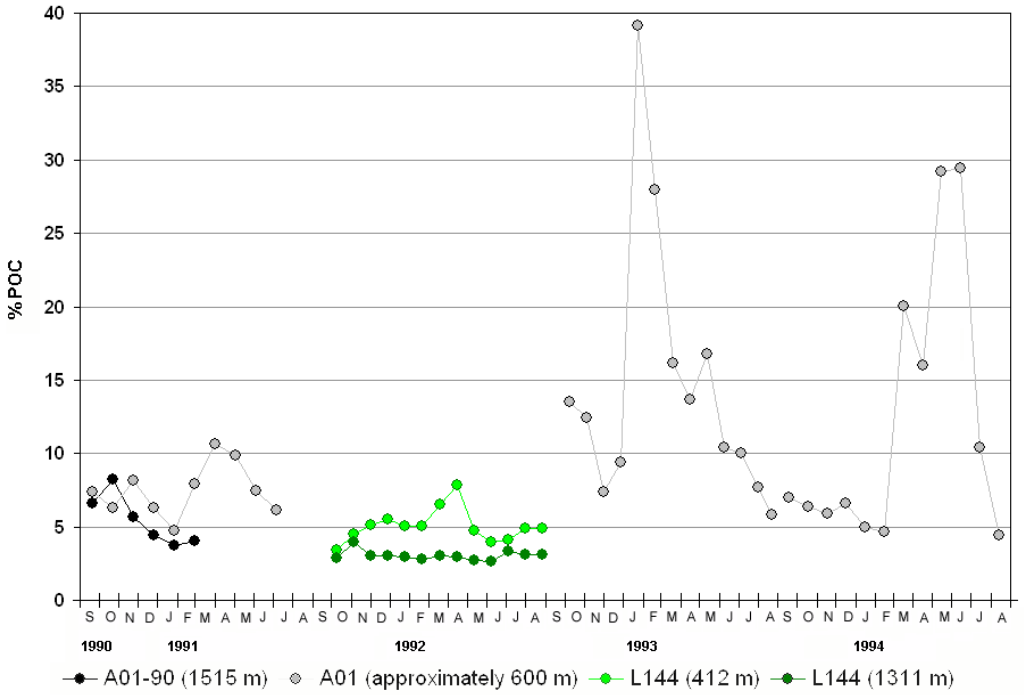

Figure 4-3 Percent organic carbon (%POC) data for stations A01-90 (615 and 1515 m), A01-92 (600m), A01-93 (568 m), and L144.

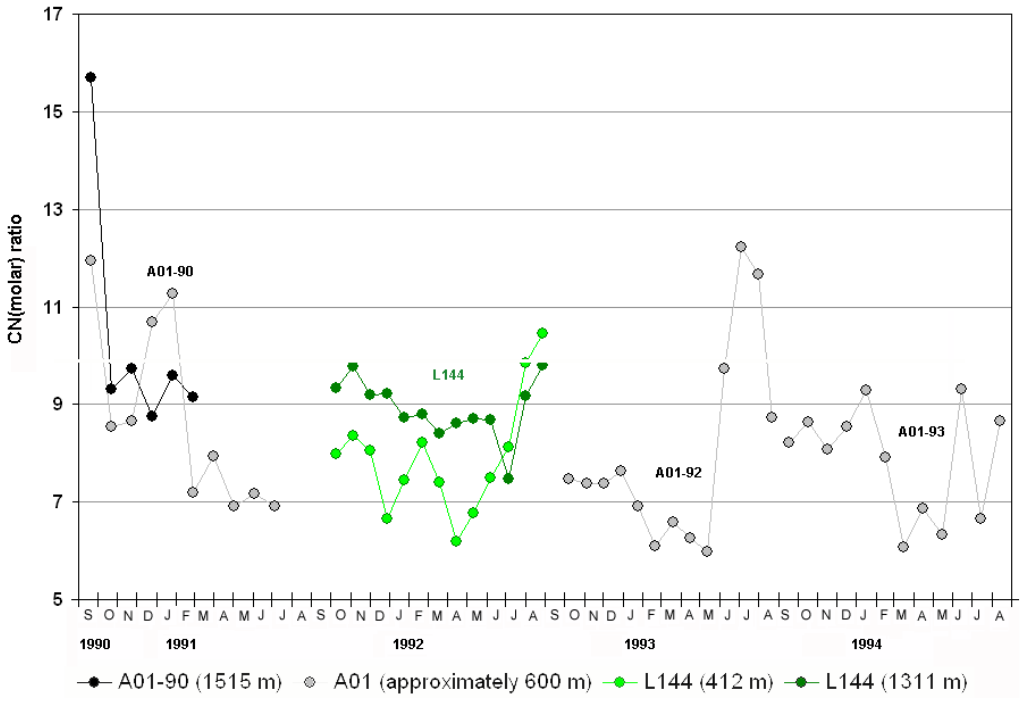

Figure 4-4 Molar ratio of organic carbon to total nitrogen (CN_{molar}) for stations A01-90 (615 and 1515 m), A01-92 (600m), A01-93 (568 m), and L144.

deep trap at A01-90, POC fluxes were low in the fall (< 0.3 mg m^{-2} d^{-1}) and markedly increased from mid-December to mid-March (~ 1to 1.6 mg m^{-2} d^{-1}).

There is a very broad temporal pattern in %POC at 600 m water depth at A01-90 and A01-93. Minima of several per cent occurred in late fall/early winter and maxima (up to ~39 %) in mid-winter to mid-spring (Figure 4.3). A much narrower range of %POC values (3.4 to 7.9%; Figure 4.3) was measured in the L144 samples.

$C:N_{molar}$ ratios (Figure 4.4) ranged from ~6 to ~12 in the A01 traps at ~600 m, and from ~8.7 to nearly 16 in samples from the A01-90 trap at 1515 m depth. $C:N_{molar}$ ratios show a weak negative correlation with %POC and %TN (r = -0.41 and -0.55 respectively) and a weak positive correlation with BIOSI flux and %BIOSI (r = 0.44 and 0.50 respectively), and no correlation with TDW flux, POC flux or TN flux. Very generally, ratios are lowest in the spring (roughly 7 to 9) and highest in the summer (>9, and as high as nearly 16 in September, 1990), the one exception being a maximum in January/February at 600 m depth at A01-90.

The temporal pattern of BIOSI fluxes differs substantially between the A01 deployments (Figure 4.5). There are few BIOSI data for A01-90 but at the 1515 m trap, fluxes are elevated in the winter coinciding with the peaks in POC and TDW flux. At A01-92, very low fluxes in the fall and winter give way to increases in spring/summer and subsequent decreases. At L144, BIOSI fluxes are substantially higher (Figure 4.5) Temporal variability in %BIOSI at A01-93 differs markedly from that at A01-92: highest values occur in mid-winter at A01-93 and are relatively low in the spring/summer period (<4.5%; Figure 4.6).

The CHLA and PHAEO fluxes (Figures 4.7 and 4.8) correlate strongly with each other (r = 0.96) across the data set for site A01. Peaks in CHLA and PHAEO flux coincide with the POC flux peak in late-July/early-August at A01-92, while at A01-93, CHLA and PHAEO fluxes are very low in the spring and summer and elevated in the early fall and during the winter.

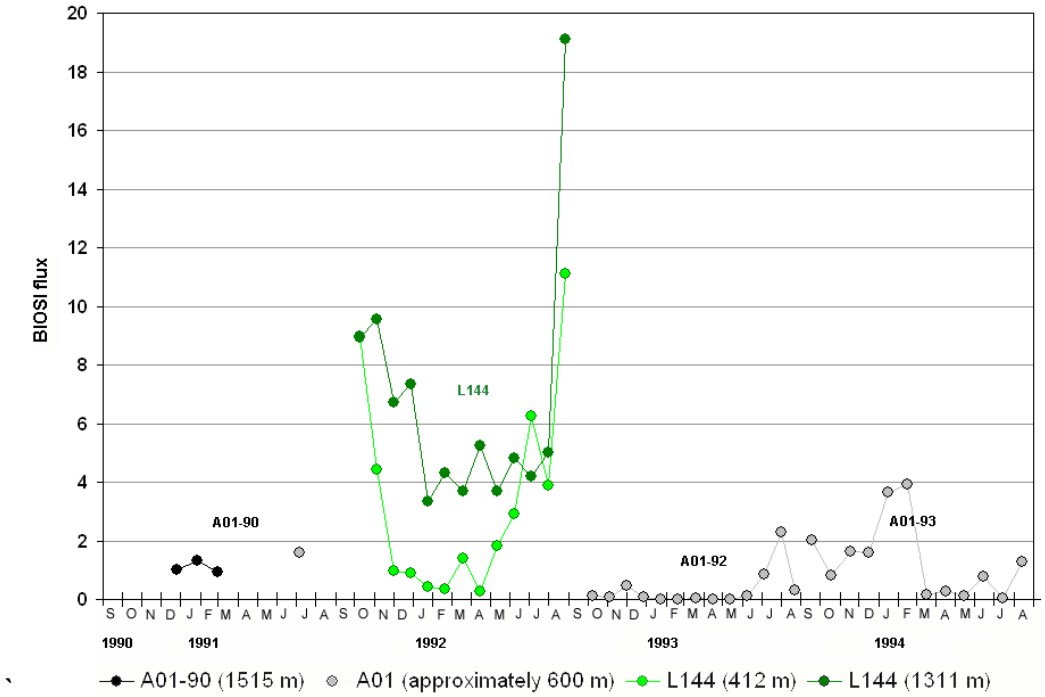

Figure 4-5 Biogenic silica (BIOSI) flux data for stations A01-90 (615 and 1515 m), A01-92 (600m), A01-93 (568 m), and L144. The units for BIOSI flux are mg m^{-2} d^{-1}.

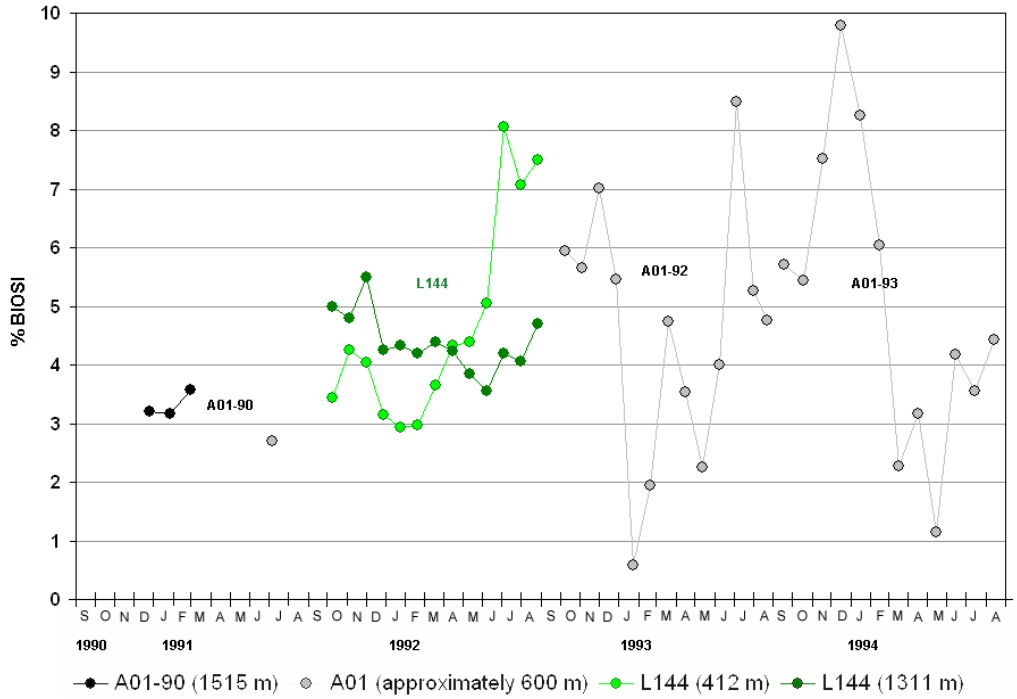

Figure 4-6 Percent biogenic silica (%BIOSI) data for stations A01-90 (615 and 1515 m), A01-92 (600m), A01-93 (568 m), and L144.

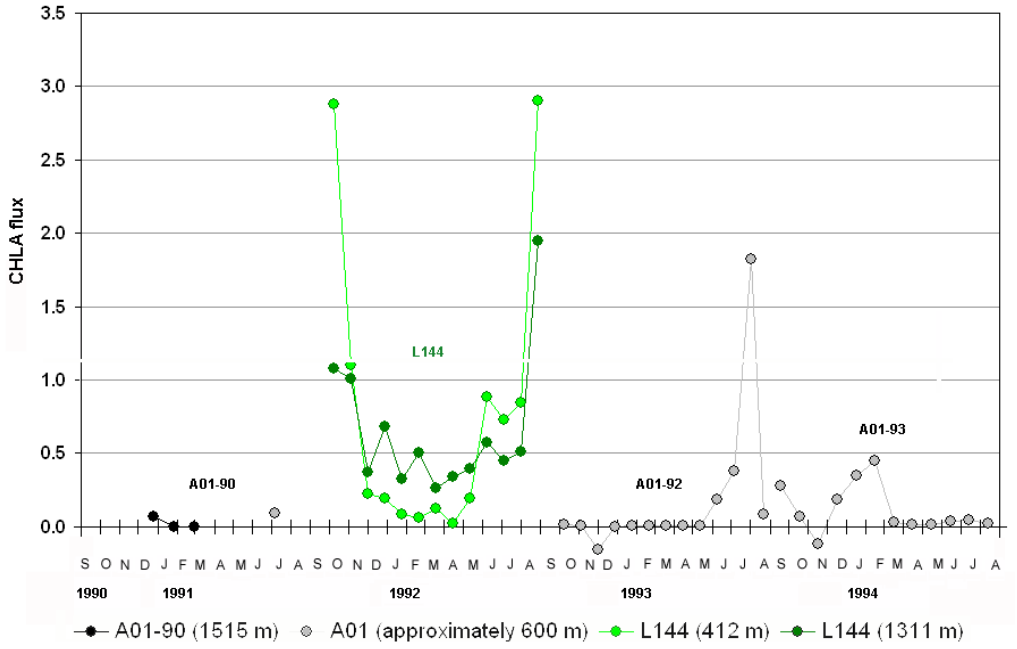

Figure 4-7 Chlorophyll *a* (CHLA) flux data for stations A01-90 (615 and 1515 m), A01-92 (600m), A01-93 (568 m), and L144. The units for CHLA flux are µg m^{-2} d^{-1}.

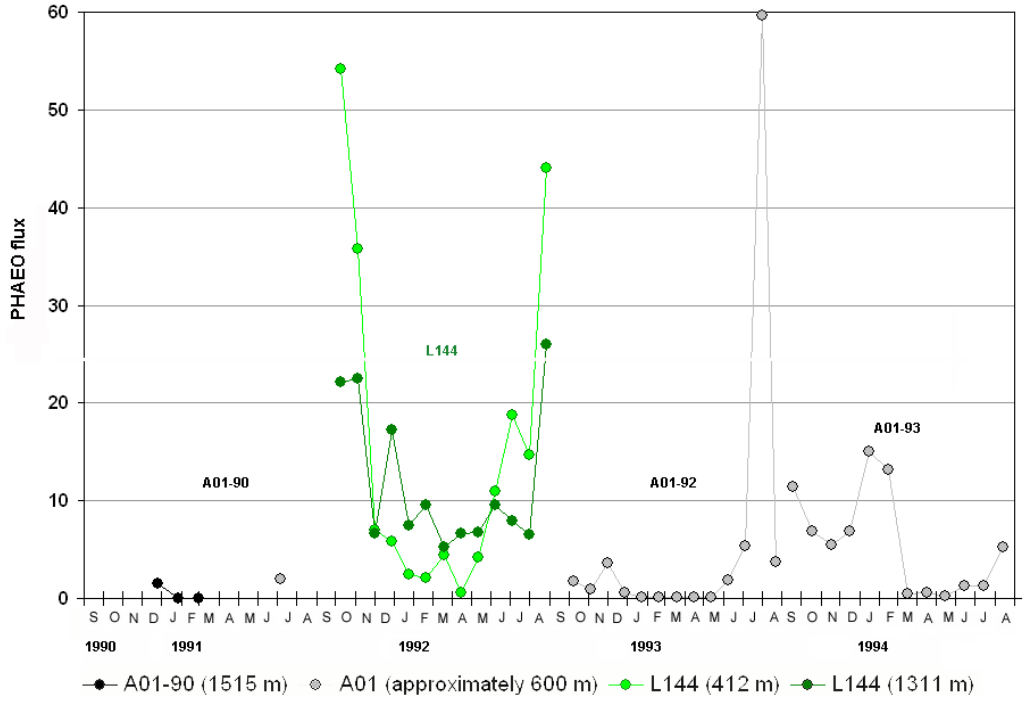

Figure 4-8 Phaeophytin (PHAEO) flux data for stations A01-90 (615 and 1515 m), A01-92 (600m), A01-93 (568 m), and L144. The units for PHAEO flux are µg m^{-2} d^{-1}.

Chapter 5 Annual fluxes and composition

Both terrestrial and marine sources of particulate matter influence annual fluxes and their seasonality at the four mooring sites (Figure 1.1), and the balance between them reflects processes important to shelf-basin exchanges. Toward improving understanding of the system in the particular context of the Beaufort Sea, a method is developed and described in this chapter that allows biogenic and terrigenous components of the sediment trap material to be distinguished.

The Beaufort shelf is highly impacted by the delivery of terrestrial suspended and bedload material from the Mackenzie River and to a lesser extent from coastal erosion (Macdonald et al., 1998). Most riverine matter is delivered to or beyond the shelf via spring flooding of the Mackenzie River, typically between the third week of May and first week of July (O'Brien et al., 2006, HYDAT CD-ROM from the Water Survey of Canada; see Figure 2.4). Coastal erosion from the combined effects of gradual sea level rise, storm surge activity, and disintegration of weakened ice-bonded banks along the shore (Hill et al., 1991) contributes a considerable but lesser amount of terrigenous material to the shelf than does the riverine source. The redistribution and transport of these terrigenous inputs on and to the shelf, slope, and deep basins can be driven by winds (O'Brien et al., 2006, Hill et al., 1991; Giovando and Herlinveaux, 1981) and ocean currents (Giovando and Herlinveaux, 1981; Aagaard, 1984; Carmack, 1998), as well as ice rafting (Eicken et al., 2005), eddy formation (D'Asaro, 1988; Plueddemann et al., 1998; Mathis et al., 2007), and/or density driven currents (Pickart et al., 2004; Aagaard et al., 1985).

Marine biogenic matter in the Arctic is subject to the same modes of redistribution and transport as terrestrial matter, and may derive from primary production associated with polynya formation (Lovejoy et al., 2002) and ice edge retreat (Tremblay et al., 2006; Andreassen and Wassmann, 1998) as well as open-water blooms. The establishment of water column stratification as a result of river input and seasonal ice melt is critically important to primary production in the region (Tremblay et al., 2002; Macdonald and Yu, 2006; Carmack et al., 1989). Other important influences on

production and the settling of biogenic material include nutrient injections to the euphotic zone from rivers or upwelling events (Macdonald et al., 1987), the liberation of ice algae due to seasonal sea ice melt (Horner and Schrader, 1982), the presence of ballasting materials (Passow, 2004), temporal mismatches between primary producers and grazers (Wassmann, 1998), the nature of the ecosystem (Wassmann, 1998), and the intensity of biogenic recycling processes in the water column (Wassmann, 1998).

Size sorting of particles occurs extensively in this area during the transport and redistribution of sediments on the shelf, to the slope and rise, and eventually to the deep basin (Pelletier, 1975), and is influenced by the differential densities of organic versus lithogenic particles (Goñi, et al., 2000; Yunker et al., 1995). Moreover, biogeochemical transformations of biogenic material occur in the cryosphere, the pelagic zone, and via the activities of the benthos. Flocculation of particles within the Mackenzie Estuary at the interface between fresh- and seawater (Droppo et al., 1998) as well as the formation of marine snow (Sarthou et al., 2005, Ashjian et al., 2005) all play a role in influencing the transport of suspended sediments in this area. In addition, differential densities of material such as terrestrial organic debris versus lithogenic material result in differential extent of transport on the shelf (Goñi, et al., 2000; Yunker et al., 1995).

Previous work using organic biomarkers has shown that 50 % to 80 % of the POC in the Beaufort shelf surface sediments is of terrigenous origin, and was delivered to the shelf by the Mackenzie River in a highly degraded form (Goñi et al., 2000; Yunker et al., 1995). Such material is also old and highly altered (Goñi et al., 2005); > 60 % of the organic carbon in riverine SPM and shelf sediments is highly degraded and ancient (Goñi et al., 2005). Yunker et al., (1995) showed that there is a general similarity in organic composition between the shelf sediments and the Mackenzie River sediment load, and that riverine terrestrial organic material is transported on particles.

Suspended silts and clays originating from the Mackenzie River are ubiquitous in the Mackenzie River/Beaufort shelf system and dominate the benthos, water-column nepheloid layers, and the spreading river plume (O'Brien et al., 2006; Bornhold, 1975). It is reasonable to assume that there is interaction between the transport of this massive

Table 5-1 Estimated annual fluxes (g m-2 a-1) (TDW, POC, TN, and BIOSI) and composition (CNmolar ratio, % POC, % TN, and % BIOSI).

Station	Trap depth	Period of estimation	# days	TDW	POC	TN	BIOSI	CN_{molar}	POC	TN	BIOSI
	m				$g\ m^{-2}\ a^{-1}$			ratio	%	%	%
SS-5	199	spring91 to spring92	365	26.47	2.07	0.25	5.98	9.46	7.81	0.96	22.59
SS-5	349	spring91 to spring92	365	37.20	2.36	0.29	5.47	9.38	6.35	0.79	14.69
SS-5	499	spring91 to spring92	365	44.71	2.64	0.31	6.89	9.90	5.90	0.70	15.41
SS-5	199	fall 91- fall 92	365	17.09	1.02	0.16	0.62	7.28	6.00	0.96	3.62
SS-5	349	fall 91- fall 92	365	31.91	1.46	0.21	1.13	8.08	4.58	0.66	3.54
SS-5	499	fall 91- fall 92	365	45.14	1.63	0.23	1.42	8.36	3.61	0.50	3.14
L144	412	fall 91 to fall 92	365	26.31	1.14	0.16	1.32	8.33	4.33	0.61	5.02
L144	1311	fall 91 to fall 92	365	56.04	1.73	0.22	2.52	9.15	3.08	0.39	4.49
AM1-92	290	fall 92 to fall 93	365	68.55	3.84	0.40	2.14	11.08	5.60	0.59	3.12
AM1-92	490	fall 92 to fall 93	365	128.65	6.87	0.82	9.44	9.78	5.34	0.64	7.34
A01-90	615	fall 90 to fall 91	365	4.20	0.27	0.04	no data	7.30	6.38	1.02	no data
A01-92	600	fall 92 to fall 93	365	2.08	0.18	0.02	0.12	9.78	8.80	1.05	5.68
A01-93	568	fall 93 to fall 94	365	8.29	0.71	0.10	0.50	7.98	8.61	1.26	5.98

Table 5-2 Seasonal fluxes. Seasons are defined as spring/summer (early May to the end of August) and fall/winter (early September to late April).

station	trap depth	% in summer TDW	% in fall/winter TDW	% in summer POC	% in fall/winter POC	% in summer TN	% in fall/winter TN	% in summer BIOSI	% in fall/winter BIOSI
SS-5	199 m	91.5	8.5	89.0	11.0	84.0	16.0	98.6	1.4
SS-5	349 m	71.1	28.9	74.9	25.1	70.6	29.4	90.8	9.2
SS-5	499 m	81.1	18.9	81.9	18.1	78.9	21.1	91.3	8.7
AM1-92	290 m	26.1	73.9	51.1	48.9	33.4	66.6	46.8	53.2
AM1-92	490 m	53.0	47.0	66.9	33.1	62.4	37.6	77.2	22.8
L144	412 m	39.0	61.0	41.3	58.7	38.6	61.4	53.2	46.8
L144	1311	41.5	58.5	40.5	59.5	40.9	59.1	39.5	60.5
A01-90	615 m	87.2	12.8	83.4	16.6	87.2	12.8	-	-
A01-92	600 m	77.7	22.3	71.8	28.1	61.9	38.1	78.0	22.0
A01-93	568 m	41.4	58.6	42.1	57.9	41.4	58.6	15.1	84.9

terrigenous input and the marine production, but the nature of that interaction is not yet clear.

In such a complex river-dominated system, distinguishing the relative proportions of allochthonous and autochthonous contributions to export fluxes is challenging but essential to understanding the ultimate fate of carbon in the system. Important questions remain. Is this arctic shelf/slope/basin unit a location of carbon sequestration? Which physical factors control the balance between a system acting as a source or a sink for carbon? What time frames of change are important to this balance (e.g. will anticipated climate warming spell catastrophic or more gradual changes to this balance?). Toward answering such questions, this chapter offers a method for separating contributions from terrigenous and biogenic sources, important because of the high impact of terrigenous material on the Beaufort Shelf. The following chapter discusses and interprets fluxes at each mooring site in terms of biogenic and terrigenous contributions and physical forcings within the Beaufort-Mackenzie system.

5.2 Annual flux estimates of TDW, POC, TN, and BIOSI

Annual fluxes at the continental slope (SS-5 and AM1-92) and base of the slope (L144) sites (Table 5.1, Figure 5.1) were comparable to ranges observed previously (20 - 140 g m^{-2}; O'Brien et al., 2006; see Figures 4b and 6). In Canada Basin however, annual fluxes (~600 m traps) were significantly lower (2.0 – 8.3 g m^{-2}; Table 5.1; Figure 5.1) and the winter fluxes at 1515 m exceeded the fluxes during the same period at the 615 m depth (Figure 4.1). Annual POC fluxes measured in this study (~0.3 - 7 g m^{-2} m) fall within ranges published for other Arctic regions (0.07 to 13.8 g m^{-2}; Forest et al., 2007; Fahl and Nöthig, 2007, Wassmann et al., 2004).

Estimates made to fill gaps in the data introduce little uncertainty in most cases because the periods of missing data were short (Table 5.1). In the case of the spring/summer deployment at station SS-5, estimates for the fall and winter period were computed by averaging early fall and late winter fluxes and in this case, the uncertainty is much larger, but the results are comparable with other mid-winter fluxes in the area (O'Brien et al., 2006).

Table 5-3 A) Integrated terrigenous and biogenic fluxes (g m-2) and B) Percent terrigenous and biogenic fractions of total dry weight (TDW). Note that for site SS-5, the130 day period represents the spring and summer of 1991 and the 381 day period represents the single interval collections from the fall of 1992 to the fall of 1993. Also note that due to small sample sizes for site A01, the total biogenic fraction was estimated using total carbon values and no distinction is made for POMbiogenic and POMrefractory.

A) Integrated fluxes of terrigenous and biogenic fractions

				TERRIGENOUS			BIOGENIC			
Station	Depth m	Duration days	Total flux g m^{-2}	Total terrigenous fraction g m^{-2}	Inorganic (clays and carbonates) g m^{-2}	$POM_{refractory}$ g m^{-2}	Total biogenic fraction g m^{-2}	$POM_{biogenic}$ g m^{-2}	$OPAL_{new}$ g m^{-2}	$OPAL_{old}$ g m^{-2}
SS-5	199	130	24.21	6.78	6.67	0.10	17.42	3.28	13.99	0.15
	349	130	26.43	11.53	11.33	0.20	14.90	3.00	11.60	0.30
	499	130	36.25	17.67	17.34	0.33	18.58	3.54	14.54	0.50
SS-5	199	381	17.83	14.63	14.41	0.23	3.20	1.65	1.21	0.34
	349	381	33.30	28.35	27.87	0.47	4.95	2.12	2.12	0.70
	499	381	47.10	41.64	40.82	0.83	5.46	1.92	2.32	1.22
AM1-92	290	365	68.55	57.81	56.78	1.02	10.75	5.61	3.61	1.52
AM1-92	490	365	128.65	95.77	94.05	1.72	32.88	10.23	20.11	2.55
L144	412	365	26.31	21.60	21.20	0.39	4.70	1.53	2.58	0.59
L144	1312	365	56.04	48.09	47.22	0.87	7.95	1.90	4.76	1.29
A01-92	600	339	1.97	1.38			0.60	0.33	0.27	
A01-93	568	360	8.13	5.65			2.49	1.32	1.17	

B) Percent of total flux for terrigenous and biogenic fractions

				TERRIGENOUS			BIOGENIC			
Station	Depth m	Duration days	Total flux g m^{-2}	Total terrigenous fraction % of total	Inorganic (clays and carbonates) % of total	$POM_{refractory}$ % of total	Total biogenic fraction % of total	$POM_{biogenic}$ % of total	$OPAL_{new}$ % of total	$OPAL_{old}$ % of total
SS-5	199	130	24.21	27.99	27.56	0.43	71.95	13.54	57.80	0.61
	349	130	26.43	43.63	42.86	0.77	56.35	11.33	43.87	1.15
	499	130	36.25	48.75	47.83	0.92	51.23	9.75	40.11	1.37
SS-5	199	381	17.83	82.08	80.80	1.28	17.92	9.24	6.77	1.91
	349	381	33.30	85.14	83.71	1.42	14.87	6.37	6.38	2.11
	499	381	47.10	88.41	86.65	1.75	11.59	4.07	4.93	2.60
AM1-92	290	365	68.55	84.32	82.83	1.49	15.68	8.19	5.27	2.22
AM1-92	490	365	128.65	74.44	73.11	1.33	25.56	7.95	15.63	1.98
L144	412	365	26.31	82.09	80.61	1.49	17.87	5.83	9.82	2.22
L144	1312	365	56.04	85.82	84.27	1.55	14.18	3.40	8.49	2.30
A01-92	600	339	1.97	69.70			30.30	16.56	13.72	
A01-93	568	360	8.13	69.40			30.60	16.19	14.39	

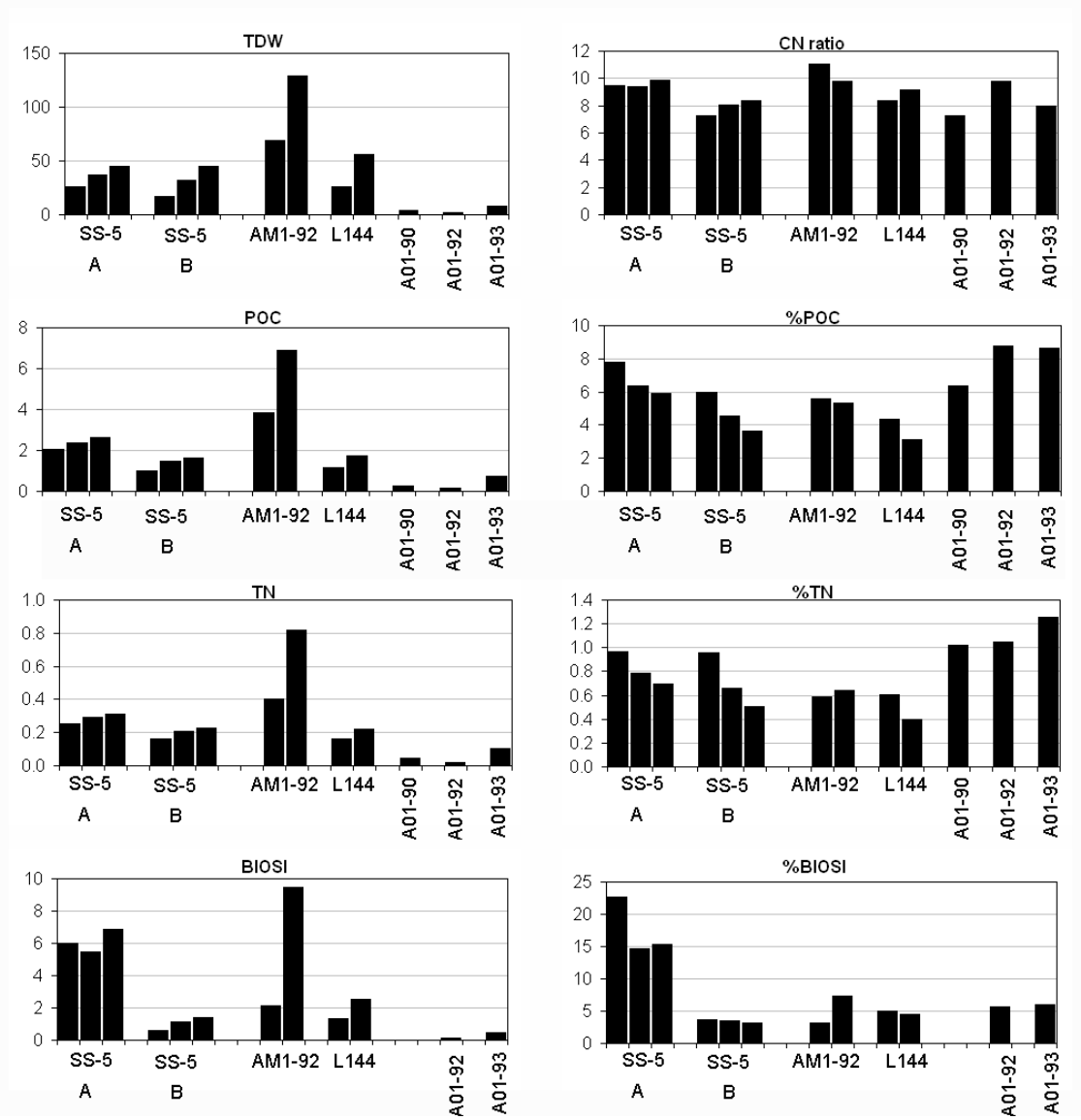

Figure 5-1 Estimated annual fluxes of TDW, POC, TN, and BIOSI (units are g m^{-2} a^{-1}) are shown in the left-hand plots. Estimated values for annual CNmolar ratio, % POC, %TN, and %BIOSI are shown in the right-hand plots. Data are for stations SS-5 (trap depths 199, 349, and 499 m), AM1-92 (trap depths 290 and 490 m), L144 (trap depths 412 and 1311 m), and Canada Basin stations A01-90, A01-92, and A01-93 at ~600 m. The two estimates shown for SS-5 are as follows: A. estimate from the 130-day spring/summer period of 1991with the fall/winter portion estimated as the average of the early fall and the late winter fluxes and B. estimate from the fall 1991 to fall 1992 single-interval period. The BIOSI data at SS-5 clearly show that the B interval did not have the large diatom bloom that was evident in A.

a)

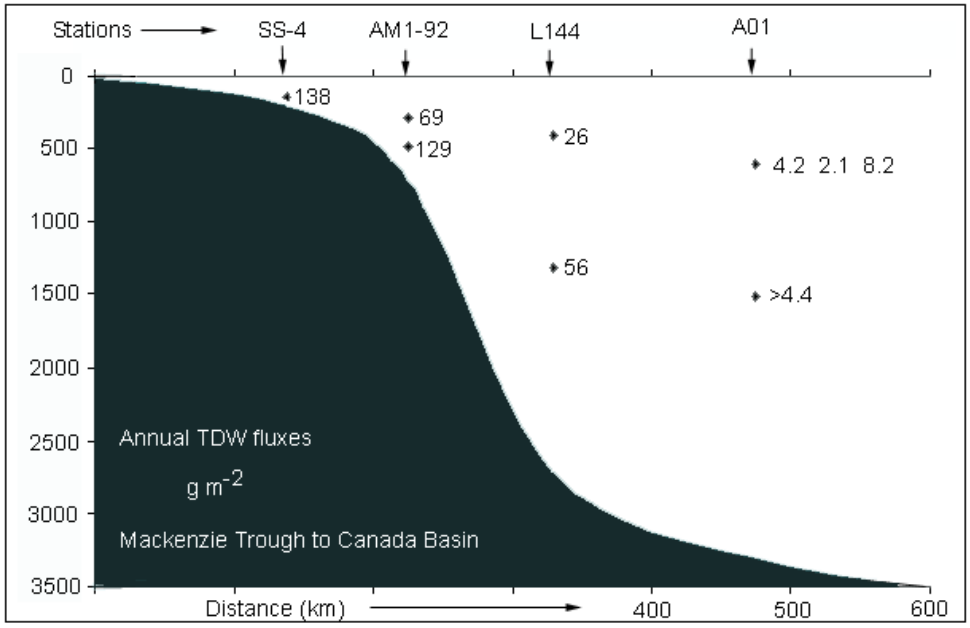

b)

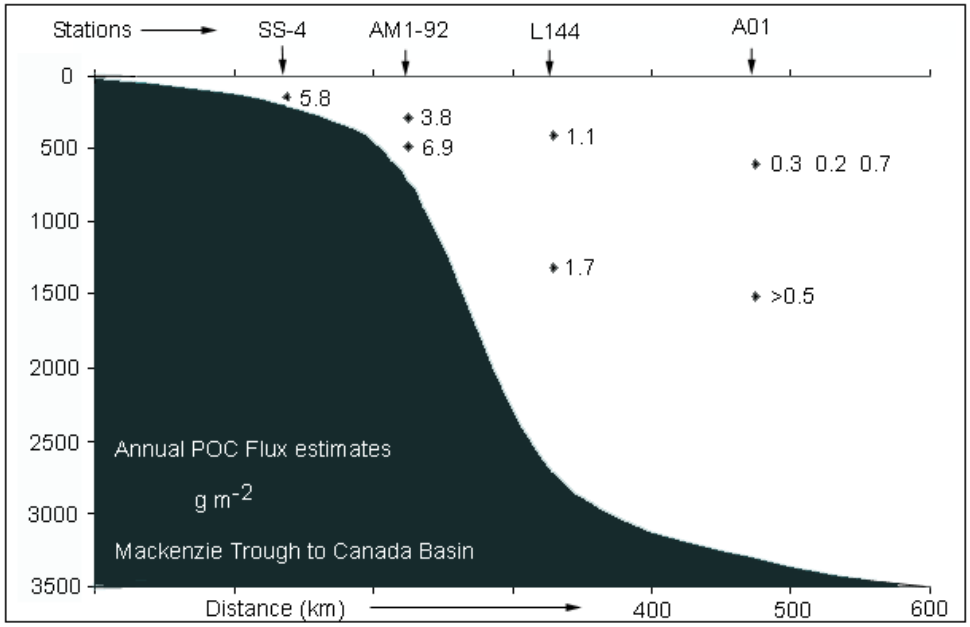

Figure 5-2 Vertical transects from Mackenzie Trough to Canada Basin representing the annual fluxes (g m-2) of a) total dry weight (TDW); b) particulate organic carbon (POC); c) and biogenic silica (BIOSI). The figure includes station SS-4 (from O'Brien et al. 2006) and stations AM1-92, L144, and A01 from this study (for map see Figure 1.1). See Table 5.1 for annual fluxes of total nitrogen (TN). Note that c) is on following page.

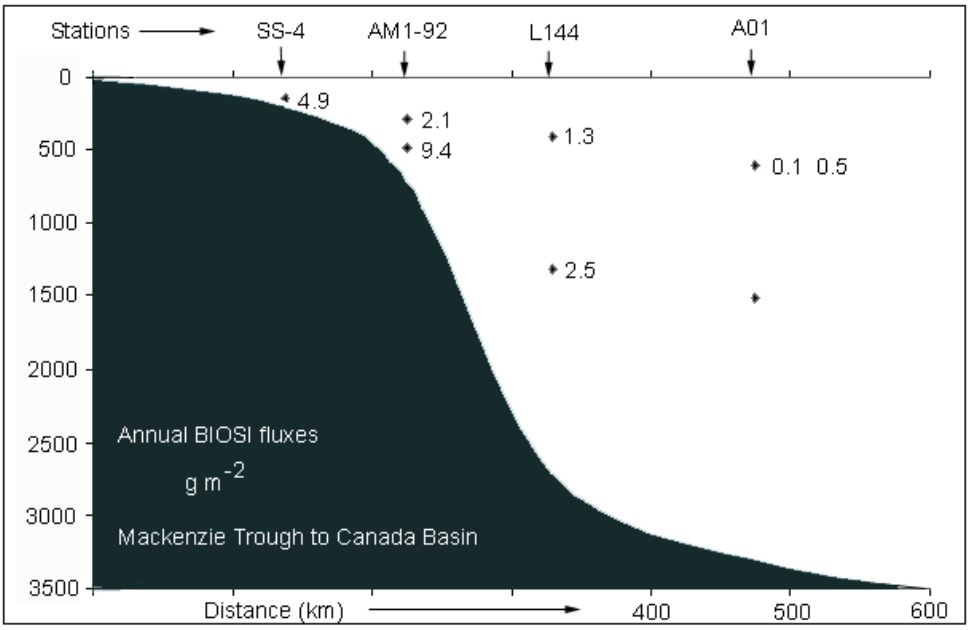

Continuation of Figure 5.2 (5-2 c)

Annual fluxes of TDW, POC, TN, and BIOSI clearly show variations with location, increases with depth, and decreases with distance offshore (Figures 5.1 and 5.2). The fluxes are consistently highest in the deepest traps indicating an increasing importance of lateral transport of material with depth. In terms of the mass of material collected, the distance of the trap off the bottom may be a more important consideration than the distance of the trap from the ocean surface. A vertical transect showing fluxes from Mackenzie Trough to Canada Basin (Figures 5.2a and 5.2b; Figure 2.2) implies the occurrence of lateral transport in mid-water. Nepheloid layers near the bottom may also play a significant role in transporting particulate matter seaward, but the available data do not allow that hypothesis to be appropriately tested. Such considerations raise the questions as to how to estimate the fraction of the material that has undergone lateral transport, and what are the expected extent and characteristics of lateral transport into the deep basin?

In both this study and the one described by O'Brien et al. (2006), the Mackenzie Trough location has higher annual TDW and POC fluxes than the adjacent slope sites suggesting that this is an area of enhanced export of material from the shelf to the deep basin. There are a number of factors important to this apparent enhancement. First, the

bulk of Mackenzie River inputs of freshwater and suspended particulate material are injected onto the shelf on the west side of Richards Island at the head of Mackenzie Trough (Carson et al., 1998, 1999; Figure 2.2). Second, local topography suggests that transport of suspended sediments and dense water might be channelled, leading material directly offshore. Third, upwelling and river inputs both supply nutrients for primary production, supporting enhanced primary and export production (Williams et al., 2006; Carmack and Kulikov, 1998; Macdonald et al., 1987).

5.3 Seasonality in fluxes

Defining seasons in the Arctic is difficult due to large inter-annual extremes with respect to ice coverage and other physical parameters. For the purposes of comparison, two seasons are defined here, fall/winter between early September and late April, and spring/summer from early-May to the end of August. For each site, the closest intervals from the collection periods define the start and end of the seasonal periods.

Percent seasonal fluxes (of TDW, POC, TN, and BIOSI; see Figure 5.3 and Table 5.2) vary between stations, and in some cases with the depth of the traps. For station SS-5 (assuming that the estimate of the winter portion of the collection is representative), 70 to 98% of TDW, POC, TN, and BIOSI is delivered in the 1991 spring/summer season as compared to 26 to 77% spring/summer delivery for stations AM1-92 and L144 (Figure 5.3, Table 5.2). The high proportional delivery in summer at SS-5 is due to the large diatom bloom in 1991; the following spring, a bloom either did not occur at this site or was much smaller. Similarly, the highest percentage summer delivery of BIOSI at AM1-92 (77%) is attributable to a large diatom bloom.

About 40% of the annual flux of TDW, POC, and TN was delivered at station L144 in spring/summer, and this proportion was approximately the same at both the trap depths. In contrast, more BIOSI was intercepted at 412 m (~53%) than at 1311 m (~40%). The 60% delivery of the TDW, POC, and TN in winter under conditions of complete ice cover and severe light limitation suggests that the bulk of the winter material is laterally exported from the shelf. It is likely that, in addition to refractory carbon associated with the inorganic terrigenous fraction, the organic matter consisted of production from the past summer or from recent heterotrophic production. The 40 % of

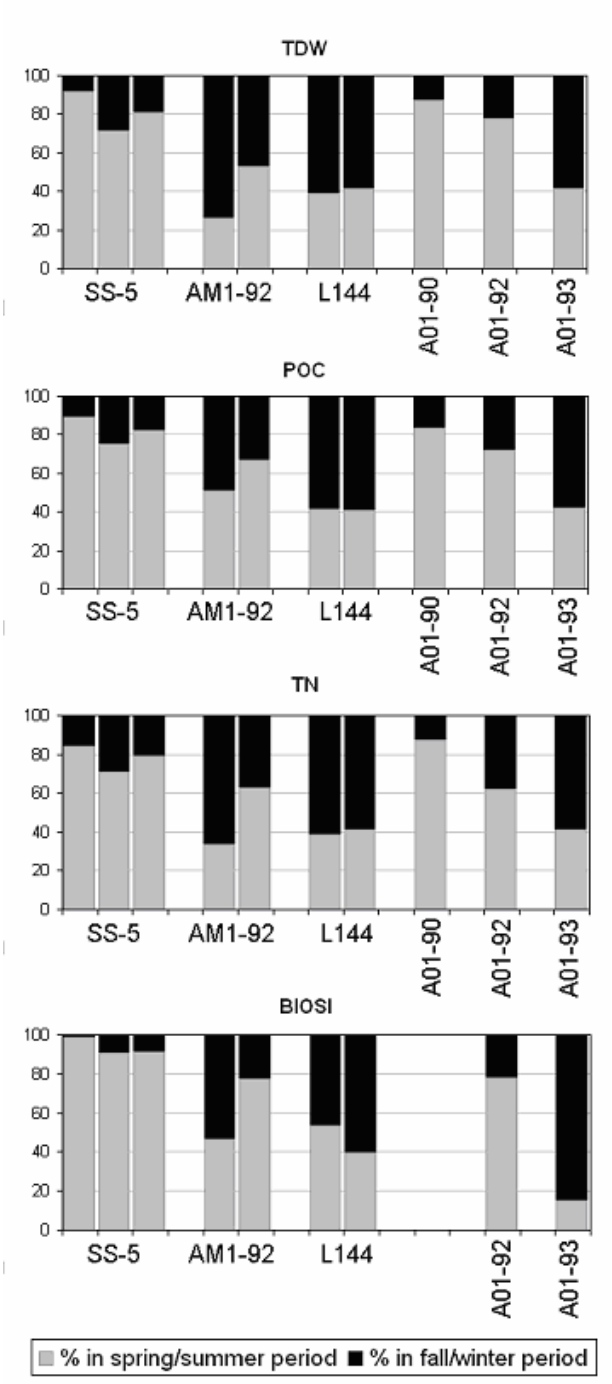

Figure 5-3 Seasonal delivery of material to the traps showing the percent of total annual fluxes of TDW, POC, TN, and BIOSI delivered in the spring/summer period vs. the fall/winter period. Data are for stations SS-5 (199, 349, and 499 m), AM1-92 (290 and 490 m), L144 (412 and 1311 m), and Canada Basin stations A01-90, A01-92, and A01-93 (at ~600 m). See Table 5.2.

material delivered in summer is more likely to include a portion of vertically exported new production along with laterally exported shelf material.

At the shallow trap at station AM1-92 (290 m below surface), 26, 51, 33 and 47% of the annual fluxes of TDW, POC, TN, and BIOSI respectively were delivered in spring/summer. In the same season at 490 m subsurface, 53, 67, 62, and 77% respectively were intercepted. Notably in summer at 290 m, only about one quarter of the total annual TDW was intercepted while about half of the total annual POC and BIOSI (51 % and 47 % respectively) was collected. Interestingly, only 33 % of the total annual TN was collected in the summer at 290 m.

At the ~600 m traps in Canada Basin at the A01 site, the percent split of annual fluxes between spring/summer and fall/winter periods varied markedly between the A01-92 and the A01-93 collections (Table 5.2 and Figure 5.3). Over 60% of the annual flux of TDW, POC, and TN was collected in the summer period at A01-92 compared to ~40% at A01-93. Nearly 80% of the annual flux of BIOSI was collected in the summer period at A01-92 but only 15 % at A01-93.

5.4 Differentiating the terrigenous and biogenic fractions

The discussion of carbon by source is fraught with difficulties of definition, and it is important to keep in mind the specific definitions and their inherent assumptions. While the terrestrial organic carbon delivered to the shelf by the Mackenzie River is biogenic in origin, a large portion of it is old refractory carbon which is resistant to recycling and therefore, has a tendency to be preserved in the sediments. While not all of the terrestrial carbon is refractory, the term terrestrial carbon comes with the assumption that the bulk of this carbon pool is old and refractory. Likewise, the term biogenic as utilized in this document comes with the assumption that the bulk of the more recent aquatic primary production is a more labile, relatively easily recycled carbon pool. This is also not strictly correct as there are refractory compounds preserved in the sediments that originated from algal production (see Goñi et al., 2005). The important thing to keep in mind is that the specific operational definitions are based on analytical methodologies and, while they provide a convenient first order approximation of the more refractory carbon with a terrestrial “biogenic” source (the terrigenous carbon) and the more labile

carbon with an aquatic "biogenic" source (the biogenic carbon), they do not perfectly separate the two sources.

The total biogenic fraction ($BIOG_{total}$) is defined here as the sum of the total opaline silica ($OPAL_{total}$) and the autochthonous biogenic portion ($POM_{biogenic}$) of the total organic matter (POM_{total}), which is the sum of the autochthonous biogenic portion ($POM_{biogenic}$) and the refractory organic matter ($POM_{refractory}$). Refractory organic matter is introduced into the water column by sediment resuspension and river input and is thought to have a close association with fine clay particles. It may have both terrigenous and marine precursors but biomarker evidence suggests that the source is mainly from allochthonous inputs from the Mackenzie River (Yunker et al., 1991, 1995). No attempt is made here to distinguish between marine and terrigenous sources of refractory material. The $OPAL_{total}$ content consists, in varying proportions of both recently produced opaline planktonic tests ($OPAL_{new}$) as well as the fragments of older opaline tests ($OPAL_{old}$) previously deposited, reworked, and then resuspended by various means from bottom sediments.

The allochthonous terrigenous fraction ($TERR_{total}$) is defined here as the sum of inorganic components ($TERR_{inorganic + CaCO3}$) and $POM_{refractory}$. $TERR_{inorganic + CaCO3}$ consists of clays, other minerals, and (Ca, Mg) carbonates. The latter are derived from the biogenic production of calcium carbonate shells (e.g. by foraminifera and/or coccolithophoridae), inorganic precipitation, and/or dolomite and limestone rock fragments. Ideally, the fraction represented by $CaCO_3$ would be identified and an estimate made as to what portion is biogenic but unfortunately, the data to do this are not available. As seen in scanning electron microscope (SEM) photographs, foraminifera are present only as a minor contribution so this omission is not likely to be significant. In addition, no coccolithophorids were observed in the SEM samples. Therefore, the contribution by newly-produced marine carbonate shells is likely to be insignificant. Carbonates in Mackenzie Shelf surface sediments are present mainly as dolomite (Pelletier, 1984) and occur in higher concentrations inshore (~16 - 27% by weight) versus ~8 - 16% offshore.

The relationships between the components described above are summarized as follows:

$$TDW = BIOG_{total} + TERR_{total}$$
$$BIOG_{total} = POM_{biogenic} + OPAL_{total}$$
$$OPAL_{total} = OPAL_{new} + OPAL_{old}$$
$$POM_{total} = POM_{biogenic} + POM_{refractory}$$
$$TERR_{total} = TERR_{inorganic+ CaCO3} + POM_{refractory}$$

Finally, the percent terrigenous fraction (% $TERR_{total}$) was determined as 100 minus the sum of % POM_{biog} and % $OPAL_{total}$. Note again that with the available data, it is not possible to separate % $TERR_{inorganic}$ from the % $CaCO_3$.

$$100\ \% = \%\ TERR_{total} + \%\ BIOG_{total}$$
$$\%\ TERR_{total} = 100\ \% - [\%\ POM_{biog} + \%\ OPAL_{total}]$$
$$= (\%\ TERR_{inorganic+CaCO3}) + \%\ POM_{refractory}$$
$$100\ \% = [\%\ TERR_{inorganic+CaCO3} + \%\ POM_{refractory}] + [\%\ POM_{biog} + \%\ OPAL_{new}]$$

5.4.1 Estimation of biogenic and refractory carbon reservoirs

The measured % POC_{total} in the trap material is discriminated into biogenic and refractory carbon following O'Brien et al. (2006). Briefly, this method uses the assumption of a constant ratio between the refractory carbon content ($POC_{refractory}$) and the aluminum content in the trap material. While refractory carbon can have both terrigenous and marine sources, biomarker measurements made on Mackenzie Shelf surface and suspended sediments demonstrate that the source is predominantly terrigenous (Gõni et al., 2000; Yunker et al., 1991, 1995). For greater clarity, the terminology for the refractory carbon and refractory organic matter in this study is $POC_{refractory}$ and $POM_{refractory}$ instead of POC_{terr} and POM_{terr} as was used in O'Brien et al. (2006). A ratio % $POC_{refractory}$:% Al of 0.16 was used to calculate the $POC_{refractory}$ content in a sample (% $POC_{refractory}$ = 0.16 x % Al) and is based on an investigation of aluminum contents of surface sediments at the Mackenzie Shelf edge (data from Pelletier, 1984; O'Brien et al., 2006). Regardless of the delivery process, this ratio is assumed to be representative of the relationship between aluminum and refractory carbon in sediment

delivered to the traps, an association based on evidence that refractory organic matter is closely associated with the inorganic matrix of fine clay sediments (Hedges and Keil, 1995). It is further assumed that the proportions of this association do not change significantly during transport in the short time frame represented by this study. The terrigenous fraction in the traps could derive from melting ice cover, from the spread of the river plume, and/or from the remobilization of bottom sediments due to the influence of winds, ice keel gouging, bioturbation, and/or currents.

The biogenic fraction (% $POC_{biogenic}$) is determined as the difference between the % POC_{total} and the % $POC_{refractory}$. The corresponding refractory and biogenic organic carbon fluxes are calculated as the corresponding proportions of the TDW flux. In cases where there are no aluminum data due to small sample size, the biogenic and refractory carbon fractions are estimated by using the average of the % $POC_{refractory}$ in the $TERR_{total}$ fraction for each trap, as described more fully below.

Percent $POC_{biogenic}$ and % $POC_{refractory}$ data are converted to particulate organic matter (POM) by multiplying by conversion factors representative of the POM:C ratios for the respective reservoirs. For the biogenic organic matter, a conversion factor of 1.87 (POM:C) is used. This is based on a mean algal elemental composition of $C_{106}H_{175}O_{42}N_{16}P$ as proposed by Anderson (1995). For the refractory terrigenous carbon, a conversion factor of 1.22 is used and this value was chosen to represent Kerogen Type III that originates from terrestrial plant matter lacking in lipids or waxy matter, and which has formed from cellulose, lignin, terpenes, and phenolic compounds. This material is complex and has a variable composition with an H:C ratio < 1 and an O:C ratio that ranges from 0.03 to 0.3 (Vandenbroucke and Largeau, 2007; see Figure 29 on p. 773 and Figure 32 on p.780). Using H:C ratios (atomic) from 0.5 to 1 and O:C ratios (atomic) from 0.03 to 0.3 yields POM:C ratios (by weight) from 0.96 to 1.48. The average of these two values (1.22) was chosen here to convert the % $POC_{refractory}$ to % $POM_{refractory.}$ This is a rough approximation only but given that kerogen has a complex nature and a variable composition, and contains elements besides hydrogen and carbon (notably sulphur and nitrogen), further refinement was not possible.

For very small samples where aluminum analysis was not possible, an alternate method of estimating $POC_{refractory}$ and $POC_{biogenic}$ was used. For each trap, the average

percent of terrigenous organic matter in the total terrigenous fraction ($TERR_{total}$) was calculated for samples where aluminum measurements were available. These averages were then used to represent of the expected percent terrigenous organic matter in the total terrigenous fraction ($TERR_{total}$) at a particular depth. In turn, these were used to calculate the $POM_{refractory}$ flux for samples where aluminum data is not available, and the % $POM_{refractory}$ of the TDW (% $POM_{refractory}$ = [$POM_{refractory}$ flux] / [TDW flux] *100). In these cases, the % $POC_{refractory}$ of the TDW is determined by dividing by the % $POM_{refractory}$ of the TDW by 1.22. The % $POC_{biogenic}$ is then calculated by the difference between the % POC_{total} and the calculated % $POC_{refractory}$.

Finally, the % $POM_{biogenic}$ was calculated by multiplying % $POC_{biogenic}$ by the factor 1.87 as described above, and the $POM_{biogenic}$ flux was computed as the product [% $POM_{biogenic}$/100] * TDW flux. Appendix 3 summarizes the results for the average % $POM_{refractory}$ and % $POC_{refractory}$ in $TERR_{inorganic + CaCO3}$. Given the assumptions employed, the % $POC_{refractory}$ results (range of 1.27 to 1.56 %) compare well with the percent organic content of surface sediments from the shelf and slope area (range of 1.0 to 1.3 %) (Pelletier et al., 1975).

5.4.2 Estimation of newly produced and "old" biogenic silica

It is challenging but important to distinguish between biogenic silica newly produced within a given year and older biogenic silica previously deposited, reworked, and subsequently resuspended by various means along with bottom sediments. It is postulated here that the transport and settling of "new" diatoms may be important in the transfer of nitrogen, carbon, and silica to the deep Arctic basins, as it is in other oceans. Also, it is expected that the ratios BIOSI:POC and BIOSI:TN will differ between recently settled diatoms and those that have been reworked by benthic organisms and are resuspended as finer, less carbon-rich fragments of diatom tests. While recognizing that this is a difficult distinction to make precisely, a first order estimation is presented here. It is assumed that biogenic silica originating from new production in a given year either settles directly from the surface or is remobilized (i.e., resuspended and transported) after sinking to the bottom. Once at the bottom, the newly deposited diatom-rich particles are likely to spend some time as a loose flocculated layer at the sediment surface. Such material is relatively easily resuspended by bottom currents (Walsh et al., 1991;

Thomsen, 1999). In addition, the newly settled material rich in biogenic silica may resist compaction and incorporation into the sediment surface for a period of time, especially where bottom currents are high (Thomsen, 1999). Older biogenic silica which has become more solidly incorporated in the surface sediments will likely have been reworked by micro- and macrobenthos, and can be expected to be transported in resuspension events along with the surface sediments.

The concept used to distinguish between the newly produced and the older biogenic silica is essentially the same as was used for estimating the portion of POC that is from a refractory, largely terrigenous source. Data for biogenic silica contents of surface sediments from sediment cores close to the mooring sites were used to represent the older, re-worked biogenic silica that would resuspend along with the terrigenous inorganic fraction (data from Gobeil et al., 1991). The biogenic silica content of the surface sediments of five cores had a narrow range between 0.81 to 1.10 wt. % BIOSI (1.94 to 2.64 wt. % OPAL), and the range including the down-core data was 0.51 to 1.15 % BIOSI (1.22 to 2.76 % OPAL). For the estimates here, the BIOSI core-top data for the three cores closest to the SS-5, L144, and AM1-92 moorings (cores L-050, SS-3, and SS-4, Gobeil et al., 1991) were averaged, yielding 1.0 % BIOSI (2.4 % OPAL) which represents the biogenic silica content associated with the terrigenous portion of the collected material. The ratio of % BIOSI: % Al for these core tops ranged from 0.094 to 0.14 (average 0.12), and the % $BIOSI_{old}$ was then calculated as the product 0.12 x % Al. This provides a rough estimate only. In particular, it is recognized that there may be differential rates of transport between resuspended biogenic silica frustules and fragments and clay particles. In addition, biogenic silica is not bound to the clay particles in the same way that refractory carbon appears to be, and is subject to dissolution.

Finally, % BIOSI was converted to % OPAL by multiplying by 2.4 to account for the average water content of diatomaceous silica (Mortlock and Froelich, 1989). The OPAL fluxes were determined from the % OPAL of the TDW flux. The % $OPAL_{new}$ was calculated as the difference between % $OPAL_{total}$ and % $OPAL_{old}$. Where samples are too small to allow for analysis of aluminum, the average $OPAL_{old}$ in the $TERR_{inorganic + CaCO3}$ fraction was calculated for each trap and used to estimate $OPAL_{old}$ in the small samples (see Appendix 3).

Using the methods outlined above, the biogenic and terrigenous fractions of the trapped material at each of the four mooring sites were calculated and discussed in the next section. The biogenic and terrigenous fluxes are discussed along with physical forcing in Chapter 6.

5.5 Composition of trapped particles

The annual integrated estimates for CN_{molar} ratios (Figure 5.1) range from 7.3 to 11.1 and show no consistent pattern with depth, the ratios increase slightly with depth at SS-5 and L144 and decrease at AM1-92. The annual integrated % POC decreases with depth at all sites (Figure 5.1) and ranges from 3.1 % (deep trap at L144) to 8.6 % (at 600 m at A01-93), and this decreasing trend with depth likely reflects the increasing content of resuspended terrigenous material. The annual integrated % TN data follows the same decreasing pattern with depth except at station AM1-92 where there is a slight increase with depth (Figure 5.1). In the estimate based on the spring/summer period of 1991, the highest % BIOSI occurs at SS-5 (199 m trap) but this did not coincide with the highest BIOSI flux which was at the 490 m level at station AM1-92 (Figure 5.1).

The material intercepted by the sediment traps at sites SS-5, AM1-92, and L144 is highly terrigenous with the exception of the period at SS-5 in the spring/summer period of 1991during the export of a large diatom bloom. For data integrated over the sampling periods, both the terrigenous and biogenic fluxes (g m^{-2}) increase with depth at all sites, and with the exception of site AM1-92, the terrigenous content increases with depth while the biogenic content decreases (Table 5.3). At site AM1-92 however, the terrigenous content of the deep trap is lower due to the input of a high pulse of biogenic material (largely diatoms) by lateral transport during one interval in June/July. The composition of the trapped material is highly terrigenous (> 80%; Table 5.3) at SS-5 (381 day period), at AM1-92 (290 m trap), and at L144 (both depths). The higher biogenic component at SS-5 during the spring/summer period of 1991 is clearly due to a sustained diatom bloom. At A01 (~ 600 m) in Canada Basin, the higher biogenic content is likely due to a reduced transport of terrigenous material to the site.

At site SS-5, the increase in the OPAL content in the third interval (May 18 to 31, 1991) in the 199 and 499 m traps indicates that export of the bloom began during this

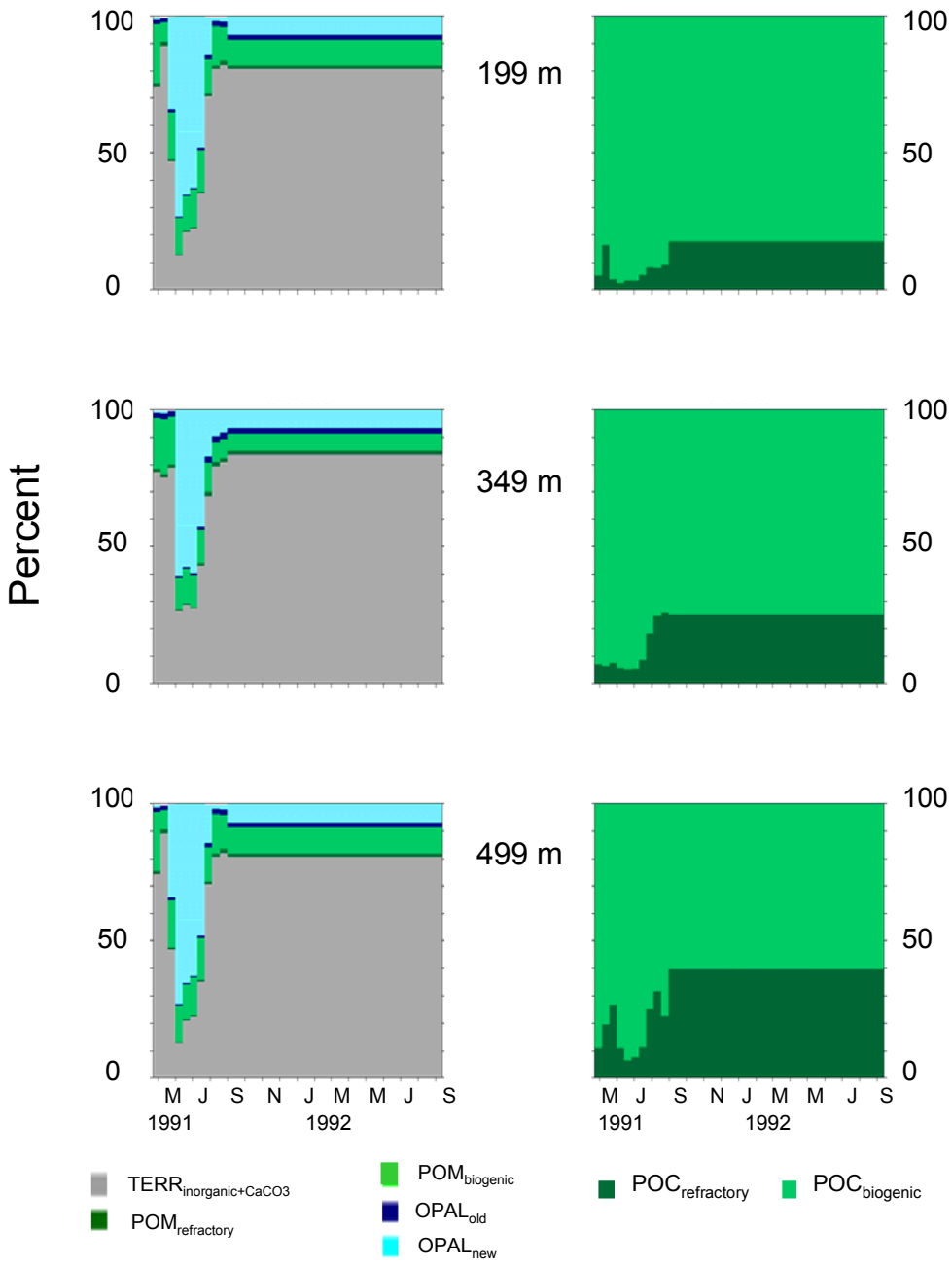

Figure 5-4 Terrigenous and biogenic components of the material intercepted by the sediment traps for A) site SS-5, B) site AM1-92, C) site L144, and D) site A01. Plots on the left show the percentages of the terrigenous ($TERR_{inorganic+CaCO3}$ and $POM_{refractory}$) and the biogenic ($POM_{biogenic}$, $OPAL_{old}$, and $OPAL_{new}$) components. Plots on the right show the percentages of the total particulate organic carbon (POC) represented by $POC_{biogenic}$ and $POC_{refractory}$. Note that due to small sample sizes for site A01, the total biogenic fraction was estimated using total carbon values and no distinction is made for $POM_{biogenic}$ and $POM_{refractory}$. Figures 5.4 B), C), and D) are on following pages.

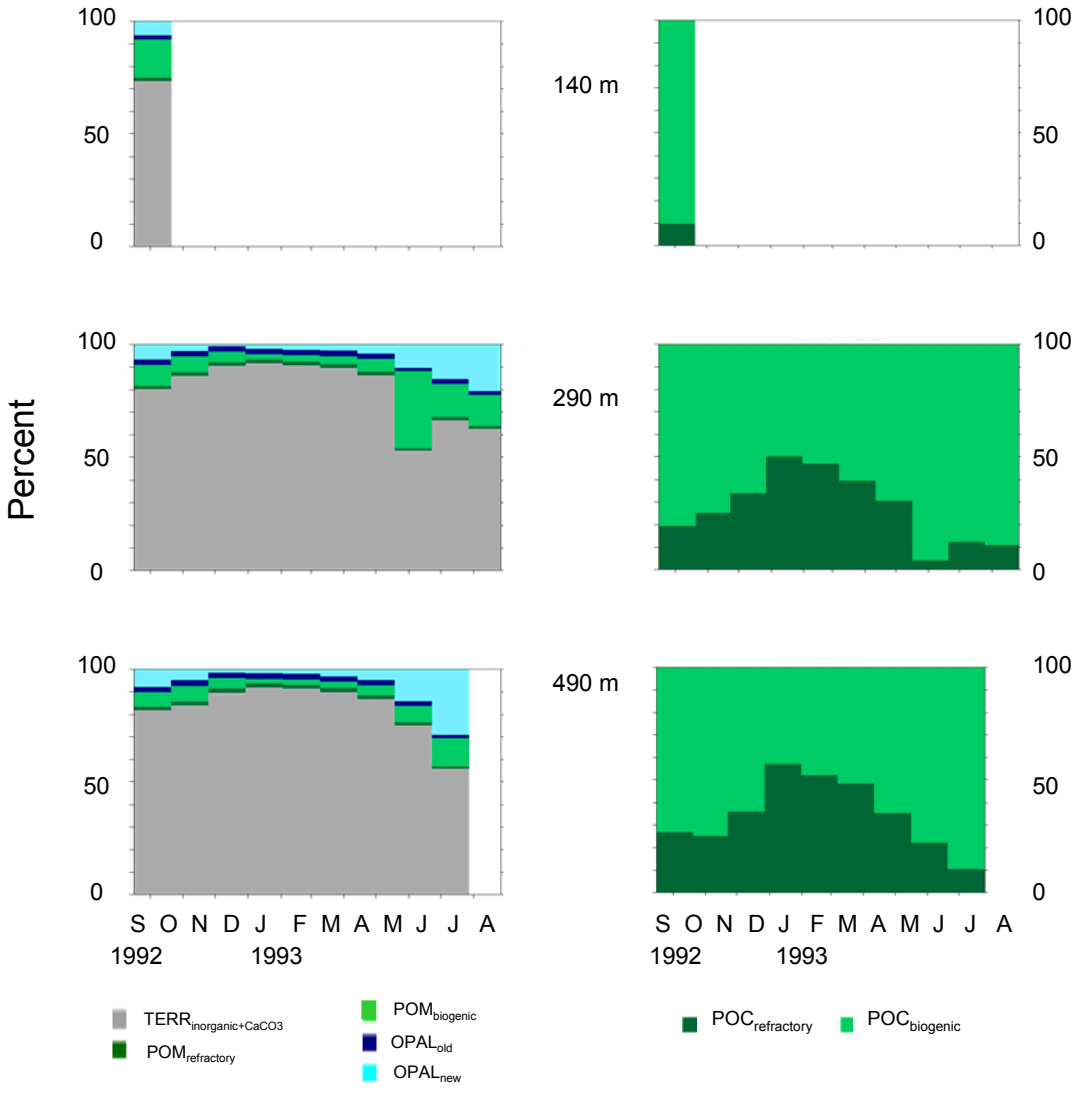

Continuation of Figure 5.4 (5.4B)

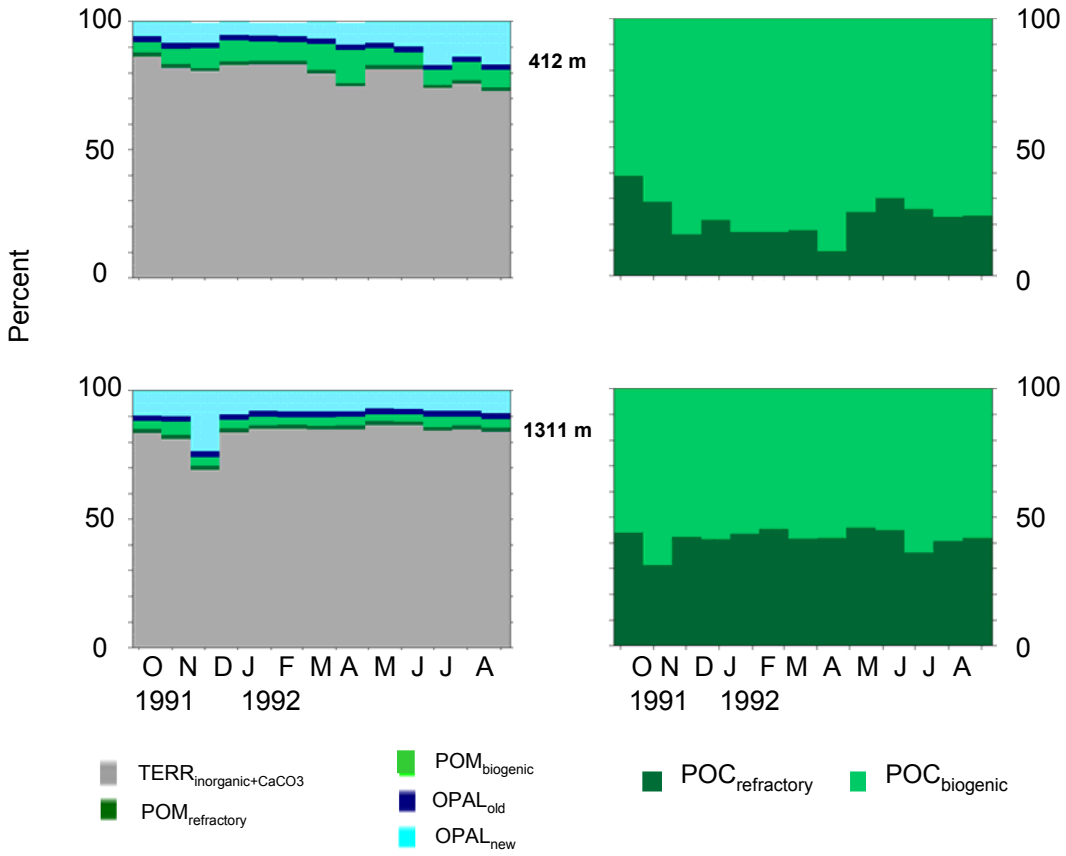

Continuation of Figure 5.4 (5.4C)

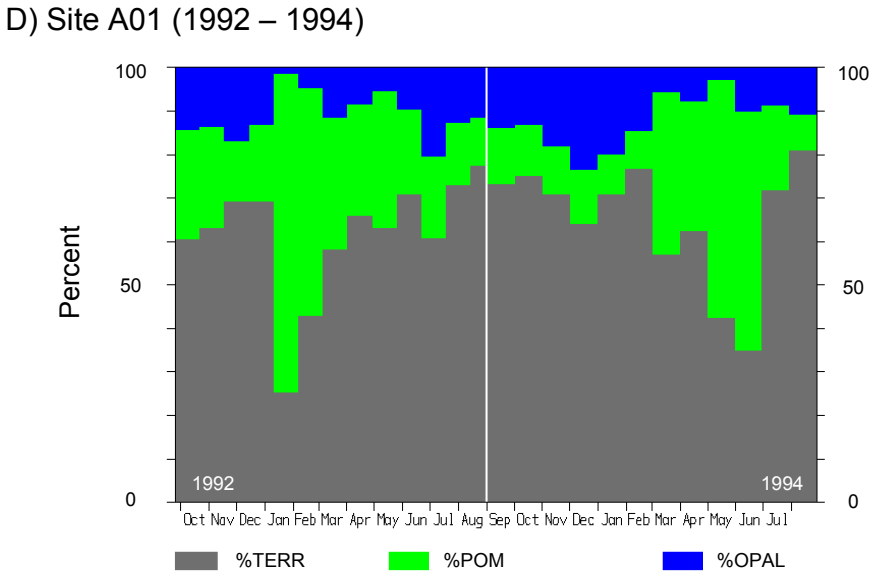

Continuation of Figure 5.4 (5.4D)

period (Figure 5.4A). The absence of an increase in OPAL content in the 349 m trap at interval 3 indicates that transport processes in addition to vertical export are involved. The majority of the particulate organic matter (POM) is biogenic at all depths although the proportion decreases as the terrigenous portion increases with depth (Figure 5.4A).

At AM1-92, the terrigenous and biogenic composition of the trapped material shows seasonality with a higher biogenic component in the fall and spring/summer than in the winter (Figure 5.4B). Throughout the whole collection, the POM is dominated by biogenic material but the relative proportion of refractory POM increases over the winter months.

At L144, the increased biogenic component at 412 m in the spring and summer suggest a seasonal signal but the material in the 1311 m trap is remarkably uniform in composition suggesting a uniform source (Figure 5.4C). At this site, the POM is again dominated by biogenic material and there is relatively little variation in the proportions of biogenic and refractory POM throughout the collection (Figure 5.4C).

The Canada Basin site exhibits considerable variation in composition but there is no discernable pattern (Figure 5.4D). For most intervals, the material is > 50% terrigenous but there are two periods of time when the material is > 50% biogenic; one in the winter of 1992 and the other in the summer of 1994. There was much more variability in the composition than was seen at site L144.

In summary, there is a strong terrigenous component in the material collected at all the mooring sites and there is considerable variability between sites. The following chapter examines physical processes that may account for these differences.

Chapter 6 Influence of physical forcing on sediment fluxes

The trajectory of biological material from its point of production in the surface waters to interception by the sediment traps depends critically on water column stratification, ocean currents, and sinking rates of particles. The time spent along this trajectory as well as the biogeochemical agents and processes acting during transit dictate the biochemical composition of the trapped biological material.

The availability of light and nutrients fundamentally affect the input of primary production that occurs, and differential recycling and predation dictate which biological particles are exported to deeper waters. The export production may sink rapidly to the bottom or travel large horizontal distances during descent depending on the influence of currents, differential settling rates, water column structure, and the dynamics of mid-water and bottom nepheloid layers. Moreover, before interception by traps, biological material may have settled to the bottom on the shelf or shelf slope before remobilization and transport to deeper waters (Thomsen and van Weering, 1998; Thomsen, 1999).

Reworking and redistribution of newly settled biogenic material in the Arctic occurs by a variety of biological, chemical, and physical benthic processes. For example, arrival of the early ice algal bloom at the bottom stimulates activity in the benthic community (Grebmeier and Barry, 1991; Gooday et al., 1990; Renaud et al., 2007). Because of all these influences, the biological material caught in the traps only partially reflects the community of primary producers in the surface layer directly above the traps.

Inorganic material intercepted by the sediment trap originates from a number of sources and arrives via trajectories that respond to physical forcing. In a highly episodic fashion, the Mackenzie River supplies most of the inorganic suspended material to this region. The river plume distributes sediments on the shelf and the shelf slope, and the interplay of winds, ice cover, and coriolis forcing controls the disposition of the plume on and beyond the shelf. In the absence of other dominant factors, the coriolis force acts to direct the plume eastward along the Tuktoyaktuk Peninsula. Mid- and bottom water nepheloid layers transport particles in this area, and material is entrained into them via sinking from the river plume and resuspension from the bottom. Resuspension arises

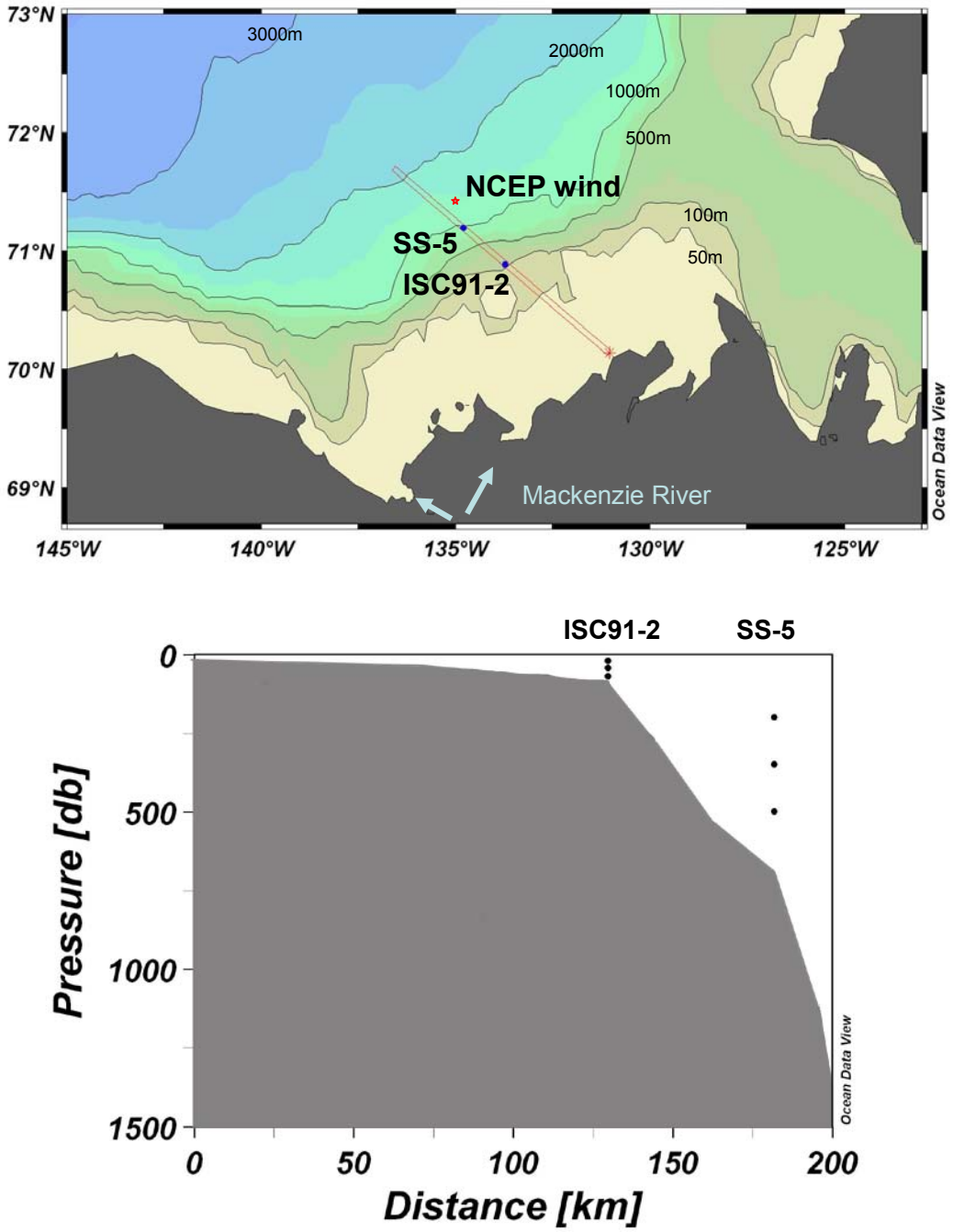

Figure 6-1 Map showing the locations of mooring sites SS-5 and ISC91-2 and the location of the NCEP wind data used in the discussion. A cross-section of the shelf indicates the sediment trap depths at site SS-5 (199, 349, and 499 m) and the depths of the current data at site ISC91-2 (20, 43, and 70 m). At site SS-5, currents, temperature, and salinity were measured at 99, 206, and 506 m. (Plot done using Ocean Data View software, Schlitzer, R., Ocean Data View, http://odv.awi.de, 2009)

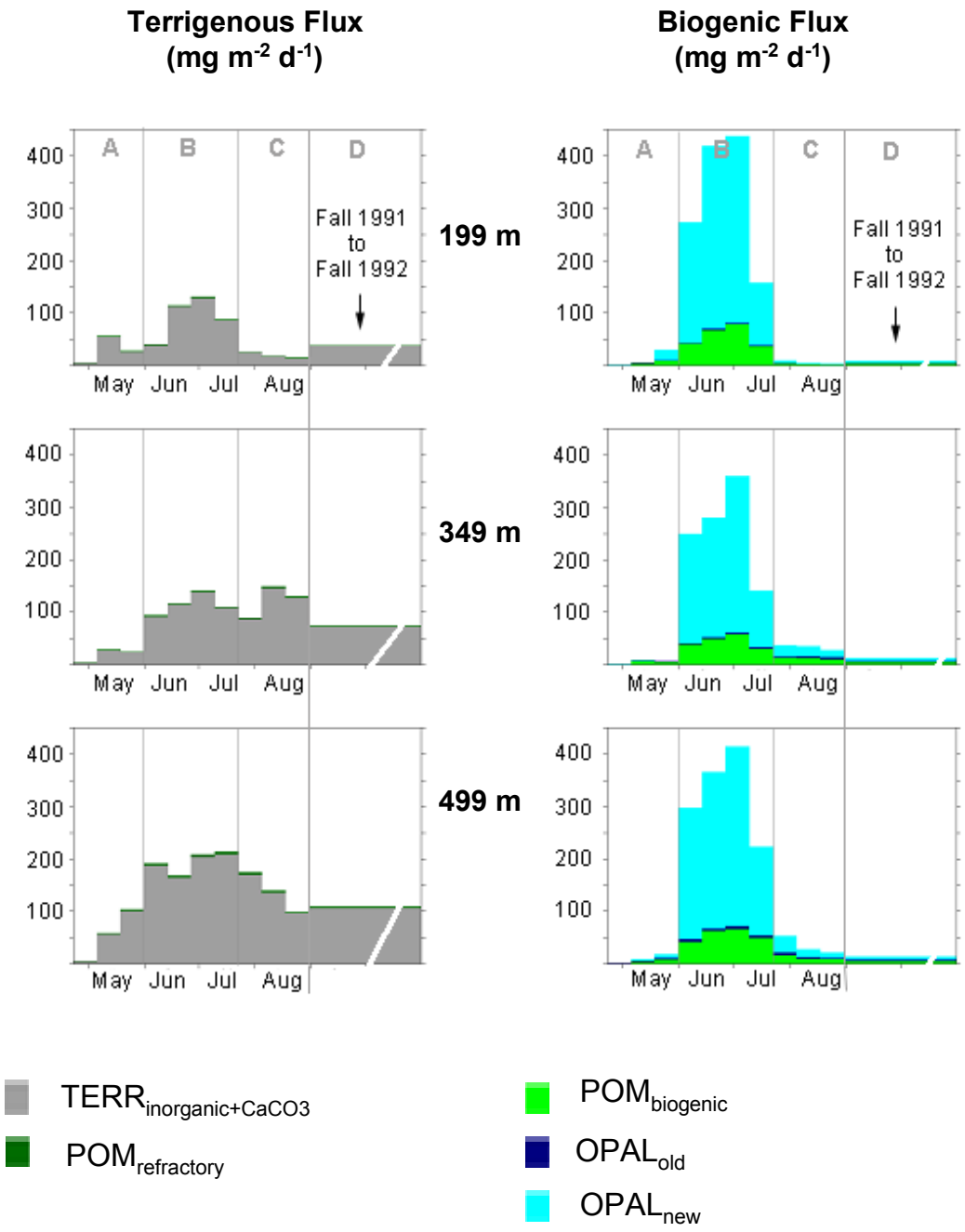

Figure 6-2 Plots showing the terrigenous and biogenic fluxes at site SS-5 at the 199, 349, and 499 m sediment traps. For the purpose of discussion, the collection period is divided into periods A) pre-export, B) export, C) post-export, and D) August 30 to September 12, 1992. See Section 5.4 for definition of terrigenous and biogenic as used in this plot.

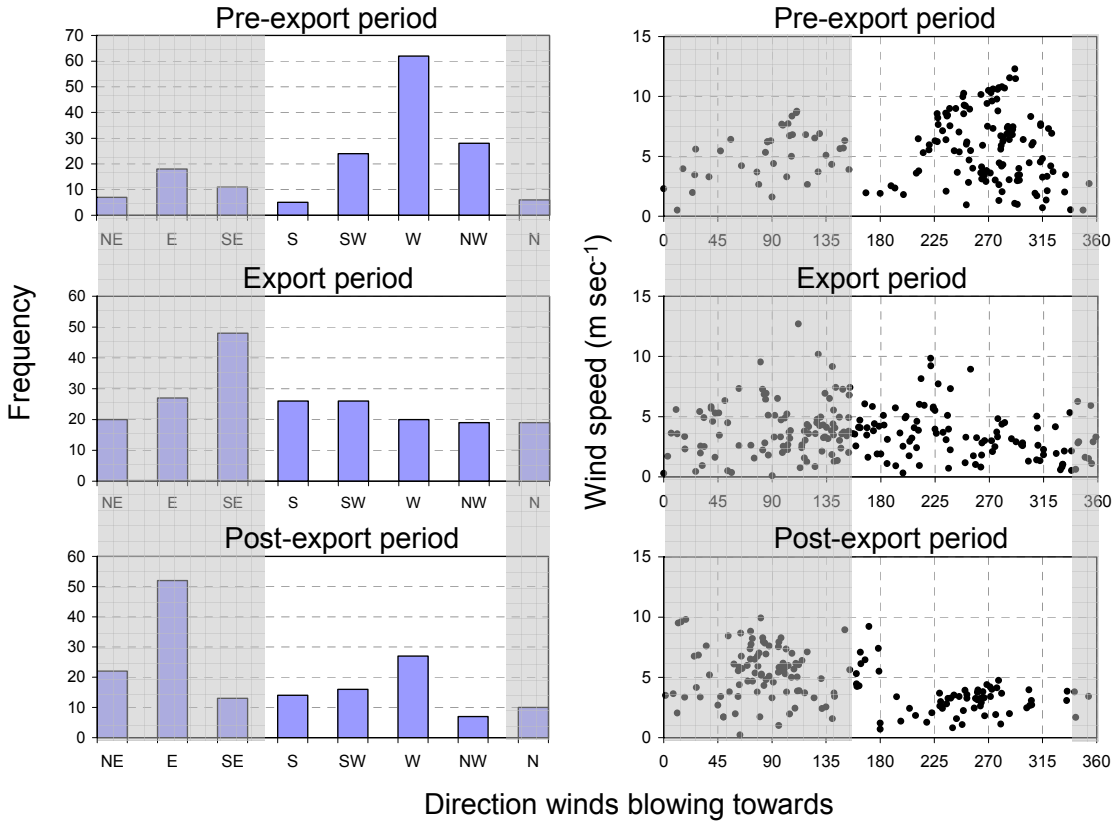

Figure 6-3 Histograms of wind directions (NCEP 10-meter winds, see Figure 6.1 for location of grid point) for the spring/summer season of 1991 in the three periods (pre-export, export, and post-export) corresponding to the trap collection as shown in Figure 6.2. The plots to the right show the wind direction for events with the highest wind speeds. The shaded areas indicate downwelling favourable wind directions at the shelf edge.

from such mechanisms as ice keel gouging, bioturbation, bottom currents, upwelling and relaxation of upwelling at the shelf edge, ocean currents, and wind induced mixing. Strong winds from the northwest during periods of open water promote massive resuspension events close to the shore and produce downwelling favourable conditions capable of transporting sediments seaward. In addition, storms and storm surges add to the load of suspended material by erosion of sensitive coastal areas. Moreover, inorganic material released into the water column from melting ice can originate locally or from far-flung regions of the Arctic depending on where and how incorporation into the ice occurred. Once initially mobilized, particles may experience a series of deposition and resuspension events.

In the remainder of this chapter, physical factors important to the patterns of biogenic and terrigenous material observed in the sediment traps are described for each of the four mooring sites. Related discussions focus on central questions arising from the data and these questions are listed at the beginning of each section.

6.1 Influence of physical forcing at Site SS-5

Conditions on the shelf affecting the terrigenous and biogenic fluxes at the SS-5 mooring are discussed here, along with current meter and ice data from a mooring at site ISC91-2, located at the shelf edge about 52 km to the SE (Figure 6.1). The terrigenous and biogenic fluxes at site SS-5 (Figure 6.2) are calculated as described in section 5.4 and delineate three periods (pre-export, export, and post-export). Data are also included from a single cup collection that ran from the fall 1991 to the fall of 1992 (Figure 6.2).

A diatom bloom dominated the spring/summer collection of biogenic material at site SS-5 (Figures 6.2 and 3.10). The development and fate of this 52-day long bloom and the pattern of terrigenous input is examined below. Several questions are explored:

1) What are the sources and trajectories of the highly terrigenous material in the pre-export period in May? What turns the system on?
2) What factors initiate, sustain, and terminate the early spring bloom? What factors control the export of the bloom? What are the sources and trajectories of the trapped biogenic material?
3) What are the sources and trajectories of the terrigenous material in the export and post-export periods? What are the controlling physical factors?
4) What are the expected sinking rates of the terrigenous and biogenic particles? How much horizontal advection occurs during descent of the particles? What evidence, if any, is there of a “ballasting effect” which alters the settling rates and trajectories of either or both the biological and terrigenous particles? Does the stickiness of diatoms play a dominant role and sweep up terrigenous particles during descent? If present, can this “ballasting effect” reach a saturation point?
5) How do the spring/summer conditions of 1991 and 1992 differ? How does this manifest itself in the shelf slope fluxes?

Ice cover, winds, seasonal warming, river inputs, water properties, nutrient availability, and ocean currents all conspire to varying degrees and with different timing to the observed patterns of fluxes. All are important in the context of the above questions and are considered in the following sections.

6.1.1 Wind and ice

Episodes of high winds and accompanying ice displacement are expected to be strong drivers in this system. Wind data from 1991 show that during the pre-export period, the winds blew most frequently to the W with wind speeds averaging 5.5 m sec^{-1} and ranging up to 12.3 m sec^{-1} (Figures 6.3 and 6.4A). The directions and the changes in direction of the ice displacement agree remarkably well with the wind, and the net displacement of the ice at the shelf break is to the SW (Figures 6.5A and 6.5B, see direction changes on May 18 and 27). There was very little movement of the ice cover during the first interval of the trap collection in late April and early May even though there were strong winds throughout this period. In the second interval, the winds were to the SW and the ice moved rapidly to the WSW. Between May 18 and May 27, the wind shifted to the SE as did the ice.

During the export period, the winds blew most frequently to the SE, the average wind speed was lower than over the pre-export period at 3.7 m sec^{-1}, and the strongest wind event blew to the E with a maximum speed of 12.7 m sec^{-1} (Figures 6.3 and 6.4B). After mid-June, the direction of ice displacement differed from the wind direction, with the winds blowing predominantly to the E and SE while the net ice displacement was to the SW (Figures 6.5A and 6.5B). In the post-export period, the winds blew most frequently to the E with an average speed of 4.5 m sec^{-1} and a maximum speed of 9.9 m sec^{-1} (Figures 6.3 and 6.4C). During this period with the winds blowing predominantly to the east, the net ice displacement was to the SE (Figures 6.3, 6.4C, 6.5A,B).

The ice conditions at site SS-5 were pieced together using satellite images (Figure 6.6), data from the ISC91-2 mooring (Figures 6.4A,B,C and 6.5B), and Canadian Ice Service maps (http://ice-glaces.ec.gc.ca/App/WsvPageDsp.cfm?ID=1&Lang=eng&Clear=true). The Amundsen Gulf polynya and leads beyond the landfast ice bordering Banks Island and Tuktoyaktuk Peninsula opened relatively early in the spring of 1991 (Figures 6.6 and 2.2). Heavy ice

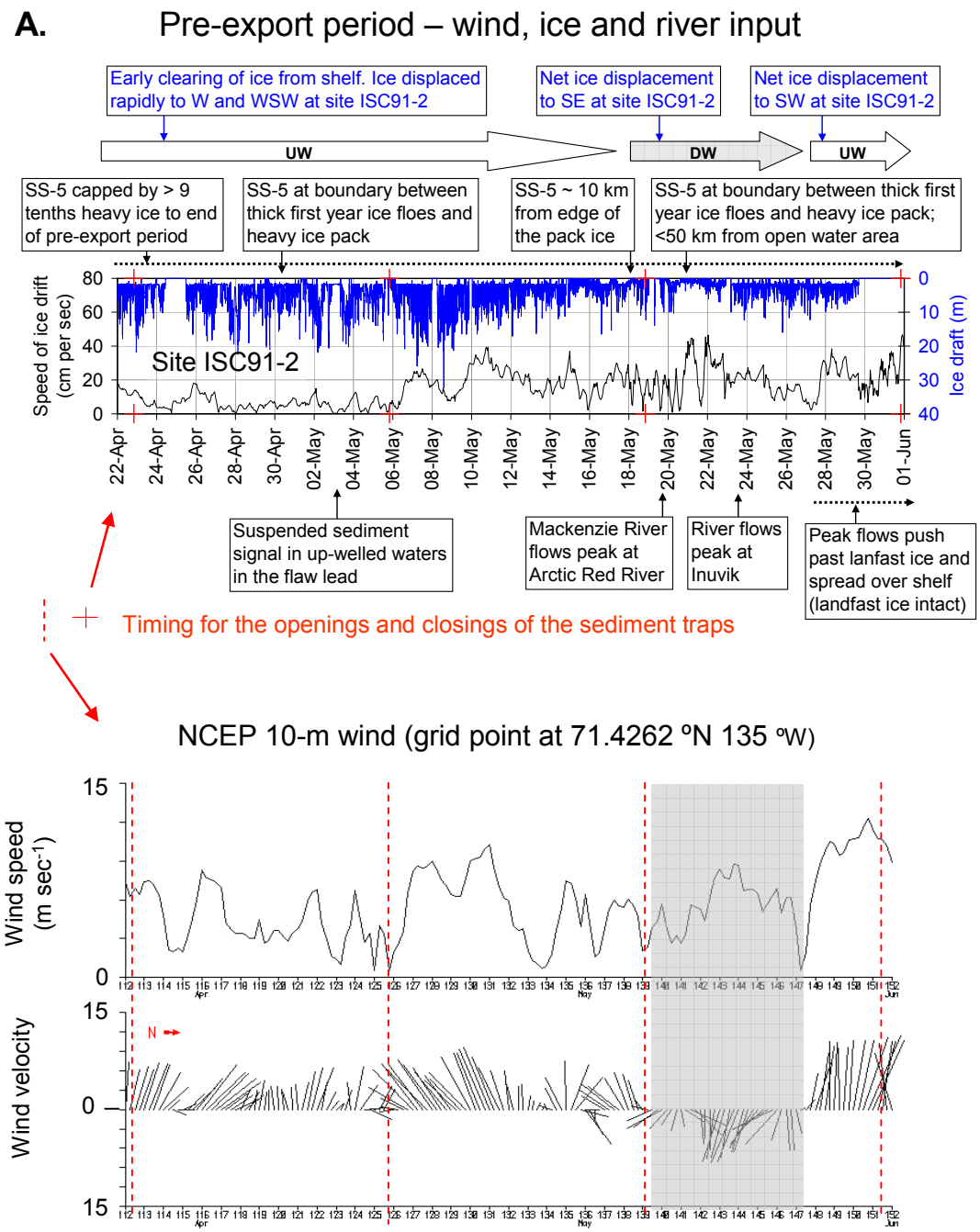

Figure 6-4 Time line plots of conditions on the Mackenzie shelf in the spring/summer season of 1991 covering the A) pre-export, B) export, and C) post-export periods of the sediment trap mooring at site SS-5. The top chart is the ice draft and the speed of ice drift at site ISC91-2 (70.886 ºN 133.732 ºW; bottom depth 81 m). The ice draft data is from a Water Structure Profiler (WASP; acoustic frequency of 200 kHz and a 90 second sampling interval) located at 5 m above the bottom and the ice speed data is from an Acoustic Doppler Current Profiler (ADCP; acoustic frequency of 307.2 kHz and a 45 minute sampling interval) located 6 m above the bottom. Melling and Riedel, 1994 describe this data in detail. The wind data is from the NCEP data set (http://www-pord.ucsd.edu/~sgille/sio221c/ncep_wind.html), the river data is from the HYDAT data set, and the ice coverage at site SS-5 is from the CIS charts (http://ice-

glaces.ec.gc.ca/App/WsvPageDsp.cfm?ID=1&Lang=eng&Clear=true). The upwelling (UW) and downwelling (DW) arrows on the top chart depict the conditions expected at the shelf edge due to the direction of ice drift, and the shaded grey in the bottom chart depict downwelling (DW) conditions due to winds.

B. Export period – wind, ice and river input

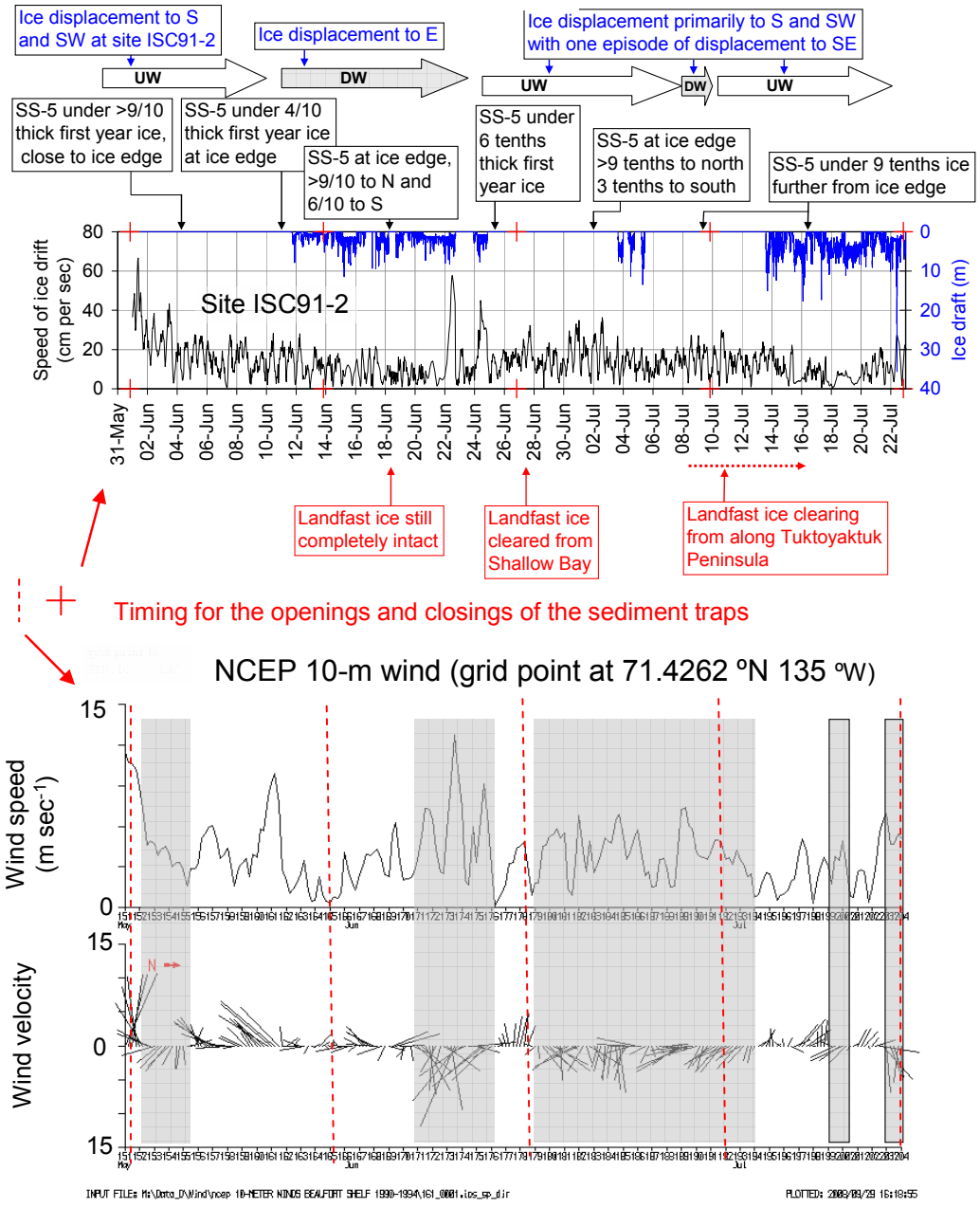

Continuation of Figure 6.4 (6.4B)

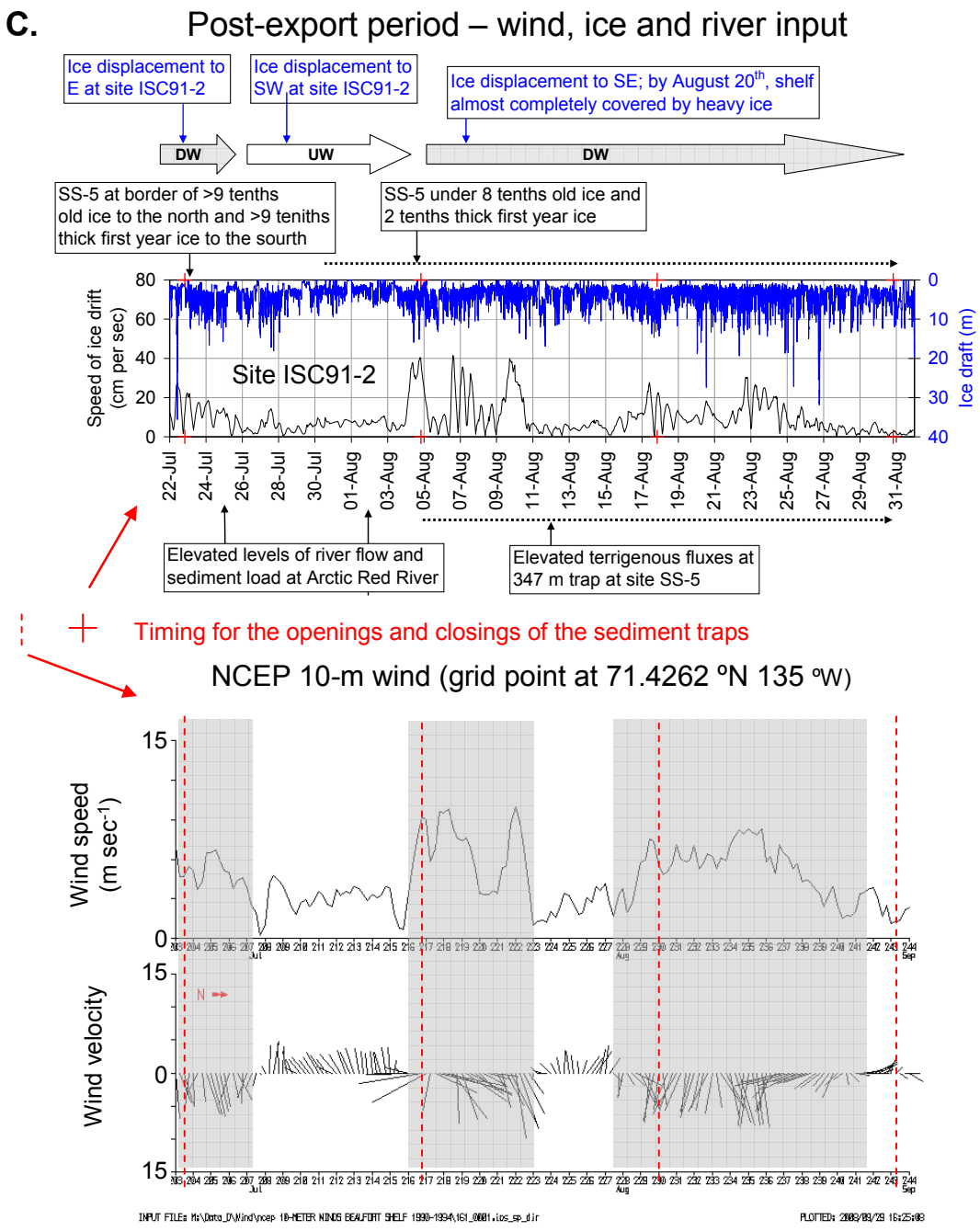

Continuation of Figure 6.4 (6.4C)

with keel depths frequently in excess of 10 m covered much of the Mackenzie Shelf in early spring 1991 (Figure 6.4A). Small leads opened up at the end of March and expanded slowly during April. At site ISC91-2 on the Shelf ice displacement to the west began on April 14 and an expanding area of open water developed over the eastern and southern areas of the Shelf and on the west side of Banks Island (Figures 6.5B and 6.6). From April 21 to May 18, ice moved rapidly to the W and SW (Figure 6.5B) under the combined influences of the large scale movement of the pack ice and winds (Figures 6.4A, 6.5A,B, and 6.6). By May 21, the drift of the ice pack had created a large Y-shaped area of open water in the mouth of Amundsen Gulf and beyond the landfast ice bordering Banks Island and Tuktoyaktuk Peninsula (Figure 6.6).

The water was open at Site ISC91-2 from May 30 to June 11 (Figures 6.1 and 6.4A,B). However, site SS-5, located ~52 km to the NW of ISC91-2 remained under heavy ice approximately 10 km from the edge of the pack ice. For the pre-export period, this was probably the closest approach of the ice edge to site SS-5, as after May 18, the ice moved to the ESE under the influence winds from the NW and increased the distance of SS-5 from the ice edge. For the last few days of May, the ice displacement was again to the SW (Figure 6.5B). Over the full pre-export period, site SS-5 was at least 90% covered by heavy ice and severe light limitation would have prevented the initiation of a diatom bloom at that location. In contrast, light conditions in the expanding pool of early opened waters would have supported primary production.

Over the export period, ice coverage at SS-5 ranged from 90 to 30 %, and during most of that period, the site was close to the edge of the heavy pack ice (Figure 6.4B). From the end of the first week of June to the end of the first week of July, ice cover at SS-5 was reduced, but from July 9 to the end of the export period the ice edge moved south and the site was again covered with heavy ice. In contrast, at the shelf edge, at Site ISC91-2, ice-free conditions prevailed for over half of the export period. The export period is the only interval with stretches of open water over site SS-5. Light availability would at times have been sporadic but clearly was adequate overall to sustain a diatom bloom. It is very likely that advection of settling particles from the open water areas occurs during this period.

A. NCEP 10-meter winds (grid point location 71.426 ºN 135.000 ºW)

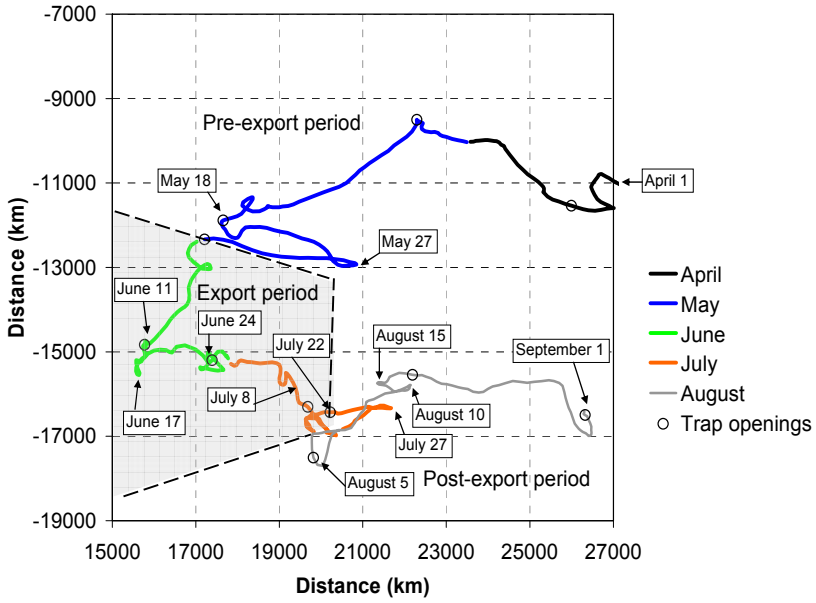

B. Ice displacement at site ISC91-2

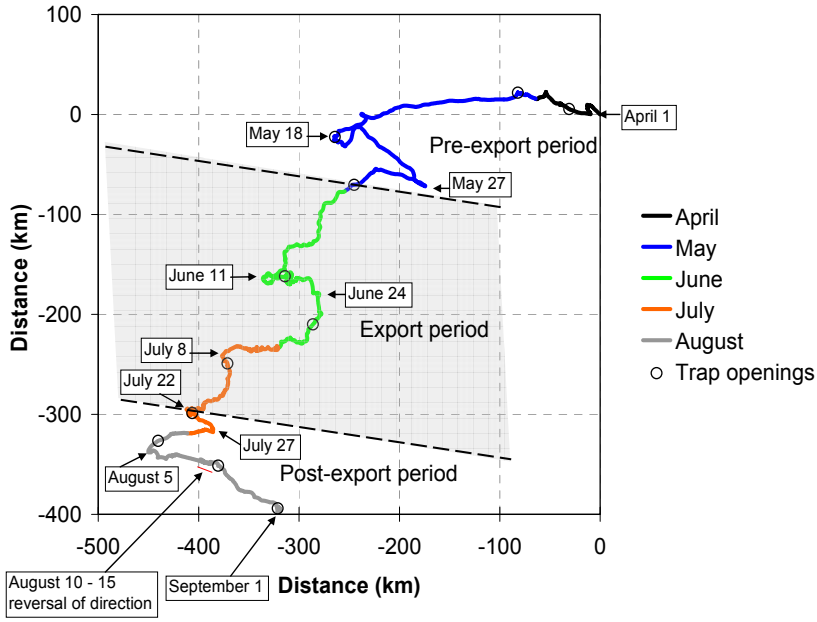

Figure 6-5 Progressive vector plots of a) NCEP 10 meter wind at 71.4262 ºN 135.0000 ºW and b) Ice displacement at station ISC91-2 (70.886 ºN 133.732 ºW; bottom depth 81) for spring/summer season of 1991. Ice displacement data is from an Acoustic Doppler Current Profiler (ADCP) located 6 m above the bottom (acoustic frequency of 307.2 kHz and a 45 minute sampling interval; this data is described in detail in Melling and Riedel, 1994. Dates marking the changes of direction of wind and ice displacement are indicated and these changes of wind direction are used to infer the switching between upwelling and downwelling conditions.

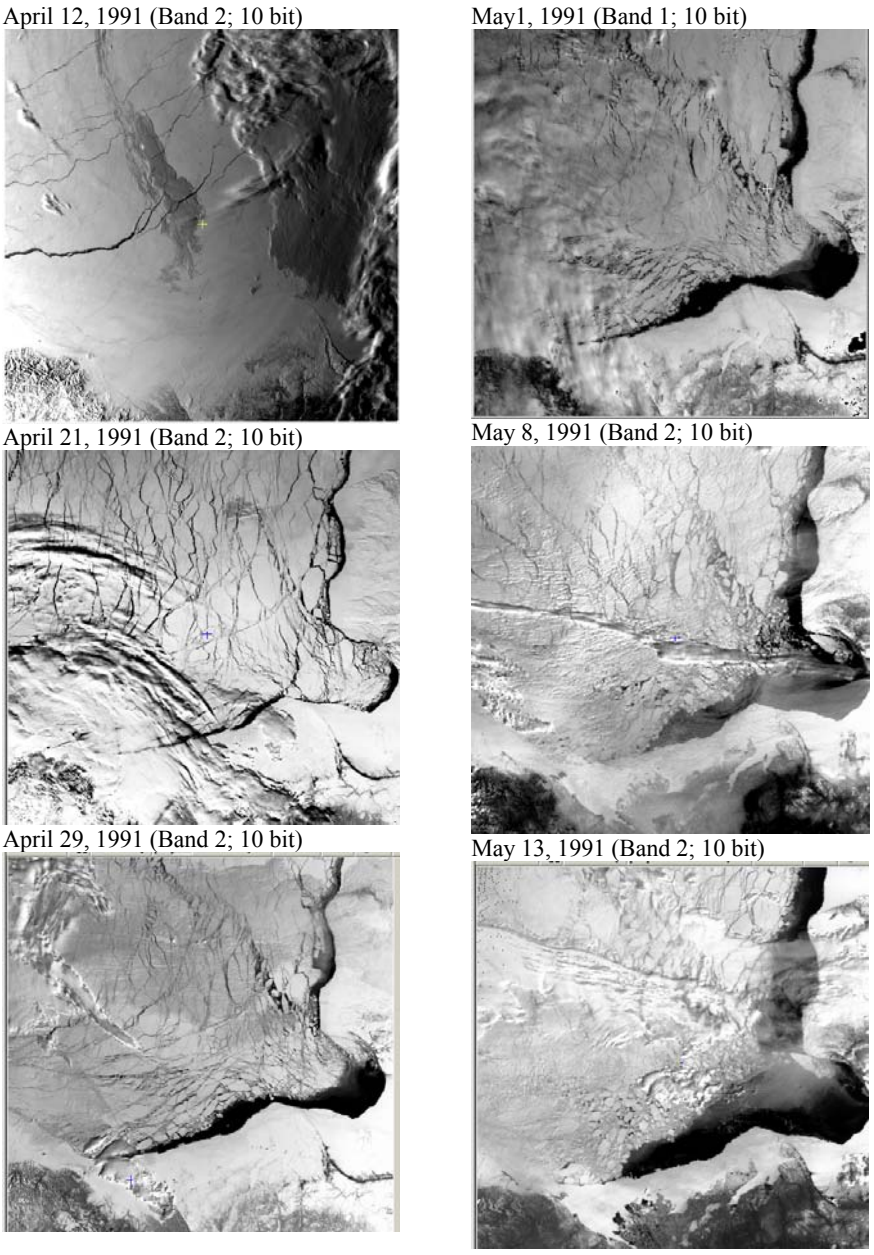

Figure 6-6 Satellite images depicting the ice cover over the Beaufort Shelf for the spring and summer of 1991. Note the early clearing of the ice from Amundsen Gulf and the eastern side of Mackenzie Shelf. Note also that the ice pushed back in over the shelf by the end of August. The data is from the Advanced Very High Resolution Radiometer (AVHRR) on board the National Oceanic and Atmospheric (NOAA) series weather satellites. Band 1 (visible red, 0.58-0.68 µm) and Band 2 (near IR, 0.725-1.10 µm) images were chosen to best represent the ice cover over the period.

May 16, 1991 (Band 2; 10 bit)

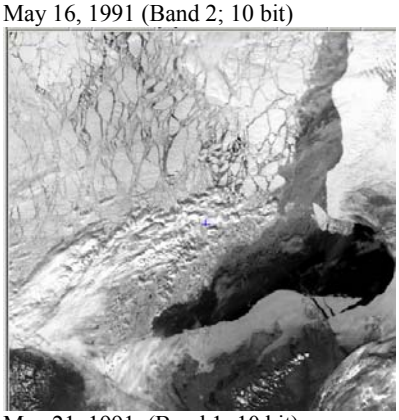

June 28, 1991 (Band 2; 10bit)

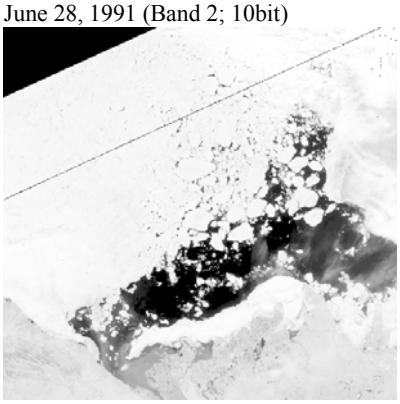

May 21, 1991 (Band 1; 10 bit)

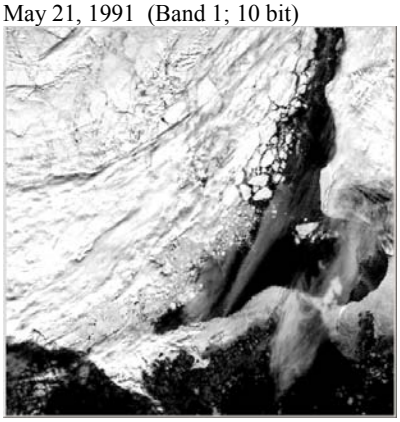

July 5, 1991 (Band 2; 10 bit)

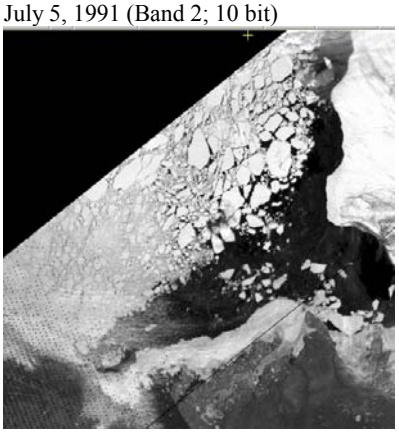

June 7, 1991 (Band 2; 10 bit)

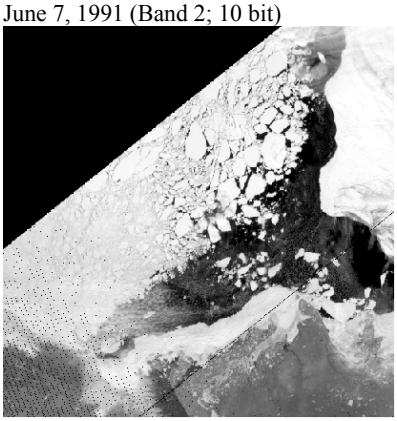

August 29, 1991 (Band 2; 10 bit)

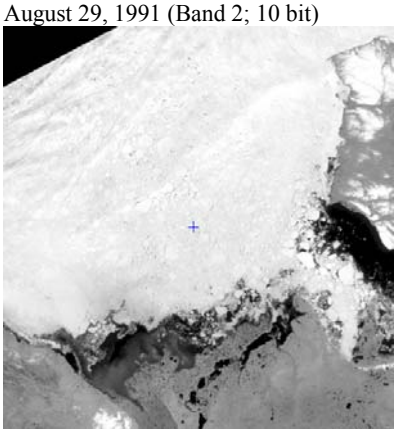

Continuation of Figure 6.6

Over the full post-export period, heavy ice covered site SS-5 and the ice edge had moved far to the south (Figure 6.4C). At ISC91-2, heavy ice with frequent deep keels moved to the SW for the last few days of July and the first five days of August after which the ice pushed strongly to the SE for the remainder of the month (Figures 6.5B and 6.6). By late August, there was very little open water left on Mackenzie Shelf and primary production would have been severely light limited over the shelf and shelf slope due to the heavy ice cover. The movement of the heavy ice back over the shelf coincides with the abrupt decrease in exported biogenic material at all trap depths (Figure 6.2), a decline attributed to the severe reduction of light availability under the heavy ice cover. The small amount of biogenic material collected in the traps during the post-export period is likely due to lateral advection of material previously settled on the shelf.

During the single long sediment trapping interval at SS-5 (fall of 1991 to the fall of 1992) (Figure 6.2), the ice initially cleared from large portions of the eastern side of the Alaskan and Mackenzie shelves and from Amundsen Gulf, and remained clear until mid-October. Freeze up was complete by October 22. At SS-5, ice coverage was >90 % over the fall; the ice edge was close, only for a period around October 8.

The spring/summer seasons in 1991 and 1992 were very different with respect to the ice coverage on the shelves. Unlike the spring/summer of 1991, when there was an early season opening, ice completely covered Mackenzie Shelf until mid-June in 1992, and site SS-5 remained far from the ice edge until the third week of July. For the last half of August 1992, site SS-5 was at the edge of heavy ice to the north and more open water to the south. In the last half of August 1992, large areas of open water covered Mackenzie Shelf while in the same period in 1991 little open water was present. Severe light restriction would have prevented a diatom bloom from occurring close to site SS-5 in the spring of 1992 and this probably constitutes the main reason for the much lower estimated annual flux of BIOSI in 1992 than in 1991 (see Figure 5.1 and Table 5.1). It is clear that the ice cover as a controller of light availability is a key factor in determining the location and extent of phytoplankton production and export. Moreover, the contrasting conditions in 1991 and 1992 with respect to the timing of the ice cover highlight the importance of conducting long time series studies if system variability is to be reasonably captured.

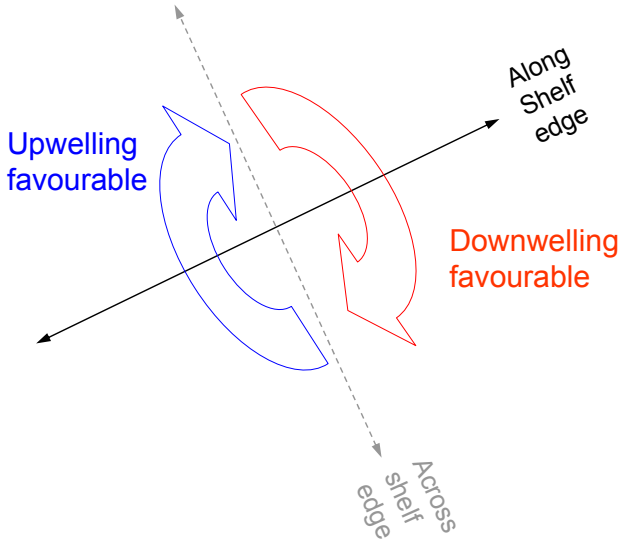

Figure 6-7 Relationship between wind direction and upwelling and downwelling conditions on the Mackenzie shelf and Shelf edge.

The release of sediments from melting ice during the pre-export period is an unlikely contributor to the terrigenous sediment flux at that time. Average air temperature at Sachs Harbour in May was -3.8 ºC, and this is likely a good representation of temperatures at site SS-5. Although there were periods in May with temperatures above freezing, these periods were not high enough for long enough for any significant melting and particle release to occur before the beginning of June.

6.1.2 Upwelling and downwelling

The Mackenzie Shelf edge runs SW to NE, and the relationship between wind direction and upwelling/downwelling favourable conditions is shown in Figure 6.7 (adapted from Williams et al., 2008). Over the spring/summer period of 1991, the edge of the heavy pack ice ran parallel to the shelf edge (Figure 6.6). Wind stress over the open water to the SE would force surface currents to the right, whereas under heavy ice cover, the direction and speed of ice drift, forces the surface currents. This distinction is important in the scenarios discussed here. In the spring and summer of 1991, the movement of ice would have governed rates of upwelling or downwelling at the shelf edge, as summarized in the top plots of Figures 6.4A,B,C. The early opening of shelf waters in that year coupled with the inferred episodes of upwelling and downwelling were important factors in influencing fluxes observed in the sediment traps at site SS-5.

Furthermore, there is evidence that mid- and bottom nepheloid layers are common on the Mackenzie Shelf edge and shelf slope (Bornhold, 1975; Giovando and Herlinveaux, 1981; O'Brien et al., 2006) and downwelling events would favour the transport of suspended material offshore (O'Brien et al., 2006).

During the pre-export period, two periods of UW favourable conditions and one of downwelling are indicated (Figure 6.4A). West and southwest displacements of ice over the shelf and shelf edge at the end of April into May and the movement of deep ice keels (Figures 6.4A and 6.5B) would likely have driven the displacement of surface waters offshore and upwelling of deep, nutrient rich waters onto the shelf. From May 18 to May 27, the net displacement of ice changed to the ESE creating downwelling conditions at the shelf edge (Figures 6.4A and 6.5B). For the last few days of May, ice displacement changed again to the W and SW, once again favouring upwelling conditions (Figure 6.4 A). Similar alternations between up- and downwelling occurred during the export and post-export periods (Figures 6.4B,C and 6.5A,B), albeit with a higher degree of physical complexity as the directions of ice drift and the wind are often not in as good agreement as they were in the pre-export period.

The inferred UW and DW episodes and the displacement of large ice keels have important implications with respect to the biogenic and terrigenous fluxes observed in the spring/summer period at site SS-5. First, episodes of UW likely result in resuspension of bottom sediments over the slope, as has been observed on a continental shelf elsewhere (for example the continental slope off Oregon in Perlin et al., 2005). Relaxation of UW and DW conditions in that study were associated with the thickening of a bottom nepheloid layer (identified by an enhanced backscatter signal) and with the formation and spreading of mid-water nepheloid layers. Second, UW of nutrient replete waters onto the shelf enhances primary production, assuming light availability, water column stratification, and ecosystem dynamics are amenable, as they were during the prolonged diatom bloom in the early opened waters in the spring of 1991. There is clear evidence of upwelling of nutrient-rich waters in the mid-shelf region in early May 1991, and the surface waters in the open lead appeared to originate from a mixing of deep Polar Mixed Layer (PML) water with offshore surface water (Borstad and Kerr, 1994; Macdonald et al., 1992). Third, observations show that movements of ice keels over Arctic shelves

correlate with increased backscatter in the water column above the sea bottom (personal communication with Humfrey Melling; ADCP data). Such implied resuspension of shelf sediments would have contributed to off shelf transport during downwelling conditions especially in the presence of heavy deep-keeled ice on the shelf. In the pre-export period, only an insignificant biogenic signal accompanied an increasing terrigenous signal. The sudden appearance of the predominantly terrigenous material in the second interval of the collection coincides with the rapid westward movement of the ice over the shelf and is attributed to resuspension and transport of shelf sediments. In early May, a small concentration of suspended inorganic solids was detected in the water column, and an investigation of water properties ruled that the source was resuspension of bottom sediments and not horizontal advection of Mackenzie River water out from under the land-fast ice (Borstad and Kerr, 1994). Resuspension of shelf sediments may also have occurred during strong wind events over the open waters in May and June. This is consistent with the general increase of terrigenous sediment with depth of the traps in the water column. Particulate transport of resuspended terrigenous and recently settled biological material beyond the shelf edge likely occurs in bottom and mid-water nepheloid layers via a series of depositions and re-suspensions (similar to the process reported by Thomsen and van Weering, 1998 and Ashjian et al., 2005). Fourth, upwelling and enhanced primary production at the edge of the pack ice are reported phenomena in the Arctic (e.g. Wu et al., 2007 and references therein), probably resulting from smaller scale, shallower upwelling/downwelling strictly associated with the pack edge. Thus, the location of the edge of the ice pack with respect to site SS-5 is an important consideration. At all three trap depths, the highest biogenic fluxes indeed coincide with the period of closest proximity to the ice edge and lowest ice cover. Fifth, resuspension in shallow coastal waters during high wind events and downwelling conditions have been observed to correlate with increases in trapped terrigenous material at the shelf edge (O'Brien et al., 2006).

6.1.3 River input and landfast ice

The spring discharge at Inuvik in 1991 was one of the top four earliest discharge peaks on record with the flows peaking on May 20 at Arctic Red River and on May 24 at Inuvik (Figures 2.3 and 6.4A). Flows increased by 22,620 m^3 sec^{-1} over the 12 days prior

to the peak flow. The peak flow was of short duration and dropped off sharply (Figure 2.3). Compared to the average monthly flows for 1980 to 1997, flows for 1991 were about 4 % higher than average in April/May, about 12% lower than average in June, and about 12 % higher than average in July/August, due to the high flows that peaked on July 25 and August 2 (Figures 2.3 and 6.4.C).

Without direct evidence, it is difficult to determine the exact timing of the freshwater push beyond the landfast ice or the behaviour of the plume as it spreads into the open lead beyond. Landfast ice remained intact in Mackenzie Bay until at least June 18, but it is reasonable to expect that the peak flows had traversed the Mackenzie delta by the end of May or possibly even a few days earlier (see Figure 6.4B for timeline). During the last few days of May and the first week of June, the full force of the peak flow must have pushed in under the landfast ice, broached the stamukhi zone (an area of thick rubble ice at the edge of the landfast ice), and begun to spread out over the waters in the lead to the north and east of Richards Island. The sediment laden freshwater plume may also have spread north under the thick first year ice over Mackenzie Trough though it is also probable that the buoyant river plume is deflected by the ice edge to a degree dependant on the ice thickness; the thicker the ice, the greater the degree of deflection. In addition, given the thickness of the ice at the north edge of the lead, it is possible that the buoyant plume was able to spread to the NE along the north edge of the lead despite the predominant winds to the west at the end of May.

On June 4, the lead to the north of the landfast ice adjacent to Richards Island and Tuktoyaktuk Peninsula was 10 % covered by thick first year ice. At about this time, the peak flows were delivered into the lead beyond the landfast ice and likely with considerable force (Figure 6.4A). Massive resuspension of sediments likely occurred under these circumstances and would have augmented the high riverine suspended sediment loads transported during spring flood conditions (Carmack and Macdonald, 2002). There is no direct evidence as to the dynamics of the spreading of the river plume north of the landfast ice in 1991. However, since river plumes are responsive to winds (Macdonald and Yu, 2006), the plume in the open lead was likely constrained by easterlies to the west side of the lead in the last few days of May (Macdonald and Yu,

2006). After mid-June, the plume most probably swung to the E-SE under the influence of predominantly SE winds (Figure 6.5A,B).

The spreading speed of the plume in the lead is likely quite high. A drifter study at the mouth of the Rhone River reported drift speeds in the plume as high as 85 cm sec^{-1} with much lower river flows (Naudin et al., 1997). Without considering wind influences, estimating the speed of the plume advance at a modest 30 cm sec^{-1} suggests a possible plume advance of over 250 km in 10 days. This was easily sufficient time for the plume to spread east along the lead to beyond the location of site SS-5 at least within the second trap interval of the export period at site SS-5. This suggests that for the last half of the export period, the stratification and nutrient influx provided by the spreading river plume could well have been significant factors in supporting the diatom bloom exported to depth at site SS-5.

In June, the downwelling conditions due to episodes of strong winds from the northwest likely directed the plume to the southern edge of the lead. The downwelling coincided with a large influx of turbid river water into the open waters of the lead and this may explain, via nepheloid layer transport, the large increase in terrigenous material in the traps in the beginning of June. Transport via nepheloid layers is known to occur in this area (Bornhold, 1975; O'Brien et al., 2006; Forest et al., 2007).

Terrigenous sediment delivery beyond the shelf via the peak river flows of July 25 and August 2 and subsequent nepheloid transport in downwelling favourable conditions may have contributed to the terrigenous fluxes observed in the 349 m trap at site SS-5 in the last two intervals in August (Figure 6.4).

6.1.4 Stratification and water column structure

The development of water column stratification is critically important to the degree of primary production realized in the early opened waters such as occurred in the spring of 1991 (Niebauer, 1991). Processes capable of influencing the degree and timing of stratification in these waters are solar heating, melting of the ice cover, wind-induced mixing, mixing due to ice displacement, and freshwater inputs by the Mackenzie River. All play a role to varying degrees, albeit with different timing related to the extremes of weather, ice cover, and seasonality.

In the spring of 1991, the exact timing and extent of the developing stratification in the expanding lead is difficult to establish. In late March 1991, before the lead opens, the mixed layer extends down to about 40 m on and beyond the shelf (Figure 6.8). During May, the rapid movement of heavy ice cover to the west, the generally windy conditions, and the low average temperatures would have acted against the development of stratification in the early opened waters, while solar heating, sea ice melt, and increasing freshwater inputs would have acted to increase the stratification. In early May, waters in the lead were well mixed, and surface water properties indicated the presence of upwelling from about 40 m depth and the absence of leakage of river water at the landfast ice edge (Borstad and Kerr, 1994; Macdonald et al., 1992; Figures 6.10 and 6.11). In addition, temperatures in the open lead in early May showed evidence of warming mixed down to about 20 m and of surface temperatures raised above the freezing point, but this warming translated to only very weak diurnal stratification in the lead (Figure 6.10; Macdonald et al., 1992; Borstad and Kerr, 1994). It is likely that at the outer shelf, stratification due to ice melt was not significant until after the beginning of June when the temperatures were consistently above freezing (Appendix 4). The air temperatures measured at Tuktoyaktuk Airport were considerably higher than those at Sachs Harbour, so it is possible that stratification due to ice melt began earlier along the southern edge of the open waters (Appendix 4).

Stratification due to river inputs would have increased dramatically during the last few days of May and the first week of June as the peak flows of the Mackenzie River spread beyond the landfast ice into the open lead (Figure 6.4A). Strong winds to the W and NW in late May and to the SW in early June (Figures 6.4A,B) likely contained the river plume to the west side of the shelf, initially minimizing the influence of the spreading plume on stratification in the waters close to the mooring sites SS-5 and ISC91-2. At least until about June 10, the stratification of the water column to the south and east of ISC91-2 and SS-5 was likely relatively weak and more easily disrupted by winds and ice movement. After June 10 in the export period, the winds favoured the spread of the river plume to the E and SE. It is not possible to determine definitively whether the river plume extended to the shelf break after June 10 or whether the predominant SE winds in the export period directed the plume predominantly to the SE

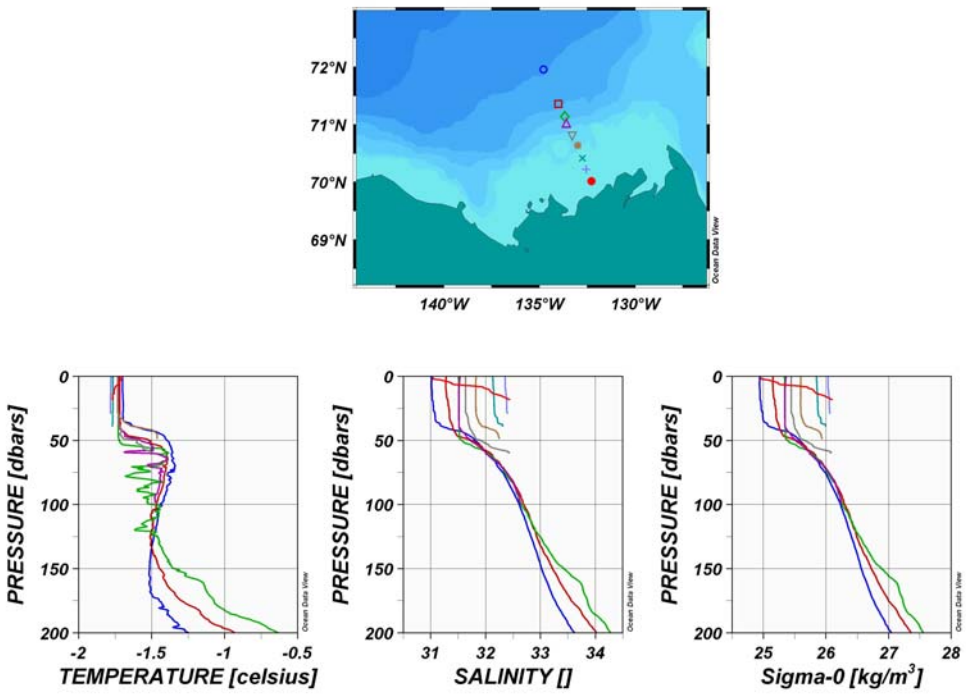

Figure 6-8 Temperature, salinity and density profiles of the top 200 m in CTD line across the shelf in early spring of 1991 (March 21 to 24, 1991). Map shows locations of the stations and the depth contours are at 50, 100, 500, 1000, 2000, and 3000 m. Data courtesy of Dr. H. Melling, Institute of Ocean Sciences. (Plot done using Ocean Data View software, Schlitzer, R., Ocean Data View, http://odv.awi.de, 2009)

along the Tuktoyaktuk Peninsula. Given that the winds during June and July were weaker than during May, the plume most likely extended out as far as the shelf break at least intermittently enhancing the stratification near the mooring sites.

6.1.5 Shelf edge currents (site ISC91-2)

Over the pre-export period, net current flow at site ISC91-2 (20, 43, and 70 m; Figure 6.1) is to the SW, in general agreement with the direction of ice displacement (Figures 6.5B and 6.12). Both the speed of the ice displacement and the current speeds at ISC91-2 are much lower during the first trap interval than during in the second and third intervals (Figure 6.4A). The increase in current speeds coincides with the increase settling of terrigenous sediment in the traps at site SS-5 during the pre-export period, likely reflecting increased resuspension of shelf sediments on the NE portion of the Mackenzie shelf or the Banks Island shelves.

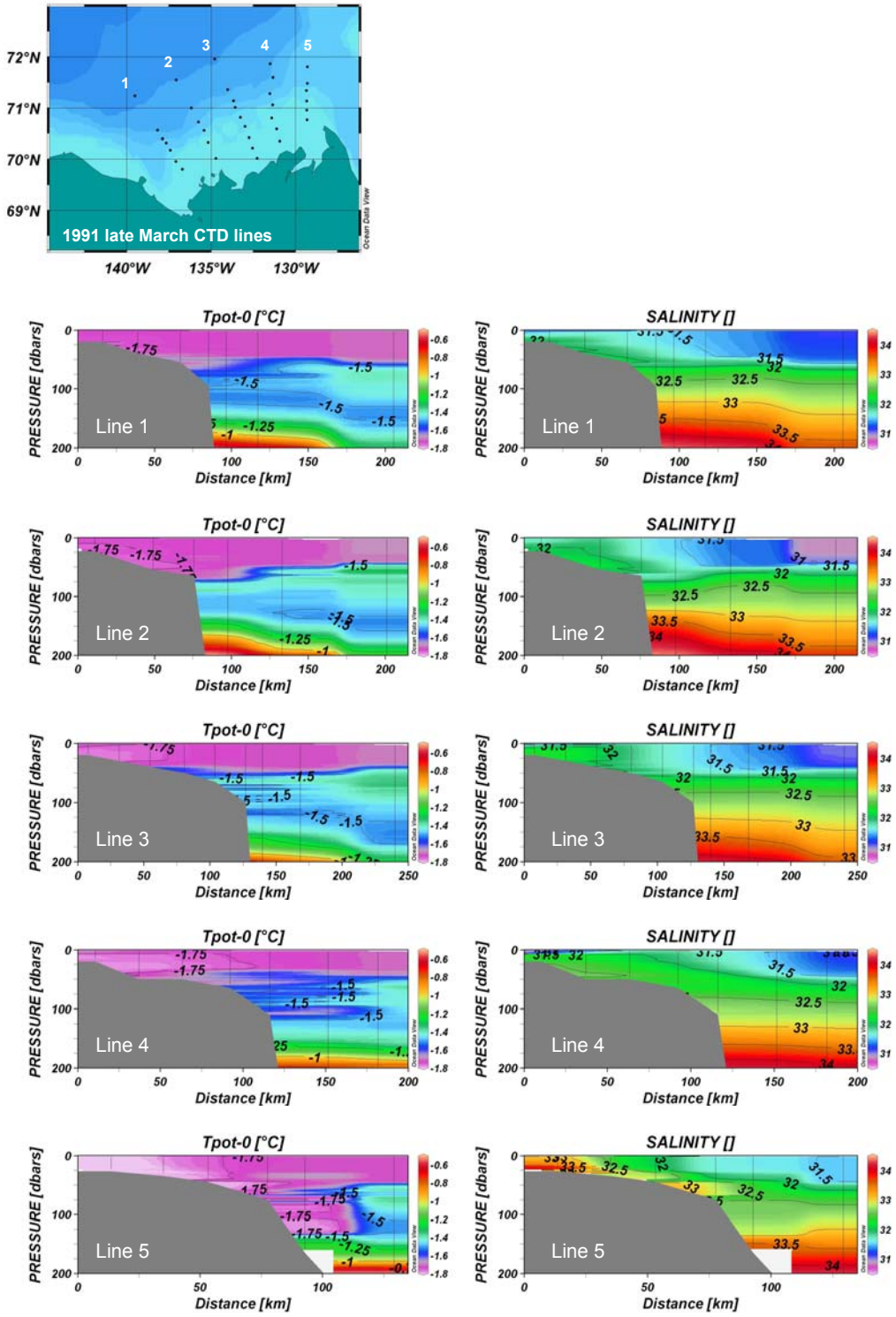

Figure 6-9 CTD lines across the shelf in late March of 1991. Solid lines on the contour plots indicate the positions of the stations. Data courtesy of Dr. H. Melling. (Plot done using Ocean Data View software, Schlitzer, R., Ocean Data View, http://odv.awi.de, 2009)

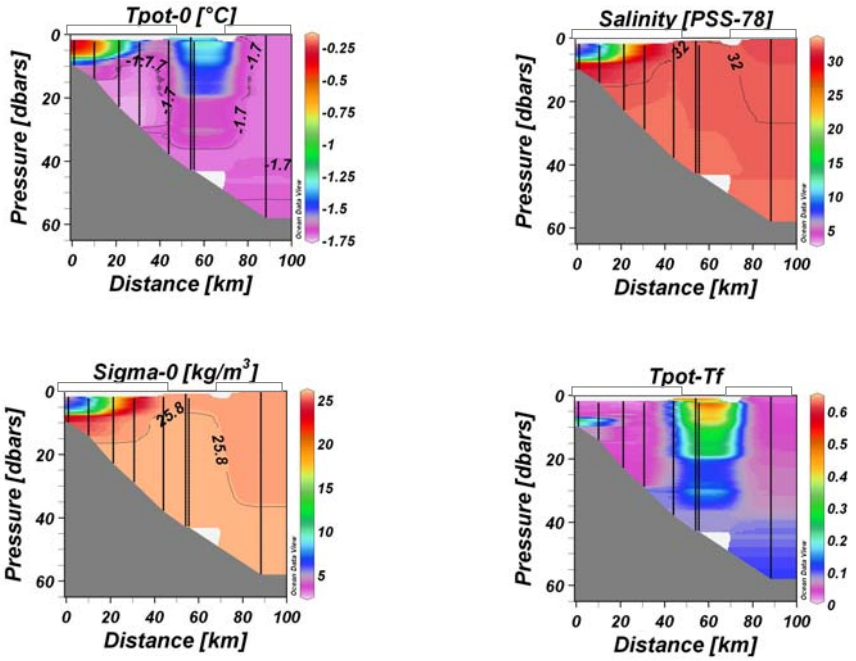

Figure 6-10 Cross-sections of Mackenzie Shelf showing early spring conditions in the early opening lead on May 3, 1991 before the onset of the bloom. Also shown on the cross-section plots is the approximate position of the ice (only one station is in the open lead, all others are ice covered). See the map in Figure 6.10 for the location of the section and the position of the ice edges relative to the transect stations. Plots are of potential temperature (Tpot-0), salinity, density (sigma-0), and the difference between the potential temperature and the freezing temperature (Tpot-Tf). (Plot done using Ocean Data View software, Schlitzer, R., Ocean Data View, http://odv.awi.de, 2009)

From the beginning of June to July 22, the 20 m currents at the shelf edge at ISC91-2 follow the same general trajectory as ice displacement (Figures 6.5B and 6.12) but directions are not as coherent at the 43 m and 70 m depths. However, the net displacement over the upper 70 m is to the SW (Figure 6. 12). Notably, there are features suggestive of eddies at the 43 and the 70 m depths. At 70 m, the currents make two full 360 º rotations in the first two weeks of July, once clockwise and once counter clockwise. It is possible that the inferred eddies formed on the shelf and subsequently transported water and suspended sediments seaward.

Over the post-export period (July 22 to August 30), current trajectories at site ISC91-2 followed a line predominantly SW to NE with a net displacement to the NE despite five distinct reversals. (Figure 6.12). In contrast, the net displacement of heavy ice over site ISC91-2 during this period is to the SE (Figure 6.5B). Although the water column and ice displacement trajectories differ, the timings of changes in direction

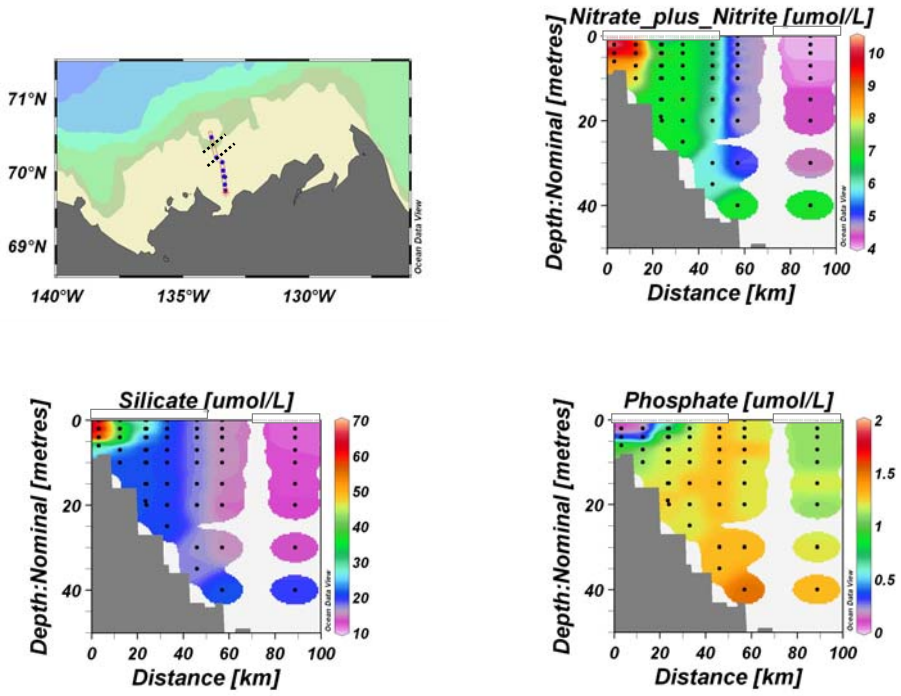

Figure 6-11 Cross-sections of nutrient levels (nitrate plus nitrite, silicate and phosphate) on the Mackenzie Shelf on May 3, 1991 showing the early spring conditions on the shelf before the onset of the bloom and during the very early opening of the lead. Also shown on the cross-section plots is the approximate position of the ice (only one station is in the open lead, all others are ice covered). The map shows the transect location and the dotted lines show the approximate location of the ice edge relative to the stations. (Plot done using Ocean Data View software, Schlitzer, R., Ocean Data View, http://odv.awi.de, 2009)

between the ice and the water column at site ISC91-2 match closely. The current patterns suggest that the resuspended sediments derive from the W and SW.

6.1.6 Currents over the shelf slope (site SS-5)

In the pre-export period, the currents at site SS-5 over the slope are markedly different from those at site ISC91-2. Current data at 99 and 206 m at site SS-5 are represented by a progressive vector diagram (Figure 6.13) and a plot of current speeds over the mooring deployment period (Figure 6.14). At 99 m, from April 22 to about May 8, the current direction changes from south to southeast and remains southeast until the end of May (Figure 6.13). At 206 m depth, the current speed is generally higher (Figure 6.14) and the direction swings from south to the east during the same period (Figures 6.13). These swings are towards the shelf break suggesting that water from 99 m may be

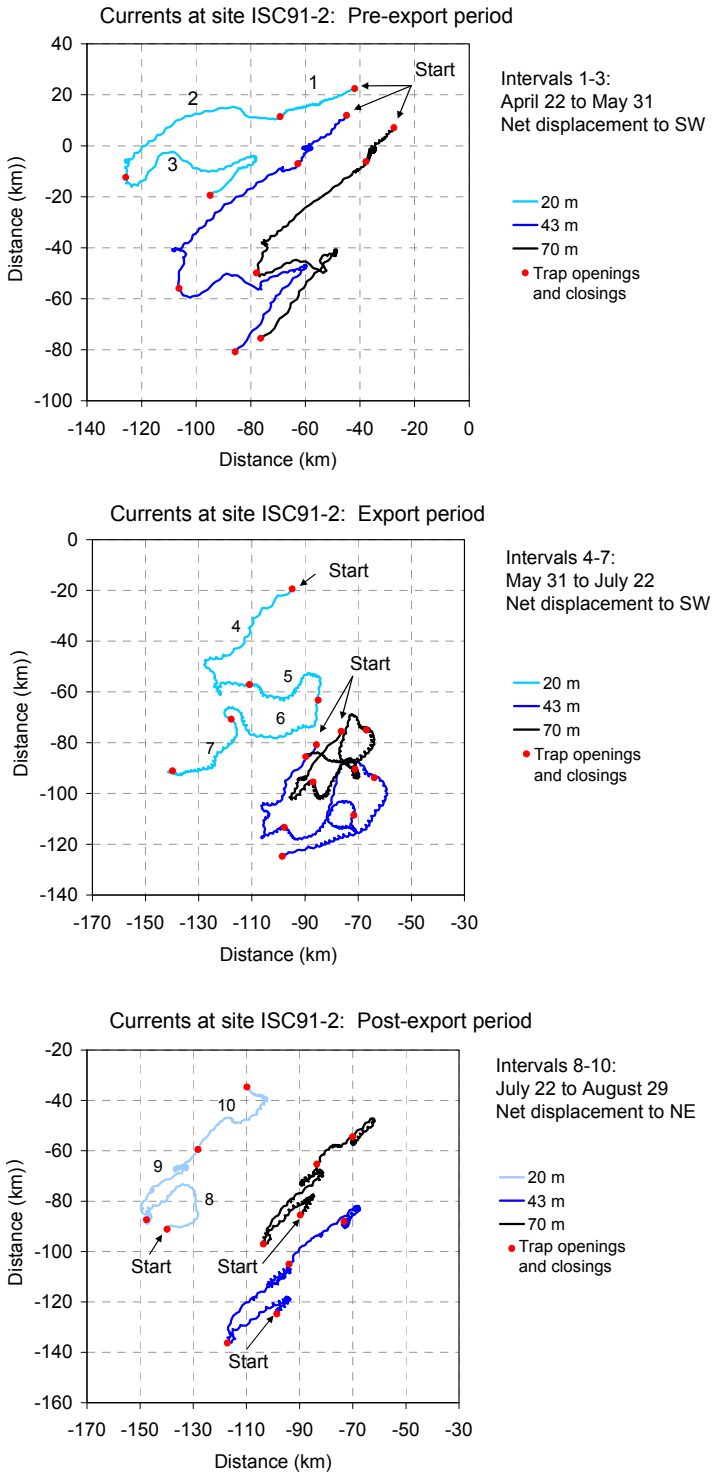

Figure 6-12 Progressive vector diagram of currents at the shelf edge (site ISC91-2). Periods coinciding with trap openings and closing of sediment traps at site SS-5 are shown.

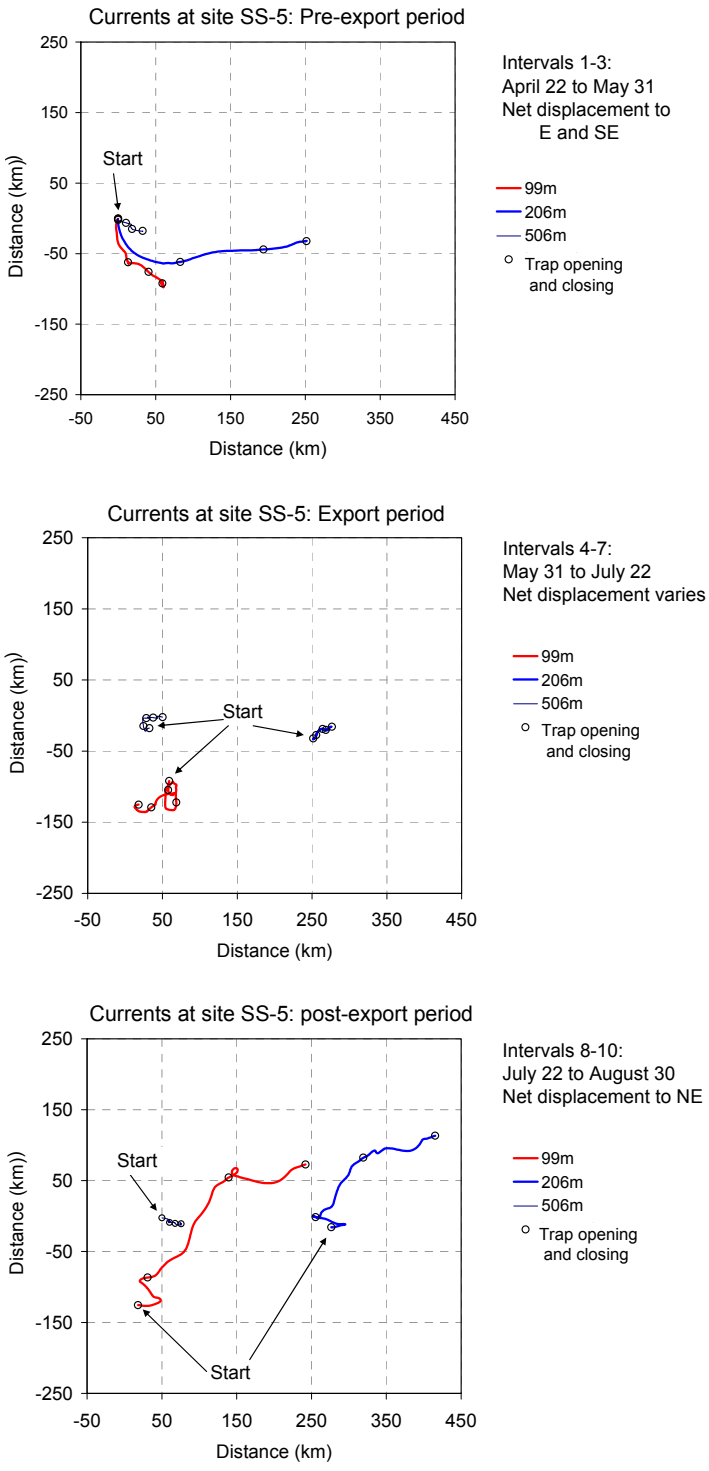

Figure 6-13 Progressive vector diagram of currents over the slope at site SS-5 showing timing of sediment trap intervals.

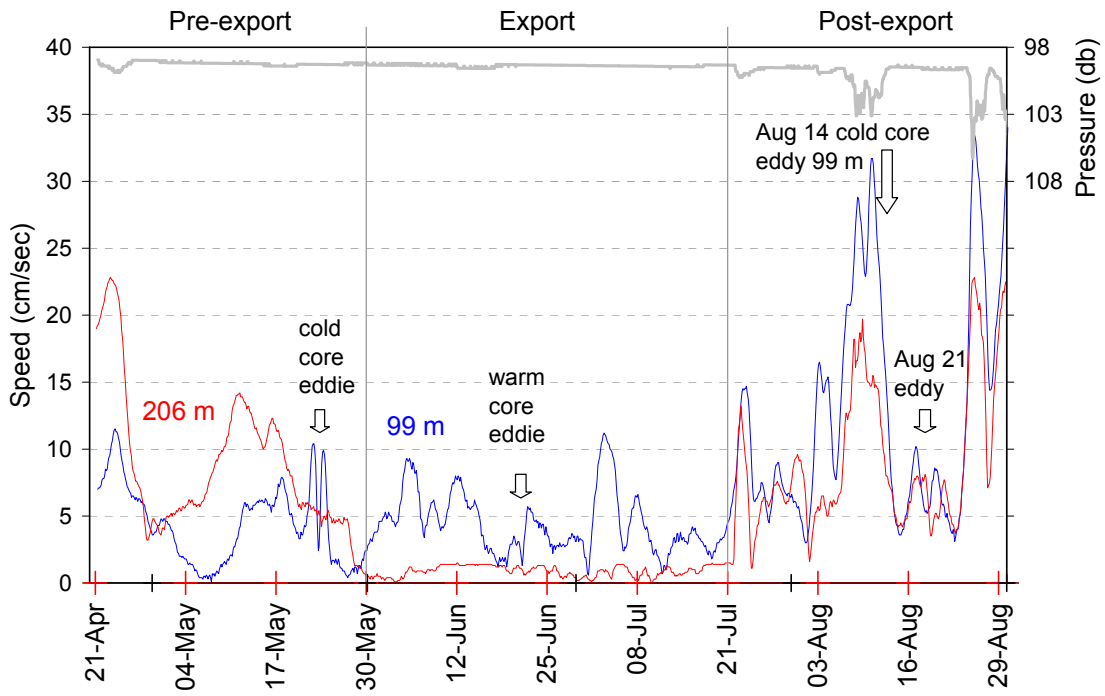

Figure 6-14 Current speeds at site SS-5 represented by red at 206 m and blue at 99 m. A pressure sensor at 99 m monitors where high current speed pulled the mooring down.

welling up onto the shelf during this period. At the same time, water from 206 m may move up the slope closer to the shelf edge.

A small distinct cold-temperature core anticyclonic eddy that very likely formed on the shelf passed over site SS-5 from May 23 to May 26, and rotated 360 degrees (Figure 6.15; also see Section 6.1.7). Maximum current speeds of 10.4 cm sec^{-1} in the southeast direction and 9.9 cm sec^{-1} in the northwest direction suggest that the center of the eddy passed directly over site SS-5. The core temperature of -1.73 ºC, some 0.3 ºC colder than the waters through which it passed, matches temperatures seen on the shelf and in the surface layer at the end of March, suggesting the eddy was of at least a two-month duration. Given ~10 cm sec^{-1} current speeds as observed, such features could theoretically contribute to the transportation of particles or aggregates finer than (roughly) medium sand to and beyond the shelf break, although they would not exert sufficient critical shear stress to resuspend cohesive fine particulates (Hjulstrom, 1939).

During the export phase at SS-5 (May 31 to July 22), the current speeds at 99 m ranged from 0.3 to 11.1 cm sec^{-1} and the net displacement was about 50 km to the SW.

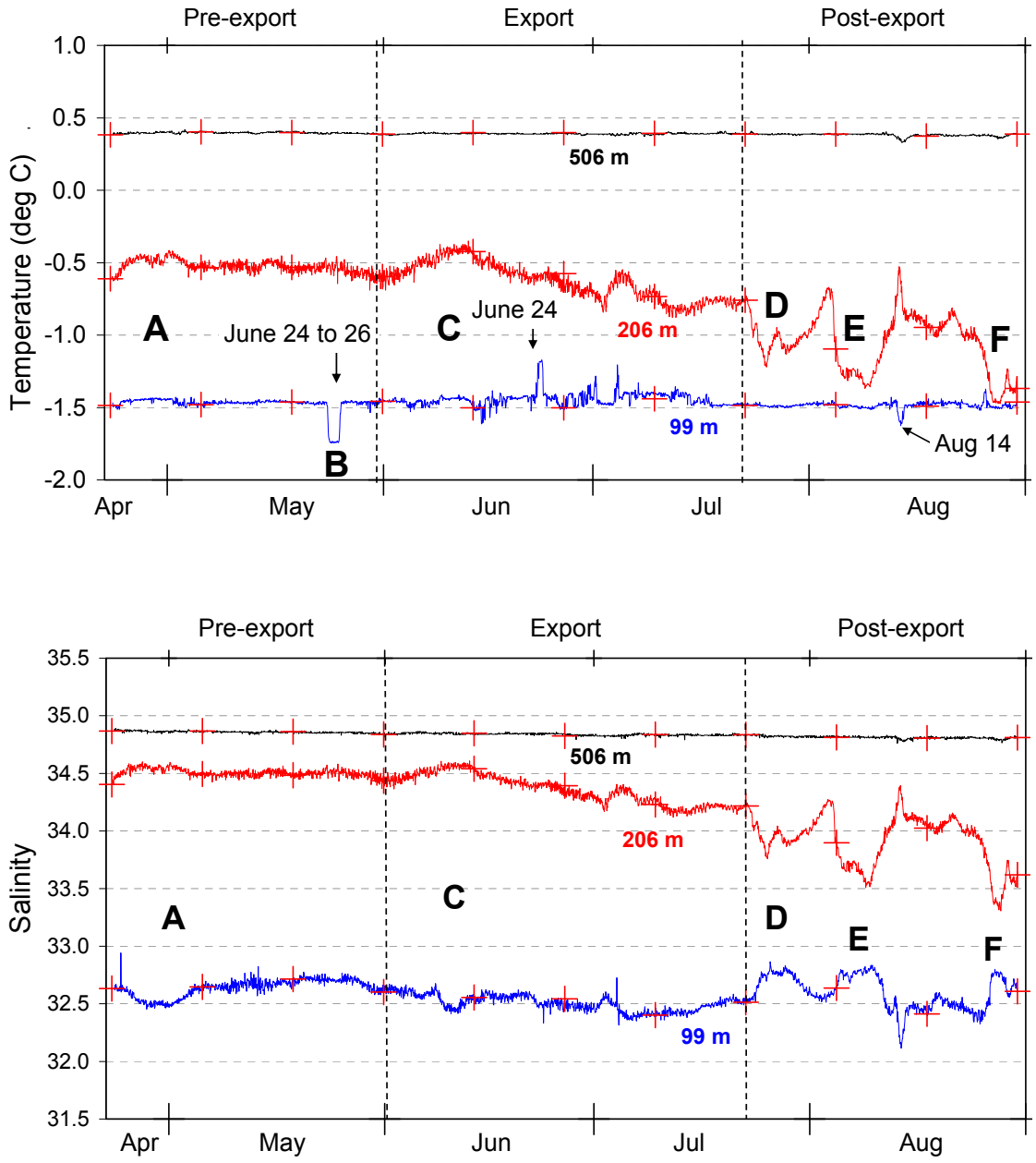

Figure 6-15 Temperature and salinity records for site SS-5 at 99, 206, and 506 m for the pre-export, export, and post-export periods of the trap deployments. The red crosses indicate the trap intervals.

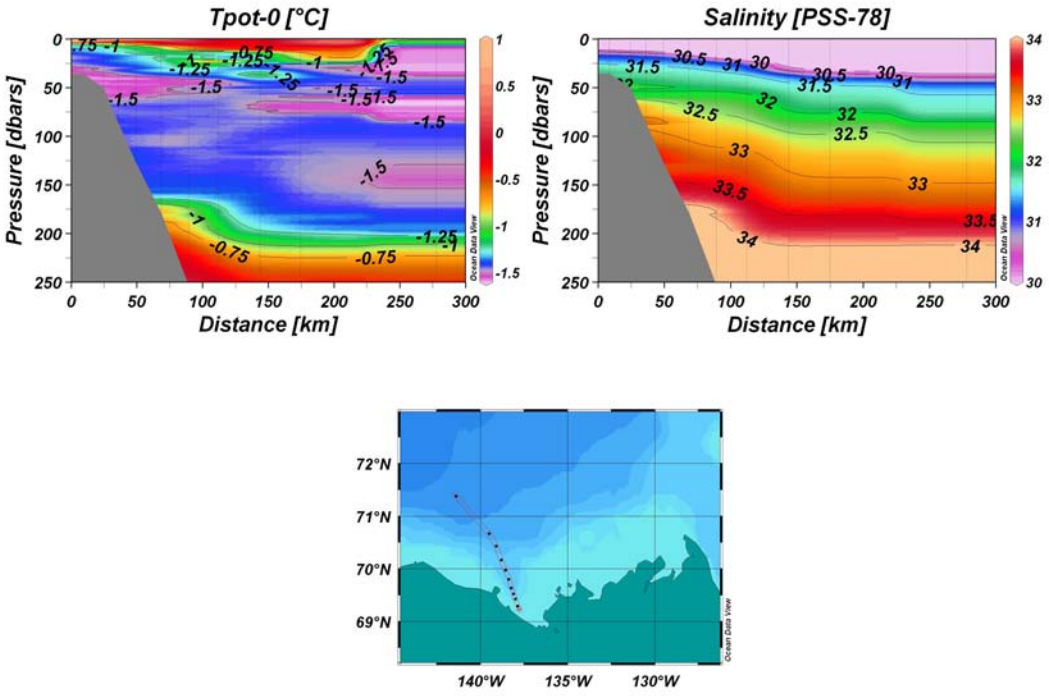

Figure 6-16 Cross-section of Mackenzie Trough in September 1991. (Plot done using Ocean Data View software, Schlitzer, R., Ocean Data View, http://odv.awi.de, 2009)

The current direction varied considerably, exhibiting circular rotations, again suggestive of the passage of eddies (Figures 6.13 and 6.14) or reversals of motion related to upwelling and downwelling. Temperature and salinity data discussed in the next section do however lend some support to the idea of eddies at site SS-5 during this period. During the export period, measured current speeds at 206 m of < 1.5 cm sec^{-1} (Figures 6.14 and Table 6.1 – average speeds at the two mooring sites) may be real or may reflect a temporary stalling of the rotor. However, there does not appear to have been any problem with the rotor in the later part of the record. Regardless, at such very low current speeds, the direction data are not useable (Figure 6.14).

During the post-export period, the net displacement is to the NE for both sites SS-5 and ISC91-2 (Figures 6.12 and 6.13). There is no obvious evidence of eddies passing over the site during this time, and current speeds are generally higher at 99 m than at greater depth (206 m, Figure 6.14), reaching episodic maxima of ~33 cm sec^{-1} (Figure 6.14).

6.1.7 Temperature and salinity relationships

A series of CTD lines over the Mackenzie Shelf provide an early spring snapshot of the distribution of water properties in the top 200 m under complete ice cover (Figure 6.9) before the onset of primary production. At that time, a surface pool of cold low salinity water ~ 40 m deep sat off the shelf (31 to 31.5 PSU; -1.6 to -1.7 ºC), while cold, higher salinity water lay over the shelf (~ 32 PSU, -1.7 to -1.8 ºC). This distribution indicates a pre-conditioning over the fall and winter (1990 - 1991) that moved fresh shelf waters offshore under the influence of westerly winds and later brought higher salinity waters up onto the shelf when easterlies were prevalent. In addition, brine rejection during the formation of new ice likely contributed to the higher salinities on the shelf (Melling, 1993). The observed temperature maximum at about 60 m is most probably a remnant of warming from the previous summer (Figures 6.8 and 6.9).

In this early spring period of 1991, the mixed layer extends down to a maximum of 50 m over the shelf and the slope. From about the 100 to the 500 m isobaths, across the shelf break, density differences controlled by temperature drive an interleaving between cold dense shelf waters and waters over the slope. Significant interleaving occurs between the depths of about 50 and 150 m (Figures 6.8 and 6.9), and it is likely that this process continued throughout April and May (and possibly into June) along with the westward displacement of the sea-ice. Interleaving waters may entrain resuspended sediments, and may contribute to the off-shelf transport of resuspended sediments in the spring. Similar phenomena occur in other continental shelf/slope areas (see for example Heussner et al., 2006; Perlin at al., 2005; Monaco et al., 1990).

Keeping in mind that the T and S data represent only three levels in the water column (99, 206, and 506 m) at site SS-5, they provide a good indication of the complexity of the physical processes occurring over the slope. When examined along with the current records, some of the temperature and salinity changes at 99 and 206 m are consistent with the pattern expected for cyclonic eddies that span the two depths (see for example features A and C in Figure 6.15). Note that with the data available, positive confirmation that these are eddies is not possible. An alternate explanation invoking upwelling with deformation of the isopycnals also fits the observed data.

In the post-export period, water column temperature and salinity changes were much more dynamic. The salinities at both 99 and 206 m were more variable and the changes at the two depths occurred in opposition (see features D, E, and F in Figure 6.15). At 206 m, the temperature and salinities increases and decreases tracked each other, whereas at 99 m the temperature varied relatively little as compared to the changes in salinity. The pattern observed in the salinity and temperature record in the post-export period is consistent with the passage of a front that possibly preconditioned earlier in the year and on a shelf much further to the west. The front spans the depths 99 and 206 m, and the water properties at each of these depths approach the water properties in the core of the front with a salinity of between about 32.8 and 33.3 PSU and a temperature close to -1.5 ºC. These properties are in keeping with winter-transformed Pacific waters described by Pickart et al., 2005 and Nikolopoulos et al., 2008. A cross-section from September 1991 of Mackenzie Trough to the west displays a core of water between about 100 and 200 m with these characteristics (Figure 6.16). This water mass could have been formed off the shelf in the Chukchi Sea or along the Alaskan Shelf. To the west and east of Barrow Canyon, an eastward flowing boundary current has these characteristics and in addition, is associated with increased levels of suspended sediments (Pickart et al., 2005; Nikolopoulos et al., 2008). Water formed 900 km to the west off the Chukchi shelf would take about 3.5 months to arrive at site SS-5 at an average current speed of 10 cm sec^{-1}. At a distance of 500 km to the west, the water mass would take about 2 months to arrive at site SS-5.

6.1.8 Nutrients in the water column in spring and late summer

Phytoplankton require the major nutrients nitrate (N), silicic acid (Si), and phosphate (P) for growth and cannot take advantage of other favourable conditions (light and stratification) unless these nutrients plus other major and trace nutrients are available. The relative proportions of these nutrients affect the growth rates, the relative uptake rates, and the composition of the phytoplankton community (Sakshaug, 2004).

At SS-5, the biogenic export peak is dominated by a diatom bloom, and the Si:N ratios of the settled material are very high (Figure 3.9e; maximum Si:N ratio ~ 20). The Si:N uptake ratio (mol:mol) of diatoms is ~1 for diatoms cultured in nutrient replete conditions (Brzezinski, 2003), so the high Si:N ratios of the exported material almost

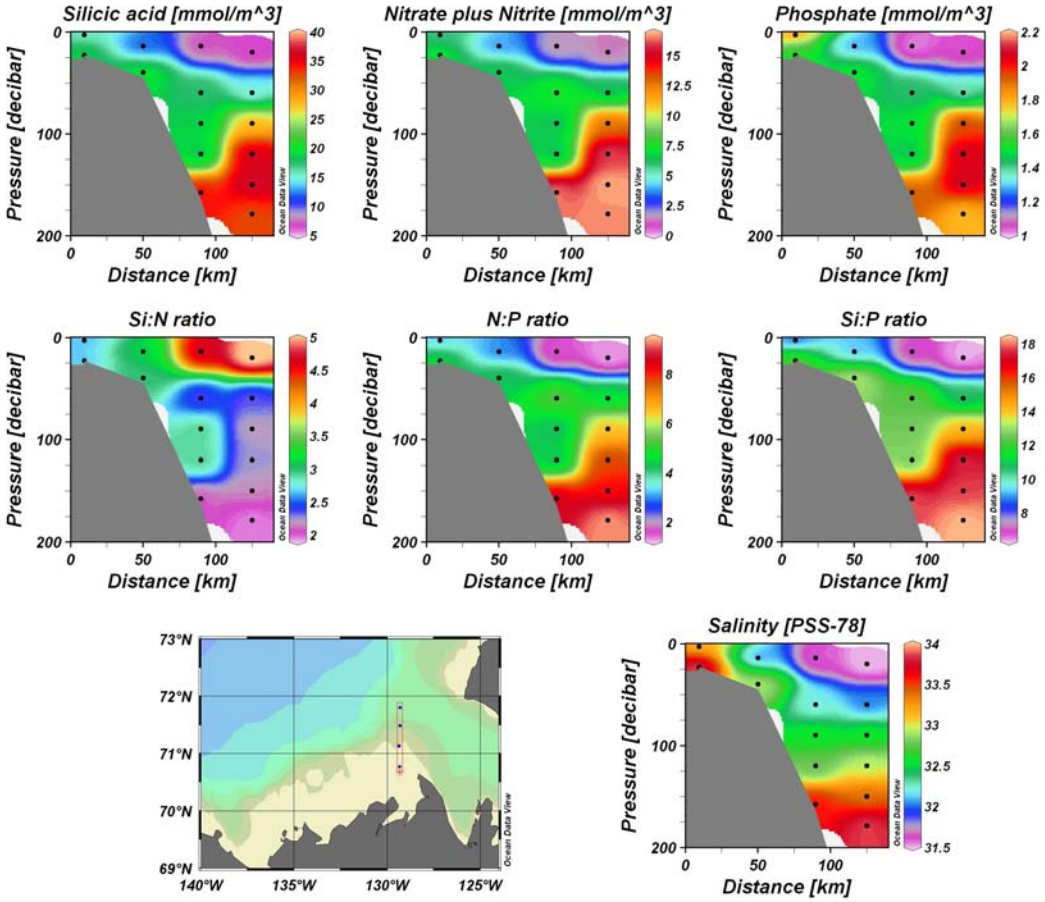

Figure 6-17 Cross-section on eastern side of Mackenzie Shelf of nutrients (N, Si, and P), nutrient rations, and salinity in late March 1991. (Plot done using Ocean Data View software, Schlitzer, R., Ocean Data View, http://odv.awi.de, 2009)

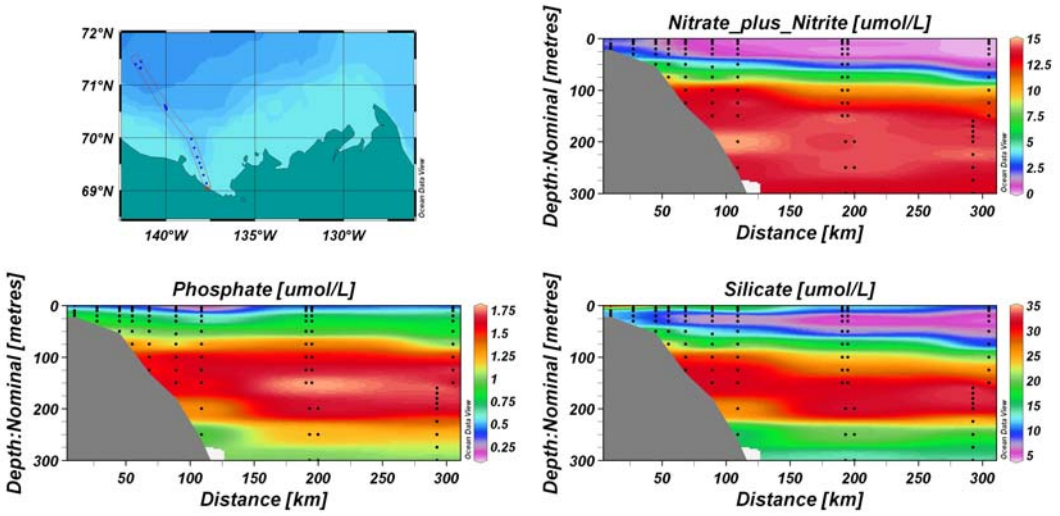

Figure 6-18 Cross-sections of nutrient data over the Mackenzie Trough in late summer of 1991. (Plot done using Ocean Data View software, Schlitzer, R., Ocean Data View, http://odv.awi.de, 2009)

certainly indicate rapid remineralization of N after export relative to slow dissolution of opaline frustules. They may also indicate that Si becomes limiting before N in circumstances where N is recycled quickly in the surface waters; this can lead to the termination of a diatom bloom and the ascendance of other phytoplankton species (Sakshaug, 2004). Alternatively, high Si:N ratios are also typical of Fe-limited diatoms (Hutchins and Bruland, 1998) but it is not at all certain that this area is iron limited.

Nutrient data collected by sampling through the ice, on and beyond the Mackenzie Shelf in late March in five consecutive years (1986-1991) are summarized in Table 6.2. Although N, Si, and P concentrations vary considerably at all depths, concentrations are lower in the top 50 metres and increase in underlying waters. The data available for late March 1991 were obtained from four stations on the eastern side of the shelf (Figure 6.17). Samples were collected through the ice at least two weeks before open water appeared on the east side of the shelf. The nutrient distributions indicate that denser shelf waters may have flowed seaward and been redistributed at a depth of ~100 m. Indeed, nutrient concentrations were higher in shelf waters that in similarly shallow waters offshore and matched properties extending down to at least 125m along the shelf slope (Figure 6.17).

Nutrient depletion typically occurs in the surface waters over the shelf by the end of the summer (Macdonald et al., 1987), with some fraction of the nutrient inventory exported in dissolved or particulate form, and the remainder primarily recycled. A comparison of the Si and N inventories in the surface layer in March to the inventories of BIOSI and N collected in the traps over the spring/summer period highlights the relative export of Si and N at site SS-5, and allows the degree of recycling to be estimated. Based on the data in Table 6.2, the inventory of dissolved inorganic N in the top 50 m of water column in late March 1991 ranged from 60 to 375 mmoles m^{-2}. The amount of particulate N collected in the three traps at site SS-5 over the 130-day spring/summer period represented only 24 to 30 % (14.8 to 17.5 mmoles m^{-2}) of the lowest value calculated for the surface-layer dissolved N inventory (60 mmoles m^{-2}). Assuming that N was fully depleted over the course of the light-replete period, and considering only the vertical dimension then at least 70% of the surface-layer dissolved N sequestered by phytoplankton was recycled back into the water column before the descending particles

reaching the trap depths. Substituting the upper range of the inventory in the same comparison yields a recycling rate >95%. One possibility that should be investigated is that significant dissolution occurs in the sampling cups after the particles have been trapped (Anita, 2005).

In contrast to N, the recycling rate of Si is much lower: the inventory of dissolved Si in the top 50 m ranges between 250 and 1050 mmoles m^{-2} and the amount of particulate Si collected in the traps over the same period (176 to 223 mmoles m^{-2}) represents 17 to 89 % of the surface-layer inventory. Thus, proportionally much more Si than N is exported to depth at the shelf edge. In late summer 1991, the few available nutrient data show that except for stations closest to shore in the 30 to 50 m depth interval, N was depleted (Figure 6.18). A thin fresh layer, almost certainly of riverine origin, was present at the surface at this time, and extended all the way to the farthest station offshore. The layer was depleted in P and N but contained moderate levels of Si, suggesting that phytoplankton growth had reached a point of nitrogen limitation.

6.1.9 Physical factors important to primary productivity

At site SS-5, primary productivity was light limited in May due to heavy ice cover over the site (see section 6.1.1), and yet, the abrupt export of a diatom bloom in early June (Figure 6.2) indicates that the bloom was well underway in May in the open waters of the expanding lead over the shelf. It likely proceeded as a spring ice-edge bloom following the westward displacement of the ice-edge and leaving nutrient depleted water in its wake. Light conditions, nutrient levels, and the developing thermal stratification within the lead in May favoured high primary productivity (Figures 6.10 and 6.11; Macdonald et al., 1992; Borstad and Kerr, 1994). Minimal primary production had occurred by late April / early May as indicated by very low chlorophyll a levels (< 0.2 mg m^{-3}) in the surface waters in the lead and at the lead edge (Borstad and Kerr, 1994). Since neither light nor nutrients were limiting within the lead in early May, the development of thermal stratification in the lead was the key factor for the initiation of the bloom. The bloom took on strength during May as the thermal warming of surface waters, and eventually the fresh water from ice melt, increased the stability of the water column sufficiently to counteract mixing due to winds and ice displacement. There are numerous examples in the Arctic of blooms depleting the surface waters of nutrients as they follow

a retreating ice-edge, and the timing of these ice-edge blooms varies widely (April to July) depending on the geographical area and the specific physical forcing (Sakshaug, 2004 and references therein).

As the ice edge moved beyond site SS-5 in early June, the bloom was already well underway and export of material from the euphotic zone was occurring. The mechanism for the prolongation of the diatom bloom over the 52-day export period is a combination of adequate light and stratification combined with an adequate supply of nutrients. Although a conservative inventory of nutrients in the top 50 m indicates adequate nutrients to account for the fluxes of N and Si in the traps, renewal of nutrients may have been occurring through upwelling, from the advancing river plume, and/or by wind mixing. In addition, with an ice-edge bloom, waters replete in nutrients may be uncovered as the ice-edge moves. In the spring of 1991, the nutrient profile across the shelf in early May suggests that the westward moving ice edge may uncover relatively nutrient depleted waters from the previous season (Figure 6.11) but it is uncertain how this would change as the lead expands. Using semi-continuous culture techniques, Lovejoy et al. 2002 have demonstrated that renewing nutrient supplies by advective processes is the key factor in the maintenance of a prolonged diatom bloom. Good spatial and temporal information on nutrients throughout the pre-export and export periods would help resolve important questions regarding the progress of the bloom.

The timing and extent of this early opening on southern and eastern portions of the Mackenzie Shelf in 1991 is very similar to the early opening in the same area observed in 1998 (Arrigo and van Dijken, 2004; see Figure 2.2) where a phytoplankton bloom was well underway by mid-May following anomalous warming and very early stratification. In 1991, the spring warming was not as early or as dramatic as that experience in 1998.

Mechanisms leading to the export of the bloom over the 52-day period are not clear. It is very likely that there was more than one mechanism responsible for export of the bloom and there may be species-specific factors. Diatoms may have run their course to natural senescence according to specific growth cycles, and in the absence or incomplete grazing by zooplankton, been exported to depth (Passow, 1991; Sakshaug, 2004). Some diatom populations have subpopulations of paired cells, one that is sinking

and one that is actively dividing, and so there may be a certain proportion of the population being exported at any one time (Passow, 1991). If a shallow mixed layer developed due to melting ice cover, then depletion of N and/or Si may have contributed to export as well (Sakshaug et al., 2004 and references therein). Export of the diatom bloom was likely triggered in part by strong wind events that caused an increase in the depth of the mixed layer and a transport of cells below the euphotic layer such as is described for a study in the Northeast Water (NEW) polynya (Peasant et al., 2002). The 13-day collection intervals of the traps are too long to establish precise links between specific wind events and export events. Termination of the diatom bloom at site SS-5 in mid-July was clearly due to light limitation resulting from the southward displacement of the heavy ice pack back over the mooring site and over the nutrient depleted waters over the shelf. The position of the ice edge is clearly the key controlling factor for primary production at site SS-5 in the spring of 1991.

Identification of the factors determining the settling rates of the biological material is beyond the scope of this study. However, the collection of roughly equivalent amounts of biological material at the trap depths (199, 349, and 499 m) during the export period suggests that the settling rates were very high. Diatom aggregates have sinking rates between 50 and 200 m d^{-1} (Passow, 1991 and references therein; Sarthou et al., 2005 and references therein). At these rates, the material would descend to the 499 m trap in 2.5 to 10 days, and travel horizontally with the prevailing currents in the order of 11 to 86 km during the descent (for a range of current speeds estimated at 5 to 10 cm/sec). Given this and the net displacement to the SW of currents at the shelf edge during the export period, the biogenic material collected in the traps could be the remnants of a bloom from a considerable distance to the NE of the mooring site.

The dramatic increase of both terrigenous and biogenic fluxes at SS-5 over the export period at all three trap depths suggests a relationship between the diatom bloom and the large inputs of freshwater and suspended particulate material by the Mackenzie river in late May/early June (Figures 6.2 and 2.3). For the first half of June, it is unlikely that the river plume had a direct affect on the diatom bloom at site SS-5 as the wind likely contained the plume to the west side of the shelf. On the other hand, in the last half of June with the winds favourable for a swing of the plume to the east, the plume could have

extended sporadically beyond the shelf edge near site SS-5. This may have resulted in enhancement of the diatom bloom due to increased stratification and injection of nutrients from the plume. Acting in the opposite direction, the presence of high levels of suspended particles in the plume could have increased export rates of the bloom due to a reduction of available light and to possible unfavourable effects on the viability of the cells. As described for other large river systems, the spreading of the forward edge of the Mackenzie River plume is likely favourable to diatom blooms (McKee, 2003). The river plume spreading into the early opened waters over the shelf would have divested itself of most of the riverine particulate matter at the leading edge (McKee, 2003 and references therein) such that adequate light penetration and surface layer stratification at the leading edge would favour primary production. These favourable light levels along with stratification, mid-range salinities, and nutrient availability all favour the boom and bust style of diatom growth (Ragueneau et al., 2000, Dagg et al., 2004). Given that the plume is mobile and can spread quickly, it is important to keep in mind that the river plume could have been important at least sporadically in the prolongation of the diatom bloom or to the initiation of export from the euphotic zone at site SS-5. There is not enough information to clearly establish either the behaviour or the particulate load of the plume over the export period, and these are important considerations for future studies.

The high levels of both terrigenous and biogenic material during the bloom period strongly suggest an association between these particles during the export of the bloom. The sinking diatoms may have facilitated the sinking of fine terrigenous particles in the water column by processes of aggregation and flocculation during descent. In addition, the presence of fine particles in the plume may have influenced the export of the diatoms from the surface waters by acting as ballast. It is possible that during the descent, the "stickiness" of the diatom cells accumulate suspended inorganic particles that act as ballast and increase sinking rates. A reasonable maximum estimate of total suspended solids in waters at the shelf edge in spring would be around 0.1 g m^{-3}, which represents 50 gm of material in a column of water 500 m deep by one square meter. Sinking chains of diatoms, especially if the cells are intact, may sweep up some of this suspended material during descent and in addition may reach a saturation point in their ability to do so. It is possible that both these mechanisms contributed to the export of material to the

sediment traps but there is no direct evidence to support or disprove the existence of these mechanisms. This is a large area of debate and worthy of further investigation (Passow, 2006 and references therein).

6.1.10 Summary of physical data for site SS-5

Based on sediment trap data and physical evidence, particle fluxes over the slope reflect interactions between solar radiation, winds, ice cover, ocean currents, water column structure, and turbid river inputs. The biogenic and terrigenous components exhibit some similarities, but also distinct differences, both in temporal patterns of fluxes and in trajectories inferred from physical forcing. The three periods, initially chosen solely based on the biogenic export peak (pre-export, export, and post-export), exhibit unique and markedly different combinations of physical forcing integrally important to the observed flux patterns.

Upwelling conditions and a rapid early opening of the waters over the shelf characterized the pre-export period. In addition, increasing solar warming led to progressive stratification in the opening lead in May due initially to surface warming and later to ice melt. The injection of freshwater and suspended sediments from the Mackenzie River freshet occurred at the end of this period and was not important to the pre-export fluxes over the slope at site SS-5.

The highly terrigenous fluxes at site SS-5 in the pre-export period that occurred under heavy ice cover are attributable to resuspension of bottom sediments and movement of the resuspended material out over the slope with ocean currents and in bottom and mid-water nepheloid layers. As early as the beginning of May, there was clear evidence of inorganic resuspended shelf sediments in the opening lead (Borstad and Kerr, 1994). The movement of heavy ice keels over the shelf likely resuspend sediments either by direct gouging of the bottom sediments or by increasing bottom currents sufficiently to cause resuspension commensurate with the cohesiveness of the sediments. Upwelling, relaxation of upwelling, and downwelling cycles likely resuspend sediments on the slope (as described by Perlin et al., 2005). Finally, strong winds to the west over stretches of open water may resuspend sediments over shallower areas of the shelf. Once resuspended, particles are subject to transport with the prevailing ocean currents, in mid- and bottom nepheloid layers, and through the interleaving of cold dense shelf waters with

the waters over the slope. As emphasized in O'Brien et al., 2006, these mechanisms of resuspension and particle transport all warrant further investigation as the presence of nepheloid layers, although widely reported in this area, are poorly understood. In addition, the currents to the SW at the shelf edge and over the slope to the S and SE during this period suggest that the suspended particles are transported preferentially along the slope rather than across the slope to the deep basin.

Small increases in biogenic flux at the end of the pre-export period (at 199 and 499 m) coincide with the approach of the ice edge to site SS-5 and are the first evidence of the diatom bloom already underway in the lead. The cells arriving at the bottom trap may have travelled a horizontal distance up to about 85 km and taken 2.5 to 10 days for the descent following roughly the trajectory of the shelf edge water in the third interval of the trap collection (Figure 6.12). The biogenic material at the end of the pre-export period in the 499 m trap shows increasing values of $\delta^{13}C$ (Figure 3.7a). This provides evidence for the release of ice algae from melting ice (Tremblay et al., 2006; Belt et al., 2008) at the end of the pre-export period, and the development of stronger stratification of the water column due to ice melt providing a favourable environment for primary productivity.

The bloom period is characterized by alternating episodes of upwelling and downwelling favourable conditions, a large expanse of open water over the shelf, massive inputs of turbid Mackenzie River water onto the shelf, rapid melting of pack ice, net displacement of ice to the SW, shelf edge currents to the SW, and low apparent currents over the slope. For the first interval of the export period, it is unlikely that the river plume reached site SS-5, but after that, the plume may have sporadically extended beyond the shelf break near SS-5 but this is difficult to establish. During the bloom period, the ice edge is close to site SS-5 and the mooring is under reduced ice cover.

The terrigenous fluxes during the bloom period are elevated and the source is likely resuspended sediment from the slope and from shelf areas to the east. The behaviour of bottom and mid-water nepheloid layers following the large influx of riverine sediments onto the shelf is unknown.

The position of the ice edge as a controller of light availability appears to be the key factor controlling the diatom bloom. The export of biological material increases over

the first three intervals of the bloom period when site SS-5 is close to the ice edge under reduced ice cover and light is not a limitation. The biogenic fluxes decrease sharply as the ice edge moves south of the mooring site and light becomes limiting. Over this period, nutrients do not appear to be limiting and may be supplied by advection or localized upwelling at the ice edge. Minimum inventories for N and Si in the top 50 m are sufficient to account for the exported N and Si at site SS-5. Export of the diatom bloom over the 52-day period from the beginning of June to the third week of July is most likely due to a combination of natural senescence, disruption of weak stratification by wind mixing, nutrient limitation if the mixed layer is shallow, and sporadic light limitation if the bloom is carried under the pack ice. The relatively high (heavy) stable carbon isotope ratios ($\delta^{13}C$) in the exported material in early June provide evidence for the development of stratification due to ice melt at that time. These higher $\delta^{13}C$ values are indicative of the release of ice algae from the under side of the ice during ice melt (Belt et al., 2008 and references therein). This melt water likely contributed to stratification of the surface waters at the ice edge during June supporting the continued development of the bloom. The trajectories of the terrigenous and biogenic material may overlap if the exported diatoms act as a net and sweep up some of the fine terrigenous material during descent but this remains uncertain.

The post-bloom period is characterized by predominant downwelling favourable conditions and displacement of heavy ice to the SE back over the shelf. In addition, the net displacement of the currents both at the shelf edge and over the slope was to the NE, and there were frequent current reversals with a NE-SW alignment at the shelf edge. This period exhibited the highest current speeds over the slope and the T-S record identified the presence of a water mass with unique water properties consistent with winter-transformed Pacific waters (Pickart et al., 2005 and Nikolopoulos et al., 2008). Terrigenous fluxes in this period remained high at the middle and bottom traps and the source of this material was likely resuspended sediments from the slope and shelf to the W and SW of the site. It is possible that suspended particles transported down Mackenzie Trough are transported in a boundary current beyond the shelf break. There is no evidence of cross-shelf transport at this during this period, and the trajectory appears to be parallel to the shelf break and to the NE. The small biogenic fluxes in the post-bloom

period are likely the final remnants of the bloom that was terminated as the ice moved back over the nutrient depleted shelf waters.

Outstanding questions remain regarding sources and trajectories of both terrigenous and biogenic particles at this site. Most notably, many questions remain regarding the nature and behaviour of nepheloid layers and the dynamics of the river plume. The increase of terrigenous fluxes with depth clearly indicates that advective processes are important, and implies that key information is missed by not capturing transport processes close to the bottom on the shelf and over the slope. In addition, there are many questions remaining about the progress and termination of the diatom bloom and about the possible interactions between settling biogenic and terrigenous particles. Clearly, caution is required in extrapolating from these sediment trap fluxes without specific knowledge of the physical context.

6.2 Influence of physical forcing at site AM1-92

This section focuses on sources and trajectories of the terrigenous and biogenic materials delivered to the sediment traps at 290 and 490 m at site AM1-92(Figures 6. 19 and 6.20). There are two prominent features with respect to the fluxes at the site (Figure 6.20). The first is the highly terrigenous winter peak (December 29, 1992 to March 7, 1993; intervals 4 and 5 at the 290 and the 490 m traps). This peak defies conventional wisdom, in that sediment transport under full ice cover should be low, given minimal river inputs and lack of resuspension due to winds. The second feature is the summer peak with significant fluxes of both terrigenous and biogenic material (May 16 to July 25). Notably, the high fluxes in late June/July occurred only at 490 m and not at 290 m (Figure 6.20). Explanations for the occurrence of the prominent flux features are provided in the following sections.

6.2.1 Ice cover at site AM1-92 from fall 1992 to fall 1993

Descriptions of ice conditions on the Beaufort Shelf leading up to and during the September 1992 deployment of the mooring at site AM1-92 are based on Canadian Ice Service charts (http://ice-glaces.ec.gc.ca/App/WsvPageDsp.cfm?ID=11872&Lang=eng), Upward Looking Sonar (ULS) data from the AM1-92 mooring, and drifting ice buoy #

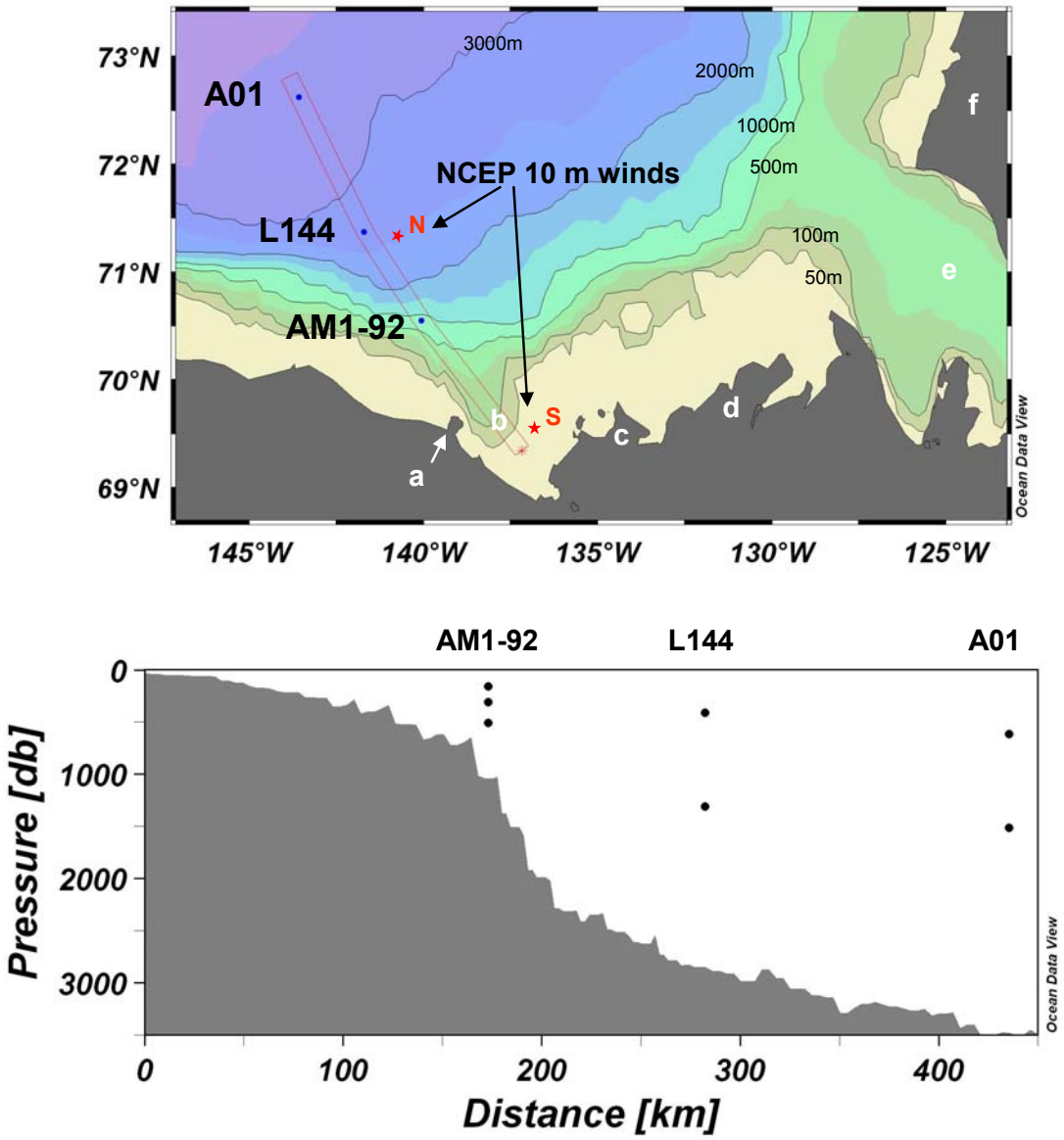

Figure 6-19 Locations of moorings AM1-92, L144, and A01. The location of the NCEP wind grid points used are indicated by the red stars and designate N and S. Also shown is a cross section of the shelf through the mooring sites and down Mackenzie Trough. Place names used in the text are indicated as follows: Herschell Island (a), Mackenzie Trough (b), Richards Island (c), Tuktoyaktuk Peninsula (d), Amundsen Gulf (e), and Banks Island (f). Ocean Data View program was used to create the plots. (Plot done using Ocean Data View software, Schlitzer, R., Ocean Data View, http://odv.awi.de, 2009)

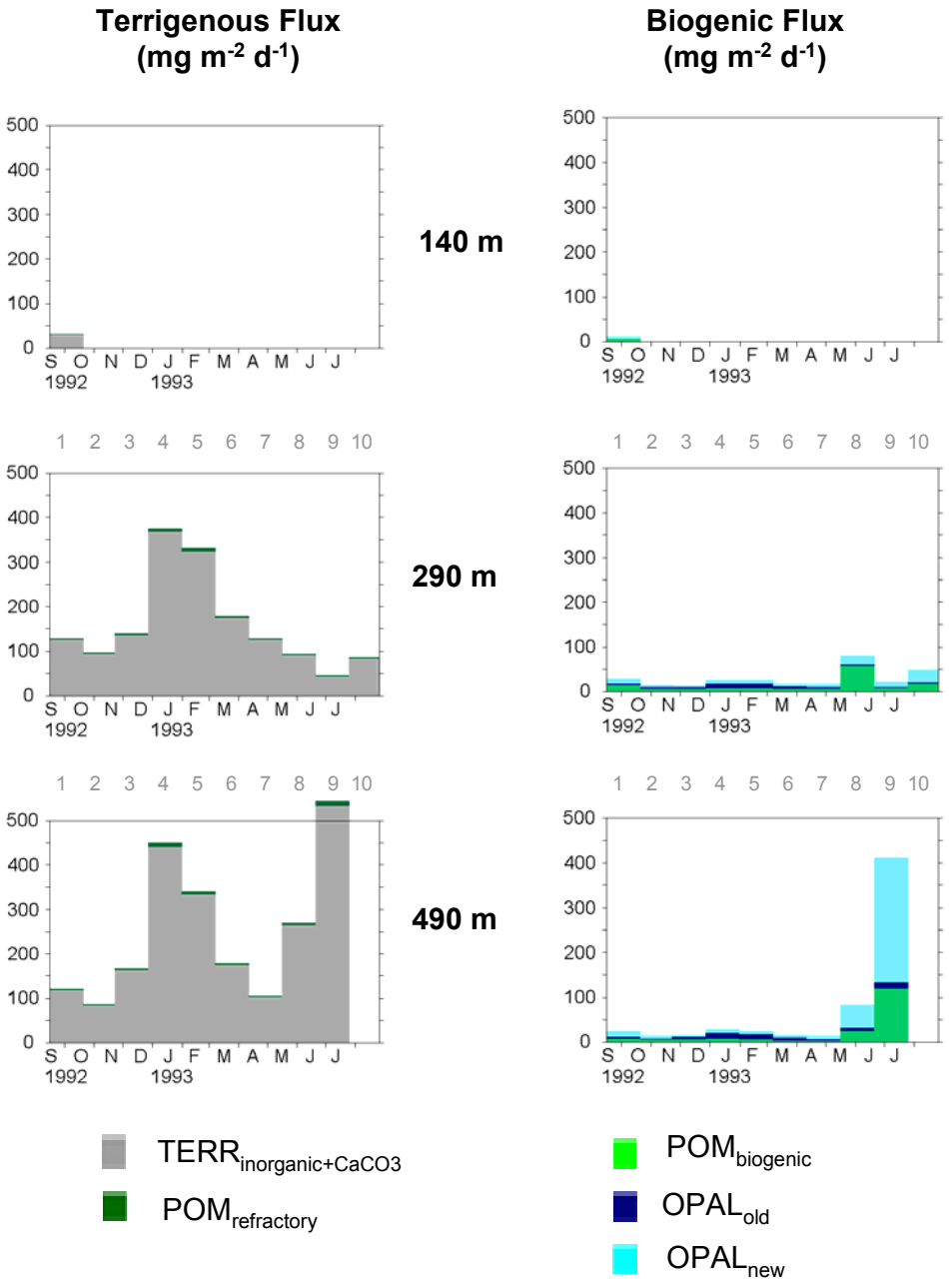

Figure 6-20 Terrigenous and biogenic fluxes (mg m-2 d-1) for site AM1-92 at the 140, 290, and 490 m sediment traps. The terrigenous fraction includes the inorganic material (TERRinorganic+CaCO3) and an estimate of the refractory organic mater (POMrefractory). Note that calcium carbonate produced by foraminifera and coccolithophorids could not be separated from the inorganic portion. The biogenic fraction includes the biogenic organic matter (POMbiog), the recently produced opal (OPALnew), and opal produced in an earlier season that has been resuspended along with bottom sediments (OPALold). See Sections 3.1.3 to 3.1.6 for a description of the methodology used to calculate the biogenic and terrigenous fluxes. The numbers (1-10) above the 290 and 490 m plots refer to the sediment trap interval number. The 140 m trap collected only one sample before it malfunctioned.

Table 6-1 Summary of data for IABP buoy number 11252. Buoy positions were recorded every twelve hours. The asterisks indicate that the periods do not cover the full period of the sediment trap intervals as follows: 1-3* indicates the period September 29 to December 27 and 8 indicates May 16 to June 2 after which the buoy lost.**

Sediment trap intervals	Number of days	Maximum distance in 12-hour period (km)	Maximum speed in 12-hour period (cm sec^{-1})	Average speed of 12-hour periods over period (cm sec^{-1})	Cumulative distance covered (km)	Average daily distance covered (km day^{-1})
1-3 *	89	17.7	41.0	10.1	775.9	8.7
4-5	70	19.9	46.1	8.6	516.1	7.4
6-7	70	9.9	22.9	5.9	410.3	5.9
8 **	17	11.4	26.5	9.7	189.7	11.2

11252 (Colony and Rigor, 1993; Colony and Rigor, 1995). The Mackenzie Shelf remained heavily clogged with ice until the end of June, 1992. While the ice cover over the site was light for the first three weeks of July, heavy pack ice sat just to the north. In August, a large patch of open water developed from 146 ºW to Amundsen Gulf, and by the end of August, AM1-92 was in open water. By early September, the ice had retreated north to about 71 ºN across the western side of Mackenzie Shelf and to beyond 72 ºN on the eastern side such that the lead-up to the mooring deployment saw large expanses of open water over the shelf and slope. Winds were bimodal to the W and to the E over this period of open water, and likely created alternating upwelling and downwelling favourable conditions, while periodically shifting the plume beyond the shelf break, and resuspending sediment in the shallower waters close to shore. Such conditions likely favoured resuspension and transport of fine suspended particles beyond the shelf break (O'Brien et al., 2006).

The mooring at AM1-92 was deployed in mid-September 1992 in a period of extensive area of open water over the shelf and the winds were predominantly to the E and the SE (Figure 6.23). By September 22, the area of open water was significantly reduced by ice pack drift and growing sea ice, and landfast ice formation had begun. A week later the site was > 90 % covered by large floes of old ice and thick first-year ice, and by October 6, 90 % covered by multi-year, second year, and grey ice. Ice cover was

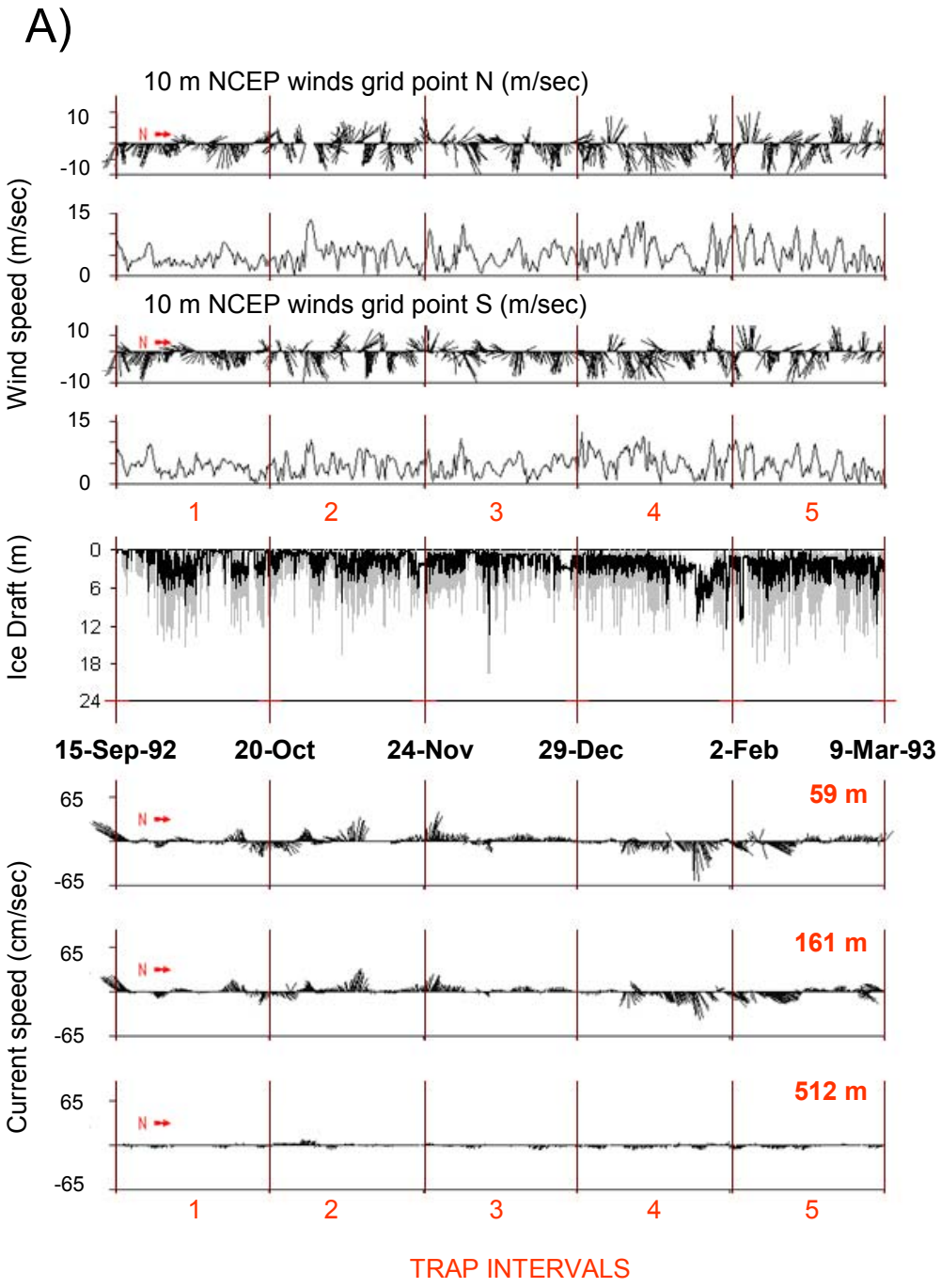

Figure 6-21 Winds, ice draft, and current velocities at site AM1-92 for: A) sediment trap intervals 1 to 5 and B) sediment trap intervals 6 to 10. The top plot is the 10 m NCEP winds at a grid points N and S (see Figure 6.19). The second plot is the ice draft in metres from Upward Looking Sonar data at the AM1-92 mooring. The lower group of plots show the current velocities (cm sec-1) at 59, 161, and 512 m at the mooring site. The numbers in red at the bottom and center of the figure designate the trap intervals and the red lines mark the start and end of each interval. The dates of the sediment trap openings and closings are shown below the ice draft plot.

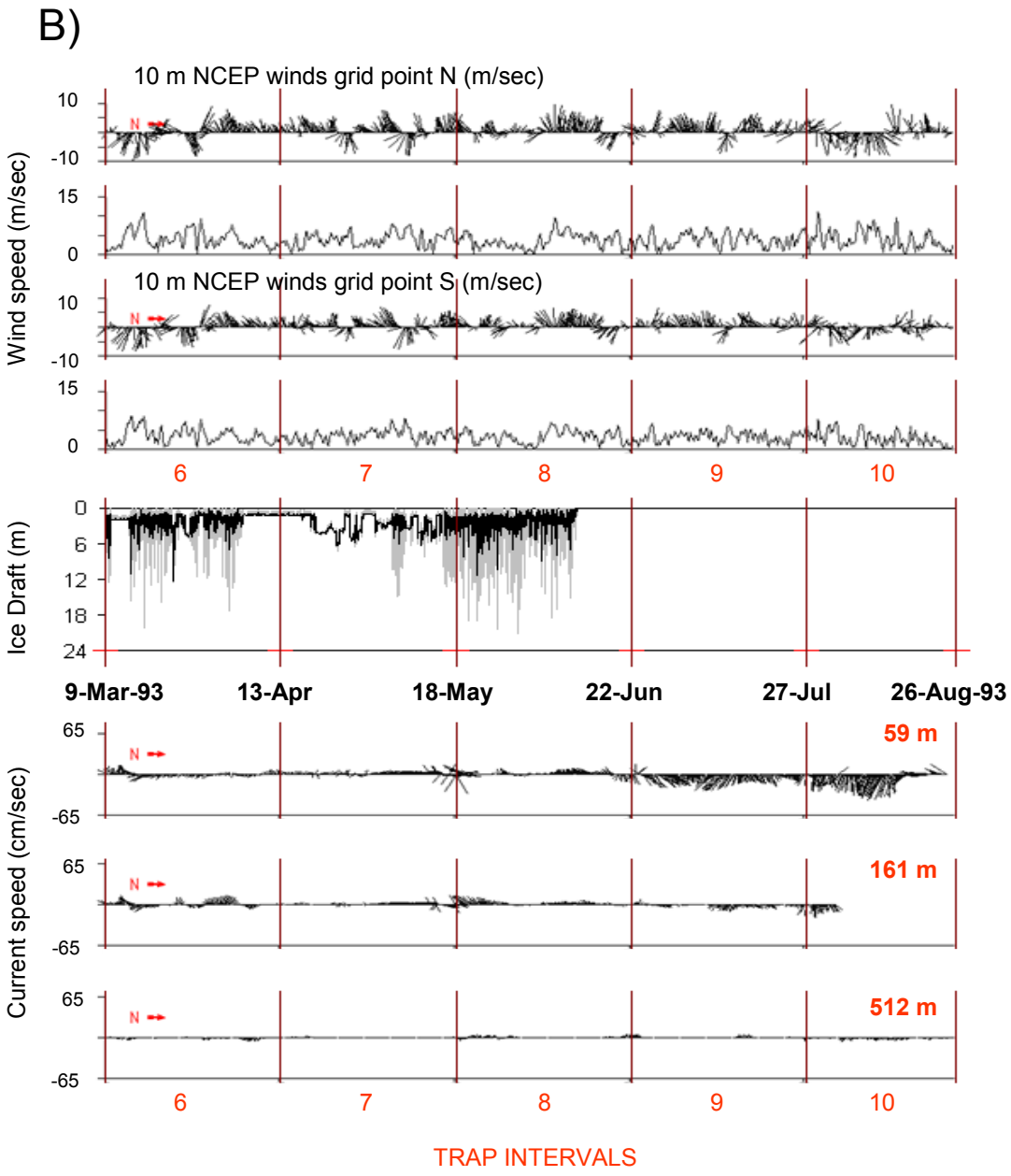

Continuation of Figure 6.21 (6.21B)

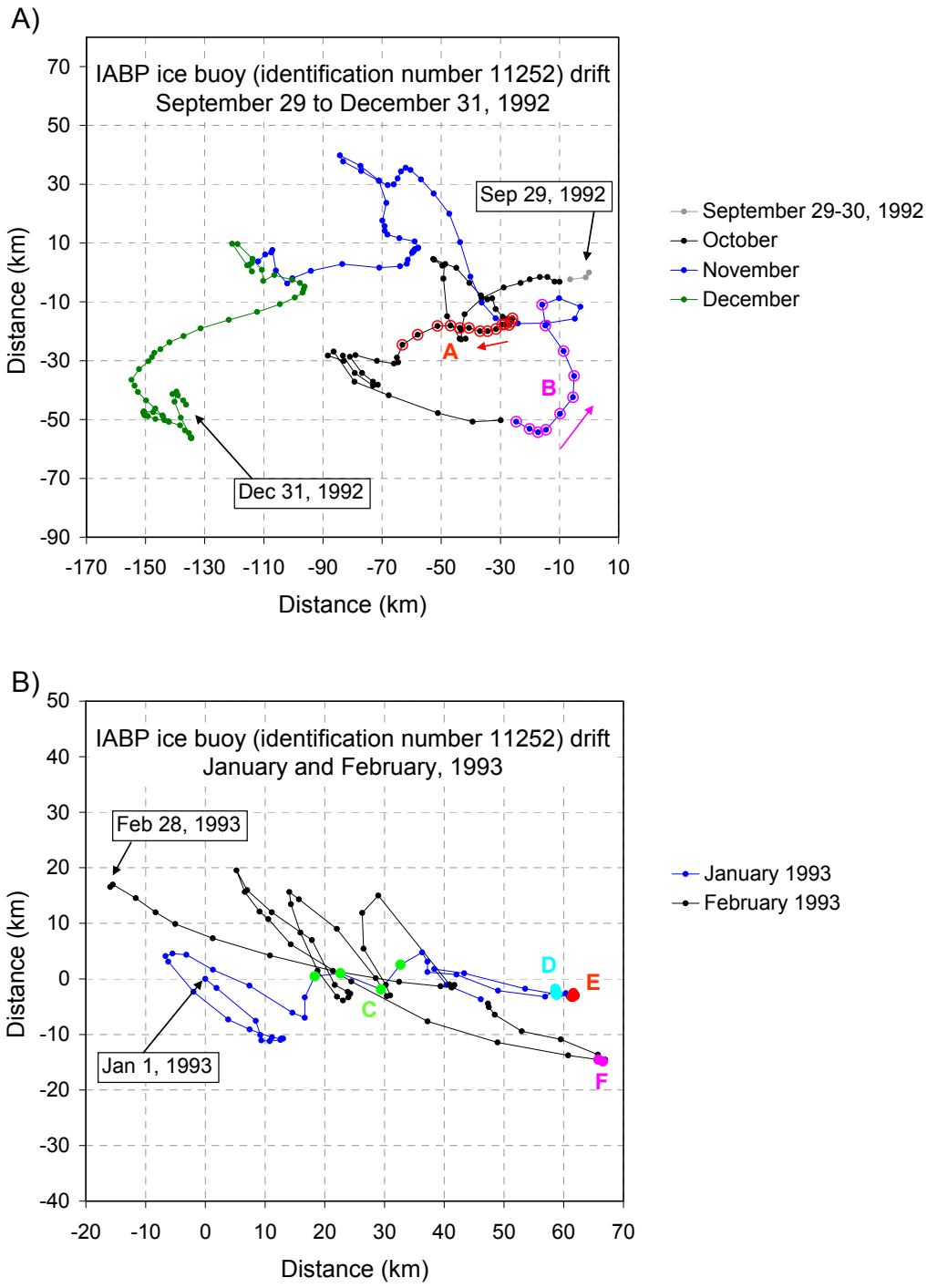

Figure 6-22 Distance covered by IABP drifting buoy (identification number 11252; Colony and Rigor, 1993) during the periods A) September 29 to December 31, 1992, B) January and February 1993, and C) March 1 to June 2, 1993. Also included on plots A and B are the timing of passing eddies at site AM1-92 (see features A to F in Figure 6.27A).

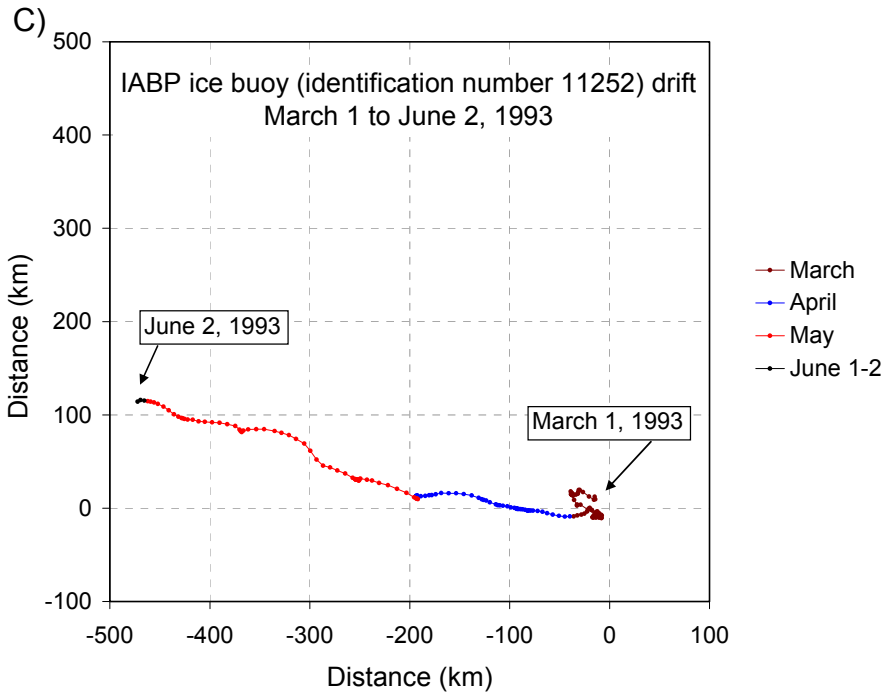

Continuation of Figure 6.22 (6.22C)

complete over the whole shelf by October 20. ULS data show that from the beginning of December 1992 to June 12, 1993, the site remained at least 90 % covered by mostly heavy ice (Figure 6.21).

By May 21, 1993, a band of open water had developed across Mackenzie Shelf beyond the landfast ice edge from 142 º W to 118 º W. It is likely that ice melt contributed to stratification of the upper water column in the area between May 21 and June 15. Progressive melting and drift of the ice pack extended the area of open water and by the end of June/early July, landfast ice broke free. ULS data shows site AM1-92 in open water from June 12 until the end of the trap collection on August 28 (Figure 6.21B). Extensive open water on and beyond the shelf (extending beyond 73ºN at times) persisted throughout the whole summer and fall season of 1993 and freeze-up was complete by November 9, 1993.

IABP buoys drifting with the ice pack during this period demonstrate considerable forcing due to ice drift. Even under complete ice cover in the dead of winter, the pack ice moved significant distances and with surprisingly high speeds (Figure 6.22). Indeed, over one 12-hour period during sediment trap intervals 4 and 5, IABP buoy #

A)

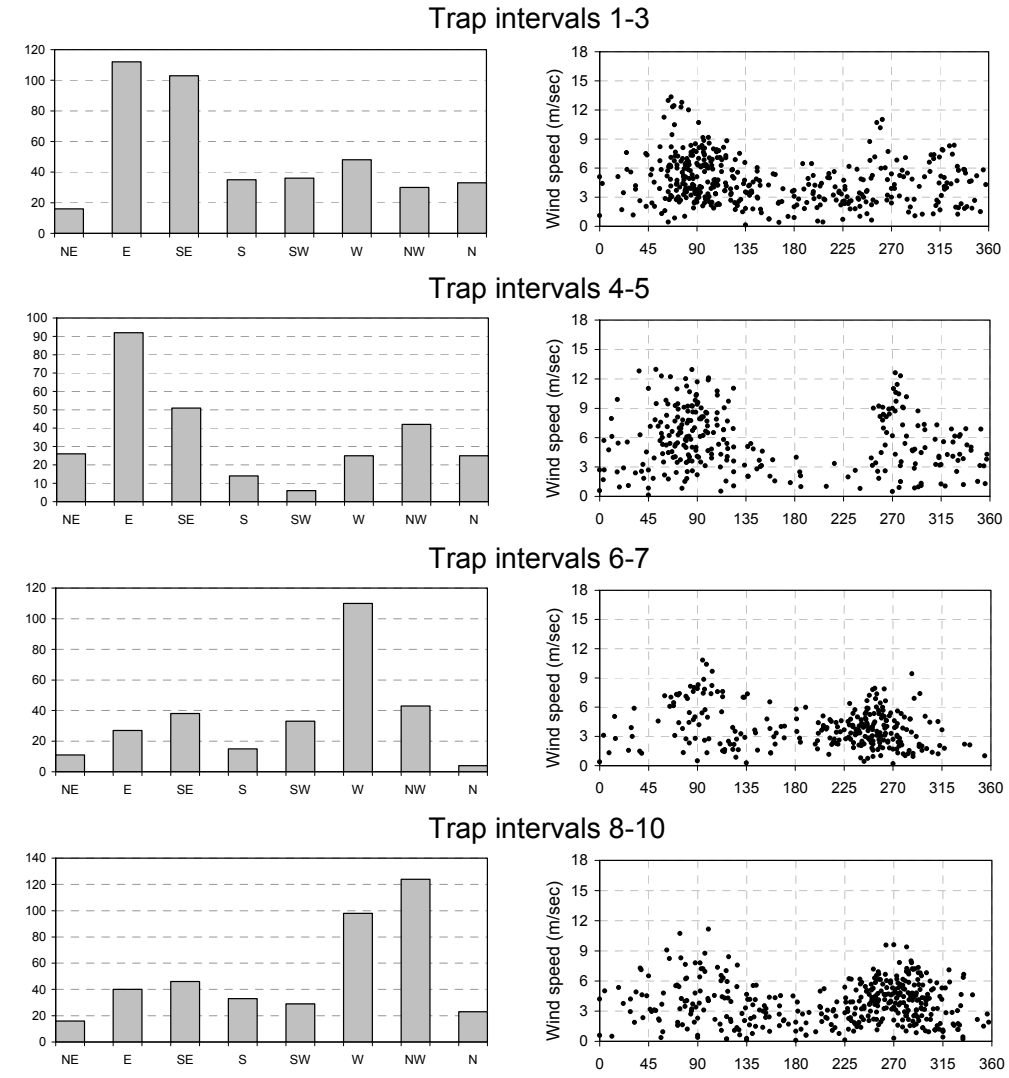

B)

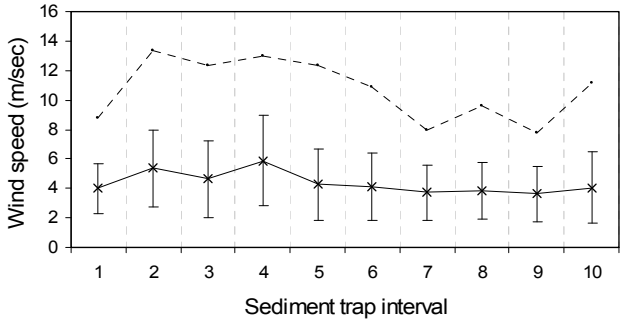

Figure 6-23 A) Histograms of wind directions and plots of winds speed (m sec-1) and wind direction according to trap intervals 1-3, 4-5, 6-7, and 8-10 at mooring site AM1-92. B) Average and maximum wind speeds during the sediment trap collection intervals at site AM1-92. Winds are 10 m NCEP data from grid point N (see figure 6.19).

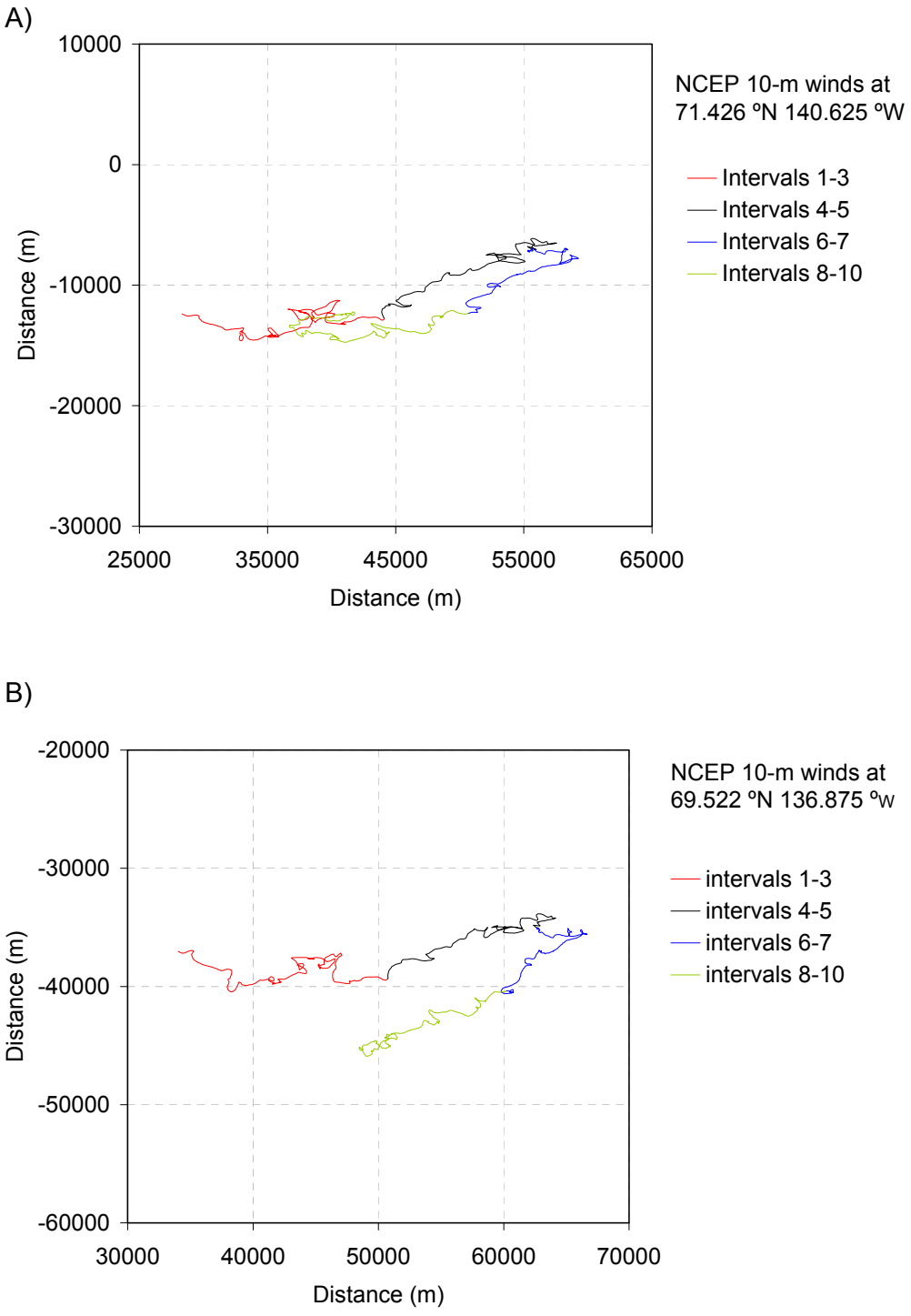

Figure 6-24 Progressive vector plot of 10 m NCEP winds at the two grid points (N and S) indicated in Figure 6.19. The sediment trap intervals 1-3, 4-5, 6-7, and 8-10 are plotted in different colours as indicated in the legends.

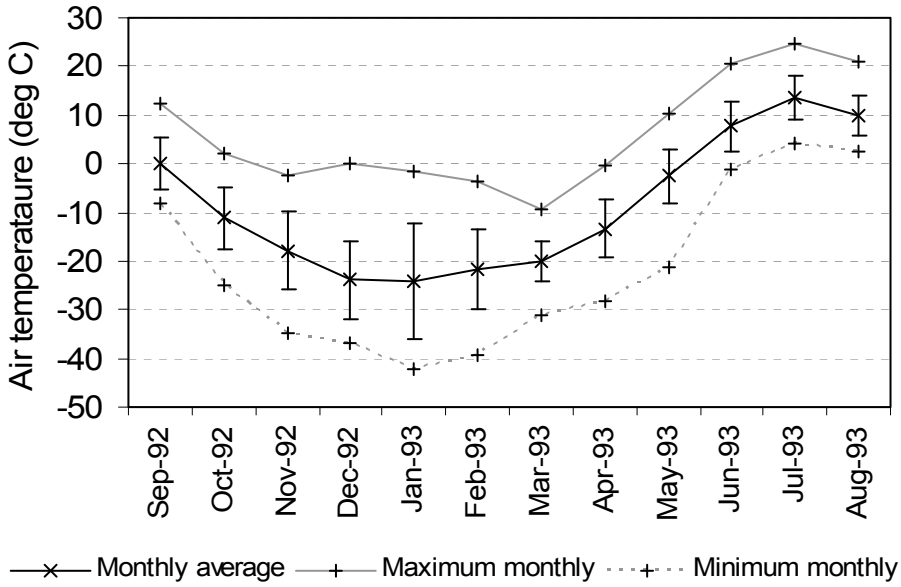

Figure 6-25 Air temperatures at Tuktoyaktuk Airport showing the monthly averages, maximums and minimums. Data is from the Meteorological Services of Canada.

11252 drifted at an average rate of 46 cm sec^{-1} (Table 6.1). While the direction of ice displacement was quite variable over the fall and winter of 1992-1993, displacement after the beginning of April was steadily to the WNW: strongly upwelling favourable. Such motion has been associated with large upwelling events in Mackenzie Trough; an indication of strong coupling between ice movement and the underlying waters (Williams et al., 2006).

6.2.2 Winds and air temperature

Over the first five intervals of the deployment (September 15 to March 7), the net wind displacement was to the NE (Figure 6.24), the wind direction was most frequently to the E and SE (Figure 6.23A), and the highest average wind speeds occurred during sediment trap interval 4 (Figure 6.23B). For the later half of the trap collection (intervals 6 to 10), the net wind displacement was to the SW (Figure 6.24) and the winds blew preferentially to the W and NW (Figure 6.23). Conditions were predominantly downwelling favourable for the first five intervals and upwelling favourable thereafter (Figure 6.21A, 6.23 and 6.24). It must be noted however that over the whole period there

A. PVD plot for 59 m current meter at site AM1-92 (sediment trap intervals 1-5)

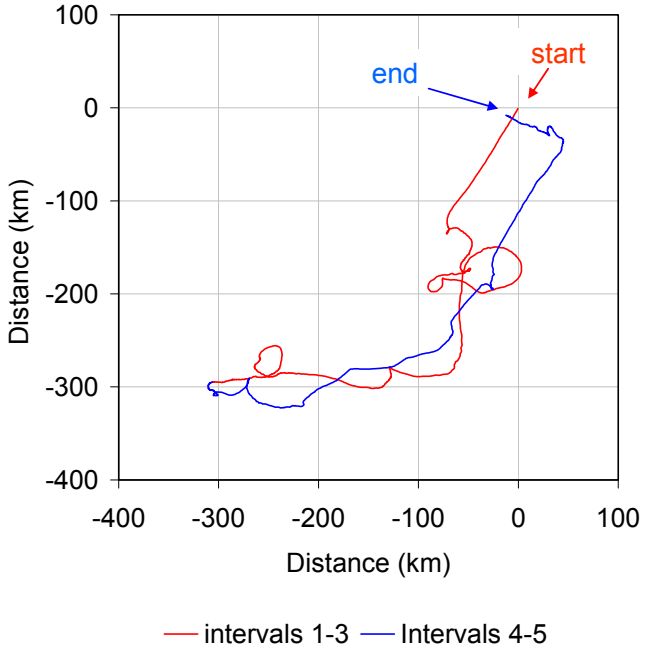

B. PVD plot for 59 m current meter at site AM1-92 (sediment trap intervals 6-10).

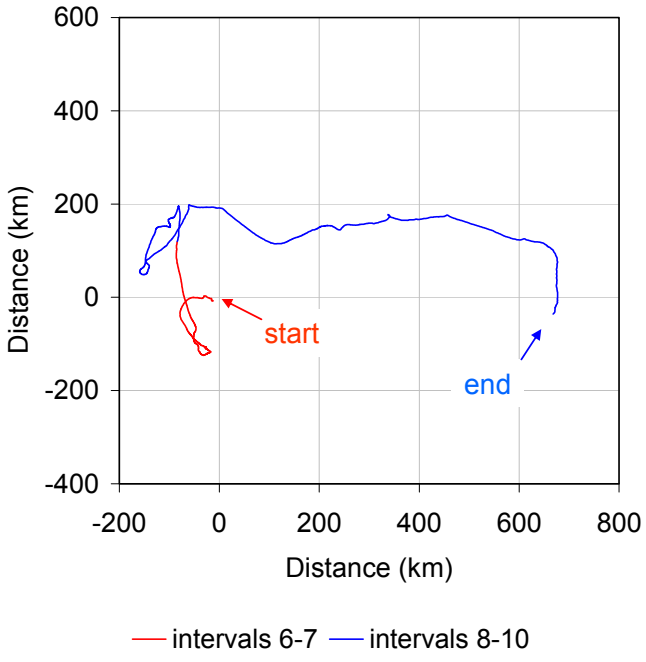

Figure 6-26 Progressive vector plots of currents at mooring site AM1-92 at A) 59 m for sediment trap intervals 1 to 5, B) 59 m for intervals 6 to 10, C) 161 m intervals 1 to 5, D) 161 m for intervals 6 to 10, and E) 512 m for intervals 1 to 10. Note that the current record for 161 m only goes until August 3, 1993 so that for interval 10 the record is incomplete (see Figure 6.27).

C. PVD plot for 161 m current meter at site AM1-92 (sediment trap intervals 1-5).

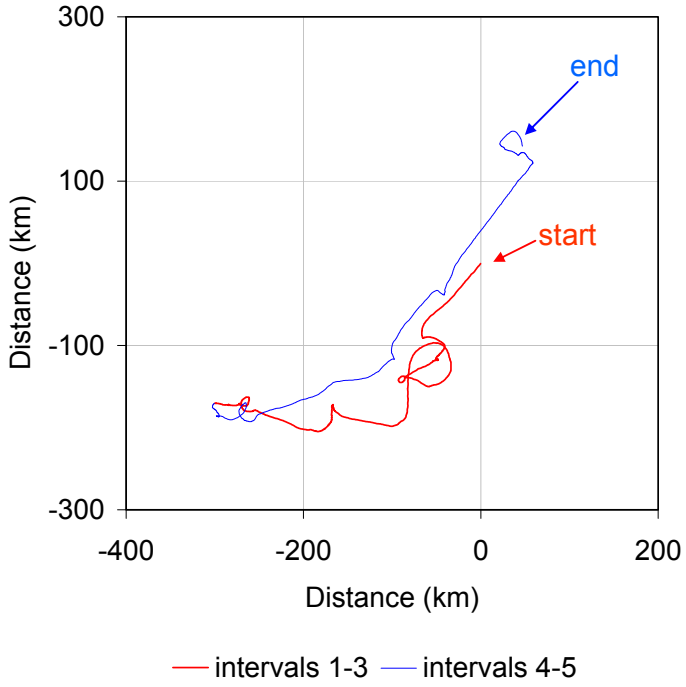

D. PVD plot for 161 m current meter at site AM1-92 (sediment trap intervals 6-10).

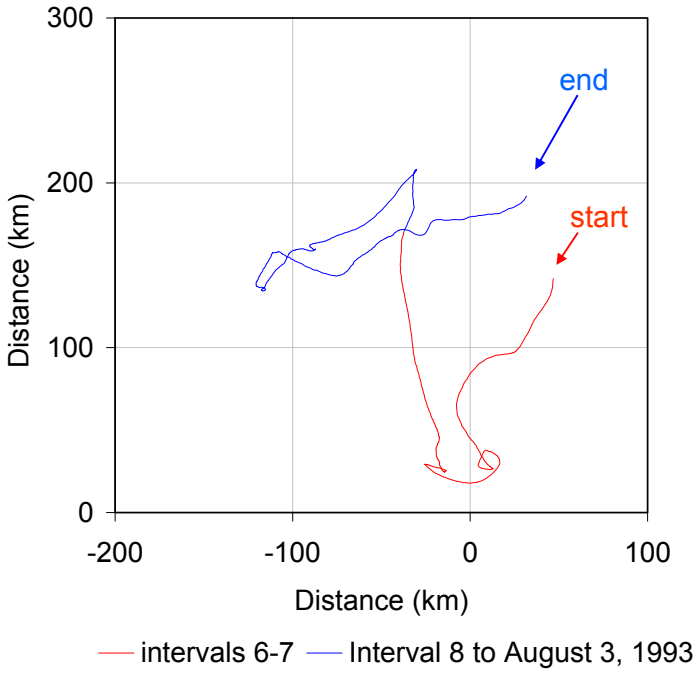

Continuation of Figure 6.26 (6.26C and 6.26D)

E. PVD plot for 512 m current meter at site AM1-92 (sediment trap intervals 1-10).

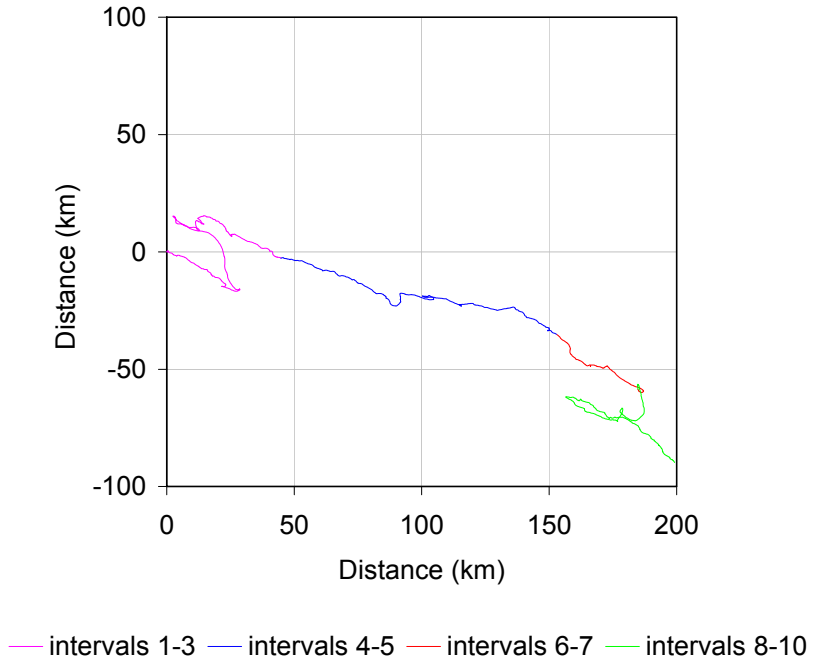

Continuation of Figure 6.26 (6.26E)

were frequent changes in wind direction with an overall bimodal E-W pattern particularly with respect to the elevated wind speeds (Figure 6.23).

Monthly average temperatures were well below freezing from October to April (Figure 6.25). No significant stratification of the water column due to melting of the ice cover was likely before late-May/early-June in the spring of 1993.

6.2.3 Currents, temperature and salinity relationships, and resuspension

Current (from 59, 161, and 512 m) and temperature-salinity (T-S) data (from 60 and 162 m) shed important light on the dynamics of the water column during the collection period and point to processes capable of transporting sediments over the continental slope and into deeper waters.

During the fall/early winter of 1992 (trap intervals 1 – 3), the favoured range of current direction at 59 and 161 m was between 180 and 300 degrees (Figure 6.26A and Appendix 5), with episodic maximum speeds of 55.7 and 49.3 cm sec $^{-1}$ to 210 º and to

A)

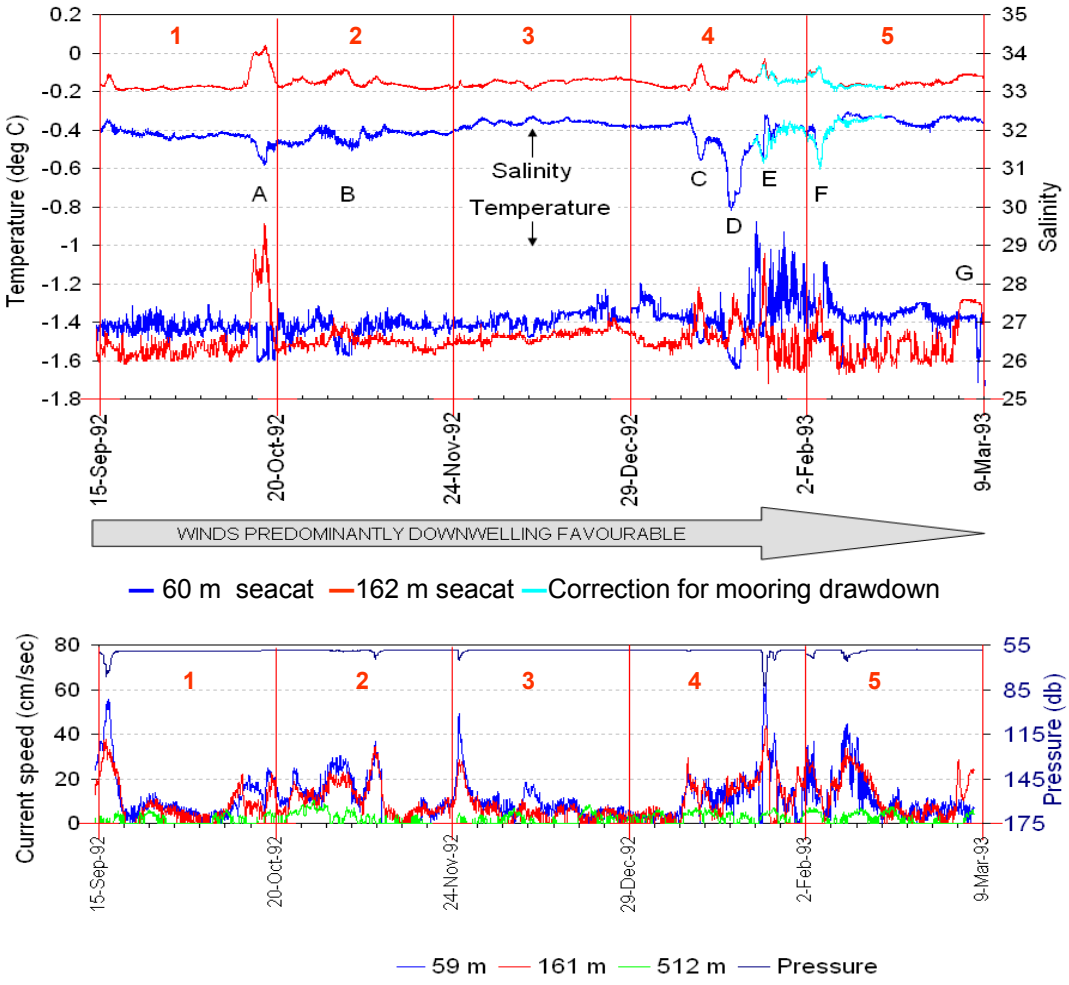

Figure 6-27 Data from AM1-92 mooring. Temperature and salinity at 60 and 162 m (top two plots) and current speed data from 59, 161, and 512 m (bottom two plot) are plotted for: A) sediment trap intervals 1 to 5 and B) intervals 6 to 10. The red numbers indicate the trap intervals and the arrows between the plots indicate upwelling or downwelling favourable winds during the period as well as a period of upwelling favourable ice drift in the spring. The black letters A, B, C, D, E, and F indicate features consistent with cyclonic eddies. Features G to L are discussed in the text. Also plotted is pressure to indicate where strong currents have pulled the mooring down. See next page for Figure 27B.

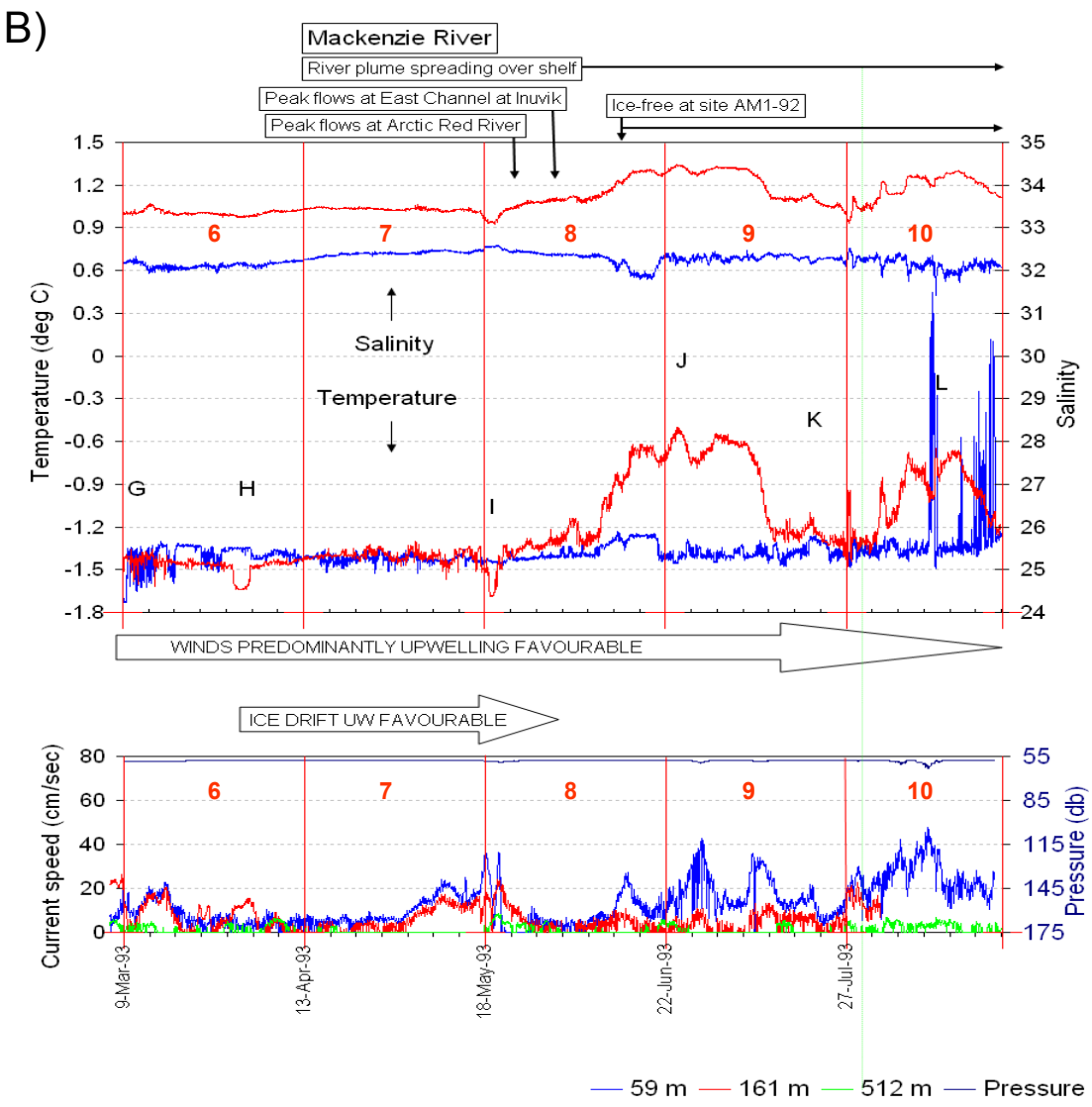

Continuation of Figure 27 (27B)

288 º respectively at 59 m, and 37.7 and 34.5 cm sec^{-1} to 214 º and 283 º respectively at 161 m. Current directions were generally coherent between the two depths, and the net displacement was to the SW (Figure 6.26A and 6.26C). Overall, the current direction in this period was to the right of the downwelling favourable wind direction (predominantly to the E) as would be expected. The movement of water onto the shelf was likely accompanied by downwelling of a bottom nepheloid layer over the slope and possibly even multiple detachments of this bottom layer to form mid-water nepheloid layers that spread out over the slope. This is the most probable mechanism for transport of the highly

terrigenous particulate material to the 290 and 490 m traps at site AM1-92 during intervals 1 to 3. In addition, during interval 1, an eddy passed over the mooring which may have contributed to the particle fluxes (Figure 6.21A; see feature A in figure 6.27A).

In contrast to the earlier intervals, trap intervals 4 and 5 during the winter show dominant current directions of between 30 and 60 º (Figures 6.26A and 6.26B; Appendix 5). The highest current speeds occurred on January 25 (62 cm sec^{-1} (to the E) at 59 m and 43.8 cm sec^{-1} (to the E-NE) at 161 m) and were largely associated with eddies that masked the background flow. By canting the line, the swift current pulled the traps down by some 25 m (Figure 6.27A). Currents at 512 m, well below the halocline, were low during intervals 4 and 5 with average speeds of < 3 cm sec^{-1} (Appendix 5) and net displacement was to the SE (Figure 6.26E). Due to the presence of eddies, no simple relationship existed between the directions of the currents, the winds and the ice displacement, and the high current speeds associated these eddies are expected to be highly effective in transporting suspended particles beyond the shelf edge.

Six features consistent with the presence of cyclonic eddies occurred during the first five trap intervals, and are clearly identifiable from the T-S records from 60 and 162 m on the AM1-92 mooring (Figure 6.27A; see features labelled A to F). The pinching of isopycnals towards a central density surface identifies these features as cyclonic eddies; these are less commonly reported than anticyclonic eddies in the Beaufort Sea (Manley and Hunkins, 1985; Krishfield et al., 2002). It is not possible to assign origin, size, or age to these eddies using the available data. The colder fresher water in the eddies at 60 m could have originated on the Alaskan Beaufort Shelf or in Mackenzie Trough during freeze-up. Mesoscale eddies have been well documented in the Arctic Ocean and their water properties strongly suggest a shelf origin (Manley and Hunkins, 1985; D'Asaro, 1988; Krishfield et al., 2002). The majority of eddies observed were anticyclonic, occurred in the depth range 50-300 m, and were particularly prevalent in the Beaufort Sea. Eddies north of the Alaskan shelf have been associated with increased levels of suspended sediments (Ashjian et al., 2005), and a similar association of suspended sediments with eddies may be important in the offshore transport of shelf sediments at site AM1-92. Indeed, the high terrigenous fluxes in trap intervals 4 and 5 (Figure 6.20) may be linked to resuspension associated with the high currents that accompanied the

Figure 6.28 A) March 17-18, 1991

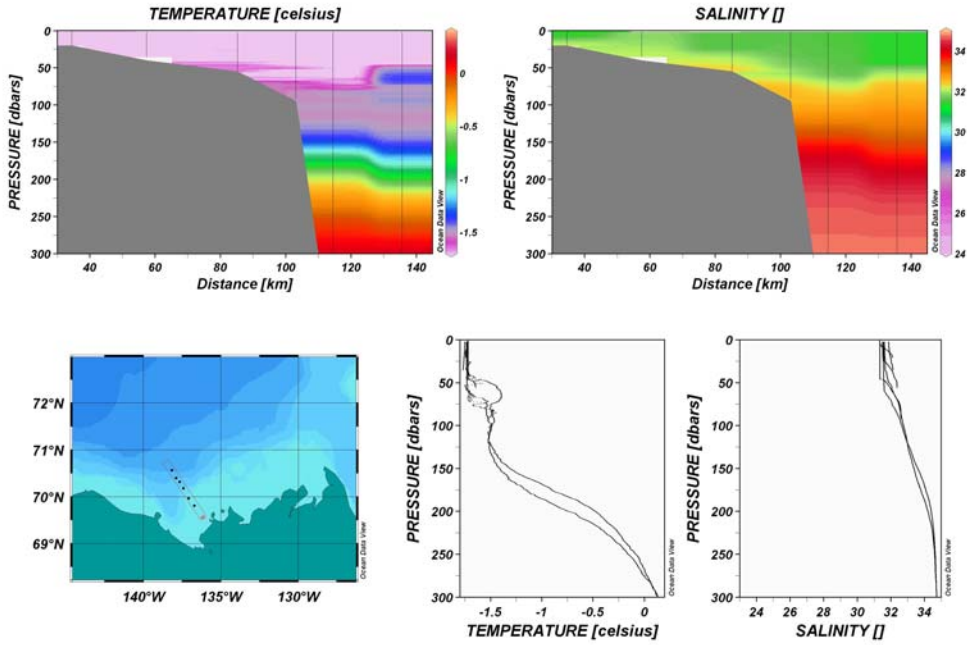

Figure 6.28 B) April 2, 1992

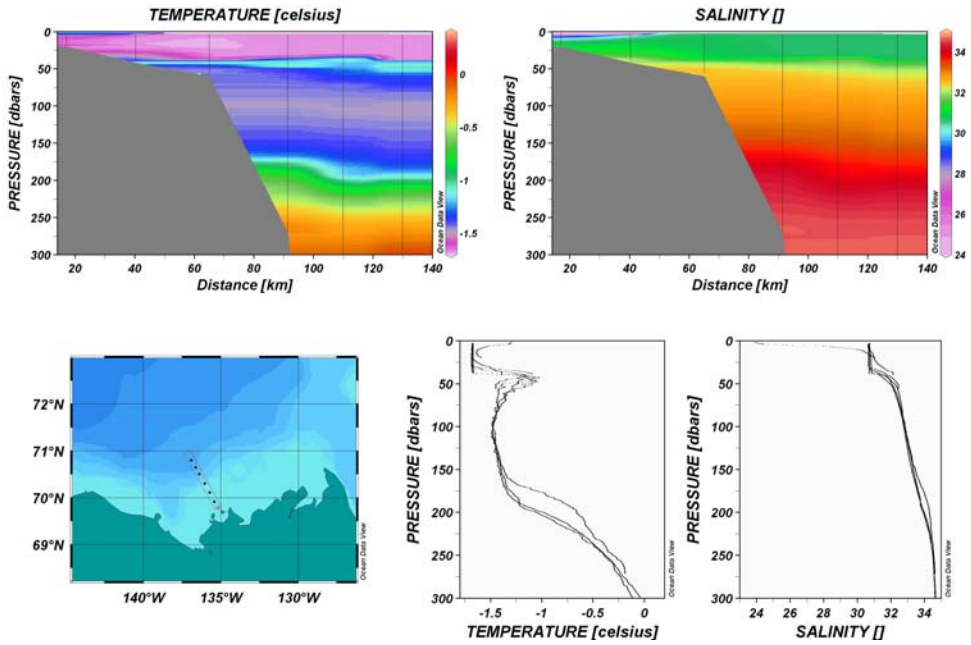

Figure 6-28 Late-winter/early-spring CTD data showing a cross-section of the shelf on the east side of Mackenzie Trough and temperature and salinity profiles down to 300 m for: A) March 17-18, 1991, B) April 2, 1992, and C) April 8, 1993. Contours shown on the map are 50, 100, 500, 1000, 2000, and 3000 m. Ocean Data View program was used to create the plots. (Plot done using Ocean Data View software, Schlitzer, R., Ocean Data View, http://odv.awi.de, 2009)

Figure 6.28 C) April 8, 1993

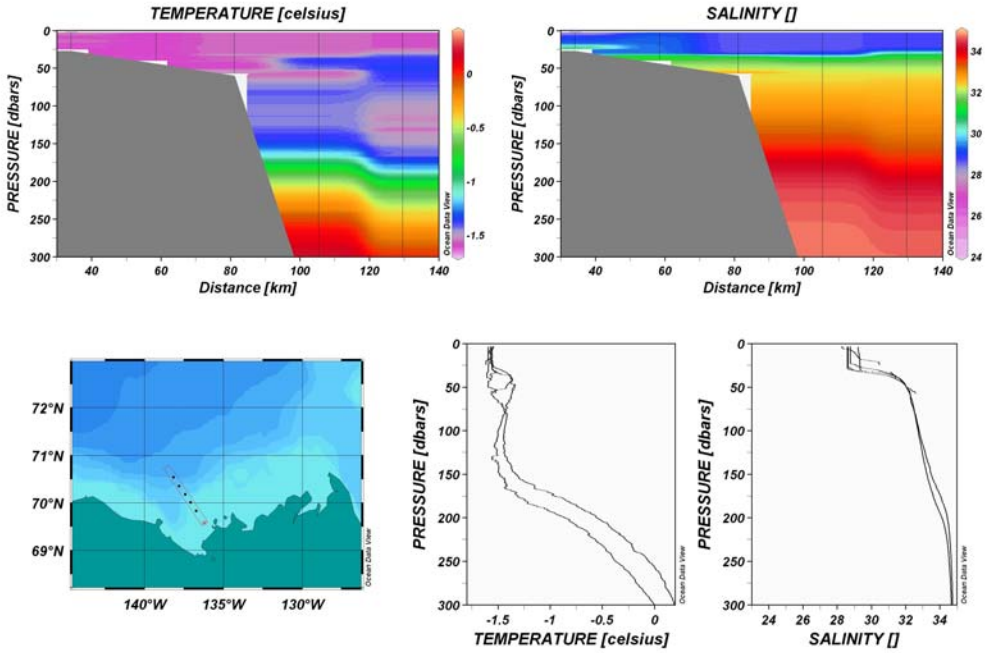

Continuation of Figure 6-28 (6.28C)

eddies (Figure 6.27; features labelled C to F). The circular motion of such eddies likely carried particulate matter further offshore to settle over the slope.

Features A and C both remained over the site for about 4 days (Figure 6.27A), and associated current speed patterns and directions with respect to the T-S anomalies are consistent with meandering over the mooring site. The maximum T-S excursions correspond with lower current speeds as would be expected in the core of an eddy (Figure 6.27A). The differences between the temporal patterns of currents and T-S at 60 and at 162 m suggest angling of eddies or different diameters at the two depths.

It is possible that features A and B are the same semi-stationary eddy that periodically moved over the mooring site to different degrees and from different directions for a period of about a month. Likewise, features C, D, E, and F may be manifestations of a meandering eddy that also stayed near the site for roughly a month (Figure 6.27). A more detailed investigation of the physics of these eddies is beyond the scope of this study but, as evidenced by the high mid-winter fluxes, it appears highly

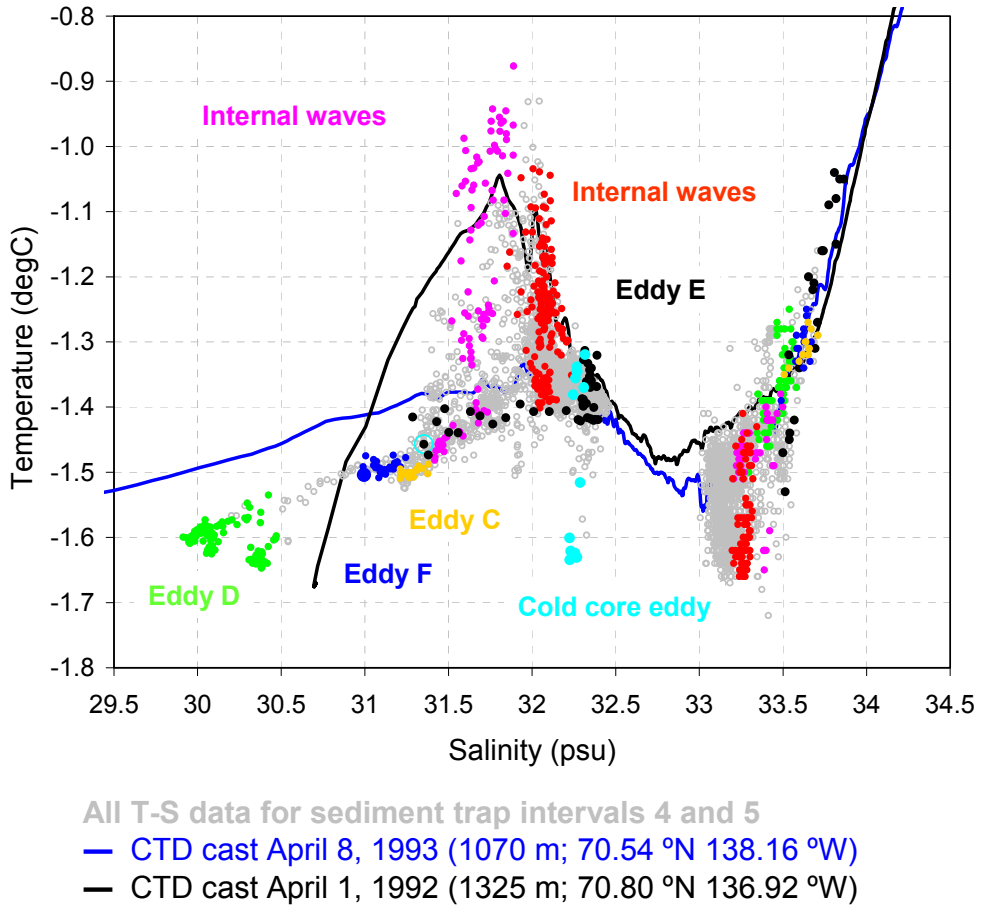

Figure 6-29 Plot of temperature and salinity data from 60 and 162 m at site AM1-92 during sediment trap intervals 4 and 5. All the data for these two intervals is plotted as open grey circles and specific features are plotted with colour-coded labels. The data chosen for plotting internal waves were not affected by drawdown of the mooring due to high currents. See Figure 6.27 for the timing of eddies A, B, C, D, E, and F. Also shown is a cold core eddy detected at 60 m on February 8, 1993. The blue line is from a CTD cast taken on April 8, 1993 (1070 m; 70.54 ºN 138.16 ºW) and the black line is from a cast taken on April 1, 1992 (1325 m; 70.80 ºN 136.92 ºW); these casts demonstrate the variability in TS in the early spring period (Data courtesy of Dr. Humphrey Melling, Institute of Ocean Sciences, Sidney, B.C.).

likely that they are important agents of cross-shelf sediment transport in this area, and as such, should be the subject of future investigations.

The ice cover over site AM1-92 was particularly heavy in the last week of January (Figure 6.21A) and the movement of this heavy ice likely delivers considerable force to the water column (see section 6.1). Figure 6.22B shows the timing of the passage of the eddy features labelled C-F (Figure 6.27A) in relation to the ice drift. The

appearance of eddies C, D, E, and F over site AM1-92 coincides with abrupt changes of direction in ice drift from SE to NE (Figures 6.22B). Although the significance of this is not clear, it leads to the speculation that there is a connection between the movement of the icepack and the generation and/or movement of eddies over the shelf and slope and in Mackenzie Trough area.

From about January 23, and into the first week of February 1993, coincident with the presence of eddies E and F, intense short-term temperature changes, which appear unrelated to eddies occur at both 60 and 162 m (Figure 6.27A), and these temperature excursions are consistent with the passage of internal waves. At 60 m, there are temperature excursions as high as -0.88 º C and as low as -1.7 º C, and at 162 m, temperatures range from about -1.5 º C down to a minimum of about -1.7 º C. The presence of the warmer waters may be due to a remnant of surface warming from the previous summer and fall. There is no CTD cast in January and February of 1993 but CTD casts from the spring of 1992 demonstrate that higher temperatures can occur in late-winter/early-spring at the bottom of the mixed layer between 30 to 60 m (Figure 6.28B). In addition, cold shelf waters flowing beyond the shelf break may interleave with existing waters and redistribute over the slope. There is evidence of this interleaving occurring in spring in 1991, 1992, and 1993 just beyond the shelf break over Mackenzie Trough (Figure 6.28 (A, B, and C)). The passage of internal waves through a water column with interleaving would produce a pattern of rapid fluctuations of temperature such as was observed in late January/early February of 1993.

In the Mackenzie Trough area, resuspended sediments carried by cold, dense flows off the shelf would be transported further offshore if caught up in the high currents associated with the cyclonic eddies over the slope. Moreover, the co-occurrence of interleaving waters and cyclonic eddies may be a very efficient mechanism for moving resuspended terrigenous material beyond the shelf break. Although it is not possible to determine the radius of the observed eddies, high currents associated with them are likely capable of resuspending sediments if they collide with the bottom topography on the slope. The high terrigenous flux peaks in mid-winter may well be a result of the co-occurrence of cyclonic eddies brushing up along the slope with interleaving cold shelf waters over the slope and the passage of internal waves. Indeed, the composition of the

material trapped during intervals 4 and 5 has the highest terrigenous content (93 to 94 %) in the whole data set suggesting that there may have been intense erosion on the slope. It is also likely that the inferred resuspension occurred over a considerable depth range on the slope given that at both 290 and 490 m, the fluxes are high and peak at the same time in trap intervals 4 and 5. The passage of internal waves may have contributed to this as has been reported elsewhere (see for example Cacchione and Drake, 1986; Cacchione et al., 2002; Puig et al., 2004). The interaction of internal waves with continental slopes and the generation of intermediate nepheloid layers is an active area of research (for review see McPhee-Shaw, 2006), and in this area, may have considerable importance in cross-margin transport of suspended particulates, nutrients, carbon and other constituents important to productivity over the slope and into Canada Basin. A TS plot for trap intervals 4 and 5 shows a summary of water column processes that likely contributed to the highly terrigenous winter peak (Figure 6.29).

Lower particle fluxes over the spring period (trap intervals 6 and 7; Figure 6.20) may be a reflection of lower current speeds in the upper and lower haloclines (59 and 161 m; Figure 6.27B and Appendix 5) along with the absence of any large eddies or major upwelling/downwelling events (Figure 6.27B). The T-S data for interval 7 is relatively featureless and this is reflected in the low particle fluxes. In contrast, during interval 6, the slightly higher fluxes may be related to the passage of internal waves (following a small upwelling event) that revealed the presence of the interleaving of cold shelf waters possibly associated with entrained resuspended sediments (feature G in Figure 6.27B) and one small minor cold core eddy (feature H in Figure 6.27B).

During the late spring/summer period (trap intervals 8 to 10) the dramatic increase in particle flux at 490 (in intervals 8 and 9) is likely due to the combination of peak Mackenzie River inputs (of fresh water and suspended particles) (Figure 6.27B) and large upwelling events punctuated by periods of relaxation of upwelling (features J, K, and L in Figure 6.27B). Upwelling during this period is favoured by three factors: winds predominantly to the W and NW, pack ice drift to the W, and spreading of the Mackenzie River plume under the influence of winds predominantly to the W. The strong upwelling signal begins towards the end of interval 8 shortly before a marked increase in current speed to the E at 59 m, shortly before site AM1-92 becomes ice-free, and as the river

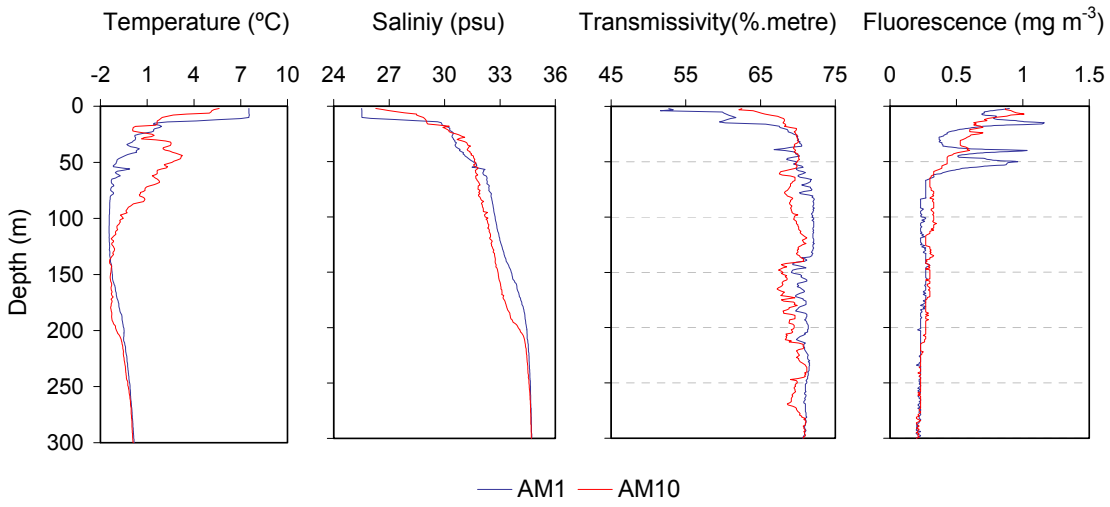

Figure 6-30 Profiles of temperature, salinity, transmissivity, and fluorescence taken August 27-28, 1993 at stations AM1 (70.396 ºN 139.872 ºW) and AM10 (70.474 ºN 136.904 ºW).

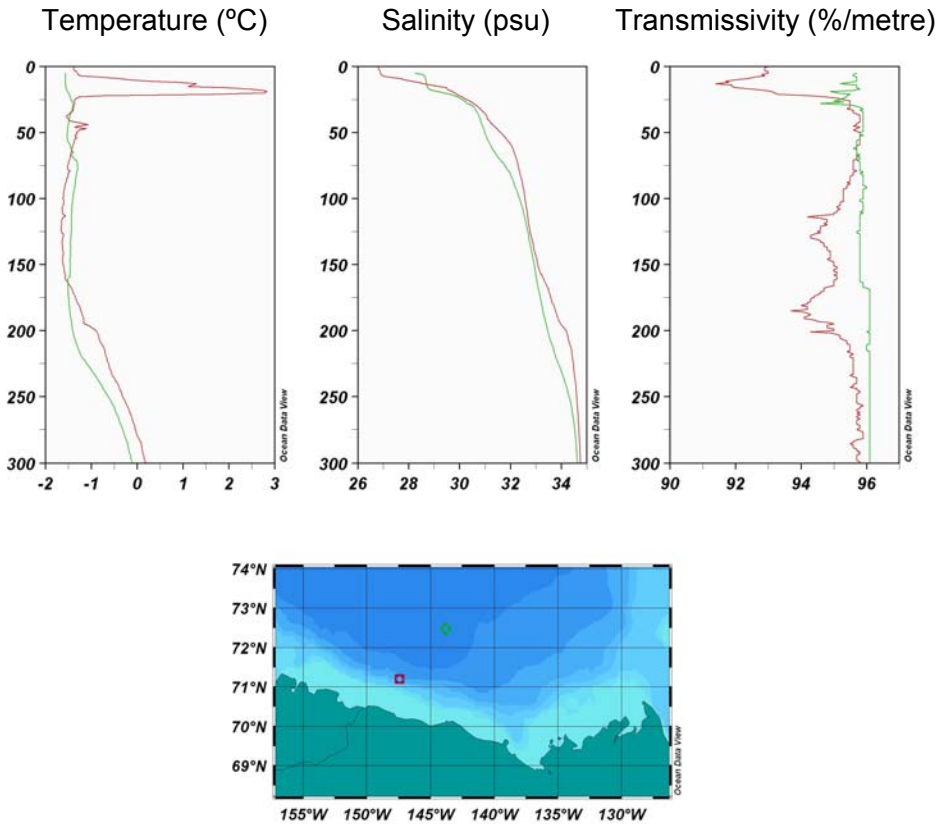

Figure 6-31 Profiles of temperature, salinity, and transmissivity for a station over the Alaskan slope on September 25, 1992 (71.202 ºN 147.439 ºW) and in Canada Basin on September 21, 1992 (72.472 ºN 143.814 ºW). (Plot done using Ocean Data View software, Schlitzer, R., Ocean Data View, http://odv.awi.de, 2009)

plume begins spreading out over Mackenzie Trough (Figures 6.21B and 6.27B). In these open water conditions with winds predominantly to the west, the river plume would be expected to be directed to the west and northwest. The spreading of the river plume in this configuration is highly favourable to a diatom bloom over Mackenzie Trough because the river provides both new nutrients and stratification to the system. In addition, it is likely that these conditions resulted in upwelling in Mackenzie Trough capable of bringing nutrients to the surface further up the canyon further enhancing conditions favourable for a spring bloom. The Mackenzie River freshet is an extremely dynamic event which supplies readily mobilized sediments to the Beaufort Sea from two main sources: eroded material from the Mackenzie River watershed and resuspended material from the extensive shallow foreshore adjacent to the delta.

The edge of the pack ice moved northward over the mooring site coincident with air temperatures rising above freezing sufficiently long enough to melt sea ice and release ice algae from the underside of the ice. The material trapped during interval 8 at 290 m had a high δ13C signature (-12.2), a high CN ratio (29.9), and a high proportion of ice algae (Nitzschia Frigida). This material may have been released from the underside of the ice as an aggregate and delivered rapidly to the bottom. It is likely that events such as this are short in duration and interception of ice algae by a sediment trap is a fortuitous occurrence rather than broadly representative of a spring release of ice algae.

In the latter part of August 1993, there are numerous excursions to very high temperatures (up to 0.4 ºC) at 60 m during periods of relaxation of upwelling (see feature L in Figure 6.27B). CTD casts from the end of August in 1993 show the interleaving of waters with different temperatures between 20 and 100 m that could account for these high temperatures (Figure 6.30). In addition, at the end of August 1993, a CTD cast at site AM1-92 reveals a mixed layer of warm, fresh, turbid water (7.5 ºC, 25.5 psu) down to about 10 m (Figure 6.30). The transmissivity profiles at these stations also show that in addition to a shallow turbid mixed layer, there is considerable interleaving of suspended sediments particularly down to 300 m (Figure 6.30). In addition, fluorescence peaks (at 16, 40, and 50 m) in these CTD casts demonstrate that in the upper 60 m, there are layers rich in phytoplankton which are distinct from deeper layers with low fluorescence due primarily to suspended material with high terrigenous content. Similarly, a CTD-

transmissivity cast taken further west (71.202 ºN 147.439 ºW; 465 m; September 25, 1992; Figure 6.31) revealed a series of nepheloid layers wherein transmissivity was particularly reduced in shallow water (<25 m) and between 100 and 200 m (where cold and warmer waters are interleaved). Other nepheloid layers extended to depths >400 m. These casts demonstrate the presence of mid-water nepheloid layers well beyond the shelf break in the Alaskan Beaufort Sea west of the mooring site as well as in the Mackenzie Trough area. Clearly, the transport of particulate material over the Beaufort Sea slope is a widespread phenomenon.

The contribution of biogenic sedimentation at the mooring site rose substantially in the late spring and summer of 1993 as the influx of warm, nutrient bearing Mackenzie River water in Late-May/early June contributed to melting of the ice cover, stratification of the water column, and phytoplankton growth. The large differences in sample mass collected by the 290 and 490 m traps over this time imply that main diatom bloom happened to the south of site AM1-92, settled to the bottom, and then moved episodically seaward in bottom or mid-water nepheloid layers along with suspended river sediments raining out of the river plume. The late summer peak of both biogenic and terrigenous material at 490 m particularly highlights the importance of such progressive and likely stepwise lateral transport of material in the Mackenzie Trough area.

6.2.4 Nutrients

A comparison of the Si and N inventories in the surface layer in March to the inventories of BIOSI and N collected in the traps over the spring/summer period highlights the relative export of Si and N at site AM1-92 (see discussion in section 6.1.8). The inventory of N in the top 50 m of the water column in early spring ranged from 60 to 375 mmoles m^{-2} as calculated from the range of concentrations in the water column in late-March/early-April (for the years 1986, 1987, 1988, 1990, and 1991). The particulate N collected in the traps over the 350-day deployment represents between 45 to 71 % (27 to 43 mmoles m^{-2}) of the lowest range of the dissolved N inventory in the top 50 m (60 mmoles m-2), somewhat higher than was calculated for site SS-5. In contrast to N, particulate Si in the traps accounts for some 28% (at the 290 m trap) to 89% (490 m trap) of the lowest range of the dissolved Si inventory in the upper 50 m (250 to 1050 mmoles m^{-2}). As for site SS-5 proportionally much more Si than N is exported to depth.

6.2.5 Summary of physical data for site AM1-92

Five processes capable of delivering sinking particles to the sediment traps at 290 and 490 m at site AM1-92 have been identified. First, the interleaving of cold waters from the shelf with water over the slope may involve the entrainment of shelf sediments into mid-water nepheloid layers. The subsequent settling of the particles from these layers is a viable source of the trapped sediments. Second, the settling out of shelf sediments entrained via resuspension by rapidly revolving migrating eddies is a possible source of the trapped particles, as inferred especially for the fall and winter of 1992/93. Third, resuspension and erosion of bottom sediment due to the interaction of internal waves with the sloping bottom of the continental slope could remobilize vast amounts of sediment in this area. Fourth, the alternations between upwelling and downwelling conditions may resuspend bottom sediments over the slope and create conditions for the entrainment of suspended particles into mid-water nepheloid layers. The tilting of isopycnal surfaces during upwelling may move suspended particles out over the slope and contribute greatly to the observed pattern of increasing fluxes with depth. And fifth, the lateral transport of riverine sediment and biological material in nepheloid layers below at least 300 m beyond the shelf break is evident following the spread of the peak river flows over the shelf. In this case, the prevailing winds confined the river plume to the west side of the shelf. Much of the terrigenous material along with the remnants of a diatom bloom (that developed in the opening lead and at the front edge of the river plume) likely settled out over Mackenzie Trough or possibly even over the eastern edge of the Alaskan shelf. This newly settled material is likely easily resuspended and moved out over the slope in a bottom boundary layer and subsequently in mid-water nepheloid layers.

The traps (290 and 490 m) are deeper than the reported record of currents, temperature and salinity (59 and 161 m), and it is therefore possible that there is an additional, deeper source of suspended sediments associated with a bottom nepheloid layer. However, the fluxes of sediment at 290 m and 490 m were very similar throughout the fall and early winter suggesting little additional nepheloid transport between 290 and 490 m water depth. This suggestion points to the need for transects of moorings with instrumentation capable of better representing full water column data for currents,

temperature, salinity and suspended particle content: these would greatly enhance the understanding of sediment transport beyond the shelf edge, and associated understanding of regional impacts on production, carbon sequestration, and nutrient cycling.

6.3 Influence of physical forcing on fluxes at site L144

Site L144 is located at the 2700 m isobath much further from the shelf break than sites SS-5 and AM1-92 (Figure 6.19). The material collected in the deep trap (1311 m) is highly terrigenous (83-89 % TERR, Figure 5.4), and with the exception of the third trap interval (which has a higher than average opal content), the composition is remarkably consistent (Figure 5.4). While the material collected in the 412 m trap has a slightly higher biogenic content (Figure 5.4), with only a few exceptions both the biogenic and terrigenous fluxes are higher in the deep trap (Figure 6.32). The fluxes vary erratically over the deployment and the largest flux peaks of both terrigenous and biogenic material occur abruptly in August/early-September, 1992. The flux data clearly indicate the occurrence of lateral transport of suspended particles, both terrigenous and biogenic. Very small, but measurable CHLA and PHAEO fluxes in fall 1991 and late summer of 1992 (Figure 3.6g and 3.6h) indicate that recently produced biological material was laterally transported to the site from the pack ice edge to the south.

The following sections examine the physical conditions at the shelf and over the slope to identify: 1) the likely sources and trajectories of the biogenic and terrigenous particles; 2) reasons for the erratic flux patterns; and 3) factors important to the fluxes of both the terrigenous and the biogenic material. Physical data include wind, ice cover, currents, temperature-salinity (T-S), and river inputs. In addition to the data from the mooring at site L144 (in 2700 m water depth), data from another mooring AM1-91 (at the 700 m isobath; see Figure 6.19 for location) deployed through the same period will be discussed to shed light on processes at the shelf edge and higher up the slope. The timing and likely fate of the massive Mackenzie River inputs of freshwater and suspended particulates is investigated in relation to the ice conditions on the shelf and to the prevailing winds to determine the both the influence on stratification over the shelf and the availability of a pool of easily resuspended sediment for potential transport beyond the shelf break.

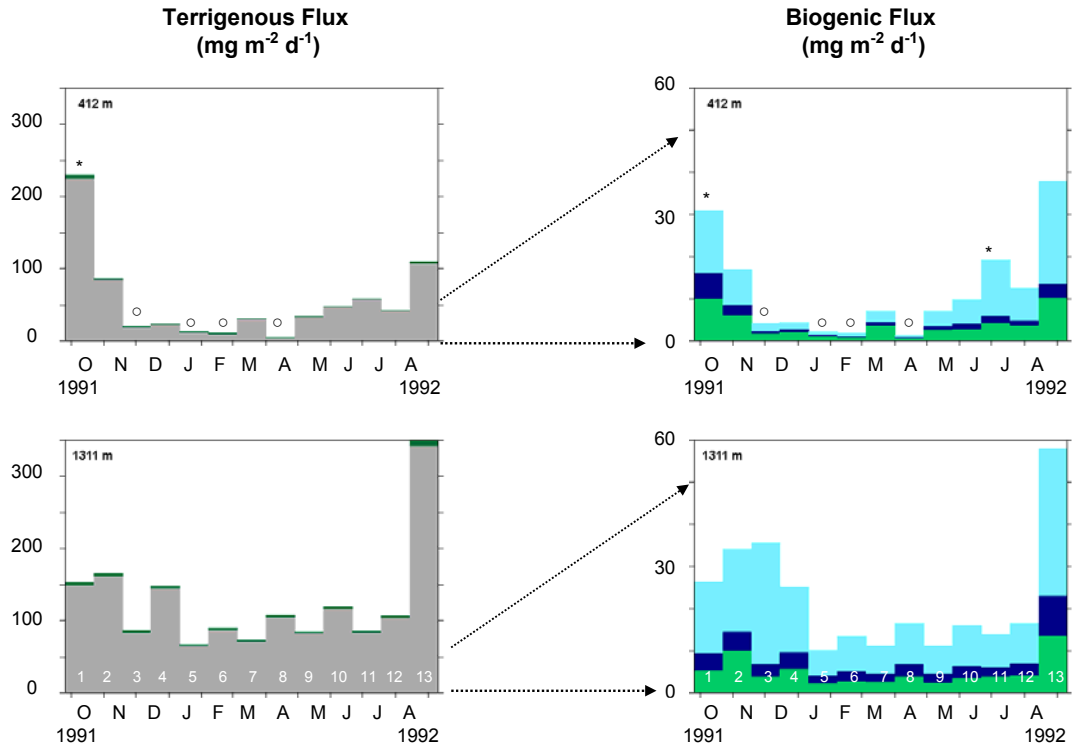

Figure 6-32 Terrigenous and biogenic fluxes (mg m^{-2} d^{-1}) for site L144 at the 412 and 1311 m sediment traps. The terrigenous fraction includes the inorganic material ($TERR_{inorganic+CaCO3}$) and an estimate of the refractory organic mater ($POM_{refractory}$). Note that calcium carbonate produced by foraminifera and coccolithophorids could not be separated from the inorganic portion. The biogenic fraction includes the biogenic organic matter (POM_{biog}), the recently produced opal ($OPAL_{new}$), and opal produced in an earlier season that has been resuspended along with bottom sediments ($OPAL_{old}$). See Section 5.4 for a description of the methodology used to calculate the biogenic and terrigenous fluxes. The numbers in white (1 to 13) at the bottom of the 1311 m plot refer to the sediment trap interval number. The asterisks (*) above interval in the 412 m plot refer to intervals where the fluxes were greater at 412 m than at 1311 m (at all other intervals, the fluxes are greatest in the deep trap). The open circles on the 412 m plot refer to very small samples where aluminum analysis was not possible and the composition of the sample was estimated according to the method outlined in section 5.4.

6.3.1 Ice cover at site L144 from fall 1991 to fall 1992

Over the summer and early fall of 1991, prior to the deployment, site L144 remained under > 90 % ice cover, and the Alaskan and Mackenzie shelves were clogged with heavy ice (Canadian Ice Service). For the first week after deployment, ice cover may have been reduced at L144 but this is uncertain due to the poor rate of good returns from the Upward Looking Sonar (ULS) possibly due to frazil ice in open leads or to fast moving ice (Figure 6.33A). For the last three weeks of October, multi-year ice

A) Upward Looking sonar data for site L144

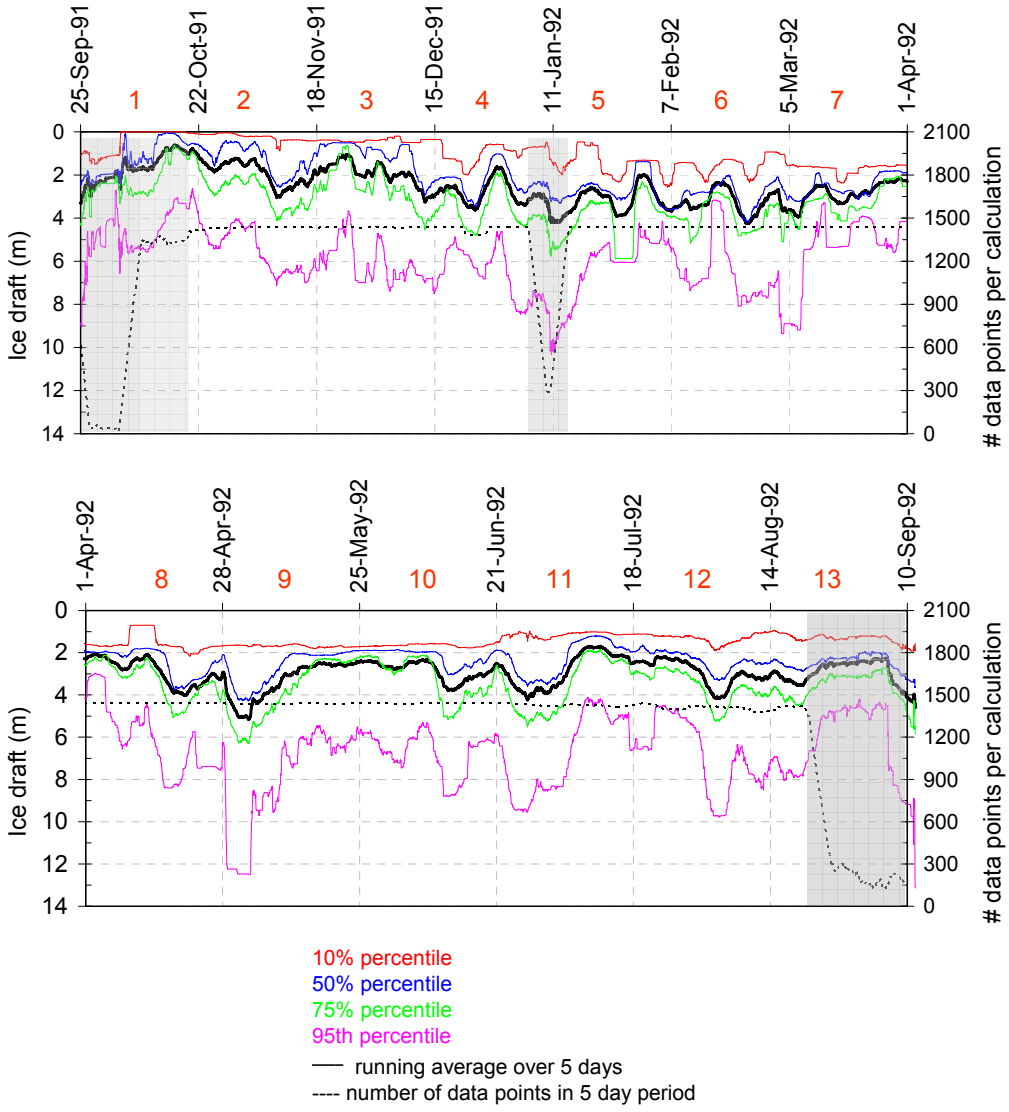

Figure 6-33 Upward Looking Sonar (ULS) data for A) site L144 where the sediment trap mooring was located and B) site AM1-91 closer to the shelf edge and deployed during the same period (see Figure 6.19 for site locations). Plots show the dates of the openings and closing of the sediment traps and the number of the trap collection interval (red numbers; 1 to 13) at site L144. The ice thickness data is presented as 5-day running averages (thick black line; data collected at 5 minute intervals) and as percentiles (also running over 5-day periods). The percentiles indicate that a given percent of the ice thickness is below the thickness represented on the graph by the 10 % (red line), 50 % (blue line), 75 % (green line), and 95 % percentiles. The periods where there were a reduced number of good returns in the ULS data (possibly due to frazil ice or to fast moving ice) are shaded in grey and the number of points used in the running average and the percentile calculations is indicated by the black dashed line. Also, because of the large file sizes, the files were split up and the number of points used in the calculations falls off at the end of the files.

B) Upward Looking sonar data for site AM1-91

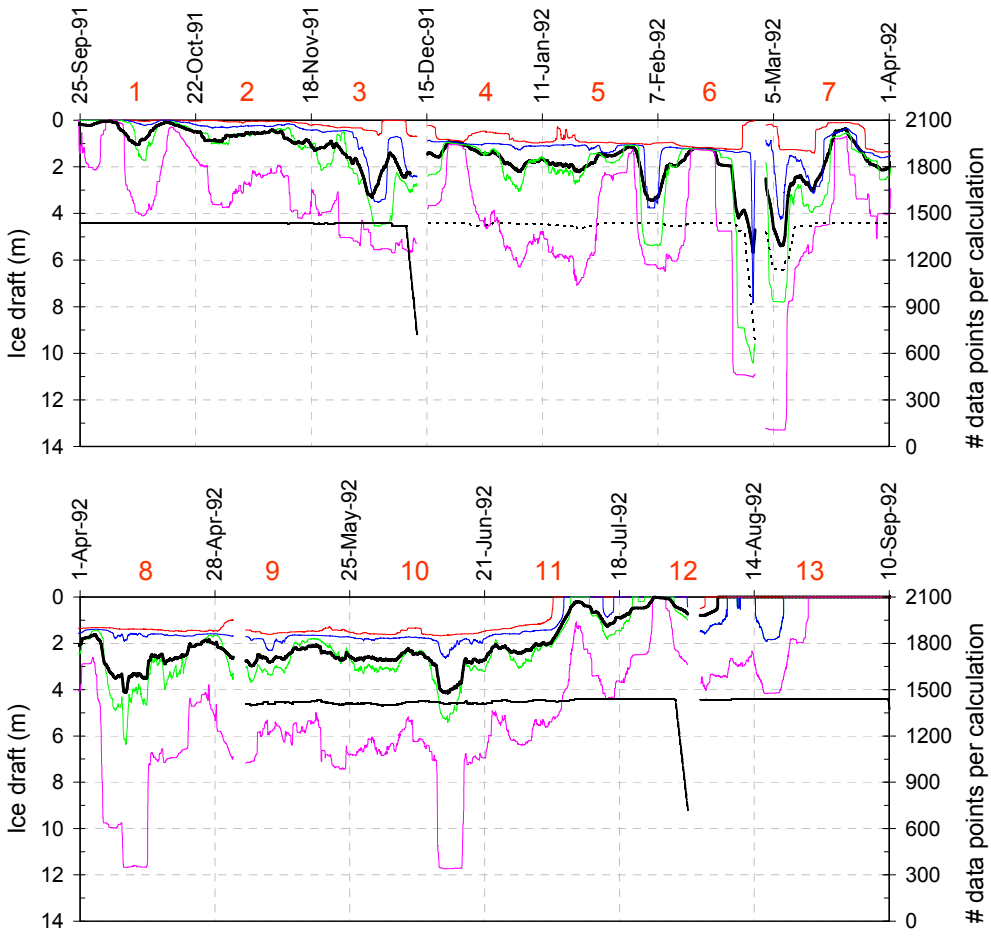

Continuation of Figure 6.33 (6.33B)

interspersed with thin new ice and open leads covered site L144 (Canadian Ice Service; Figure 6.33A). Freeze-up was complete on the Alaskan and Mackenzie shelves by October 22, 1991, and ice cover was > 90 % on the shelves until about early-June 1992 when the first small areas of open water appeared in Shallow Bay and over Mackenzie Trough. The L144 mooring site was under complete ice cover with an average ice thickness of approximately between 2 to 4 metres throughout the winter and until at least until about August 24, 1992 (Figure 6.33A). From mid-July until the end of the deployment on September 10, 1992, the mooring was close to the ice edge and after August 24, was in an area consisting of open water and pans of multi-year ice (Canadian Ice Service; Figure 6.33A). The Canadian Ice Service charts from August 24 to the end of

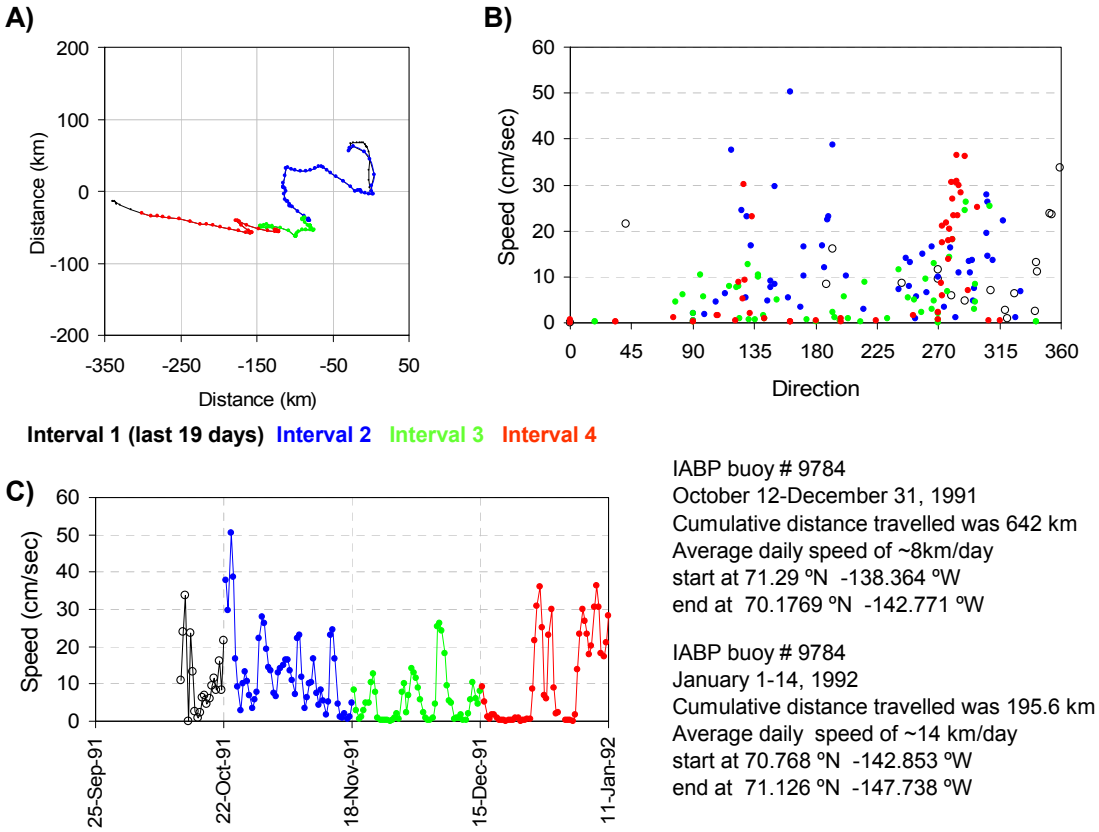

Figure 6-34 Plots of ice drift data from the International Arctic Buoy Program (IABP; buoy # 9784) during sediment trap intervals 1 to 4 at site L144 as follows: A) Progressive vector diagram of ice drift, B) Speed of ice drift plotted against direction showing the bimodal pattern in the direction of drift, and C) Speed of ice drift against time. The sediment trap intervals are color coded as noted in the figure (black for the last 19 days of interval 1, blue for interval 2, green for interval 3, and red for interval 4. In addition, at the bottom right of the figure, the buoy position and drift speeds are indicated for the periods October 12 to December 31, 1991 and January 1 to 14, 1992.

the deployment indicate some open water in the area around site L144, but there is uncertainty as to whether there was open water over the site during this period due to a poor rate of good returns from the ULS. It is clear that lateral transport of suspended particulates was occurring, and that the trapped material likely originated from resuspension of material on the shelf and slope.

Closer to the shelf edge at site AM1-91 (see Figure 6.19 for location), the ULS data from late September to mid-November 1991 indicated that there were significant periods of open water and thin ice interspersed with thick keeled ice (Figure 6.33B).

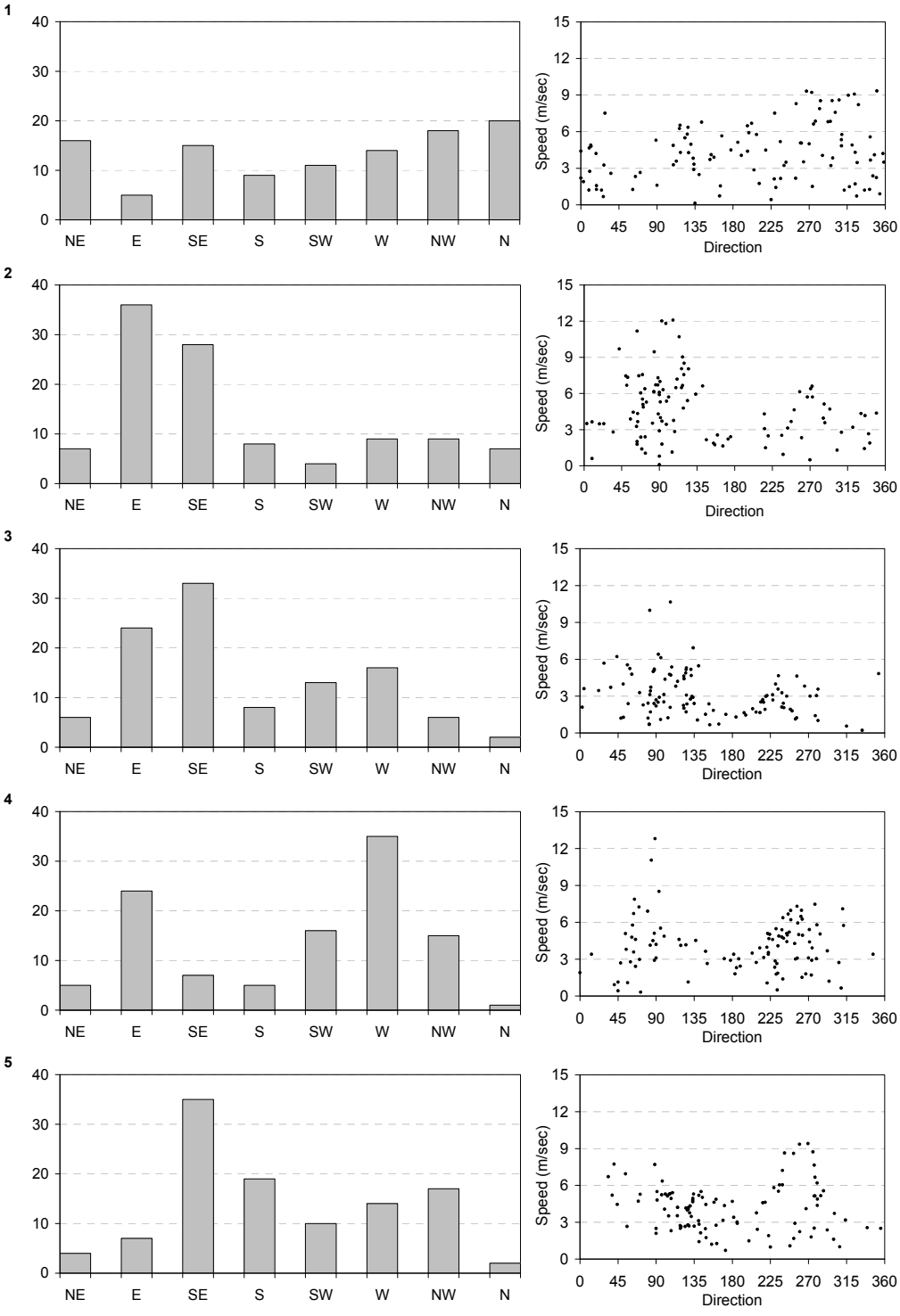

Figure 6-35 National Centers for Environmental Prediction (NCEP) 10 m wind data (at grid point labelled N in Figure 6.19) for each of the 13 sediment trap intervals at site L144. For each interval (see numbers of the far left of the plots; 1 to 13), there is a histogram of wind direction and a plot of speed against direction. The final plot of wind speed against direction is for the full sediment trap collection period at site L144. These plots highlight the strong bimodal pattern favouring the directions E-SE and W-NW.

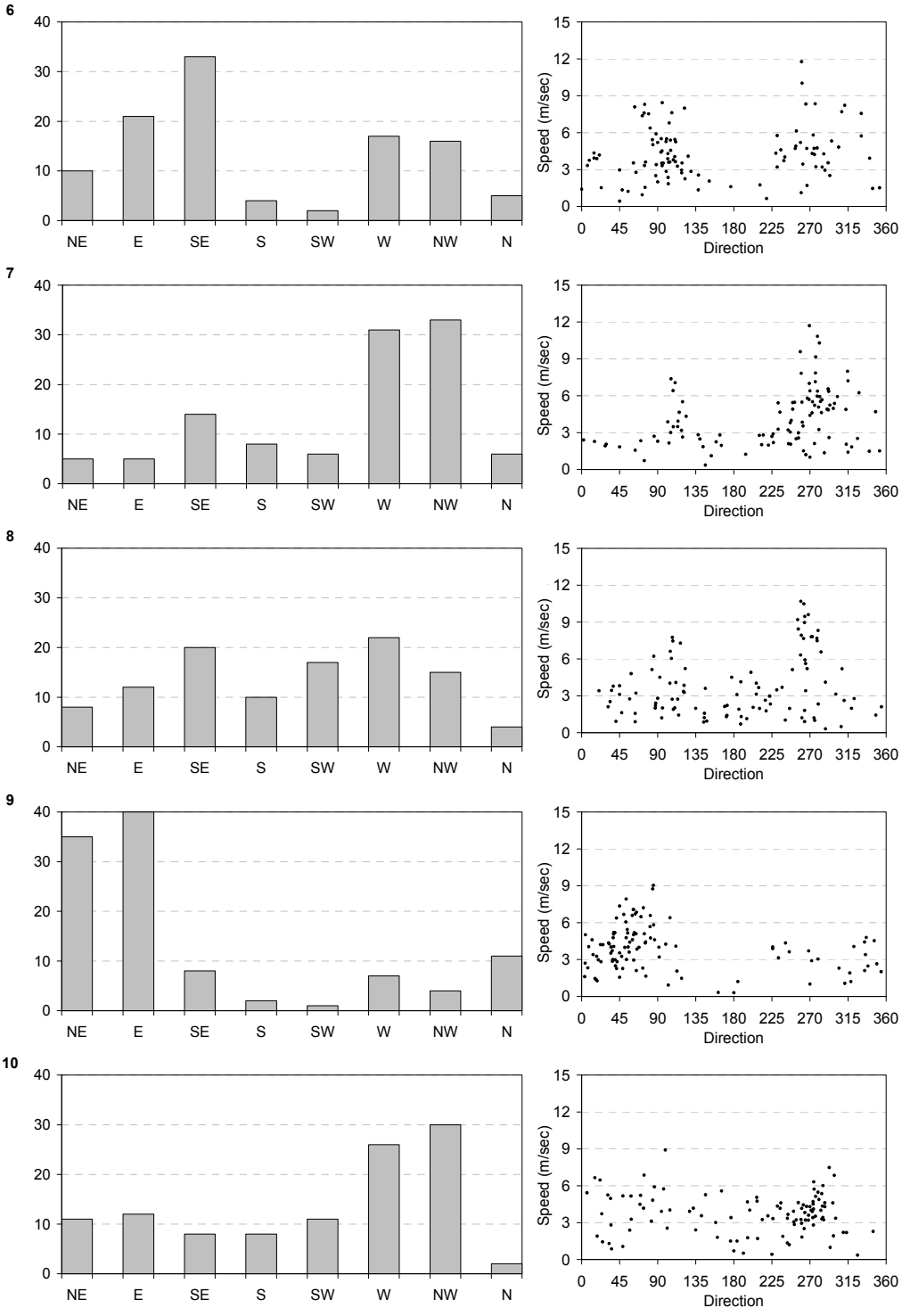

Continuation of Figure 6.35

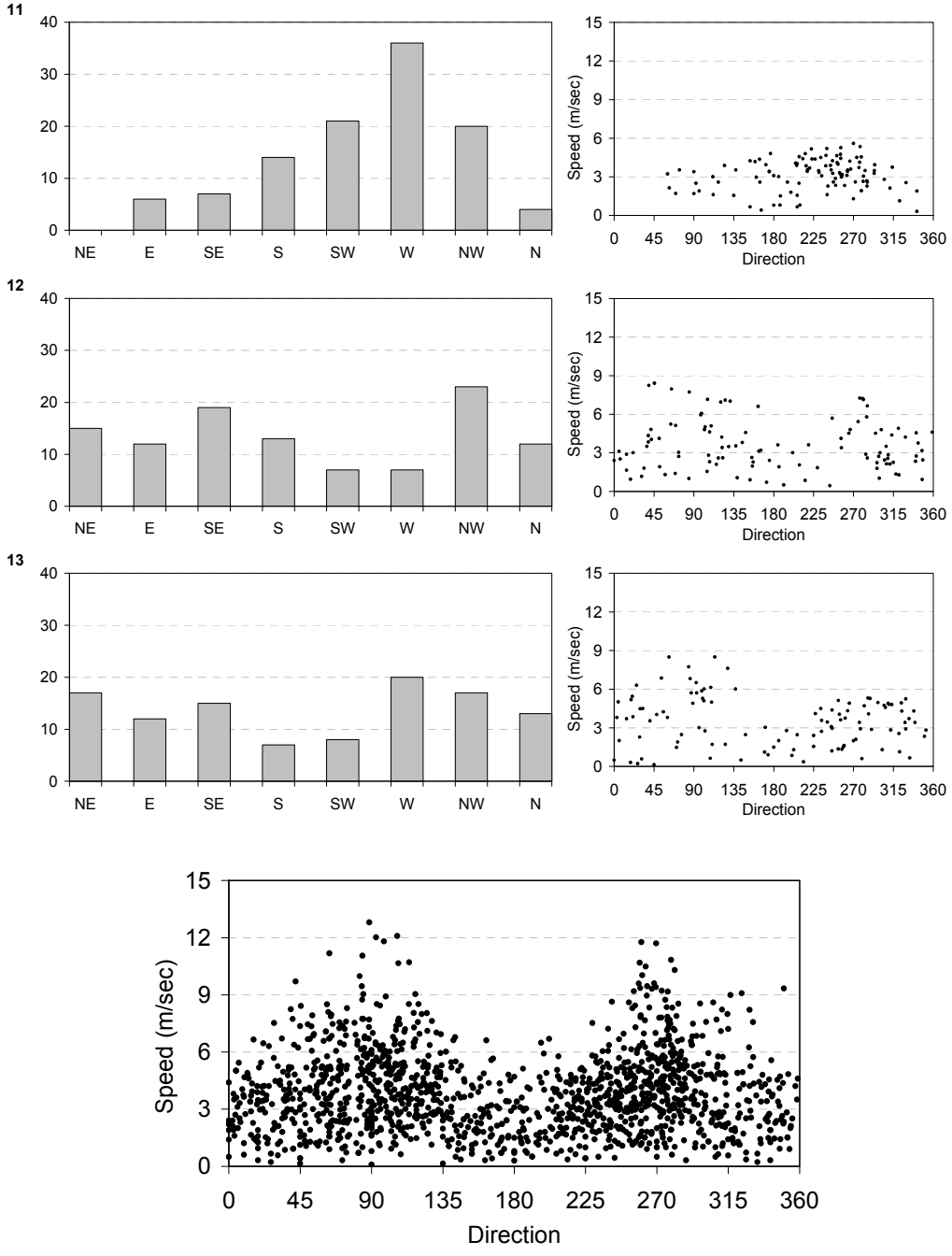

Continuation of Figure 6.35

After that, the ice cover was generally heavy (5-day averages ranged between 0.5 and 5 m) until the first week of July 1992 (Figure 6.33B). Over the remainder of the summer, the average ice thickness decreased steadily, and by the first week of August 1992, AM1-91 was essentially in open water except for the passage of pans of deep-keeled ice.

The break-up of the sea-ice was late in the spring of 1992. By late-June, heavy ice still inundated the shelves, and there was still only a small area of open water primarily over Mackenzie Trough that expanded slowly throughout July. By mid-August 1992, open water lay over the Alaskan and Mackenzie shelves out to about 71 ºN, extending to site AM1-91 but not as far as site L144.

IABP (International Arctic Buoy Program) buoy data show that the ice in this area was very mobile during the fall/early winter of 1991 and the first half of January 1992. The maximum drift speed of 50 cm sec^{-1} (12-hour sampling intervals) to the SSE occurred on October 23 during the second sediment trap interval at site L144 (Figure 6.34). From October 12 to December 31, 1991, the ice drifted an average of ~8 km day^{-1} with a net displacement to the SW but also with strong NW and SE components (Figure 6.34). In the first two weeks of January, the average drift speed was ~14 km day^{-1} with a net displacement to the NW. There were no drifting buoys to track the ice movement after mid-January. The direction of ice drift in trap periods 2-4 exhibits a bimodal pattern of SE-S and W-NW. This distinct pattern indicates high current speeds that are likely to have contributed strongly to setting up alternating upwelling and downwelling conditions along the shelf and slope.

6.3.2 Winds

The wind direction varied considerably during the trap collection period, and exhibited a bimodal pattern between E-SE and W-NW with the strongest winds blowing generally to the E or to the W (Figure 6.35). These alternately forced upwelling and downwelling. The Alaskan shelf edge has a different orientation than the Mackenzie shelf and as a rough estimation, winds blowing to between SW to NE (moving clockwise) would likely be upwelling favourable along the Alaskan Shelf edge and winds blowing to between NE to SW (moving clockwise) will likely produce downwelling conditions. In the Mackenzie Trough area, the relationship between wind patterns and upwelling/downwelling favourable conditions is likely to be much more complex.

When ice is present, the motion of the ice rather than the wind can control whether conditions are upwelling or downwelling favourable (Williams et al., 2006). For intervals 2 to 4 at L144, both the winds and the ice motion exhibit bimodal directional distributions, and the directions of ice drift tend to be to the right of the winds. In addition, peaks in wind speed and ice drift speed sometimes co-occur but not always, and there are periods, usually with dominant E and SE winds, when the winds produce no ice drift, presumably due to jamming and internal ice stresses (as was also observed by Williams et al., 2006).

As discussed earlier, alternating upwelling/downwelling conditions driven by winds and ice likely resuspend sediments on the slope and shelf edge. Because site L144 is further offshore, a lag is expected between resuspension events closer to land and the appearance of suspended particulates in the traps, which presumably were transported to the mooring site in nepheloid layers.

6.3.3 River inputs

In the spring of 1992, the peak flows of the Mackenzie River at Arctic Red River were the highest recorded in the period 1974 to 1997. The flows increased sharply from 5380 m^3 sec^{-1} on May 7 to a peak of 35,000 m^3 sec^{-1} on May 31, and stayed exceptionally high throughout June (Figure 2.3). When the peak flows spread onto the shelf beyond the landfast ice in late May/early June, there was still heavy ice inundating the Mackenzie and Alaskan shelves. The behaviour of the plume under such conditions is uncertain and decidedly understudied, but it is probable that in June, the plume and associated deposition of fluvial sediments remained contained in shallower waters, dammed up behind the heavy ice. Enhanced deposition of river sediments in shallower waters due to heavy ice on the shelf would serve to minimize or delay sediment transport off the shelf. In late June and for the first half of July, as the area of open water expanded to the west, the plume likely moved into the open waters under the influence of winds blowing predominantly to the W and NW. From mid-July to mid-September (trap intervals 12 and 13), the wind directions were more evenly distributed between upwelling and downwelling favourable. During the downwelling favourable conditions, the river sediment deposited in the nearshore is likely easily resuspended and moved offshore. The high terrigenous peak in the deep trap at site L144 (interval 13) occurs more that two

months after the Mackenzie River freshet inundated the shelf and it is difficult to make a direct link between the river freshet and that late summer accumulation in the traps. However, $\delta^{13}C$ values in the trap samples decrease sharply at this time towards values characteristic of the Mackenzie River freshet as seen at sites AM1-92 and SS-5 in this study ((intervals 11 and 12; 412 and 1311 m; Figure 3.7a) and in O'Brien et al., 2006 (particularly site SS-4). That observation points firmly to the Mackenzie River as the source of the trapped particulates.

In open water, winds to the W deliver more Mackenzie River sediments to the west over the Alaskan Shelf such that when the winds switch to the E and conditions become favourable for downwelling, there may be a ready supply of easily resuspended sediment for incorporation into nepheloid layers. Likewise, winds to the E during periods of open water and high river inputs would direct more of the new influx of river sediments to the Mackenzie Shelf. In this fashion, the location of supplies of easily resuspended sediment may vary depending on how the winds have directed the river plume. The location and availability of easily resuspended sediments may be important to the magnitude of fluxes observed beyond the shelf break.

6.3.4 Currents and temperature-salinity (T-S) relationships at site L144

The mooring at site L144 had four current meters (at 87, 106, 161, and 419 m) and one Seacat (at 98 m). When coupled with the current data (at 82, 183, and 534 m) and T-S data (at 83 and 184 m) that were collected at AM1-91 during the same period, processes that are capable of carrying suspended particulates to the traps at L144 (412 and 1311 m) can be identified.

The low background current speed at L144 was punctuated by episodes of elevated currents, many (if not all) of which were associated with passing eddies (Figures 6.36 and 6.38). Site AM1-91, closer to the shelf break, also exhibited patterns consistent with eddies (Figure 6.37 and 6.39) which occurred with a much greater frequency and with higher current speeds than at site L144. At both sites, the current speeds were higher in the top 200 m and lower at the deepest instruments (419 m at L144 and 534 at AM1-91) but the presence of eddies is evident at all the measured depths, identifiable by both

A) Currents at site L144

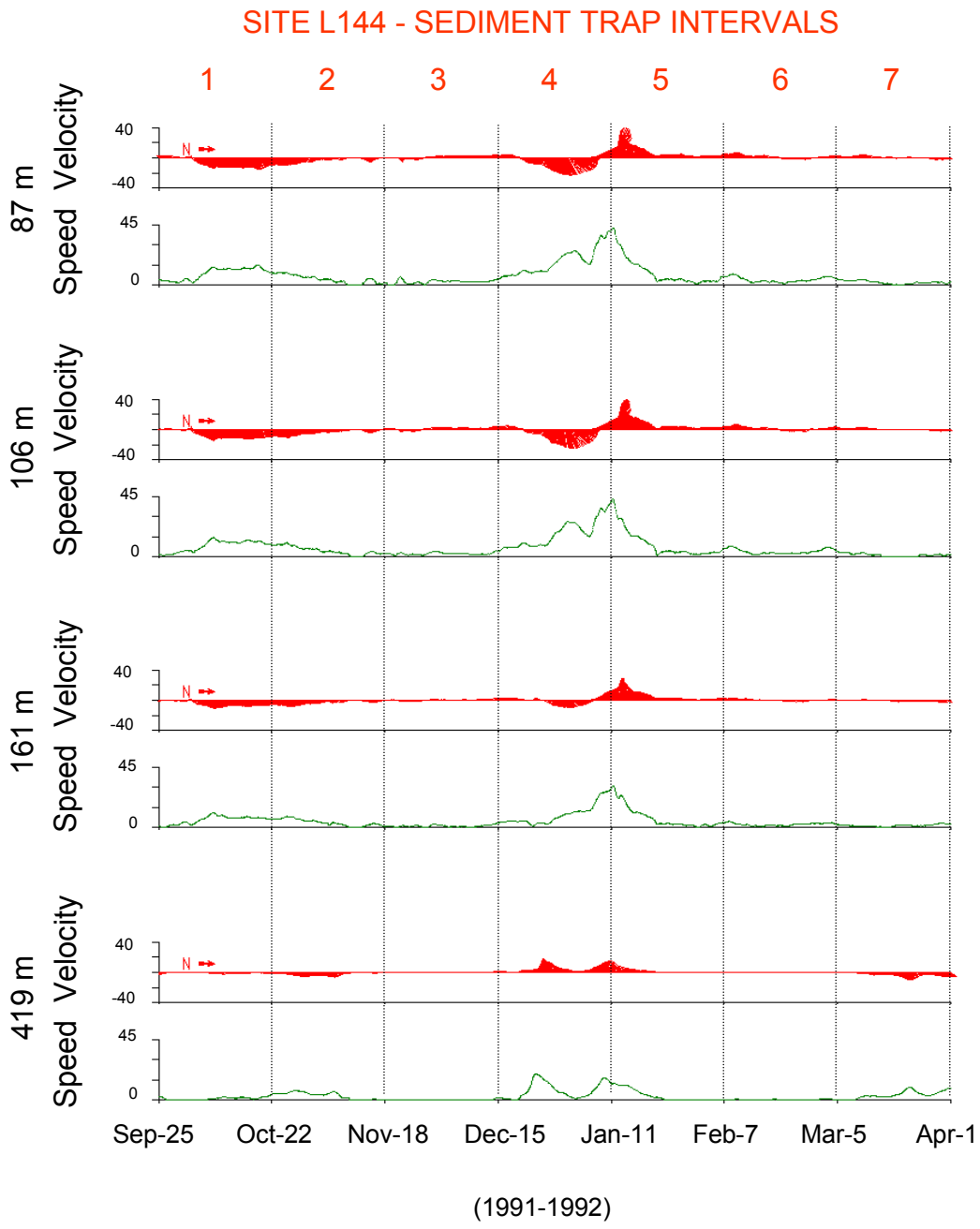

Figure 6-36 Velocity and speed data for 87, 106,161, and 419 m at site L144. Time periods on the plots are the 27 day intervals for the site L144 sediment traps as follows: A) intervals 1 to 7 and B) intervals 8 to 13. Units are cm sec^{-1}.

B) Currents at site L144

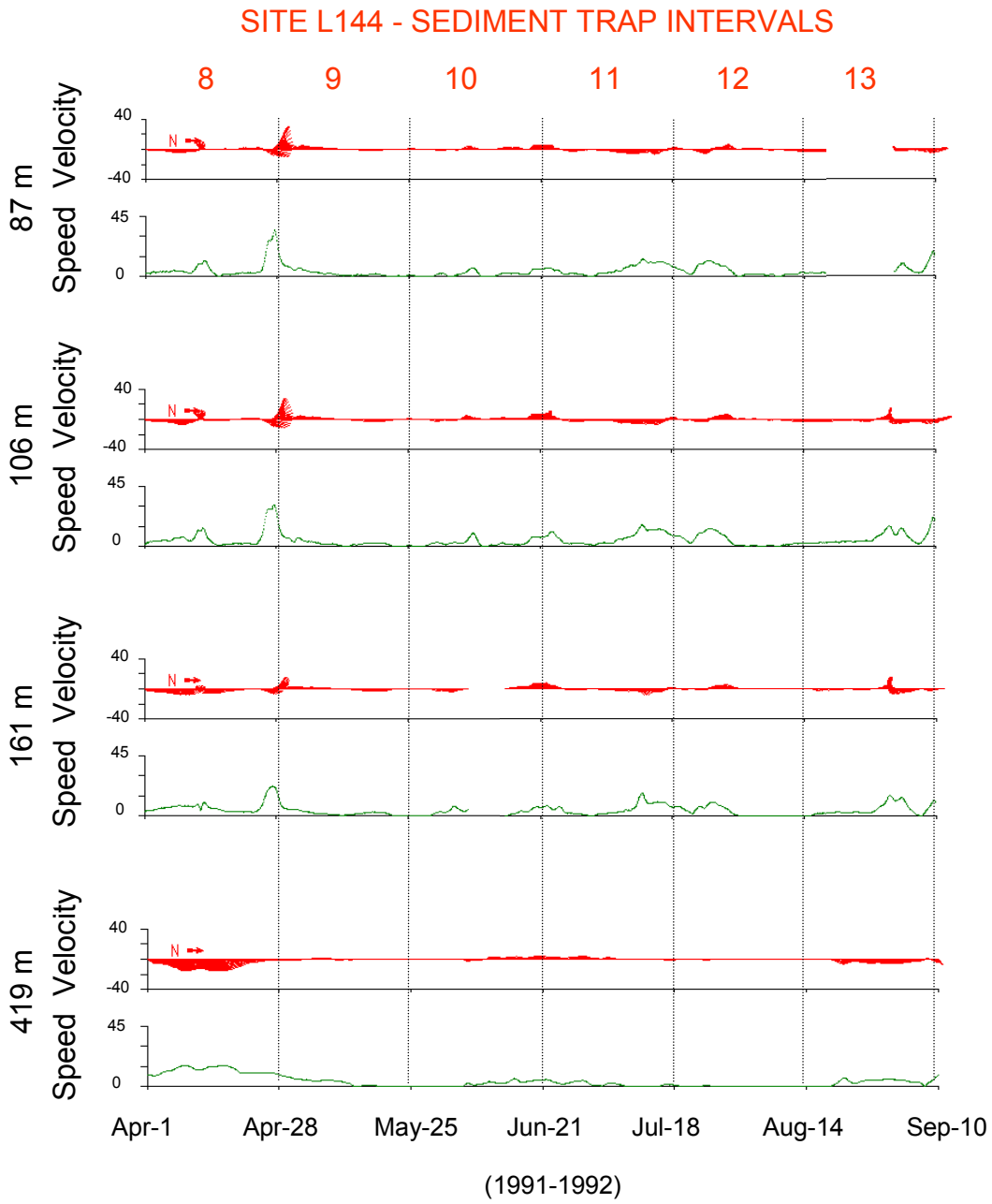

Continuation of Figure 6.36 (6.36B)

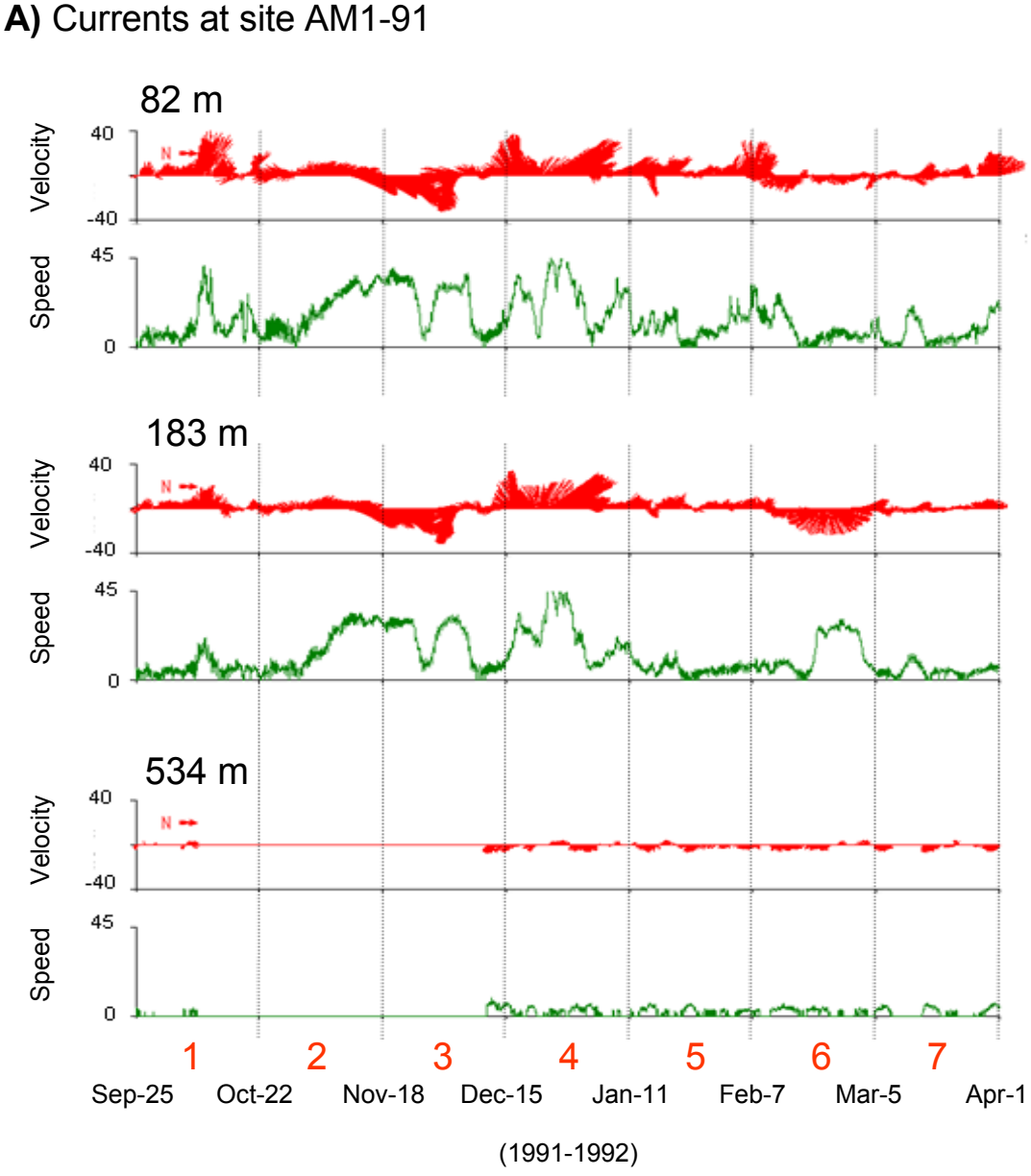

Figure 6-37 Velocity and speed data for 82, 183, and 534 m at site AM1-92. Time periods on the plots are the 27 day intervals for the site L144 sediment traps as follows: A) intervals 1 to 7 and B) intervals 8 to 13. Units are cm sec^{-1}.

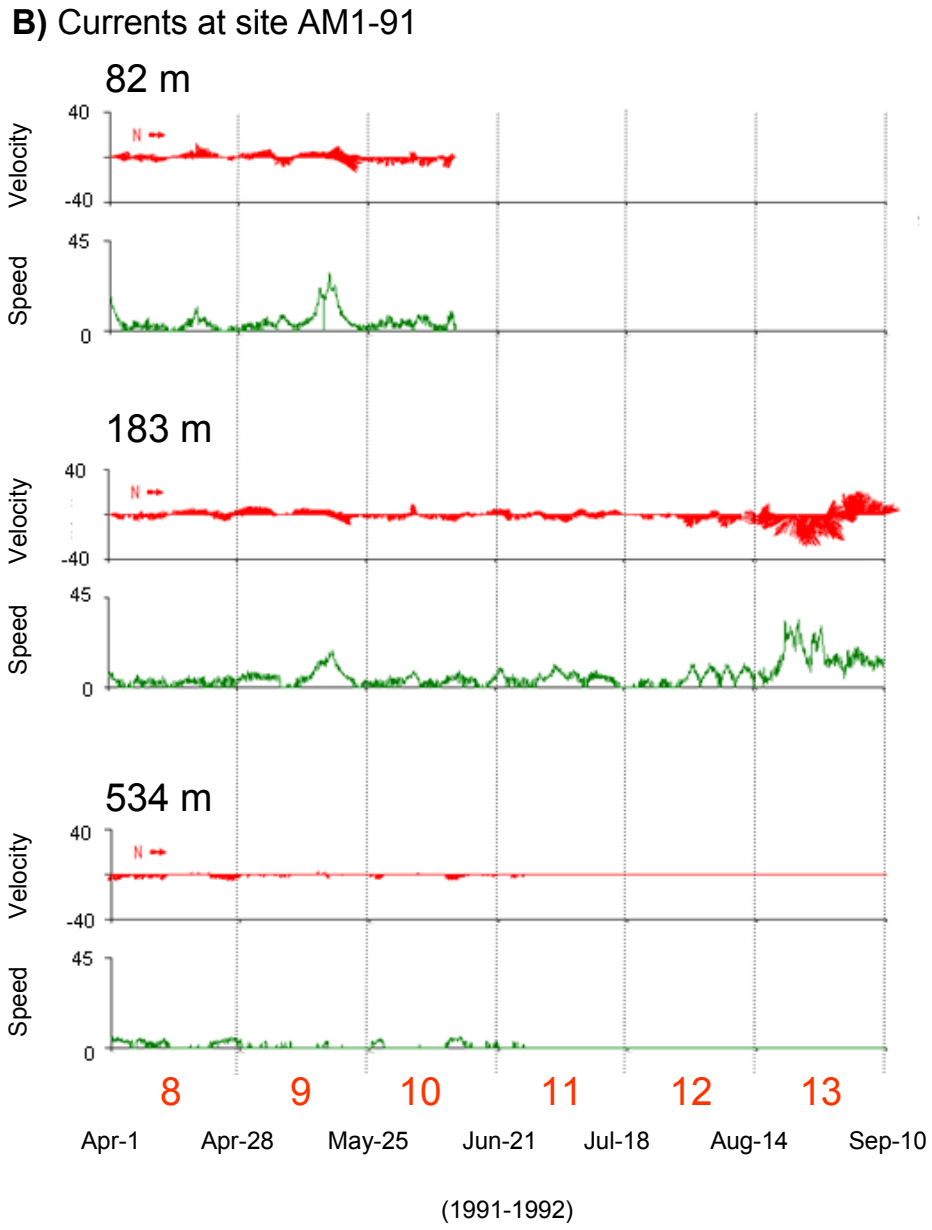

Continuation of Figure 3.37 (6.37B)

the current and the T-S records. Clearly, the currents associated with these eddies at the shelf edge and upper slope are very energetic and capable of resuspending bottom sediments and of moving suspended particles beyond the shelf break into deeper waters over the slope to settle in an generally lower energy environment.

The largest eddy at site L144 occurred during intervals 4 and 5, and extended between 87 m and at least 419 m, with associated anticyclonic current speeds ranging up

A) Site L144

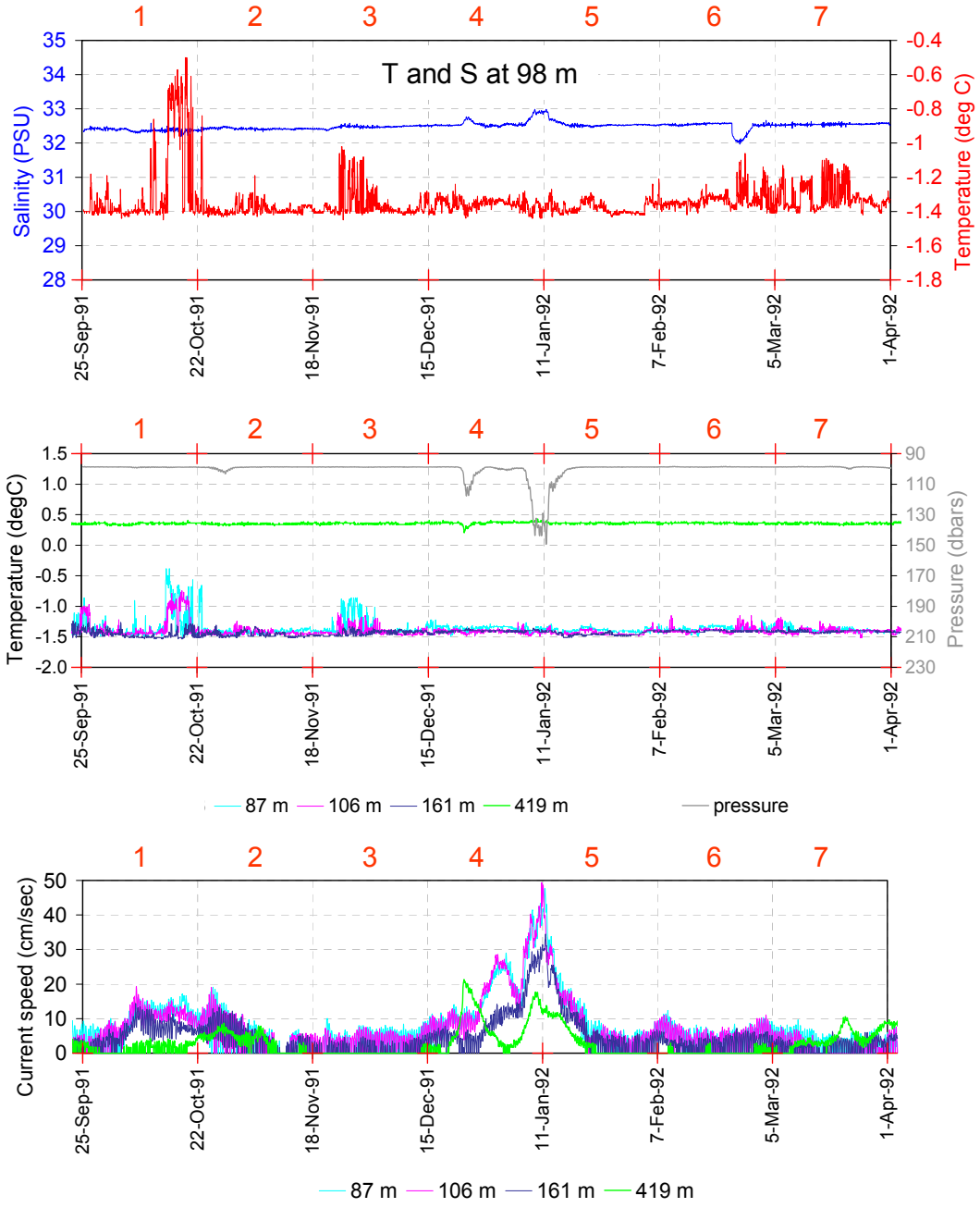

Figure 6-38 Mooring data for site L144 represented for sediment trap intervals A) 1 to 7 and B) 8 to 13. The sediment trap interval numbers are in red at the top of each plot. The top plot is the continuously recorded temperature and salinity (T-S) data at 98 m. The middle plot shows temperature data (at 87, 106,161, and 419 m; left axis) and pressure measured at 98 m (right axis; grey; units are db). The bottom plot depicts the current speeds in (cm sec^{-1}) at 4 levels in the water column (87, 106, 161, and 419 m). Note that the temperature scales are different in the top and middle plots.

B) Site L144

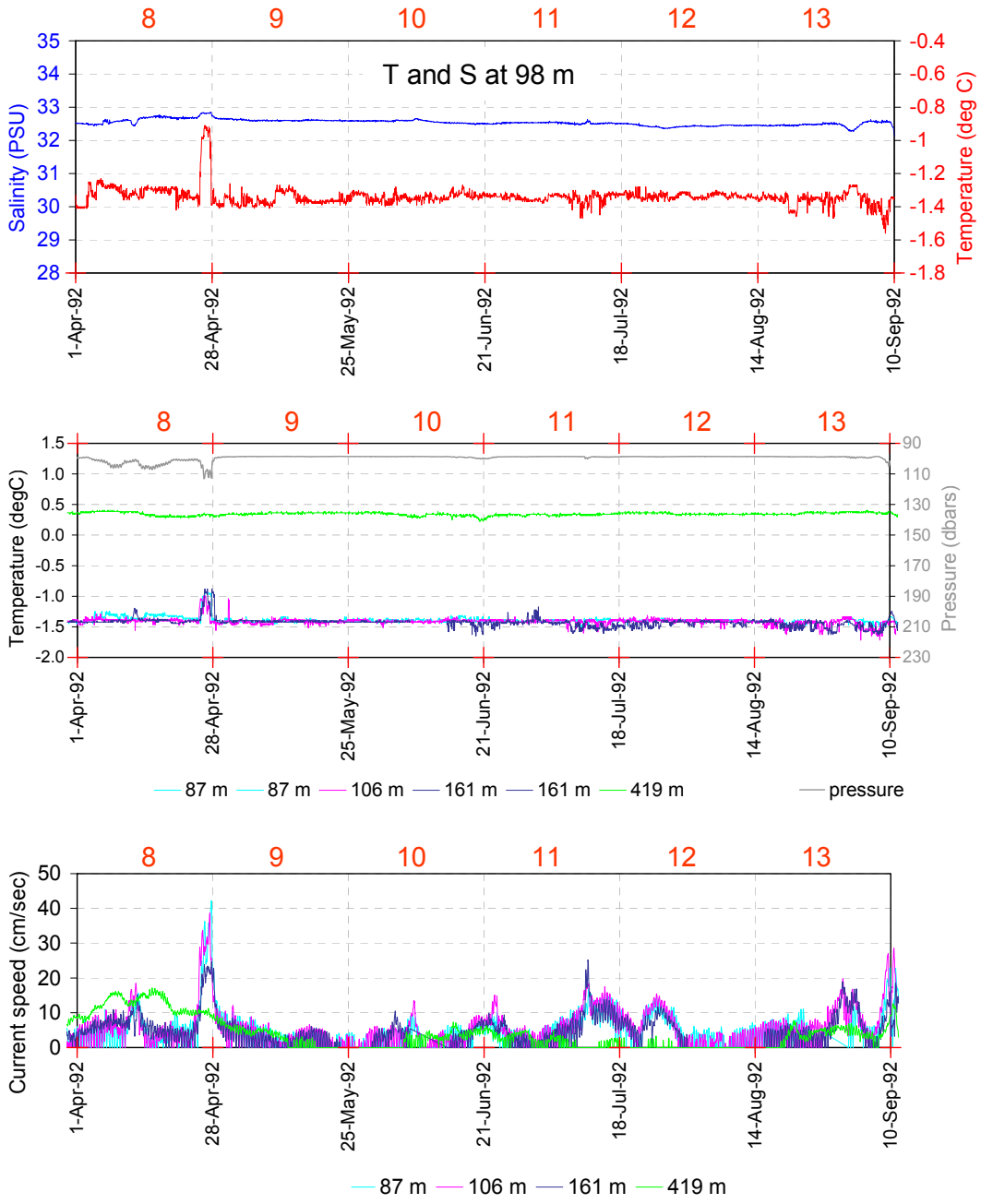

Continuation of Figure 3.38 (6.38B)

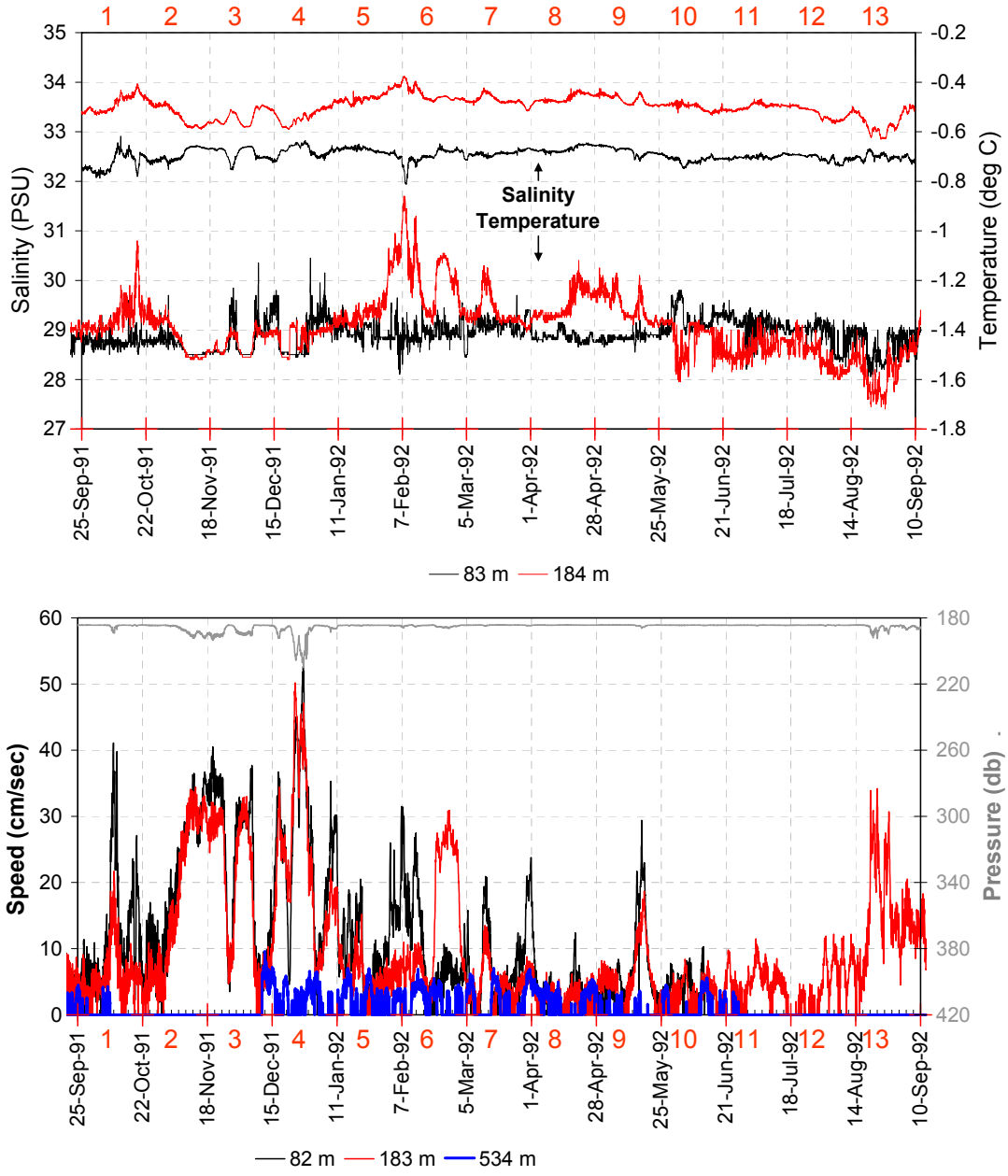

Figure 6-39 Mooring data for site AM1-91 (see Figure 6.19 for location). For convenience, the sediment trap intervals for the L144 trap intervals are represented on the time scale with all 13 intervals on each plot. The top plot is the continuously recorded temperature and salinity (T-S) data at 83 (black lines) and 184 m (red lines). The bottom plot depicts the current speeds (in cm sec^{-1}) at 3 levels in the water column (82,183, and 534 m).

to 42 cm sec^{-1} (Figure 6.36A). The passage of the eddy coincided with an increase in terrigenous sediment in the deep trap (1311 m, interval 4; Figure 6.32) of more than 100 mg m^{-2} d^{-1} but an insignificant increase in the 412 m trap. Because the current record extends only to 419 m, there is no certainty that the flux increase in the deep trap (at 1311 m) was due to the eddy but the temporal coincidence is suggestive. This particular eddy is discussed by Aagaard and Carmack (1994) who suggest that it consists of a pair of oppositely rotating eddies; an anticyclonic eddy within the pycnocline (down to at least 161 m) overlaying a deeper cyclonic eddy (manifested in the current record at 419 m). Due to lack of data, the depth to which the eddy extends is unknown.

Other eddies, both cyclonic and anticyclonic are evident in the current records at site L144 (see trap intervals 8 and 13 in Figure 6.36), and the intermittent passage of these eddies may, at least in part, be responsible for the erratic fluxes observed in the deep trap at site L144. Eddies are a common feature in this area (e.g. Newton et al., 1974; Manley and Hunkins, 1964) and are a plausible mechanism for the resuspension and movement of suspended particles seaward over the slope.

Rapid fluctuations of temperature in the T-S records at both L144 and AM1-91 most likely reflect the passage of internal waves (see Figures 6.38 and 6.39). As discussed in Section 6.2, these may also be important in the resuspension sediments along the continental slope and contributing to their delivery farther offshore via transport in nepheloid layers. Indeed, temperature interleaving and nepheloid layers are evident in CTD-transmissivity profiles over the slope from the fall of 1991, the spring of 1992, and the fall of 1992 (Figure 6.16, 6.28B, and 6.31). The interleaving is most intense in the top 200 m and is present, but much more subtle, at greater depths. Although detailed investigation of the relationship between internal waves, resuspension over the slope, and subsequent transport of particles in nepheloid layers is beyond the scope of this study, the data here clearly indicate that the topic warrants future attention.

6.3.4 Summary physical data and relationship to fluxes at site L144

The importance of lateral vectoring of particles is reinforced by the observation that site L144 was under heavy ice cover for virtually the full deployment period. Clearly, the trapped particles at L144 must have originated from resuspension of bottom sediments on the shelf and shelf slope and subsequently been transported laterally over

the slope either in association with eddies or within nepheloid layers. Resuspension and incorporation into nepheloid layers was likely due at least in part to: 1) the movement of bottom waters up and down the slope during alternating upwelling/downwelling cycles due to the E-W bimodal wind patterns and to ice drift; and 2) the passage of internal waves. In addition, resuspension of bottom sediments and a more rapid transport seaward likely occurred due to the interaction energetic eddies and boundary currents with the bottom sediments at the shelf edge and on the slope.

The irregular pattern of fluxes in the deep trap at site L144 suggests an episodic process that varied in intensity but continuously supplied resuspended particulates to nepheloid layers that then carried suspended particles seaward along isopycnal surfaces over distances of more than 100 km. The random passage of eddies also contributes to the episodic pattern of fluxes at L144 keeping in mind that eddies differ in suspended particle load due to variable ages and differing modes and locations of formation.

The remarkably consistent composition of the material (Figure 5.4C) in the deep trap also suggests either that the resuspended material was very homogeneous at source or that some sort of equilibrium was attained during transport. Speculatively, the available surface area of the mineral particles may determine the nature of the equilibrium between the inorganic particles and organic matter which likely consists of a host of heterotrophic organisms (bacteria and viruses) and adsorbed complex organic molecules in addition to phytoplankton debris.

The carbon isotope data make a strong link between the high flux peak (in late August/early September) and Mackenzie River inputs, and thus warrant an investigation of possible mechanisms for the transport of massive quantities of river sediments deposited in the nearshore (such as must have occurred in the heavy-ice scenario of 1992) and the subsequent across-shelf transport in bottom nepheloid layers or possibly as fluid muds as is known to occur in other large river systems (Harris et al., 2005). As this is also relevant to the high flux peak at site AM1-92, a discussion of this will be reserved for Chapter 7. Also, central to the discussion of resuspension over the slope is the assumption of sufficient flow strength at the sediment interface for resuspension to occur. This also raises the question of exactly what is being resuspended, cohesive sediments or a pool of recently deposited, and hence easily resuspended sediments? As this discussion applies to

all the sites studied, these questions will also be addressed in the final discussions in Chapter 7.

6.4 Influence of physical forcing on fluxes at site A01

The terrigenous and biogenic components of the fluxes at site A01 (A01-90, A01-92, and A01-93) are shown in Figure 6.40. At site A01-90, many of the samples were too small to allow for analysis of BIOSI so for those samples, it was not possible to calculate their terrigenous and biogenic contents (noted on plot in Figure 6.40). However, since the TDW fluxes were low, where estimates were made (range of 1.3 to 6.3 mg m^{-2} d^{-1}; see Figure 4.1), low terrigenous and biogenic fluxes can be assumed. For these estimates, a range of %TERR of 60% to 80% was used (Figure 6.41). For both A01-92 and A01-93, there is a complete set of data. Note that for the A01 sites, there is no aluminum data so it was not possible to estimate terrigenous carbon contents.

Broadly, in the fall/winter period, terrigenous and biogenic fluxes were low in 1990-91 and 1992-93 and much higher in the fall/winter period of 1993-94 (Figure 6.40). At site A01 (~600 m), the terrigenous content had no apparent correlation with season, and overall the %TERR ranged from 25 to 85 % of the TDW flux (Figure 6.41A). Mid-winter peaks in terrigenous fluxes occurred in1990-1991 at site A01-90 at 600 m (small peak; 3.8 mg m^{-2} d^{-1}) and 1500 m (larger peak; 36 mg m^{-2} d^{-1}), and both exhibited a decrease in %POC (Figure 6.41). During the fall and winter of 1992-1993, both the biogenic and terrigenous fluxes at ~600 m were low exhibiting only one small terrigenous peak in late fall 1992 (4.5 mg m^{-2} d^{-1}; Figure 6.41) and a wide range of %POC (7 to 28 %). In contrast, during the fall/winter of 1993-1994, there were significant fluxes of both terrigenous and biogenic particles, and up to the end of February 1994 (interval 6; maximum terrigenous flux of 50 mg m^{-2} d^{-1}), the %POC was lower with a narrow range of values (4.7 to 7.0 %), and lowest %POC coinciding with the high terrigenous peak in February (interval 6). Unexpectedly, the highest biogenic flux at A01-93 (15 mg m^{-2} d^{-1}) co-occurred with the highest terrigenous flux (50 mg m^{-2} d^{-1}) in mid-winter (February; interval 6) of 1994 and exhibited moderate concentrations of CHLA and PHAEO (Figure 6.41).

In all three deployments at site A01, there were spring/summer peaks in terrigenous and biogenic fluxes, albeit with different compositions, patterns, timing, and

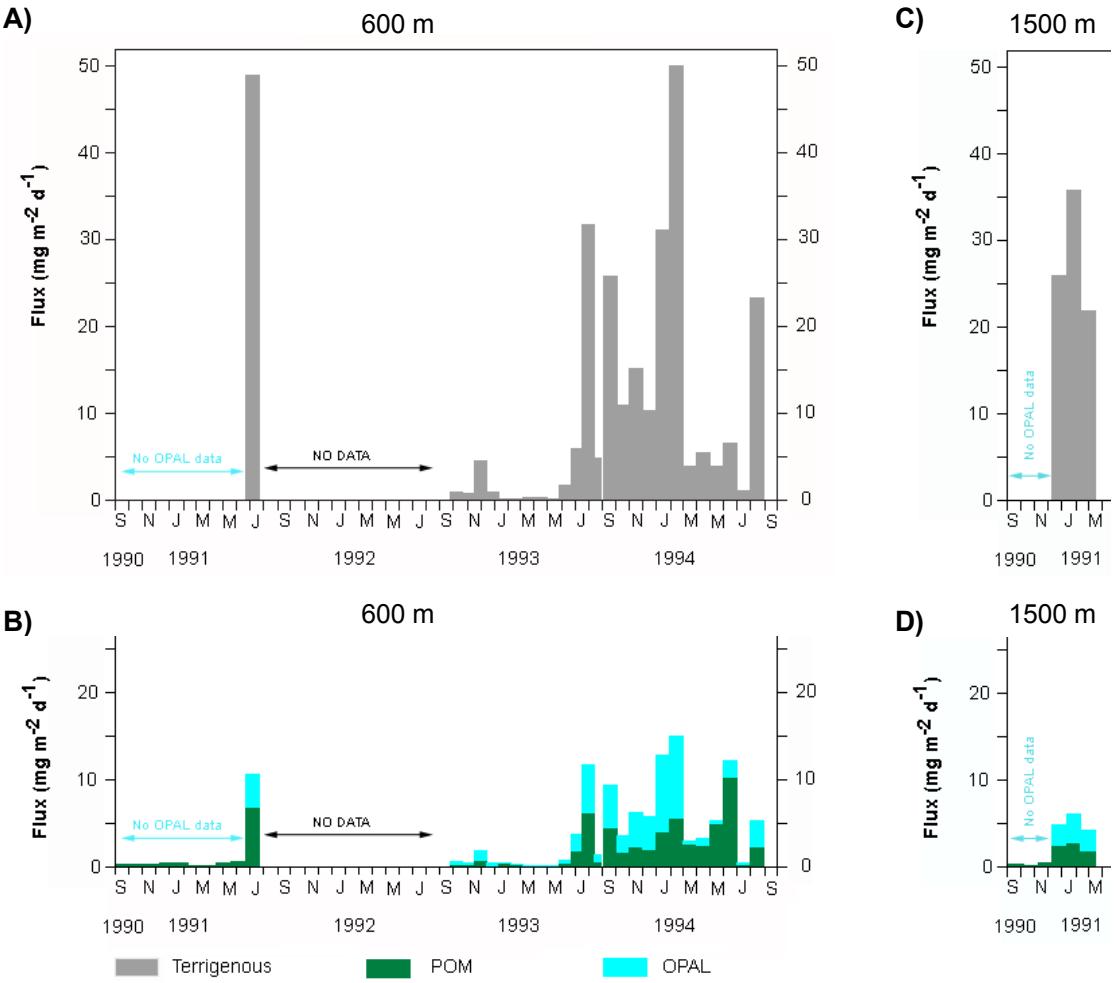

Figure 6-40 Terrigenous and biogenic components of trapped material for the three deployments at station A01 (A01-90, A01-92, and A01-93). Deployments were at ~600 m at all three sites and additionally, at 1500 m at site A01-90. Small sample sizes precluded a complete set of analysis. Where there was no OPAL data for site A01-90, terrigenous fluxes were not calculated. Note also, that with no aluminum data for the A01 site, it was not possible to estimate the terrigenous portion of the total POC. The plots represent terrigenous fluxes ($TERR_{inorganic + CaCO3}$) and biogenic fluxes (POM and OPAL) at ~600 m for all three deployments in plots a) and b) and at 1500 m for site A01-90 only in plots c) and d).

magnitudes (Figures 6.40 and 6.41). Overall, the pattern of fluxes is very similar between the biogenic and terrigenous fluxes, with the latter typically exceeding the former (Figure 6.41). There are two notable exceptions (Figure 6.41), the first being in the winter of 1992-93 (January/February; interval 5) when the fluxes were very low but the biogenic content was very high. The second, more interesting exception occurred in May/June of 1994 (intervals 9 and 10), and the composition of this material contrasted sharply with

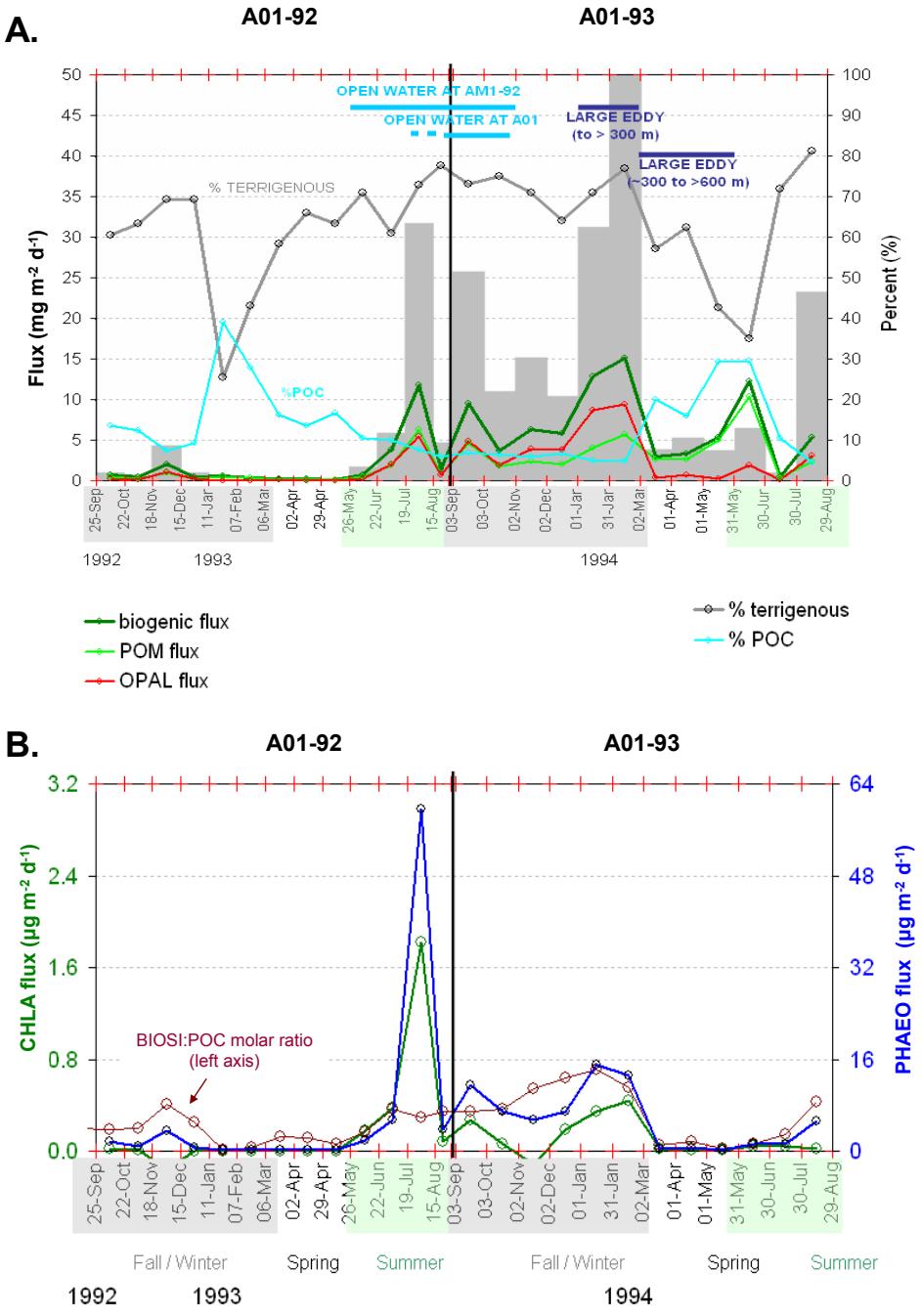

Figure 6-41 For sites A01-92 and A01-93: A) Terrigenous (grey bar plot) and biogenic (dark green line) fluxes plotted with %TERR (grey line), POM flux (light green line), OPAL flux (red line), and %POC. Plot also shows period of open water closer to the shelf edge (site AM1-92) and at site A01 in Canada Basin. The timing of two large eddies are shown (dark blue lines). B) Plots for sites A01-92 and A01-93 of chlorophyll a (CHLA), phaeophytins (PHAEO), %POC, and the molar ratio of BIOSI:POC. The time axis is colour-coded to facilitate comparison between the seasons fall/winter, spring, and summer.

the trapped material in the high terrigenous peak in February 1994; it was highly biogenic (57-65%), consisted primarily of POM with low OPAL content, and exhibited low pigment (CHLA and PHAEO) fluxes implying an origin other than primary productivity. There was an abrupt decrease in terrigenous flux after mid-February 1994, and this was accompanied by a distinct change in the composition from high terrigenous content, higher BIOSI:POC molar ratios, measurable but variable pigment fluxes, and low %POC values (intervals 5 and 6) to decreased terrigenous content, low BIOSI:POC molar ratios, very low pigment fluxes (intervals 6 to 10), and higher %POC values. Other biogenic flux peaks co-occur with high terrigenous peaks (material is >80 % TERR) but have very low pigment fluxes despite the summer season (Figure 6.41; see site A01-90 interval 10 and site A01-93 interval 12). In contrast, other biogenic peaks, which also co-occurred with a high terrigenous peaks (~73% TERR), had significant peaks in fluxes of CHLA and PHAEO pointing to that summer's primary productivity as the source (Figure 6.41; see site A01-92 interval 12 and site A01-93 interval1).

Clearly, there are significant variations, both inter-annual and seasonal, in fluxes and in composition at site A01 during the period from the fall 1990 to the fall 1994. In the remainder of this section, the physical conditions of ice cover, winds, ocean currents, river inputs, and temperature-salinity (T-S) relationships are examined to shed light on the physical forcing responsible for these observed differences. Specific questions that will be explored are: 1) What conditions are responsible for the dramatic differences between the low fall/winter fluxes of 1990-91 and 1992-93 and the high fall/winter fluxes of 1993-94?; 2) What physical processes can explain the presence of biogenic peaks in both fall/winter and in spring/summer, and what can account for the observed differences in composition with respect to OPAL and pigment contents?; 4) What transport mechanisms carry the suspended particles into Canada Basin and what is the probable source of these particles?; and 5) What is the relationship between the biogenic and the terrigenous particles?

6.4.1 Physical conditions during deployment at A01-90

Site A01-90 was under >90 % ice cover for all intervals of the sediment trap collection with the exception of a brief lead opening in October 1990 (Figure 6.42; Upward Looking Sonar (ULS) data; Canadian Ice Service Charts). Leading up to the

A.

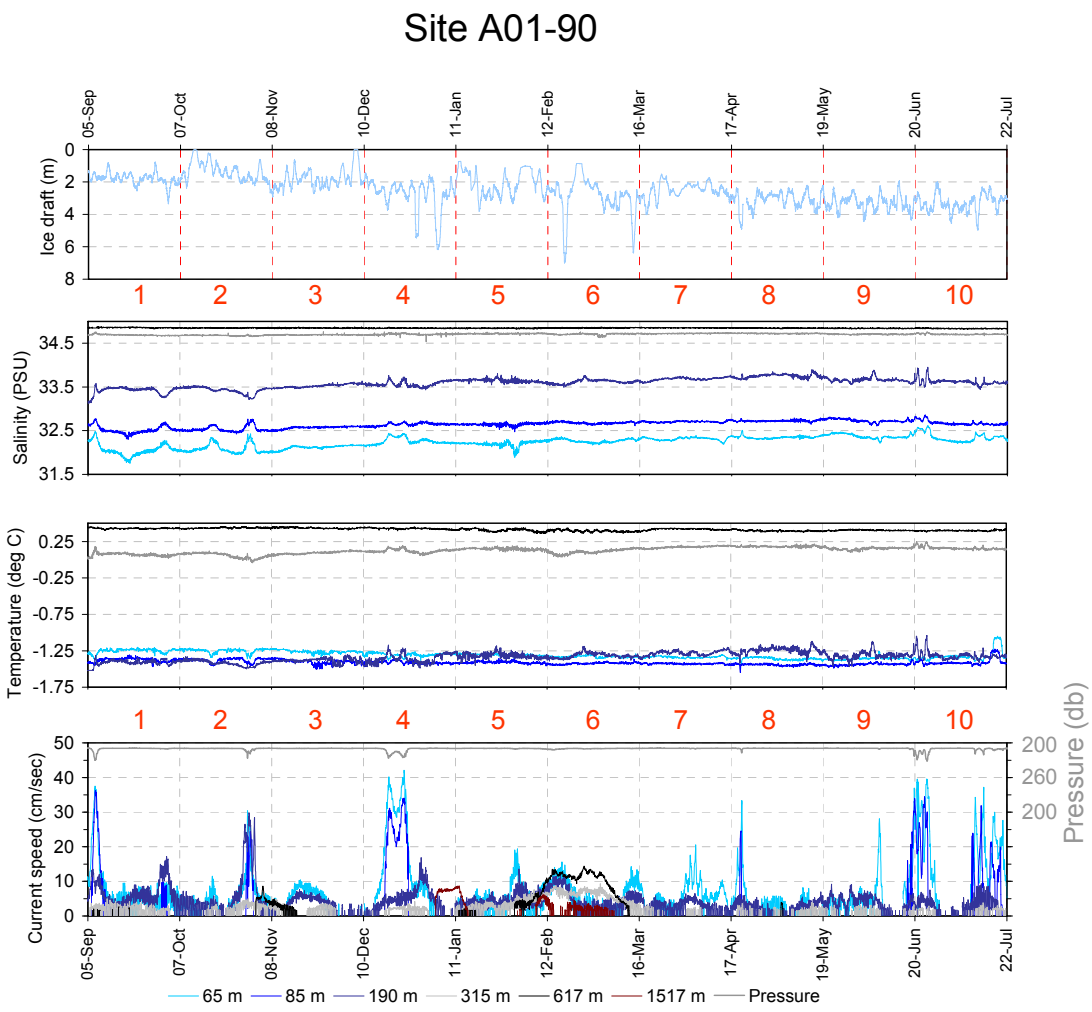

Figure 6-42 Physical parameters at site A01-90 including ice cover, T-S relationships, current speed and velocity, and 10 m NCEP wind speed and velocity A. Ice coverage from Upward Looking Sonar (ULS) data as daily averages (top plot), temperature and salinity data from the A01-90 mooring at the depths shown in the legend at the bottom of the plots (second and third plots), and the current speeds at the depths as shown in the legend (bottom plot). B. velocity and speed for 10 m NCEP data at grid point N in Figure 6.19 (top plot) and time series plots of speed and velocity at the mooring depths indicated in red on the plots (all plots below wind plots). C. Plots of wind speed and direction (10 m NCEP winds at grid point N) for specific sediment trap intervals of deployment A01-90.

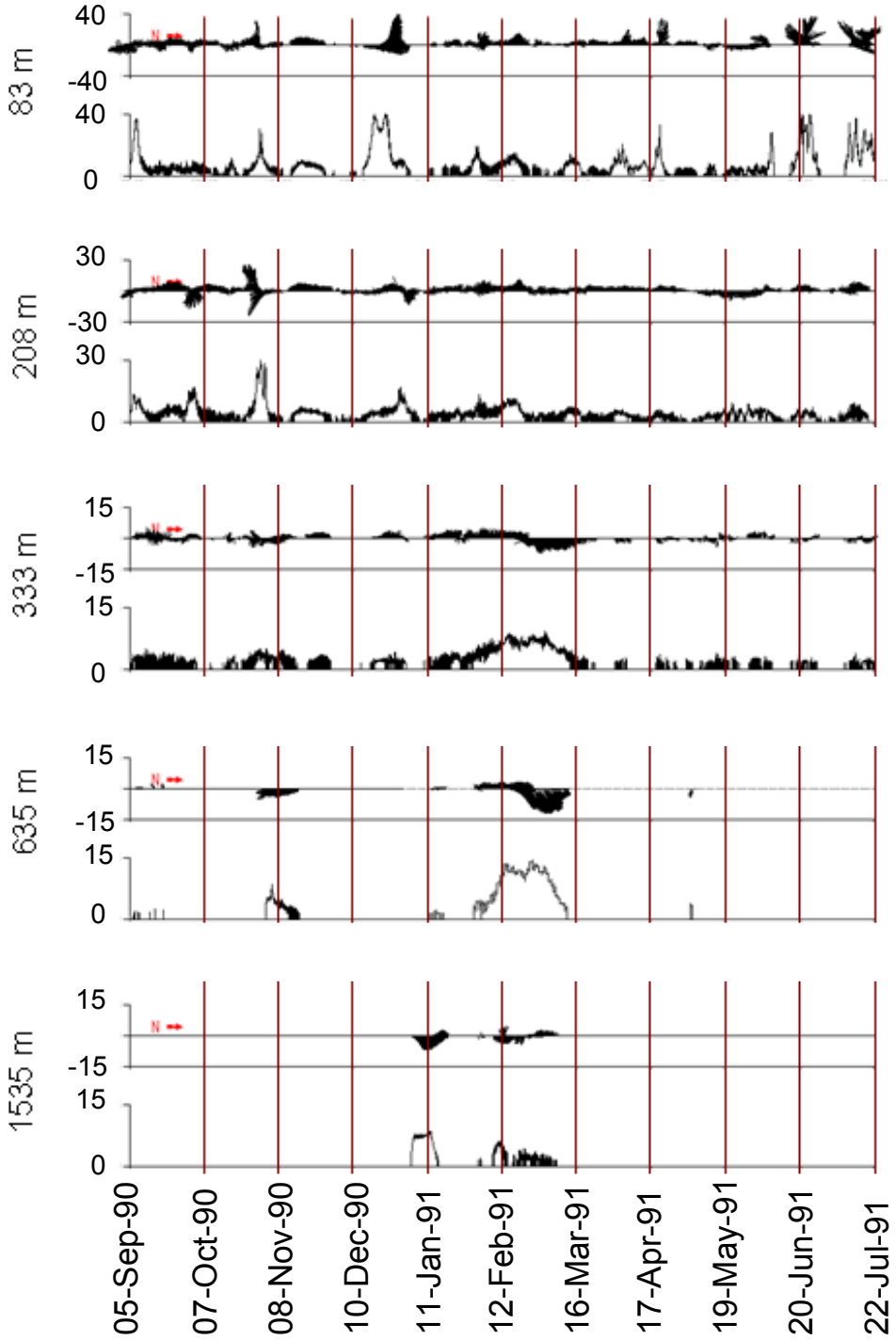

Continuation of Figure 6.42 (6.42B)

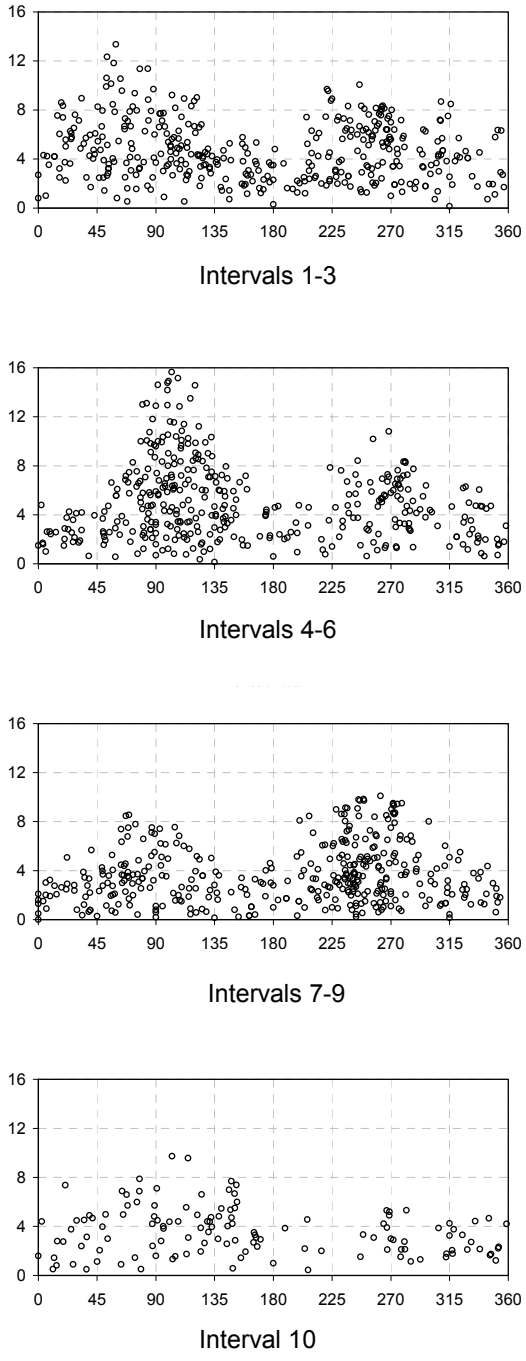

Continuation of Figure 6.42 (6.42C)

deployment in the summer of 1990, a lead opened up beyond the landfast ice on the Mackenzie Shelf relatively early in May and expanded, such that by mid-August, there was an expanse of open water out to about 71 ºN over the Mackenzie and Alaskan shelves. Up until mid-August 1990, site A01-90 was firmly ensconced below >90 % heavy ice cover far from the ice edge. After mid-August, the open water area expanded north and by the end of August 1990 (just prior to the mooring deployment) and through to early October, site A01-90 was still under heavy ice cover but much closer to the ice edge which extended at times beyond 73 ºN. Freeze-up occurred rapidly after the first week of October and after that, site A01-90 remained under heavy ice cover for the duration of the sediment trap collection which ended in late July 1991. The summer of 1991 was an exceptionally heavy ice year and ice inundated the shelves most of the summer and open water areas were very limited.

Even though site A01-90 was close to the ice edge during the fall of 1990, the daily fluxes to the trap were very low in the fall (TDW flux < 4.3 mg m^{-2} d^{-1}; intervals 1-3; Figures 4.1 and 6.41) at both the 600 and 1515 m traps (Figure 4.1). In addition, the open water over the shelves in the summer and fall of 1990 would presumably have been favourable for resuspension and off-shelf transport of suspended particles but this is not evident from the A01-90 fall trap data. During the three fall intervals, the current and T-S record at site A01-90 show evidence of the passage of eddies with high currents (up to a maximum of about 38 cm sec^{-1} (Figures 6.42A and 6.42B) between 65 and 315 m. These features evidently did not have suspended sediments associated with them or if they did, they passed by without any particles settling to 600 m and deeper. The strongest winds during the fall were to the E-NE which favours downwelling, and there was an E-W bimodal pattern favourable to alternating upwelling and downwelling at the shelf edge (Figures 6.42B and 6.432C). In the fall of 1990 (intervals 1 to 3), even though a number of physical factors associated with increased fluxes were present, the fall fluxes at site A01 were low.

In mid-winter at site A01-90, with an ice thickness ranging from 1 to 7 m, there was a significant TDW flux peak at 1500 m (intervals 4 to 6: 26 to 42 mg m^{-2} d^{-1}; Figures 4.1, 6.40, and 6.41) and a minor peak at 600 m (6.3 mg m^{-2} d^{-1}; Figures 4.1, 6.40, and 6.41). The material in the winter peak at 1500 m was 84-85 % terrigenous with %POC of

between 3.7 and 4.5 % and a BIOS:POC molar ratio of 0.31 to 0.38. During this period, there is clear evidence of eddies in the T-S and current speed records in both the upper 200 m where the current speeds are much higher (interval 4; maximum speed of 42 cm sec^{-1}) and between 300 and 1500 m where the currents are lower (intervals 4 to 6; maximum speed of 14 cm sec^{-1}) (Figures 6.42A and 6.42B). It is likely that the material trapped during mid-winter at 1500 m is associated with these eddies but, with the available data, other processes cannot be ruled out. The highest wind speeds over the whole deployment occurred during these winter intervals (4 to 6) and they were predominantly to the E-SE (Figure 6.42B), favourable to downwelling but without information on ice drift, it is difficult to assess the potential for UW/DW conditions. The winter period also had an E-W bimodal wind pattern favourable to alternations of upwelling and downwelling and under the right conditions, resuspension and formation of nepheloid layers capable of carrying suspended particles far out into Canada Basin.

In mid-summer (interval 10; late June/July 1991), there was a moderate TDW flux peak (60 mg m^{-2} d^{-1}) and POC flux peak (3.7 mg m^{-2} d^{-1}) at A01-90 (600 m) beneath an ice cover of 2 to 3 m thick. This material was highly terrigenous (82% TERR) and had a POC content of 6.2 %, low CHLA flux, low PHAEO flux, and a low BIOSI:POC molar ratio of 0.19 (Figure 41A,B). The POC content was diluted by terrigenous material from spring to summer as exhibited by a decrease from 10.6% POC in early April 1991 to 6.2% in the mid-summer peak (interval 10). The low CHLA and PHAEO fluxes suggest that this material comprised lateral transport of resuspended particulate matter and not the exported phytoplankton production from 1991. The peak in trap interval 10 (600 m) is most likely associated with the passage of two eddies during that spring period when currents ranged up to about 40 cm sec^{-1} (Figure 6.42A and 6.42B). The winds during the spring and summer exhibit the typical E-W bimodal pattern but there were fewer occurrences of high wind speed than in the fall and winter (Figure 6.42C). Moreover, the Mackenzie River peaked at Arctic Red River in mid-May in 1991 (Figure 2.4) but it was a relatively small peak and given the heavy ice conditions throughout the summer of 1991, the river plume and the massive inputs of fluvial particulates were likely contained close to shore. There is about a month between the arrival of the peak river inputs at the ice clogged shelf and the occurrence of the high flux peak at site A01-90 (600 m) in late

June/July. Without additional information (for example carbon isotope analyses), a link between the two cannot be either established or ruled out.

Given the heavy ice cover in 1991, the peak fluxes both in winter at 1500 m and in summer at 600 m are almost certainly due to lateral transport, but the precise nature of the processes involved and the origin of the particles is not clear from the available data. By implication, eddies that pass by the mooring along with prevailing upwelling/downwelling conditions in this area are the most likely means by which sediments were resuspended and carried out over the slope and into the basin. It is also clear that an increase in particle flux was not associated with every eddy that passed over the mooring.

6.4.2 Physical conditions during deployment A01-92

In the summer of 1992, the ice was very slow to break up and move off the shelf, and only by mid-August had the ice edge moved to 71 ºN. In the spring of 1992, the Mackenzie River flows peaked at Arctic Red River at the end of May, one of the highest peaks on record. Heavy ice covered the Mackenzie Shelf in June 1992, and the peak flows were most likely contained around the mouth of the river and to the shallow foreshore until the end of July 1992. Fluvial suspended material was likely deposited in relatively shallow water. The persistent heavy ice over the shelf and the containment of the freshwater would be expected to be a controlling factor for primary production over the Beaufort shelves and slope due to the light limitation and to the delay in stabilization of the water column. This implies that for the spring/summer 1992, phytoplankton production was hampered and certainly delayed due to unfavourable ice conditions.

In the fall/winter period of 1992-93, biogenic and terrigenous fluxes were low at the A01-92 in Canada Basin (Figure 6.41). Closer to the shelf edge at site AM1-92, the biogenic and terrigenous fluxes were also relatively low in the fall of 1992 (see section 6.2). In contrast, in late summer/early fall 1992, before the deployments at sites A01-92 and AM1-92, there was a peak of both biogenic and terrigenous material at site L144 at the 2700 m isobath that had a Mackenzie River carbon isotope signature (see section 6.3) implying that a late summer pulse containing fluvial sediments extended beyond the shelf break and well out over the slope before the A01-92 deployment.

Prior to the deployment of the mooring at site A01-92 on September 25, 1992, there was open water over the Mackenzie and Alaskan shelves with the ice edge at about 71 ºN. At the time of deployment, A01-92 was covered by ice of about 2 m in thickness, and the site remained under a full ice cover of between 1 and 3 m throughout the winter and until about the third week of July 1993. For the last two sediment trap collection intervals (12 and 13) in July and August 1993, there were a few periods of open water interspersed with thick ice, and the site was close to the pack ice edge. In contrast to 1992, the summer of 1993 had extensive areas of open water over the Mackenzie Shelf and there was a relatively early opening beginning in May on the central and eastern sides of the shelf which expanded westward such that by the first week of July 1993, open water extended to 72 ºN and to 140 ºW. In terms of ice conditions, the spring/summer seasons of 1992 and 1993 are completely different with 1992 representing a year of heavy ice and a late opening, and 1993 a year of large expanses of open water to beyond the shelf break and an early opening. From about mid-July to the end of the deployment in late August, the mooring was close to the edge of the pack ice. In late summer (interval 12), there was a significant peak of biogenic material along with elevated fluxes of CHLA and PHAEO which provide evidence that primary productivity in the open water close to the ice edge near site A01-92 was a probable source of biogenic material in the peak. Note that this 1992 late summer biogenic peak differs from the summer peak in 1991 (site A01-90) which did not exhibit increased fluxes of pigments. Note also, that in the summer of 1993, closer to the shelf edge at site AM1-92, there were strong biogenic and terrigenous peaks in late June/July about one month ahead of the peaks at site A01-92 further out in the basin.

From September 1992 to the end of May 1993 at site A01-92, TDW fluxes at 600 m were very low (<1 mg m^{-2} d^{-1}) with the exception of one very small peak in late fall (4.5 mg m^{-2} d^{-1}; interval 3; Figure 4.1). During this time, a number of small eddies were detected and in particular, a distinct eddy passed over the mooring during interval 3 coincident with the small flux peak (Figures 6.43A and 6.43B). As was noted for site A01-90, the presence of a specific eddy may or may not be associated with an increase in particle flux; the origin and age of an eddy are key determinants of this.

A)

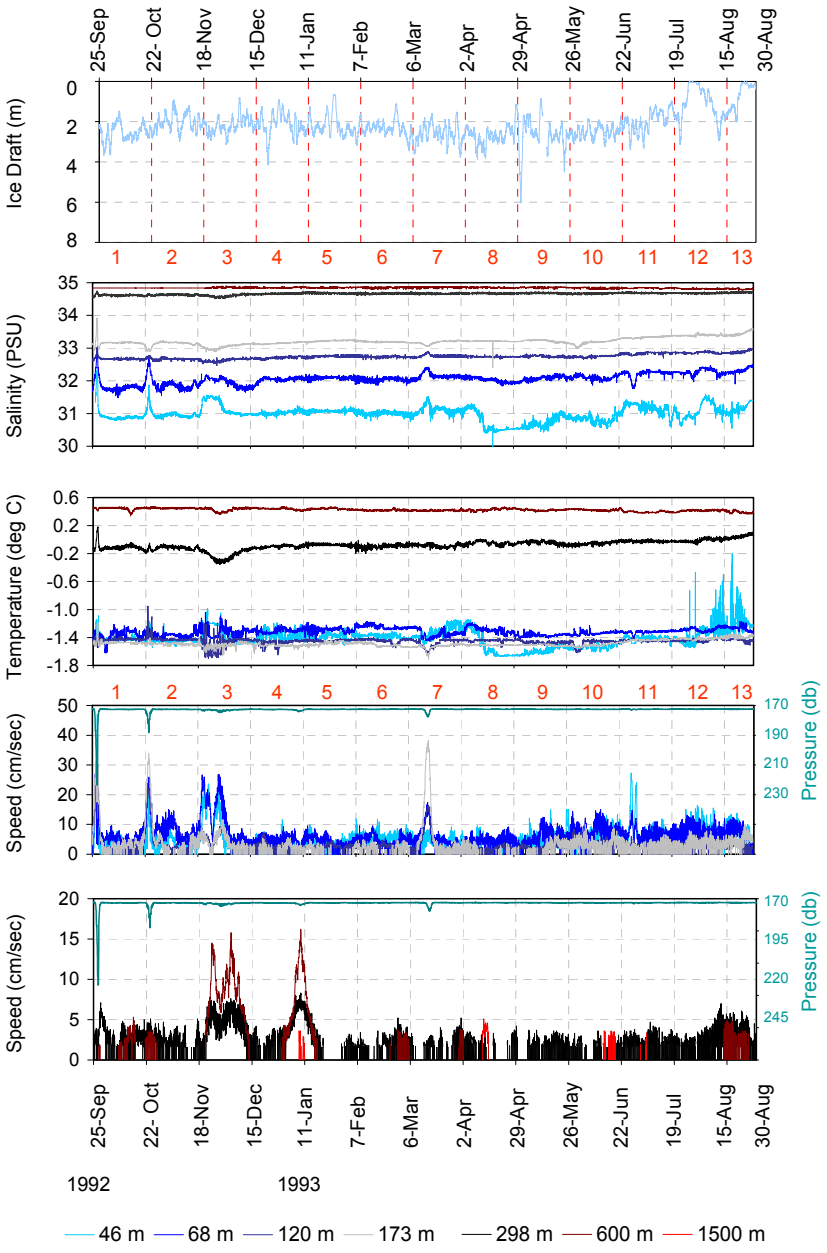

Figure 6-43 Physical parameters at site A01-92. A) Ice coverage from Upward Looking Sonar (ULS) data as daily averages (top plot), temperature and salinity data from the A01-90 mooring at the depths shown in the legend (second and third plots), and the current speeds at the depths as shown in the legend (bottom plot). B) Wind speed and velocity for 10 m NCEP data at grid point N in Figure 6.19 (top plot) and time series plots of current speed and velocity at depths indicated in red number on the plot. C) wind speed and direction (10 m NCEP winds at grid point N) for specific sediment trap intervals of deployment A01-92.

B)

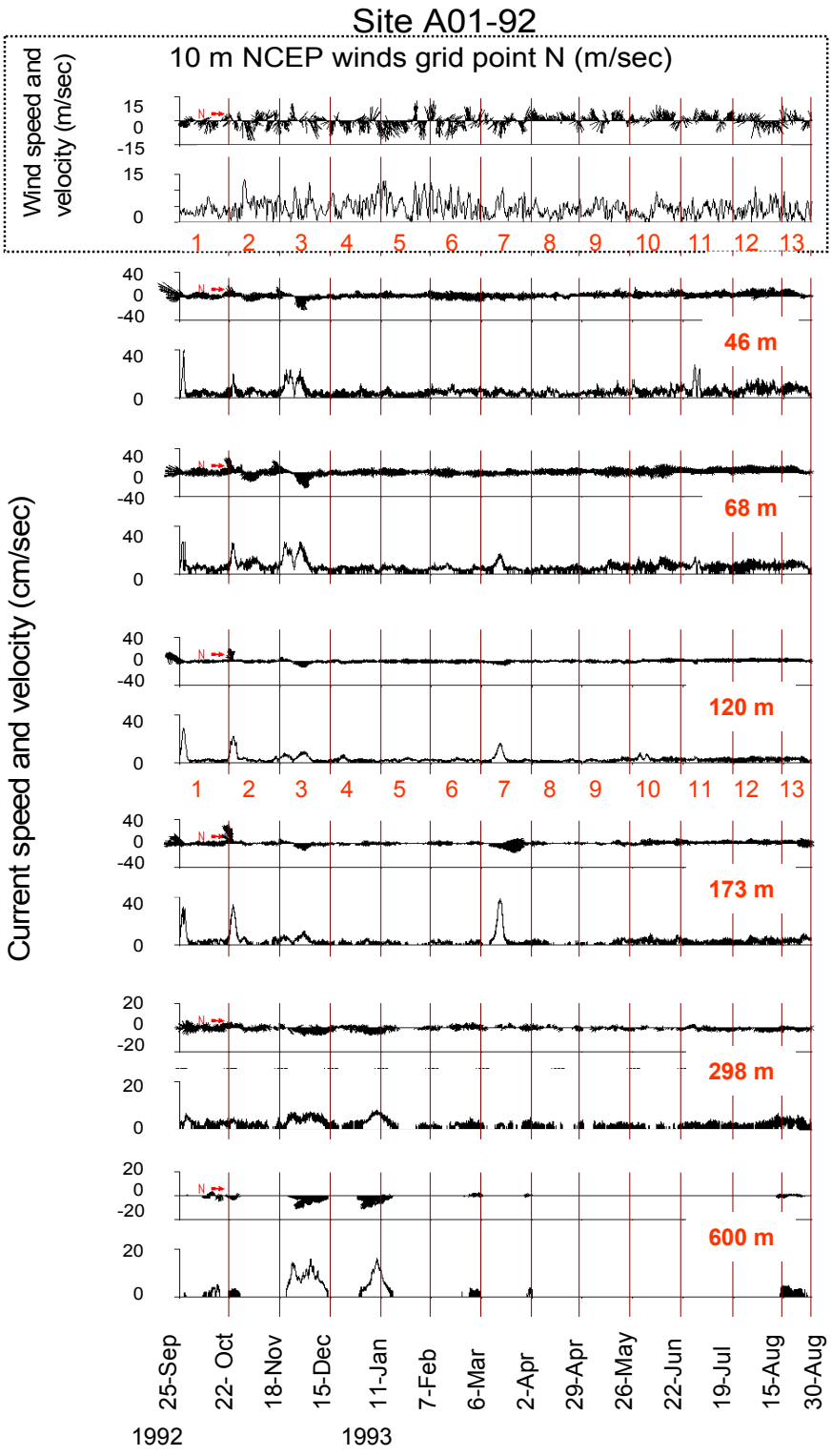

Continuation of Figure 6.43 (6.43B)

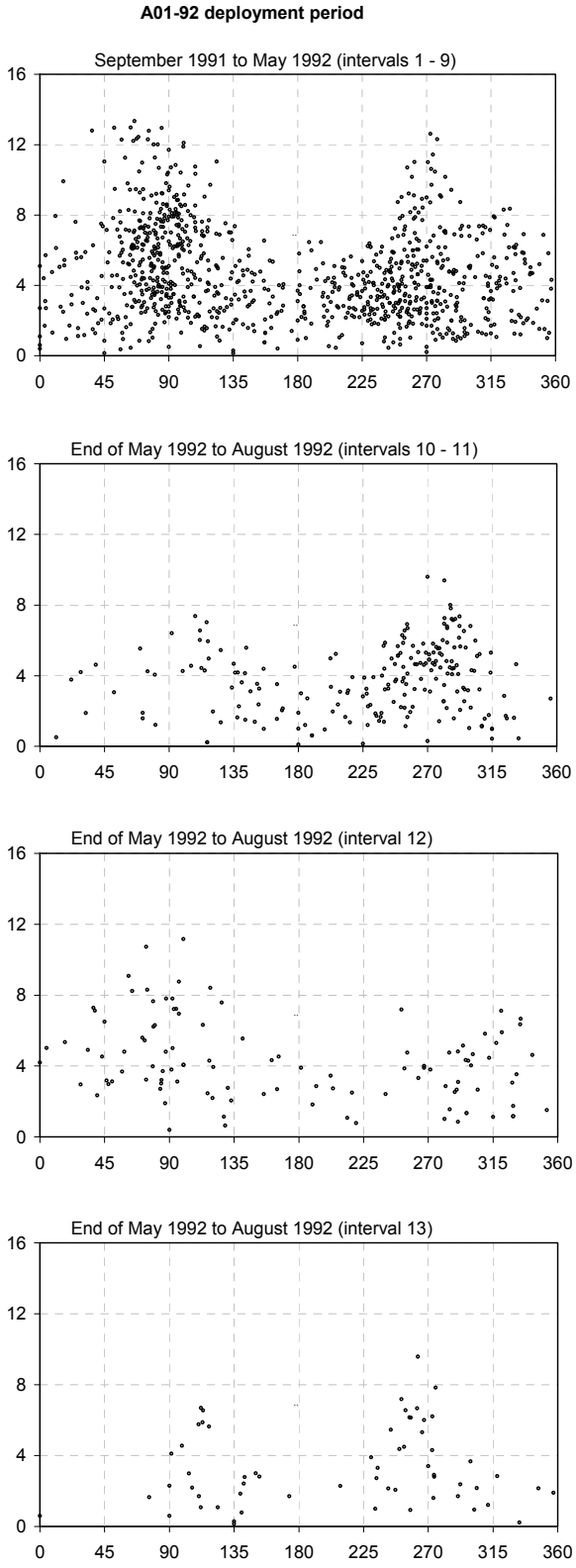

Continuation of Figure 6.43 (6.43BC)

In June 1993, the TDW flux started to increase and reached a peak in July/August 1993 (32 mg m^{-2} d^{-1}; interval 12) with a high terrigenous content (73 %TERR), a carbon content of 7.7 %, a BIOSI:POC molar ratio of 0.29, and the highest flux peaks of CHLA and PHAEO observed for the A01 mooring series. At this time, the ice edge was close to the site and there were stretches of open water over the mooring. This makes it very likely that the source of the biogenic material was phytoplankton production from within a small radius of site A01-92 which was delivered relatively quickly to the trap at 600 m. The terrigenous portion of this material was likely delivered laterally from a source on the shelf or slope or possibly gathered up during the descent of the biological material from production in the euphotic zone above the mooring.

As for other periods, the winds have E-W bimodality favourable to setting up alternating upwelling and downwelling conditions. Since the summer of 1993 had large expanses of open water over the shelf and slope, the river plume was likely highly influenced by wind direction and particularly by winds with high with speeds. The wind speeds from June to the end of August 1993 are moderate and show a slight preference for blowing towards the E which would favour downwelling. The wind direction to the E would also be favourable for generating upwelling at the ice edge. A water chemistry and CTD cast done in the fall of 1993 (Macdonald et al., 1995) showed surface waters depleted in nitrate and very low in silicate so it may be that local events of upwelling are important to regeneration of nutrients in the euphotic zone. Relatively strong, sustained winds to the E coincided with the biogenic peak in July/August of 1993 (interval 12) when site A01-92 was close to the ice edge (Figures 6.43C and 6.43C). Given the orientation of the ice edge, close to site A01-92, winds to the E could produce local upwelling. At the end of August (interval 13), the fluxes decreased abruptly coincident with winds predominantly to the W which probably terminated the local upwelling.

6.4.3 Physical conditions during deployment at A01-93

As described in Section 6.4.2, the spring/summer of 1993 saw an early clearing of ice from Mackenzie Shelf with large expanses of open water extending well beyond the shelf edge by the end of the summer. At the time of the mooring deployment in early September, there was a large area of 30 percent ice cover at site A01-93 and the pack ice was at and in places beyond 73 ºN (Canadian Ice Service). Even though the broader area

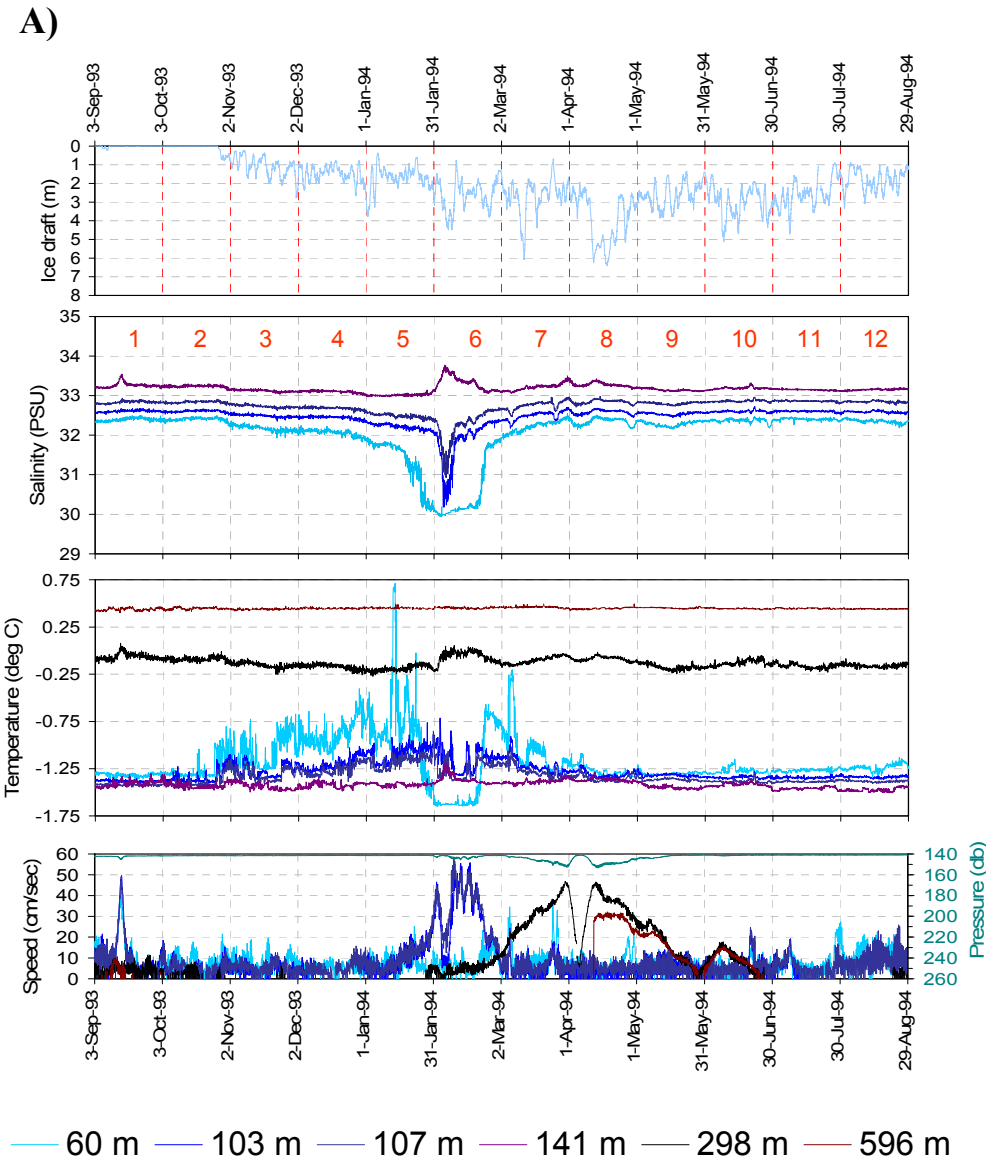

Figure 6-44 Time series plots of physical parameters at site A01-93. A. Ice coverage from Upward Looking Sonar (ULS) as daily averages (top plot), temperature and salinity data at the depths shown in the legend (second and third plots), and the current speeds at the depths as shown in the legend (bottom plot). B. Wind speed and velocity for 10 m NCEP data at grid point N in Figure 6.19 (top plot) and time series plots of current speed and velocity at the mooring depths indicated on the plots. Red numbers on plots A) and B) indicate the interval number for the sediment trap collection.

B)

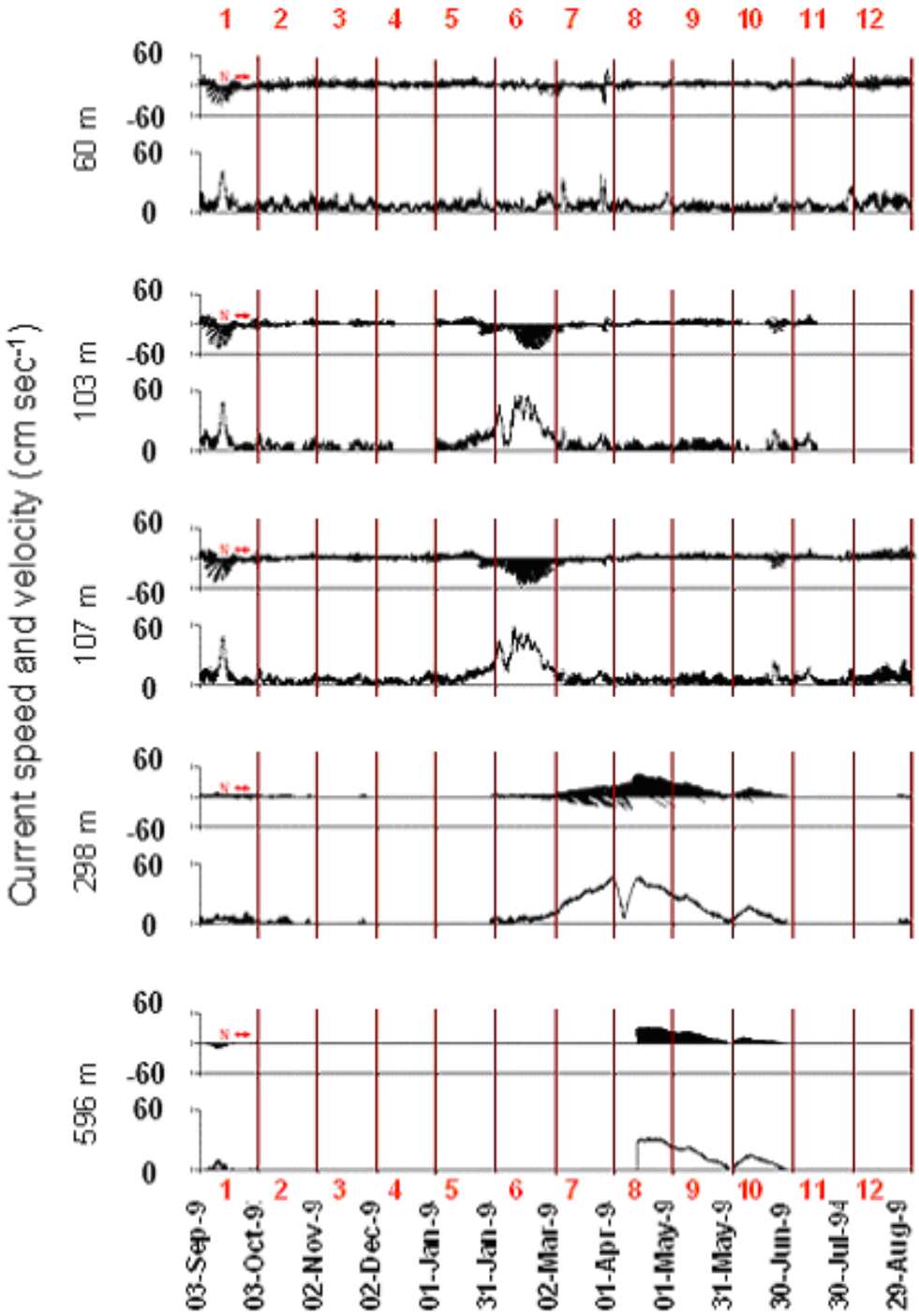

Continuation of Figure 6.44 (6.44B)

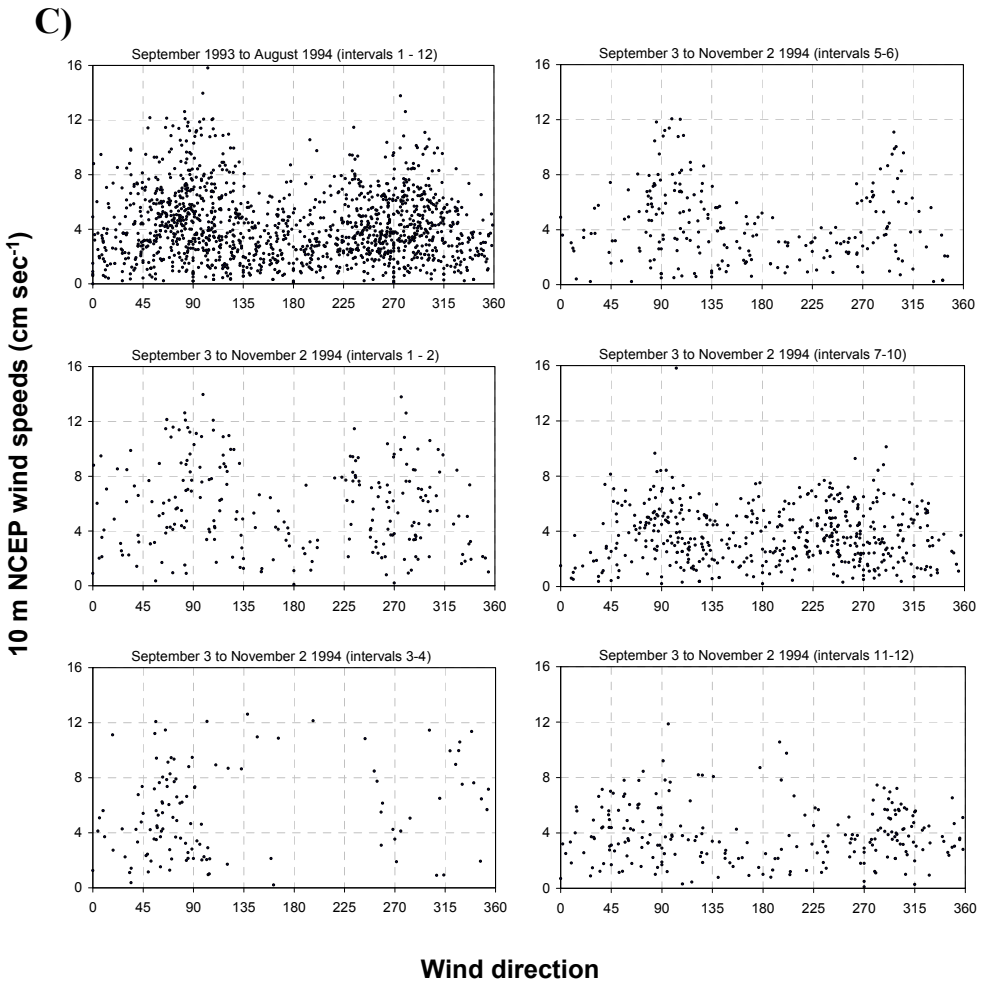

Continuation of Figure 6.44 (6.44C)

around the mooring location was initially under 30 percent ice cover, the ULS data (Figure 6.44A) shows open water over the site for all of September and most of October 1993 (intervals 1 and 2), and for most of this period, the edge of the pack ice was far to the north of A01-93 at about 74 ºN. Freeze-up had begun by the end of October, and by the end of the first week in November, freeze-up was complete over the shelves. After freeze-up, site A01-93 remained under complete ice cover until the end of the trap collection at the end of August 1994. The spring/summer of 1994 was again a year of exceptionally heavy ice over the Alaskan and Mackenzie shelves and for the duration of this period site A01-93 remained under >90 percent ice cover far from the ice edge.

In spring of 1993, when the exceptionally early Mackenzie River peak discharge reached the coast, there were already large areas of open water over Mackenzie Shelf. A large flaw lead had opened up by the third week of May and expanded throughout June such that the plume was relatively free to expand out over the shelf. This likely effected an early stratification favourable to phytoplankton production and facilitated the transport of riverine and resuspended sediment to and beyond the shelf edge during the summer and fall of 1993. In 1994, river inputs peaked at about the same time as in 1993 but peak flows were lower. In contrast to the 1993 season, when the Mackenzie River delivered its peak fluxes to the shelf in early June of 1994, the landfast ice was still intact and vast floes of heavy first year ice with traces of old ice clogged the shelf. Under these conditions, the fresh water and its load of fluvial particulates was likely contained to shallow waters as described for the 1992 spring/summer season.

In the fall and early winter of 1993 at site A01-93 (intervals 1 to 4), both the biogenic and terrigenous fluxes varied but remained elevated, and exhibited a declining trend in terrigenous content (from 75 to 64 %TERR; Figure 6.41). In September 1993 (interval 1) the peaks in terrigenous and biogenic material coincided with an eddy which was clearly recognizable from the T-S-current record, extended down to at least 596 m, and exhibited a maximum current speed approaching 50 cm sec^{-1} (Figures 6.44A and 6.44B). From October to December (intervals 2 to 4), the currents speeds were lower (< 15 cm sec^{-1}), and there was a pattern of rapid fluctuations in temperature which were quite pronounced particularly at 84 m, and which coincided with the ice cover closing over the mooring site at the end of interval 2. These rapid temperature fluctuations may have been associated with the passage internal waves through temperature interleaved waters but more likely, were associated with the edge of a large eddy (detected in intervals 5 and 6) brushing up against the mooring. It is very likely that the elevated fluxes in intervals 2 to 4 are associated with these features during this period although there are not enough data to define this association clearly.

In January/February (intervals 5 and 6), a large anticyclonic eddy within the upper halocline moved over the mooring at A01-93, and it was reflected in increased fluxes of both biogenic and terrigenous material. In addition, the composition of the trapped material in these two intervals appears to be unique to the eddy: elevated terrigenous

contents, BIOSI:POC molar ratios, and pigment fluxes combined with a low POC content. This eddy and associated elevated flux peaks is a striking example of the capacity of such physical features to transport material originating on the shelf and slope far out into Canada Basin.

In March 1994 (interval 7), the biogenic and terrigenous fluxes decreased abruptly coincident with a distinct change in composition to dramatically decreased terrigenous, OPAL, and pigment content along with increased POC content (Figure 6.41). This new composition characterized the material in the intervals 7 to 10 following the high peak in interval 6. Coincident with the change in composition from interval 6 to 7, another eddy passed by the mooring (Figures 6.44A and 6.44B). This eddy was deeper, exhibited strong currents at 298 and 596 m, spanned at least intervals 7 to 9 (and possibly 10), and was readily identifiable from the T-S-current record. Interval 10 also exhibited increases in current speed (at 298 and 596 m), and it is not clear whether or not these were associated with the same eddy that passed during the previous three intervals. However, the unique composition of the material during intervals 7 to 10 would suggest that it was (Figure 6.41). It is not known of what the biogenic material in intervals 7 to 10 consists except, that it does not appear to have originated from primary productivity or, if it did, it was excessively metabolized by heterotrophic organisms. During intervals 7 to 10, there are also at least four smaller eddies discernible in the upper halocline, which appear to be completely independent of the larger, deeper eddy in the lower halocline that likely contributed to the fluxes in intervals 7 to 10.

In July and August (intervals 11 and 12) the composition of the trapped material changed yet again (Figure 6.41), exhibiting an increased terrigenous content (72 to 81 %TERR), and an increased BIOSI:POC molar ratio. The PHAEO fluxes showed a small increase in interval 12 whereas the CHLA flux stayed essentially at zero. The peak in biogenic material was likely remnant production on the shelf and shelf edge that was laterally transported along with resuspended terrigenous material. The flux peak in interval 12 coincides with elevated currents that were most likely associated with a series of eddies or a single meandering eddy.

At site A01-93, the enhanced terrigenous and biogenic fluxes over the fall and winter were probably associated with the large expanses of open water from spring to fall

in 1993. There is a clear relationship between eddies and changes in composition and fluxes of suspended particles. The levels of CHLA and PHAEO within the mid-winter peak are unexpected and surprising, and suggest that large eddies, once initiated, may evolve quite independently with respect to the particles within them. The pigment analysis sheds important light on the nature of the trapped particles; caution must be used in interpreting peaks in biogenic material as the peaks do not necessarily coincide with a peak in primary productivity. This is particularly well demonstrated by the biogenic peaks at intervals 10 and 12 at site A01-93 and also by interval 10 at site A01-90 (Figure 6.44).

Over the duration of the A01-93 trap collection, the 10 m NCEP winds exhibited the typical E-W bimodal pattern favourable to alternations of upwelling and downwelling. The highest wind speeds occurred in the first 2 intervals during the period of open water and the wind direction was relatively evenly split between E and W (National Center for Environmental Prediction (NCEP); Figure 6.44C). In the summer and fall of 1993, there was a large fetch over the expanses of open water such that winds blowing to the E and the SE would be strong agents for resuspension in the shallow foreshore, further enhancing the availability of suspended particles for transport. In these conditions of a large fetch and strong winds to the E and SE, a previous study demonstrated a strong link between these conditions and enhanced fluxes at the shelf edge due to cross-shelf transport in a bottom nepheloid layer (O'Brien et al., 2006).

6.4.4 Summary of relationship of physical data to sediment fluxes at site A01

The patterns of fluxes at 600 m depth in the Canada Basin exhibited distinct inter-annual and seasonal variations that can broadly but not completely be explained by differences in ice conditions and the presence of eddies. Eddies formed in open water seasons such as the summer of 1993 may entrain more resuspended material than eddies formed during years of heavy ice over the slope and shelf as occurred in 1992 and 1994 (and to a lesser extent in 1990). This investigation highlights the importance of studying processes in the full water column in order to fully understand the mechanisms by which sediments are transported to Canada Basin. Clearly, these mechanisms are varied, and key factors appear to be: 1) the ice cover extent; 2) the location and availability of readily resuspended sediments; and 3) the co-occurrence of eddy formation and an abundance of

resuspended particulates. For example, in 1992, the ice would have held the peak Mackenzie River inputs of freshwater and suspended sediment closer to the coastline and rendered this material less available for transport, whereas in 1993, the plume was free to expand over and beyond the shelf at the time of the peak inputs.

There was considerable variability in composition between the biogenic peaks exhibited over the period from the fall of 1990 to the fall of 1994, and the pigment analysis provides important information regarding the probable origin of the material within the peak. The composition of biogenic material exhibited dramatic differences that were associated with passing eddies. The origin of the biogenic material associated with the deep eddy at site A01-93 (intervals 7 to 10) is unknown, but probably is largely a product of heterotrophic production. On the other hand, the biological material in the mid-winter biogenic peak at A01-93 (intervals 5 and 6), was likely entrained into the eddy in open water conditions and the composition is more typical of photosynthetic primary production.

Chapter 7 Conclusions

This study examined particle fluxes and compositions on the Beaufort slope and in Canada Basin during the period 1990 to 1994 with the aim of understanding the sources, fates, and trajectories of both terrigenous and biogenic particles through the investigation of physical dynamics. The data clearly demonstrate the need for detailed knowledge of physical processes for informed interpretation of particle fluxes and sediment transport in this area. The observed geographical, seasonal, and inter-annual variability in both fluxes and composition is intricately linked to complex interactions between ice cover, turbid river inputs, incident solar radiation, ocean currents, and winds. Due to the massive inputs of terrigenous material by the Mackenzie River, a methodology was developed to distinguish between the terrigenous and biogenic components of the fluxes such that their sources and fates could be considered separately.

Annual fluxes decreased significantly moving from the slope to the basin, and in addition, fluxes increased with depth over the slope, and probably in Canada Basin as well, although more data are needed to confirm this. Where there were sufficient data, distinct inter-annual variations in flux were observed (Canada Basin and site SS-5) and overall, the data suggest that large inter-annual variation is the norm in this area and reflect the extreme variations in the physical environment particularly with respect to responses to ice cover conditions. There were seasonal differences in fluxes between sites as well as between different collection periods at the Canada Basin site. Suspended terrigenous material was ubiquitous over the slope and biogenic inputs appear as pulses according to when and where conditions were conducive to primary production. The composition of the material collected in Canada Basin was quite variable with no apparent connection to season. At the base of the slope (2700 m isobath; site L144) the composition of the material was highly terrigenous and remarkably consistent throughout the collection period and the biogenic signal exhibited only a small increase in the shallowest (412 m) trap in early spring and summer. Higher up the slope (700 m isobath; SS-51 and AM1-92), there were biogenic peaks in the summer largely attributable to exported diatom blooms that diluted the terrigenous signal significantly.

Notable features in the flux and composition records were clearly linked to identifiable physical processes, progressions of processes, and/or combinations of physical features. Three diverse examples have been chosen from this study as illustrative of the close correlation between flux events and physical processes.

As a first example, in the spring/summer season of 1991 at Site SS-5, the three phases obvious in the flux record (pre-export, export, and post-export periods) were defined by three distinctly different physical regimes dominated by ice cover dynamics but also defined by different states of river input, ocean currents, and winds (see Section 6.1). In this case, a prolonged diatom bloom was facilitated by a dynamic early clearing of the ice from the east side of the shelf, was maintained by continued proximity to the ice edge and reduced ice cover, and was terminated as the ice swept back to the south over the shelf. In the following spring/summer season, heavy ice inundated the shelf until mid-summer and the prolonged diatom bloom seen in 1991 was absent.

As a second example, over the slope to the northwest of Mackenzie Trough (site AM1-92), an unexpected highly terrigenous flux peak (at both 290 and 490 m) occurred under heavy ice cover in the winter of 1993, and it coincided with the passage of a series of eddies associated with high currents, the transit of internal waves, strongly downwelling favourable winds, and mobile ice cover favouring upwelling/downwelling alternations (see Section 6.2). The combination of these physical processes likely conspired in the erosion of bottom sediments over the slope and in transport of the resuspended particles out over the slope in nepheloid layers.

As a third example, also over the slope to the NW of Mackenzie Trough (site AM1-92), a strong summer flux peak with high biogenic content (43%; high diatom content) occurred at 490 m but was absent at 290 m, clearly indicating a strong mechanism of lateral transport of both biogenic and terrigenous particles in mid- and bottom nepheloid layers down Mackenzie Trough and out over the slope. This flux peak coincided with a period of rapid migration of ice to the north over nutrient depleted surface waters and of strong UW favourable conditions mirrored in a strong upwelling signal in the lower halocline followed by an abrupt relaxation of UW, and the peak occurred about two weeks after the peak turbid Mackenzie River flows began to spread over Mackenzie Trough (see section 6.2). A viable picture assembled from the time-line

of events in the spring of 1993 accounts for this peak as follows: 1) favoured by upwelling of nutrients, an early spring diatom bloom developed in the expanding but still relatively narrow lead beyond the landfast ice over Mackenzie Trough far south of the mooring site; 2) termination and export of this bloom occurred following the massive inputs of turbid Mackenzie River water at peak flows; 3) easily resuspended material consisting of a combination of recently exported biogenic material and riverine sediments newly deposited at the salt/freshwater interface are transported seaward in bottom nepheloid layers; and 4) finally, separation of the bottom nepheloid layer into mid-water nepheloid layers at the shelf break carried suspended particles out over the deep waters of the slope to the mooring location. In addition, the Mackenzie River delivers massive quantities of suspended sediments to the head of Mackenzie Trough in a short period of time in spring and it is not unreasonable to speculate that bottom transport by the formation of mobile fluid mud may be a common mechanism of lateral transport of sediment in Mackenzie Trough following the spring peak inputs. Preliminary estimates indicate that flows of fluid mud are possible, even likely in Mackenzie Trough and could transit to the shelf break in a matter of two to three days. If this is occurring, high volumes of suspended particles may be transported beyond the shelf break as sporadic, short-term events.

The above scenarios from this study amply illustrate the importance of utilizing multidisciplinary approaches and of conducting multi-year investigations at carefully chosen sites extending across the shelf and into the basin if this system is to be correctly understood. For example, Mackenzie Trough appears to be a conduit for the transport of both biogenic and terrigenous material beyond the shelf break, and it warrants future intensive study over sufficient annual cycles, possibly decades to catch the variability in the system and to allow informed predictions of the consequences of climate change to the system. Unfortunately, even in recent investigations such as done by the CASES project during the International Polar Year, the moorings are of only single year duration with no overlap in site location.

The presence of mid- and bottom nepheloid layers over the shelf and slope is ubiquitous and has been repeatedly documented in the Mackenzie Shelf area but the dynamics of these nepheloid layers remains poorly understood, and the data are highly

skewed to summer open-water sampling scenarios. The fate of the massive quantities of riverine sediment delivered to the Beaufort Sea at peak river flows under different ice conditions of the shelf is poorly understood. Over the years of this study, there was considerable variability with regards to ice conditions on the shelf over the spring and summer season, implying wide variability in the fate of the huge inputs of riverine material over the spring, summer, and fall. In 1993, the ice cleared off the shelf and the ice edge moved far to the north such that there were immense areas of open water from the spring to the fall and this is reflected in increased fluxes during the fall and winter of 1993 at the Canada Basin site.

Resuspension due to ocean currents, UW/DW alternations, and passage of internal waves has been inferred in this study, and this leads to the key question as to what shear velocities are required to initiate resuspension of cohesive bottom sediments in this area. The resuspension of sediments over continental slopes in other areas has been demonstrated to occur in association with UW/DW conditions (e.g. Perlin et al., 2005) and also with the passage of internal waves (e.g. McPhee-Shaw, 2006). This very likely occurs over the Beaufort slope as well and constitutes an area for future investigations. Walker et al., 2008 determined critical erosion thresholds for sediment in this area to have a range of 1.05 to 1.30 cm sec^{-1} for resuspension of an upper less consolidated layer (type I erosion) and a range of 1.3 to 1.7 cm sec^{-1} for the lower more consolidated layer (type II erosion). Shear velocity is defined by the equation: $\tau_b = \rho(u_*)^2$ (Equation 7-1) where τ_b = shear stress at the bottom; ρ = density of the water; u_* = shear velocity. It is generally not easy to use Equation 7-1 with conventional oceanographic measurements to establish the likelihood of resuspension but in this case, since a range of values for shear velocities (u_*) in the Mackenzie Shelf region is available (Walker et al., 2008), a first order estimate of current velocities required for resuspension can be made. It is customary to estimate bottom stress using flow speed at a fixed distance off the bottom and a drag coefficient appropriate for that elevation, according to the equation: $\tau_b = \rho C_H (u_H)^2$ (Equation 7-2) where H is the elevation off the bottom; ρ is the sea water density; C_H is the drag coefficient at a height H above the bottom; and u_H is the velocity

at height H above the bottom. Values of drag coefficients (C_{100}) have been tabulated for H = 1m and typical values for mud and sand/mud are .0022 and .003 respectively (Soulsby, 1997). Equating the above two expressions for the shear stress (τ_b; Equations 7-1 and 7-2) the minimum velocity at one meter above the bottom required to initiate resuspension is related to the shear velocity by the following equation: $u_{100} = (\sqrt{1/C_{100}}) \times u_*$ (Equation 7-3). Using this equation for a mud and mud/sand bottoms, at 1 meter above the bed, velocities in the range of 19 to 28 cm sec^{-1} would be required for resuspension of an upper less-consolidated layer and velocities in the range of 24 to 36 cm sec^{-1} would be require for resuspension of the lower more-consolidated layer. Bottom flows of these magnitudes are not unheard of in this area and likely occur sporadically in association with eddies and storms (high orbital speeds of waves in shallow water).

Another key question concerns the short-term fate of the immense influxes of suspended fluvial sediments. Given the dynamic nature of the area, it is reasonable to speculate that a large portion of the newly delivered sediment may remain as a relatively easily resuspended pool and that the majority of the material in the observed nepheloid layers consists of riverine material recently delivered to the shelf by the river and/or recently settled from primary production and which undergoes multiple resuspension events and hence has never become fully incorporated as part of the cohesive bottom sediment structure.

Over the four years of this study, wind direction exhibited a strong E-W modality suggesting that alternations of UW and DW conditions were a common feature of the area. Overall, it is expected that the system is highly influenced by extreme events whether it be winds, currents, or rapid ice drift. Eddies were detected to varying degrees in the current and T-S records at all the sites and appear to be ubiquitous in the area and intricately involved in the transport of suspended particles over the slope and out into Canada Basin. The origin of the eddies as well as their trajectories remains unclear but the data suggest that Mackenzie Trough could be an important area for the generation of eddies. The data also indicate that the composition of suspended sediments can differ

dramatically between different eddies and that not all eddies are associated with enhanced levels of suspended sediments.

There is a growing consensus that in the present crisis of global warming, the Arctic will be ice-free in the summers some time before the end of this century, and it is very probable that both the presence of vast expanses of open water in the summer and thinner ice in the winter will bring with it far-reaching changes to the biological functioning of the Beaufort shelves and to the patterns of sediment transport over the shelf, slope and basin. It is useful to reiterate at this point, as aptly expressed by Creager and Sternberg (1972), that “without adequate detailed studies of both sediment distribution and water circulation over an entire shelf, we are left to intuition and deduction about sediment dispersal”.

Bibliography

Aagaard, K., 1984. The Beaufort Undercurrent. In: P.W. Barnes, D.M. Schell and E. Reimnitz (Eds.), The Alaskan Beaufort Sea; Ecosystems and Environments. Academic Press, pp 47-71.

Aagaard, K., Swift, J.H., Carmack, E.C., 1985. Thermohaline Circulation in the Arctic Mediterranean Seas. Journal of Geophysical Research 90, 4833-4846.

Aagaard, K., Pease, C.H., Roach, A.T., Salo, S.A., 1989.Beaufort Sea mesoscale circulation study - Final Report. NOAA Tech. Memo. ERL PMEL-90 (PB90-158775) 114 pp.

Aagaard, K., Carmack, E.C., 1989. The role of sea ice and other fresh water in the Arctic circulation. Journal of Geophysical Research 94, 14485-14498.

Aagaard, K., Carmack, E., 1994. The Arctic Ocean and climate: A perspective. In: O.M. Johannessen, R.D. Muench and J.E. Overland (Eds.), The polar oceans and their role in shaping the global environment, the Nansen Centennial Volume. AGU Books Board, pp 5-20.

Anderson, L., Dryssen, D., 1981. Chemical-Constituents of the Arctic Ocean in the Svalbard Area. Oceanologica Acta 4, 305-311.

Anderson, L.A., 1995. On the hydrogen and oxygen content of marine phytoplankton. Deep-Sea Research I 42, 1675-1680.

Andreassen, I.J., Wassmann, P., 1998. Vertical flux of phytoplankton and particulate biogenic matter in the marginal ice zone of the Barents Sea in May 1993. Marine Ecology-Progress Series 170, 1-14.

Anita, A.N., 2005. Solubilization of particles in sediment traps: revising the stoichiometry of mixed layer export. Biogeosciences 2, 189-204.

Armstrong, R.A., Lee, C., Hedges, J.I., Honjo, S., Wakeham, S.G., 2002. A new, mechanistic model for organic carbon fluxes in the ocean based on the quantitative association of POC with ballast minerals. Deep-Sea Research Part Ii-Topical Studies in Oceanography 49, 219-236.

Arrigo, K.R., van Dijken, G.L., 2004. Annual cycles of sea ice and phytoplankton in Cape Bathurst polynya, southeastern Beaufort Sea, Canadian Arcitc. Geophysical Research Letters 31, L08304, doi:10.1029/2003GL018978.

Ashjian, C.J., Gallager, S.M., Plourde, S., 2005. Transport of plankton and particles between the Chukchi and Beaufort Seas during summer 2002, described using a Video Plankton Recorder. Deep-Sea Research Part Ii-Topical Studies in Oceanography 52, 3259-3280.

Baker, E.T., Milburn, H.B., 1983. An instrument for the investigation of particle fluxes. Continental Shelf Research 1, 425-435.

Barwell-Clarke, J., Whitney, F., 1996. Institute o f Ocean Sciences nutrient methods and analysis. 43 pp.

Belt, S.T., Massé, G., Vare, L.L., Rowland, S.J., Poulin, M., Sicre, M.-A., Sampei, M., Fortier, L., 2008. Distinctive 13C isotopic signature distinguishes a novel sea ice biomarker in Arctic sediments and sediment traps. Marine Chemistry 112, 158-167.

Bornhold, B.D., 1975. Suspended matter in the Southern Beaufort Sea. Beaufort sea Technical Report #25b; Dept. of the Environment, Canada, 23 pp.

Borstad, G., Kerr, R., 1994. Remote sensing of an opening arctic ice lead. DSS contract # FP941-1-7544/01-XSA; Canadian Department of Fisheries and Oceans. 39 pp.

Brzezinski, M.A., Dickson, M.L., Nelson, D.M., Sambrotto, R., 2003. Ratios of Si, C and N uptake by microplankton in the Southern Ocean. Deep-Sea Research Part Il - Topical Studies in Oceanography 50, 619-633.

Cacchione, D.A., Drake, D.E., 1986. Nepheloid layers and internal waves over continental shelves and slopes. Geo-Marine Letters 6, 147-152.

Cacchione, D.A., Pratson, L.F., Ogston, A.S., 2002. The shaping of continental slopes by internal tides. Science 296, 724-727.

Calvert, S.E., Pedersen, T.F., Naidu, P.D., von Stackelberg, U., 1995. On the organic carbon maximum on the continental slope of the eastern Arabian Sea. Journal of Marine Research 53, 269-296.

Carmack, E.C., Macdonald, R.W., Papadakis, J.E., 1989. Water mass structure and boundaries in the Mackenzie Shelf Estuary. Journal of Geophysical Research 94, 18043-18055.

Carmack, E.C., 1990. Large scale physical oceanography of polar oceans. In: W.O. Smith Jr. (Eds.), Polar Oceanography Part A. Physical Science. Academic Press Inc., pp 171-222.

Carmack, E.C., 1998. Shelf-basin exchange processes in the Beaufort Sea and Canadian Arctic Archipelago. In: Proceedings international workshop on exchange processes between the Arctic shelves and basins, pp 24-27.

Carmack, E.C., Kulikov, E.A., 1998. Wind-forced upwelling and internal Kelvin wave generation in Mackenzie Canyon, Beaufort Sea. Journal of Geophysical Research-Oceans 103, 18447-18458.

Carmack, E.C., Macdonald, R.W., 2002. Oceanography of the Canadian Shelf of the Beaufort Sea: A setting for marine life. Arctic 55, 29-45.

Carmack, E.C., Chapman, D.C., 2003. Wind-driven shelf/basin exchange on an Arctic shelf: The joint roles of ice cover extent and shelf-break bathymetry. Geophysical Research Letters 30, 1778.

Carmack, E., Wassmann, P., 2006. Food webs and physical-biological coupling on pan-Arctic shelves: Unifying concepts and comprehensive perspectives. Progress in Oceanography 71, 446-477.

Carmack, E., Barber, D., Christensen, J., Macdonald, R., Rudels, B., Sakshaug, E., 2006. Climate variability and physical forcing of the food webs and the carbon budget on panarctic shelves. Progress in Oceanography 71, 145-181.

Carson, M.A., Jasper, J.N., Conly, F.M., 1998. Magnitude and sources of sediment input to the Mackenzie Delta, Northwest Territories, 1974-94. Arctic 51, 116-124.

Carson, M.A., Conly, F.M., Jasper, J.N., 1999. Riverine sediment balance of the Mackenzie Delta, Northwest Territories, Canada. Hydrological Processes 13, 2499-2518.

Cavalieri, D.J., Martin, S., 1994. The Contribution of Alaskan, Siberian, and Canadian Coastal Polynyas to the Cold Halocline Layer of the Arctic-Ocean. Journal of Geophysical Research-Oceans 99, 18343-18362.

Codispoti, L.A., 1979. Arctic Ocean Processes in Relation to the Dissolved Silicon Content of the Atlantic. Marine Science Communications 5, 361-381.

Colony, R.L., Rigor, I.G., 1993. International Arctic Buoy Program Data Report for 1 January 1992 - 31 December 1992. APL-UW TM 29-93; Applied Physics Laboratory, University of Washington. 195 pp.

Colony, R.L., Rigor, I.G., 1995. International Arctic Buoy Program Data Report for 1 January 1993 - 31 December 1993. APL-UW TM 4-95; Applied Physics Laboratory, University of Washington. 239 pp.

Comiso, J.C., Parkinson, C.L., Gersten, R., Stock, L., 2008. Accelerated decline in the Arctic Sea ice cover. Geophysical Research Letters 35, L01703, doi:10.1029/2007GL031972.

Conley, D.J., 1998. An interlaboratory comparison for the measurement of biogenic silica in sediments. Marine Chemistry 63, 39-48.

Cota, G.F., Pomeroy, L.R., Harrison, W.G., Jones, E.P., Peters, F., Sheldon, W.M., Weingartner, T.R., 1996. Nutrients, primary production and microbial heterotrophy in the southeastern Chukchi Sea: Arctic summer nutrient depletion and heterotrophy. Marine Ecology-Progress Series 135, 247-258.

Dagg, M., Benner, R., Lohrenz, S., Lawrence, D., 2004. Transformation of dissolved and particulate materials on continental shelves influenced by large rivers: plume processes. Continental Shelf Research 24, 833-858.

D'Asaro, E.A., 1988. Observations of small eddies in the Beaufort Sea. Journal of Geophysical Research 93, 6669-6684.

de Haas, H., van Weering, T.C.E., de Stigter, H., 2002. Organic carbon in shelf seas: sinks or sources, processes and products. Continental Shelf Research 22, 691-717.

Dittmar, T., Kattner, G., 2003. The biogeochemistry of the river and shelf ecosystem of the Arctic Ocean: a review. Marine Chemistry 83, 103-120.

Droppo, L.G., Jeffries, D., Jaskot, C., Backus, S., 1998. The prevalence of freshwater flocculation in cold regions: A case study from the Mackenzie River Delta, Northwest Territories, Canada. Arctic 51, 155-164.

Dunton, K.H., Weingartner, T., Carmack, E.C., 2006. The nearshore western Beaufort Sea ecosystem: Circulation and importance of terrestrial carbon in arctic coastal food webs. Progress in Oceanography 71, 362-378.

Eicken, H., Gradinger, R., Gaylord, A., Mahoney, A., Rigor, I., Melling, H., 2005. Sediment transport by sea ice in the Chukchi and Beaufort Seas: Increasing importance due to changing ice conditions? Deep-Sea Research Part II-Topical Studies in Oceanography 52, 3281-3302.

Fahl, K., Nöthig, E.-M., 2007. Lithogenic and biogenic particle fluxes on the Lomonosov Ridge (central Arctic Ocean) and their relevance for sediment accumulation: Vertical vs. lateral transport. Deep-Sea Research Part I-Oceanographic Research Papers 54, 1256-1272.

Fissel , D.B., Birch, J.R., 1984. Sediment transport in the Canadian Beaufort Sea. ASL File 35-060-F; Arctic Sciences Ltd. 165 pp.

Forest, A., Sampei, M., Hattori, H., Makabe, R., Sasaki, H., Fukuchi, M., Wassmann, P., Fortier, L., 2007. Particulate organic carbon fluxes on the slope of the Mackenzie Shelf (Beaufort Sea): Physical and biological forcing of shelf-basin exchanges. Journal of Marine Systems 68, 39-54.

Fukuchi, M., Sasaki, H., Hattori, H., Matsuda, O., Tanimura, A., Handa, N., McRoy, C.P., 1993. Temporal Variability of Particulate Flux in the Northern Bering Sea. Continental Shelf Research 13, 693-704.

Giovando, L.F., Herlinveaux, R.H., 1981. A discussion of factors influencing dispersion of pollutants in the Beaufort Sea. Institute of Ocean Sciences. 198pp.

Gobeil, C., Paton, D., McLaughlin, F.A., Macdonald, R.W., Paquette, G., Clermont, Y., Lebeuf, M., 1991. Donnees geochimiques sur les eaux interstitielles et les sediments de la mer de Beaufort. Rapport statistique canadien sur L'hydrographie et les sciences oceaniques 101, pp 92

Goñi, M.A., Yunker, M.B., Macdonald, R.W., Eglinton, T.I., 2000. Distribution and sources of organic biomarkers in arctic sediments from the Mackenzie River and Beaufort Shelf. Marine Chemistry 71, 23-51.

Goñi, M.A., Yunker, M.B., Macdonald, R.W., Eglinton, T.I., 2005. The supply and preservation of ancient and modern components of organic carbon in the Canadian Beaufort Shelf of the Arctic Ocean. Marine Chemistry 93, 53-73.

Gooday, A.J., Turley, C.M., Allen, J.A., 1990. Responses by Benthic Organisms to Inputs of Organic Material to the Ocean-Floor - a Review. Philosophical Transactions of the Royal Society of London Series a-Mathematical Physical and Engineering Sciences 331, 119-138.

Gordeev, V.V., Martin, J.M., Sidorov, I.S., Sidorova, M.V., 1996. A reassessment of the Eurasian river input of water, sediment, major elements, and nutrients to the Arctic Ocean. American Journal of Science 296, 664-691

Gosselin, M., Levasseur, M., Wheeler, P.A., Horner, R.A., Booth, B.C., 1997. New measurements of phytoplankton and ice algal production in the Arctic Ocean. Deep-Sea Research Part Ii-Topical Studies in Oceanography 44, 1623-1644.

Grebmeier, J.M., Barry, J.P., 1991. The influence of oceanographic processes on pelagic-benthic coupling in polar regions: A benthic perspective. Journal of Marine Systems 2, 495-518.

Grebmeier, J.M., 1998. The western Arctic Shelf-Basin Interactions (SBI) Program. In. K. Aagaard and T. Takizawa (Eds.), International workshop on exchange processes between the Arctic shelves and basins: Japanese Marine Science and Technology Center, 21-23.

Hargrave, B.T., Vonbodungen, B., Conover, R.J., Fraser, A.J., Phillips, G., Vass, W.P., 1989. Seasonal-Changes in Sedimentation of Particulate Matter and Lipid-Content of Zooplankton Collected by Sediment Trap in the Arctic Ocean Off Axel Heiberg Island. Polar biology 9, 467-475.

Hargrave, B.T., von Bodungen, B., Stoffyn-Egli, P., Mudie, P.J., 1994. Seasonal variablility in particle sedimentation under permanent ice cover in the Arctic Ocean. Continental Shelf Research 14, 279-293.

Harris, C.K., Traykovski, P.A., Geyer, W.R., 2005. Flood dispersal and deposition by near-bed gravitational sediment flows and oceanographic transport: A numerical modeling study of the Eel River shelf, northern California. Journal of Geophysical Research C: Oceans 110, 1-16.

Harrison, W.G., Cota, G.F., 1991. Primary Production in Polar Waters - Relation to Nutrient Availability. Polar Research 10, 87-104.

Hedges, J.I., Keil, R.G., 1995. Sedimentary Organic-Matter Preservation - an Assessment and Speculative Synthesis. Marine Chemistry 49, 81-115.

Hedges, J.I., Keil, R.G., Benner, R., 1997. What happens to terrestrial organic matter in the ocean? Organic Geochemistry 27, 195-212.

Heussner, S., de Madron, X.D., Calafat, A., Canals, M., Carbonne, J., Delsaut, N., Saragoni, G., 2006. Spatial and temporal variability of downward particle fluxes on a continental slope: Lessons from an 8-yr experiment in the Gulf of Lions (NW Mediterranean). Marine Geology 234, 63-92.

Hill, P.R., Blasco, S.M., Harper, J.R., Fissel, D.B., 1991. Sedimentation on the Canadian Beaufort Shelf. Continental Shelf Research 11, 821–842.

Honjo, S., Doherty, K.W., 1988. Large aperture time-series sediment traps: design objectives, construction and application. Deep-Sea Research 35, 133-149.

Honjo, S., 1990. Particle fluxes and modern sedimentation in the polar oceans. In: W.O. Smith (Eds.), Polar Oceanography Part B: Chemistry, Biology and Geology. Academic Press, Inc., pp 687-739.

Horner, R., Schrader, G.C., 1982. Relative Contributions of Ice Algae, Phytoplankton, and Benthic Microalgae to Primary Production in Nearshore Regions of the Beaufort Sea. Arctic 35, 485-503.

Hutchins, D. A. and Bruland, K.W., 1998. Iron-limited diatom growth and Si : N uptake ratios in a coastal upwelling regime. Nature 393, 561-564.

Jakobsson, M., 2002. Hypsometry and volume of the Arctic Ocean and its constituent seas. Geochemistry Geophysics Geosystems 3, 5, 10.1029/2001GC000302.

Krishfield, R., Plueddemann, A.J., Honjo, S., 2002. Eddys in the Arctic Ocean from IOEB ADCP data. Woods Hole Oceanog. Inst. Tech Rept. WHOI-2002-09; 145 pp.

Kulikov, E.A., Carmack, E.C., Macdonald, R.W., 1998. Flow variability at the continental shelf break of the Mackenzie Shelf in the Beaufort Sea. Journal of Geophysical Research 103, 12,725-712,741.

Kulikov, E.A., Rabinovich, A.B., Carmack, E.C., 2004. Barotropic and baroclinic tidal currents on the Mackenzie shelf break in the southeastern Beaufort Sea. Journal of Geophysical Research-Oceans 109, C05020.

Lovejoy, C., Legendre, L., Price, N.M., 2002. Prolonged diatom blooms and microbial food web dynamics: experimental results from an Arctic polynya. Aquatic Microbial Ecology 29, 267-278.

Macdonald, R.W., Wong, C.S., Erickson, P.W., 1987. The Distribution of Nutrients in the Southeastern Beaufort Sea: Implications for Water Circulation and Primary Production. Journal of Geophysical Research 92, No. C3, 2939-2952.

Macdonald, R.W., Carmack, E.C., 1991a. Age of Canada Basin Deep Waters: A way to estimate primary production for the Arctic Ocean. Science 254, 1348-1350.

Macdonald, R.W., Carmack, E.C., 1991b. The Role of Large-Scale under-Ice Topography in Separating Estuary and Ocean on an Arctic Shelf. Atmosphere-Ocean 29, 37-53.

Macdonald, R.W., Thomas, D.J., 1991. Chemical interactions and sediments of the western Canadian Arctic Shelf. Continental Shelf Research 11, 843-863.

Macdonald, R.W., Pearson, R., Sieberg, D., McLaughlin, F.A., O'Brien, M.C., Paton, D.W., Carmack, E.C., Forbes, J.R., Barwell-Clarke, J., 1992. Physical and Chemical Data Collected in the Beaufort Sea and Mackenzie River Delta, April - May 1991. Canadian Data Report of Hydrography and Ocean Sciences 104, 155 pp.

Macdonald, R.W., Carmack, E.C., Wallace, D.W.R., 1993. Tritium and Radiocarbon Dating of Canada Basin Deep Waters. Science 259, 103-104.

Macdonald, R.W., O'Brien, M., Carmack, E.C., Pearson, R., McLaughlin, F.A., Sieberg, D., Barwell-Clarke, J., Paton, D.W., Tuele, D., 1995, Physical and Chemical Data Collected in the Beaufort, Chukchi and East Siberian Seas, August - September 1993. Can. Data Rep. Hydrogr. Ocean Sci.: 139, 288 pp.

Macdonald, R.W., Paton, D.W., Carmack, E.C., Omstedt, A., 1995. The freshwater budget and under-ice spreading of Mackenzie River water in the Canadian Beaufort Sea based on salinity and 18O/16O measurements in water and ice. Journal of Geophysical Research 100, 895-919.

Macdonald, R.W., Solomon, S.M., Cranston, R.E., Welch, H.E., Yunker, M.B., Gobeil, C., 1998. A sediment and organic carbon budget for the Canadian Beaufort Shelf. Marine Geology 144, 255-273.

Macdonald, R.W., Carmack, E.C., McLaughlin, F.A., Falkner, K.K., Swift, J.H., 1999. Connections among ice, runoff and atmospheric forcing in the Beaufort Gyre. Geophysical Research Letters 26, 2223-2226.

Macdonald, R.W., 2000. Arctic estuaries and ice: a positive-negative estuarine couple. In: E.L. Lewis, E.P. Jones, P. Lemke, T.D. Prowse and P. Wadhams (Eds.), The Freshwater budget of the Arctic Ocean. pp 383-407.

Macdonald, R.W., Harner, T., Fyfe, J., 2005. Recent climate change in the Arctic and its impact on contaminant pathways and interpretation of temporal trend data. Science of the Total Environment 342, 5-86.

Macdonald, R.W., Yu, Y., 2006. The Mackenzie Estuary of the Arctic Ocean. In: (Eds.), Estuaries. Springer-Verlag Berlin Heidelberg, pp 91-120.

MacNeill, M.R., Garrett, J.F., 1975. Open water surface currents. Beaufort Sea Technical Report #17; Dept. of the Environment. 113pp.

Manley, T.O., Hunkins, K., 1985. Mesoscale eddies of the Arctic Ocean. J. Geophys. Res. 90, 4911-4930.

Mathis, J.T., Pickart, R.S., Hansell, D.A., Kadko, D., Bates, N.R., 2007. Eddy transport of organic carbon and nutrients from the Chukchi Shelf: Impact on the upper halocline of the western Arctic Ocean. Journal of Geophysical Research-Oceans 112, C05011, doi:10.1029/2006JC003899.

Mckee, B.A., Aller, R.C., Allison, M.A., Bianchi, T.S., Kineke, G.C., 2003. Transport and transformation of dissolved and particulate materials on continental margins influenced by major rivers: benthic boundary layer and seabed processes. Continental Shelf Research 24, 899-926.

McPhee-Shaw, E., 2006. Boundary-interior exchange: Reviewing the idea that internal-wave mixing enhances lateral dispersal near continental margins. Deep-Sea Research Part II: Topical Studies in Oceanography 53, 42-59.

Melling, H., 1993. The formation of a haline shelf front in wintertime in an ice-covered arctic sea. Continental Shelf Research 13, 1123-1147.

Melling, H., Riedel, D.A., 1994. Draft and movement of pack ice in the Beaufort Sea, April 1991 - April 1992. Canadian Technical Report of Hydrography and Ocean Sciences No. 162, 108 pp.

Melling, H., Moore, R.M., 1995. Modification of halocline source waters during freezing on the Beaufort Sea shelf: evidence from oxygen isotopes and dissolved nutrients. Continental Shelf Research 15, 89-113.

Melling, H., Riedel, D.A., 1996. Development of seasonal pack ice in the Beaufort Sea during the winter of 1991-1992: A view from below. Journal of Geophysical Research-Oceans 101, 11975-11991.

Melling, H., Riedel, D.A., Gedalof, Z., 2005. Trends in the draft and extent of seasonal pack ice, Canadian Beaufort Sea. Geophysical Research Letters 32, L24501.

Monaco, A., Courp, T., Heussner, S., Carbonne, J., Fowler, S.W., Deniaux, B., 1990. Seasonality and Composition of Particulate Fluxes During Ecomarge .1. Western Gulf of Lions. Continental Shelf Research 10, 959-987.

Mortlock, R.A., Froelich, P.N., 1989. A simple method for the rapid determination of biogenic opal in pelagic marine sediments. Deep Sea Research 36, 1415-1426.

Naidu, A.S., 1974. Chapter 7: Sedimentation in the Beaufort Sea: A synthesis. In: Y. Herman (Eds.), Marine Geology and Oceanography of the Arctic Seas. Springer-Verlag New York, pp 173-190.

Naidu, A.S., 1985. Organic carbon, nitrogen, and C/N ratios of deltaic sediments, North Arctic Alaska. In: E.T. Degens, S. Kempe and R. Herrera (Eds.), Transport of Carbon and Minerals in Major World Rivers. Mitt. Geol- Paläont. Inst. Univ. Hamburg, pp 311-321.

Naudin, J.J., Cauwet, G., Chrétiennot-Dinet, M.J., Deniaux, B., Devenon, J.L., Pauc, H., 1997. River discharge and wind influence upon particulate transfer at the land-ocean interaction: Case study of the Rhone River plume. Estuarine Coastal and Shelf Science 45, 303-316.

Niebauer, H.J., 1991. Bio-physical oceanographic interactions at the edge of the Arctic ice pack. Journal of Marine Systems 2, 209-232.

Nikolopoulos, A., Pickart, R.S., Fratantoni, P.S., Shimada, K., Torres, D.J., Peter Jones, E., 2008. The western Arctic boundary current at 152°W: Structure, variability, and transport. Deep-Sea Research II, doi:10.1016/j.dsr2.2008.10.014.

O'Brien, M.C., Macdonald, R.W., Melling, H., Iseki, K., 2006. Particle fluxes and geochemistry on the Canadian Beaufort Shelf: Implications for sediment transport and deposition. Continental Shelf Research 26, 41-81.

Parsons, T.R., Maita, Y., Lalli, C.M., 1984. A manual of chemical and biological methods for seawater analysis. Oxford, Pergamon Press. 173 pp.

Passow, U., 1991. Species-specific sedimentation and sinking velocities of diatoms. Marine biology 108, 449-455.

Passow, U., 2004. Switching perspectives: Do mineral fluxes determine particulate organic carbon fluxes or vice versa? Geochemistry Geophysics Geosystems 5, Q04002, doi:10.1029/2003GC000670.

Passow, U., De La Rocha, C.L., 2006. Accumulation of mineral ballast on organic aggregates. Global Biogeochemical Cycles 20, GB1013, doi:10.1029/2005GB002579.

Pelletier, B.R., 1975. Sediment dispersal in the southern Beaufort Sea. Beaufort Sea Technical Report #25a; Dept. of the Environment. 80pp.

Pelletier, B.R., 1984. Marine Science Atlas of the Beaufort Sea: Sediments. Miscellaneous Report 38; Geological Survey of Canada. 27 pp.

Perlin, A., Moum, J.N., Klymak, J.M., 2005. Response of the bottom boundary layer over a sloping shelf to variations in alongshore wind. Journal of Geophysical Research 110, C10S09, doi:10.1029/2004JC002500.

Pesant, S., Legendre, L., Gosselin, M., Bauerfeind, E., Budeus, G., 2002. Wind-triggered events of phytoplankton downward flux in the Northeast Water Polynya. Journal of Marine Systems 31, 261-278.

Pickart, R.S., 2004. Shelfbreak circulation in the Alaskan Beaufort Sea: Mean structure and variability. Journal of Geophysical Research C: Oceans 109, C04024.

Pickart, R.S., Weingartner, T.J., Pratt, L.J., Zimmermann, S., Torres, D.J., 2005. Flow of winter-transformed Pacific water into the Western Arctic. Deep-Sea Research Part II: Topical Studies in Oceanography 52, 3175-3198.

Plueddemann, A.J., Krishfield, R., Takizawa, T., Hatakeyama, K., Honjo, S., 1998. Upper ocean velocities in the Beaufort Gyre. Geophysical Research Letters 25, 183-186.

Pomeroy, L.R., 1997. Primary production in the Arctic Ocean estimated from dissolved oxygen. Journal of Marine Systems 10, 1-8.

Proshutinsky, A.Y., Johnson, M.A., 1997. Two circulation regimes of the wind driven Arctic Ocean. Journal of Geophysical Research-Oceans 102, 12493-12514.

Proshutinsky, A.Y., Polyakov, I.V., Johnson, M.A., 1999. Climate states and variability of Arctic ice and water dynamics during 1946-1997. Polar Research 18, 135-142.

Proshutinsky, A., Bourke, R.H., McLaughlin, F.A., 2002. The role of the Beaufort Gyre in Arctic climate variability: Seasonal to decadal climate scales. Geophysical Research Letters 29, 2100.

Puig, P., Palanques, A., Guillén, J., El Khatab, M., 2004. Role of internal waves in the generation of nepheloid layers on the northwestern Alboran slope: Implications for continental margin shaping. Journal of Geophysical Research C: Oceans 109, 1-11.

Rachold, V., Grigoriev, M.N., Are, F.E., Solomon, S., Reimnitz, E., Kassens, H., Antonow, M., 2000. Coastal erosion vs riverine sediment discharge in the Arctic Shelf seas. International Journal of Earth Sciences 89, 450-460.

Ragueneau, O., Tréguer, P., 1994. Determination of Biogenic Silica in Coastal Waters - Applicability and Limits of the Alkaline Digestion Method. Marine Chemistry 45, 43-51.

Ragueneau, O., Treguer, P., Leynaert, A., Anderson, R.F., Brzezinski, M.A., DeMaster, D.J., Dugdale, R.C., Dymond, J., Fischer, G., Francois, R., Heinze, C., Maier-Reimer, E., Martin-Jezequel, V., Nelson, D.M., Queguiner, B., 2000. A review of the Si cycle in the modern ocean: recent progress and missing gaps in the application of biogenic opal as a paleoproductivity proxy. Global and Planetary Change 26, 317-365.

Ragueneau, O., Savoye, N., Del Amo, Y., Cotten, J., Tardiveau, B., Leynaert, A., 2005. A new method for the measurement of biogenic silica in suspended matter of coastal waters: using Si:Al ratios to correct for the mineral interference. Continental Shelf Research 25, 697-710.

Reeder, S.W., Hitchon, B., Levinson, A.A., 1972. Hydrogeochemistry of the surface waters of the Mackenzie River drainage basin, Canada-1. Factors controlling inorganic composition. Geochimica et Cosmochimica Acta 36, 825-865.

Renaud, P.E., Riedel, A., Michel, C., Morata, N., Gosselin, M., Juul-Pedersen, T., Chiuchiolo, A., 2007. Seasonal variation in benthic community oxygen demand: A response to an ice algal bloom in the Beaufort Sea, Canadian Arctic? Journal of Marine Systems 67, 1-12.

Sakshaug, E., 2004. Chapter 3. Primary and secondary production on the Arctic Seas. In: R. Stein and R.W. Macdonald (Eds.), The organic carbon cycle in the Arctic Ocean. Springer, pp 57-81.

Sarthou, G., Timmermans, K.R., Blain, S., Treguer, P., 2005. Growth physiology and fate of diatoms in the ocean: a review. Journal of Sea Research 53, 25-42.

Schubert, C.J., Stein, R., 1996. Deposition of organic carbon in Arctic Ocean sediments: Terrigenous supply vs marine productivity. Organic Geochemistry 24, 421-436

Semiletov, I.P., Pipko, I.I., Repina, I., Shakhova, N.E., 2006. Carbonate chemistry dynamics and carbon dioxide fluxes across the atmosphere-ice-water interfaces in the Arctic Ocean: Pacific sector of the Arctic. Journal of Marine Systems, doi:10.1016/j.jmarsys.2006.05.012.

Serreze, M.C., Holland, M.M., Stroeve, J., 2007. Perspectives on the Arctic's shrinking sea-ice cover. Science 315, 1533-1536.

Soulsby, R., 1997. Dynamics of Marine Sands. Thomas Telford, London, pp249.

Stein, R., Macdonald, R.W., 2004. The Organic Carbon Cycle in the Arctic Ocean. Springer, 363 pp.

Stirling, I., Cleator, H., 1981. Polynyas in the Canadian Arctic, Occassional Paper 45, Canadian Wildlife Service, 73 pp.

Stroeve, J., Holland, M.M., Meier, W., Scambos, T., Serreze, M., 2007. Arctic sea ice decline: Faster than forecast. Geophysical Research Letters 34, L09501, doi:10.1029/2007GL029703.

Thomsen, L., van Weering, T.C.E., 1998. Spatial and temporal variability of particulate matter in the benthic boundary layer at the NW European Continental Margin (Goban Spur). Progress in Oceanography 42, 61-76.

Thomsen, L., 1999. Processes in the benthic boundary layer at continental margins and their implication for the benthic carbon cycle. Journal of Sea Research 41, 73-86.

Tremblay, J.E., Gratton, Y., Fauchot, J., Price, N.M., 2002. Climatic and oceanic forcing of new, net, and diatom production in the North Water. Deep-Sea Research Part Ii-Topical Studies in Oceanography 49, 4927-4946.

Tremblay, J.E., Michel, C., Hobson, K.A., Gosselin, M., Price, N.M., 2006. Bloom dynamics in early opening waters of the Arctic Ocean. Limnology and Oceanography 51, 900-912.

Vandenbroucke,M., Largeau, C., 2007. Kerogen, evolution and structure. Organic Geochemistry 38, 719-833.

Walsh, J.J., Dieterle, D.A., Pribble, J.R., 1991. Organic Debris on the Continental Margins - a Simulation Analysis of Source and Fate. Deep-Sea Research Part a-Oceanographic Research Papers 38, 805-828.

Waser, N.A., Harrison, P.J., Nielsen, B., Calvert, S.E., Turpin, D.H., 1998. Nitrogen isotope fractionation during the uptake and assimilation of nitrate, nitrite,

ammonium, and urea by a marine diatom. Limnology and Oceanography 43(2), 215-224.

Waser, N.A., Yin, K., Yu, Z., Tada, K., Harrison, P.J., Turpin, D.H., Calvert, S.E., 1998. Nitrogen isotope fractionation during nitrate, ammonium and urea uptake by marine diatoms and coccolithophores under various conditions of N availability. Marine Ecology Progress Series 169, 29-41.

Wassmann, P., 1998. Retention versus export food chains: processes controlling sinking loss from marine pelagic systems. Hydrobiologia 363, 29-57.

Wassmann, P., Bauerfeind, E., Fortier, M., Fukuchi, M., Hargrave, B., Moran, B., Noji, T., Nöthig, E.-M., Olli, K., Peinert, R., Sasaki, H., Shevchenko, V., 2004. Particulate organic carbon flux to the Arctic Ocean sea floor. In: R. Stein and R.W. Macdonald (Eds.), The Organic Carbon Cycle in the Arctic Ocean. Springer, Berlin, pp 101-138.

Williams, W.J., Carmack, E.C., Shimada, K., Melling, H., Aagaard, K., Macdonald, R.W., Ingram, R.G., 2006. Joint effects of wind and ice motion in forcing upwelling in Mackenzie Trough, Beaufort Sea. Continental Shelf Research 26, 2352-2366.

Williams, W.J., Melling, H., Carmack, E.C., Ingram, R.G., 2008. Kugmallit Valley as a conduit for cross-shelf exchange on the Mackenzie Shelf in the Beaufort Sea. Journal of Geophysical Research, 113, C02007, doi:10.1029/2006JC003591.

Wu, Y., Peterson, I.K., Tang, C.C.L., Platt, T., Sathyendranath, S., Fuentes-Yaco, C., 2007. The impact of sea ice on the initiation of the spring bloom on the Newfoundland and Labrador Shelves. Journal of Plankton Research 29, 509-514.

Yunker, M.B., Macdonald, R.W., Fowler, B.R., Cretney, W.J., Dallimore, S.R., McLaughlin, F.A., 1991. Geochemistry and fluxes of hydrocarbons to the Beaufort Sea shelf: A multivariate comparison of fluvial inputs and coastal erosion of peat using principal components analysis. Geochimica et Cosmochimica Acta 55, 255-273.

Yunker, M.B., Macdonald, R.W., Veltkamp, D.J., Cretney, W.J., 1995. Terrestrial and marine biomarkers in a seasonally ice-covered Arctic estuary -integration of multivariate and biomarker approaches. Marine Chemistry 49, 1-50.

Electronic references

Canadian Arctic Shelf Exchange Study (CASES), http://www.quebec-ocean.ulaval.ca/cases/network.asp

Canadian Ice Service (http://ice-glaces.ec.gc.ca/App/WsvPageDsp.cfm?ID=11872&Lang=eng)

International Arctic Buoy Program (IABP) (http://iabp.apl.washington.edu/)

International Polar Year (IPY), 2007-2008. http://www.ipycanada.ca/

Northern Contaminants Program (NCEP), http://www.itk.ca/environment/contaminants-ncp.php

Northern Oil and Gas Project (NOGAP), http://www.ainc-inac.gc.ca/oil/index_e.html

National Centers for Environmental Prediction (NCEP) (http://www.ncep.noaa.gov/)

Ocean Data View (ODV), Schlitzer, R., Ocean Data View, http://odv.awi.de, 2009

Water Survey of Canada, HYDAT CD-ROM (http://www.wsc.ec.gc.ca/products/hydat/main_e.cfm?cname=hydat_e.cfm)

Western Arctic Shelf-Basin Interactions Project (SBI), http://sbi.utk.edu/

Appendices

Appendix 1 Site and sampling information. A. Site locations, bottom depths, and overview of sequential sediment trap sampling. B. Overview of instrumentation on moorings. C. Sampling schedules for sequential sediment traps (3 pages).

1A. Site information and overview of sequential sediment trap sampling.

Station	Bottom depth	Latitude	Longitude	Trap depths	Time zone	Start time	Number of collection intervals	Duration of collection interval
	m	ºN	ºW	m		dd/mm/yyy		days
SS-5	715	71.200	134.806	199, 349, 499	UTC	22/04/1991	10	13
AM1-92	710	70.548	140.045	140, 290, 490	UTC	15/09/1992	10	35
L144	2715	71.369	141.706	412, 1311	UTC	25/09/1991	13	27
A01-90	3339	72.621	143.568	615, 1515	UTC	05/09/1990	10	32
A01-92	3375	75.542	143.830	600	UTC	25/09/1992	13	27
A01-93	3370	72.517	143.866	568	UTC	03/09/1993	12	30

1B. Instrumentation on moorings.

		Sediment traps							Current meters[1]									Seacats			ULS
Station	Bottom Depth	# on mooring	Trap-1 depth	Trap type -1	Trap-2 depth	Trap type -2	Trap-3 depth	Trap type -3	# on mooring	Depth CM-1	Depth CM-2	Depth CM-3	Depth CM-4	Depth CM-5	Depth CM-6	Depth CM-7	CM type other than RCM4 in bold type	# on mooring	Depth seacat-1	Depth seacat-2	Depth ULS
	m		m		m		m			m	m	m	m	m	m	m	m		m	m	m
A01-90	3339	2	615	B	1515	H			7	65	85	135	190	315	617	1517	All RCM4	2	66	191	59
SS-5	714	3	199	B	349	B	499	B	3	99	206	506					All RCM4	0			
L-144	2715	2	412	H	1311	H			4	84	**103**	**158**	**416**				Bold - RCM5	2	95	159	78
AM1-92	713	3	160	B	310	B	510	B	3	**65**	**166**	517					Bold - RCM7	2	66	167	60
A01-92	3375	2	605	H	1510	H			7	46	68	120	173	298	600	**1500**	Bold - RCM5	2	65	183	59
A01-93	3370	2	568	H	1482	B			7	58	77	81	137	263	570	1484	all RCM4		60	139	52

For current meters: regular type indicates RCM-4 and bold type indicates RCM-7 or RCM-5 as indicated.

1C. Sequential sediment trap schedules (page 1 of 3).

Station	trap depth	Seq#	Start date (UTC)	End date (UTC)	Mid-interval (UTC)	Interval duration	Trap collection area
	m		mm/dd/yyy hh:mm	mm/dd/yyy hh:mm	mm/dd/yyy hh:mm	days	m2
SS-5	199	1	04/22/1991 20:00	05/05/1991 20:00	04/29/1991 08:00	13	0.032
		2	05/05/1991 20:00	05/18/1991 20:00	05/12/1991 08:00	13	0.032
		3	05/18/1991 20:00	05/31/1991 20:00	05/25/1991 08:00	13	0.032
		4	05/31/1991 20:00	06/13/1991 20:00	06/07/1991 08:00	13	0.032
		5	06/13/1991 20:00	06/26/1991 20:00	06/20/1991 08:00	13	0.032
		6	06/26/1991 20:00	07/09/1991 20:00	07/03/1991 08:00	13	0.032
		7	07/09/1991 20:00	07/22/1991 20:00	07/16/1991 08:00	13	0.032
		8	07/22/1991 20:00	08/04/1991 20:00	07/29/1991 08:00	13	0.032
		9	08/04/1991 20:00	08/17/1991 20:00	08/11/1991 08:00	13	0.032
		10	08/17/1991 20:00	08/30/1991 20:00	08/24/1991 08:00	13	0.032
		11	08/30/1991 20:00	09/12/1992 23:45	03/07/1992 09:52	380.82	0.032
SS-5	349	1	04/22/1991 20:00	05/05/1991 20:00	04/29/1991 08:00	13	0.032
		2	05/05/1991 20:00	05/18/1991 20:00	05/12/1991 08:00	13	0.032
		3	05/18/1991 20:00	05/31/1991 20:00	05/25/1991 08:00	13	0.032
		4	05/31/1991 20:00	06/13/1991 20:00	06/07/1991 08:00	13	0.032
		5	06/13/1991 20:00	06/26/1991 20:00	06/20/1991 08:00	13	0.032
		6	06/26/1991 20:00	07/09/1991 20:00	07/03/1991 08:00	13	0.032
		7	07/09/1991 20:00	07/22/1991 20:00	07/16/1991 08:00	13	0.032
		8	07/22/1991 20:00	08/04/1991 20:00	07/29/1991 08:00	13	0.032
		9	08/04/1991 20:00	08/17/1991 20:00	08/11/1991 08:00	13	0.032
		10	08/17/1991 20:00	08/30/1991 20:00	08/24/1991 08:00	13	0.032
		11	08/30/1991 20:00	09/12/1992 23:45	03/07/1992 09:52	380.82	0.032
SS-5	499	1	04/22/1991 20:00	05/05/1991 20:00	04/29/1991 08:00	13	0.032
		2	05/05/1991 20:00	05/18/1991 20:00	05/12/1991 08:00	13	0.032
		3	05/18/1991 20:00	05/31/1991 20:00	05/25/1991 08:00	13	0.032
		4	05/31/1991 20:00	06/13/1991 20:00	06/07/1991 08:00	13	0.032
		5	06/13/1991 20:00	06/26/1991 20:00	06/20/1991 08:00	13	0.032
		6	06/26/1991 20:00	07/09/1991 20:00	07/03/1991 08:00	13	0.032
		7	07/09/1991 20:00	07/22/1991 20:00	07/16/1991 08:00	13	0.032
		8	07/22/1991 20:00	08/04/1991 20:00	07/29/1991 08:00	13	0.032
		9	08/04/1991 20:00	08/17/1991 20:00	08/11/1991 08:00	13	0.032
		10	08/17/1991 20:00	08/30/1991 20:00	08/24/1991 08:00	13	0.032
		11	08/30/1991 20:00	09/12/1992 23:45	03/07/1992 09:52	380.82	0.032
AM1-92	160	1	09/15/1992 11:36	10/20/1992 11:36	10/02/1992 23:36	35	0.032
AM1-92	290	1	09/15/1992 11:36	10/20/1992 11:36	10/02/1992 23:36	35	0.032
		2	10/20/1992 11:36	11/24/1992 11:36	11/06/1992 23:36	35	0.032
		3	11/22/1992 11:36	12/27/1992 11:36	12/09/1992 23:36	35	0.032
		4	12/27/1992 11:36	01/31/1993 11:36	01/13/1993 23:36	35	0.032
		5	01/31/1993 11:36	03/07/1993 11:36	02/17/1993 23:36	35	0.032
		6	03/07/1993 11:36	04/11/1993 11:36	03/24/1993 23:36	35	0.032
		7	04/11/1993 11:36	05/16/1993 11:36	04/28/1993 23:36	35	0.032
		8	05/16/1993 11:36	06/20/1993 11:36	06/02/1993 23:36	35	0.032
		9	06/20/1993 11:36	07/25/1993 11:36	07/07/1993 23:36	35	0.032
		10	07/25/1993 11:36	08/26/1993 11:36	08/10/1993 11:36	32	0.032

Station	trap depth	Seq#	Start date (UTC)	End date (UTC)	Mid-interval (UTC)	Interval duration	Trap collection area
	m		mm/dd/yyy hh:mm	mm/dd/yyy hh:mm	mm/dd/yyy hh:mm	days	m2
AM1-92	490	1	09/15/1992 11:36	10/20/1992 11:36	10/02/1992 23:36	35	0.032
		2	10/20/1992 11:36	11/24/1992 11:36	11/06/1992 23:36	35	0.032
		3	11/22/1992 11:36	12/27/1992 11:36	12/09/1992 23:36	35	0.032
		4	12/27/1992 11:36	01/31/1993 11:36	01/13/1993 23:36	35	0.032
		5	01/31/1993 11:36	03/07/1993 11:36	02/17/1993 23:36	35	0.032
		6	03/07/1993 11:36	04/11/1993 11:36	03/24/1993 23:36	35	0.032
		7	04/11/1993 11:36	05/16/1993 11:36	04/28/1993 23:36	35	0.032
		8	05/16/1993 11:36	06/20/1993 11:36	06/02/1993 23:36	35	0.032
		9	06/20/1993 11:36	07/25/1993 11:36	07/07/1993 23:36	35	0.032
L144	412	1	09/25/1991 08:00	10/22/1991 08:00	10/08/1991 20:00	27	0.509
		2	10/22/1991 08:00	11/18/1991 08:00	11/04/1991 20:00	27	0.509
		3	11/18/1991 08:00	12/15/1991 08:00	12/01/1991 20:00	27	0.509
		4	12/15/1991 08:00	01/11/1992 08:00	12/28/1991 20:00	27	0.509
		5	01/11/1992 08:00	02/07/1992 08:00	01/24/1992 20:00	27	0.509
		6	02/07/1992 08:00	03/05/1992 08:00	02/20/1992 20:00	27	0.509
		7	03/05/1992 08:00	04/01/1992 08:00	03/18/1992 20:00	27	0.509
		8	04/01/1992 08:00	04/28/1992 08:00	04/14/1992 20:00	27	0.509
		9	04/28/1992 08:00	05/25/1992 08:00	05/11/1992 20:00	27	0.509
		10	05/25/1992 08:00	06/21/1992 08:00	06/07/1992 20:00	27	0.509
		11	06/21/1992 08:00	07/18/1992 08:00	07/04/1992 20:00	27	0.509
		12	07/18/1992 08:00	08/14/1992 08:00	07/31/1992 20:00	27	0.509
		13	08/14/1992 08:00	09/10/1992 08:00	08/27/1992 20:00	27	0.509
L144	1311	1	09/25/1991 08:00	10/22/1991 08:00	10/08/1991 20:00	27	0.509
		2	10/22/1991 08:00	11/18/1991 08:00	11/04/1991 20:00	27	0.509
		3	11/18/1991 08:00	12/15/1991 08:00	12/01/1991 20:00	27	0.509
		4	12/15/1991 08:00	01/11/1992 08:00	12/28/1991 20:00	27	0.509
		5	01/11/1992 08:00	02/07/1992 08:00	01/24/1992 20:00	27	0.509
		6	02/07/1992 08:00	03/05/1992 08:00	02/20/1992 20:00	27	0.509
		7	03/05/1992 08:00	04/01/1992 08:00	03/18/1992 20:00	27	0.509
		8	04/01/1992 08:00	04/28/1992 08:00	04/14/1992 20:00	27	0.509
		9	04/28/1992 08:00	05/25/1992 08:00	05/11/1992 20:00	27	0.509
		10	05/25/1992 08:00	06/21/1992 08:00	06/07/1992 20:00	27	0.509
		11	06/21/1992 08:00	07/18/1992 08:00	07/04/1992 20:00	27	0.509
		12	07/18/1992 08:00	08/14/1992 08:00	07/31/1992 20:00	27	0.509
		13	08/14/1992 08:00	09/10/1992 08:00	08/27/1992 20:00	27	0.509
A01-90	615	1	09/03/1990 20:40	10/07/1990 05:41	09/20/1990 13:10	33.38	0.032
		2	10/07/1990 05:41	11/08/1990 05:41	10/23/1990 05:41	32	0.032
		3	11/08/1990 05:41	12/10/1990 05:41	11/24/1990 05:41	32	0.032
		4	12/10/1990 05:41	01/11/1991 05:41	12/26/1990 05:41	32	0.032
		5	01/11/1991 05:41	02/12/1991 05:41	01/27/1991 05:41	32	0.032
		6	02/12/1991 05:41	03/16/1991 05:41	02/28/1991 05:41	32	0.032
		7	03/16/1991 05:41	04/17/1991 05:41	04/01/1991 05:41	32	0.032
		8	04/17/1991 05:41	05/19/1991 05:41	05/03/1991 05:41	32	0.032
		9	05/19/1991 05:41	06/20/1991 05:41	06/04/1991 05:41	32	0.032
		10	06/20/1991 05:41	07/22/1991 05:41	07/06/1991 05:41	32	0.032

C. continued, Sequential sediment trap schedules (page 3 of 3).

Station	trap depth	Seq#	Start date (UTC)	End date (UTC)	Mid-interval (UTC)	Interval duration	Trap collection area
	m		mm/dd/yyy hh:mm	mm/dd/yyy hh:mm	mm/dd/yyy hh:mm	days	m2
A01-90	1515	1	09/03/1990 20:40	10/07/1990 05:41	09/20/1990 13:10	33.38	0.032
		2	10/07/1990 05:41	11/08/1990 05:41	10/23/1990 05:41	32	0.032
		3	11/08/1990 05:41	12/10/1990 05:41	11/24/1990 05:41	32	0.032
		4	12/10/1990 05:41	01/11/1991 05:41	12/26/1990 05:41	32	0.032
		5	01/11/1991 05:41	02/12/1991 05:41	01/27/1991 05:41	32	0.032
		6	02/12/1991 05:41	03/16/1991 05:41	02/28/1991 05:41	32	0.032
A01-92	600	1	09/25/1992 00:00	10/22/1992 00:00	10/08/1992 12:00	27	0.509
		2	10/22/1992 00:00	11/18/1992 00:00	11/04/1992 12:00	27	0.509
		3	11/18/1992 00:00	12/15/1992 00:00	12/01/1992 12:00	27	0.509
		4	12/15/1992 00:00	01/11/1993 00:00	12/28/1992 12:00	27	0.509
		5	01/11/1993 00:00	02/07/1993 00:00	01/24/1993 12:00	27	0.509
		6	02/07/1993 00:00	03/06/1993 00:00	02/20/1993 12:00	27	0.509
		7	03/06/1993 00:00	04/02/1993 00:00	03/19/1993 12:00	27	0.509
		8	04/02/1993 00:00	04/29/1993 00:00	04/15/1993 12:00	27	0.509
		9	04/29/1993 00:00	05/26/1993 00:00	05/12/1993 12:00	27	0.509
		10	05/26/1993 00:00	06/22/1993 00:00	06/08/1993 12:00	27	0.509
		11	06/22/1993 00:00	07/19/1993 00:00	07/05/1993 12:00	27	0.509
		12	07/19/1993 00:00	08/15/1993 00:00	08/01/1993 12:00	27	0.509
		13	08/15/1993 00:00	08/30/1993 00:00	08/22/1993 12:00	15	0.509
A01-93	568	1	09/03/1993 00:00	10/03/1993 00:00	09/18/1993 00:00	30	0.509
		2	10/03/1993 00:00	11/02/1993 00:00	10/18/1993 00:00	30	0.509
		3	11/02/1993 00:00	12/02/1993 00:00	11/17/1993 00:00	30	0.509
		4	12/02/1993 00:00	01/01/1994 00:00	12/17/1993 00:00	30	0.509
		5	01/01/1994 00:00	01/31/1994 00:00	01/16/1994 00:00	30	0.509
		6	01/31/1994 00:00	03/02/1994 00:00	02/15/1994 00:00	30	0.509
		7	03/02/1994 00:00	04/01/1994 00:00	03/17/1994 00:00	30	0.509
		8	04/01/1994 00:00	05/01/1994 00:00	04/16/1994 00:00	30	0.509
		9	05/01/1994 00:00	05/31/1994 00:00	05/16/1994 00:00	30	0.509
		10	05/31/1994 00:00	06/30/1994 00:00	06/15/1994 00:00	30	0.509
		11	06/30/1994 00:00	07/30/1994 00:00	07/15/1994 00:00	30	0.509
		12	07/30/1994 00:00	08/29/1994 00:00	08/14/1994 00:00	30	0.509

Appendix 2 Analytical data for sediment trap samples including the fluxes of total dry weigh (TDW), particulate organic carbon (POC), total nitrogen (TN), biogenic silica (BIOSI), chlorophyll *a* CHLA, and phaeophytins (PHAEO). Also included are percent compositions (POC, TN, BIOSI), the C:N_{molar} ratio, and stable isotopes of carbon and nitrogen ($\delta^{13}C$ and $\delta^{15}N$). (Page 1 of 2)

Station	Trap depth m	Seq #	Mid-Date mm/dd/yy hh:mm	TDW flux mg/m^2/d	POC %	POC flux mg/m^2/d	TN %	TN flux mg/m^2/d	CN Ratio molar	BIOSI %	BIOSI flux mg/m^2/d	CHLA flux ug/m^2/d	PHAEO flux ug/m^2/d	$\delta^{15}N_{tot}$ ‰	$\delta^{13}C_{org}$ ‰	%Al
SS-5	199	1	04/29/1991 02:00	6.79	12.32	0.84	2.40	0.16	5.99							
		2	05/12/1991 02:00	61.64	4.93	3.04	0.73	0.45	7.87	0.63	0.39	0.96	8.0			
		3	05/25/1991 02:00	57.42	9.85	5.65	1.20	0.69	9.61	14.46	8.30	17.20	327.8			
		4	06/07/1991 02:00	313.37	7.42	23.25	0.82	2.55	10.62	30.69	96.16	19.65	1681.9	8.17	-23.21	1.16
		5	06/20/1991 02:00	533.05	7.08	37.74	0.77	4.09	10.77	27.37	145.91	99.84	2585.3	7.72	-24.16	1.56
		6	07/03/1991 02:00	568.69	7.69	43.73	0.86	4.89	10.43	26.30	149.56	89.88	2264.2	7.64	-24.30	1.70
		7	07/16/1991 02:00	245.35	8.60	21.10	1.13	2.77	8.88	20.38	50.00	34.65	601.1	7.36	-24.32	2.89
		8	07/29/1991 02:00	36.17	7.53	2.72	1.07	0.39	8.24	6.37	2.31	4.41	56.9			
		9	08/11/1991 02:00	22.47	8.70	1.95	1.17	0.26	8.67	1.24	0.28	0.81	13.8			
		10	08/24/1991 02:00	17.43	7.72	1.35	1.16	0.20	7.76	1.38	0.24	1.33	23.6			
		11	03/07/1992 03:52	46.82	6.00	2.81	0.96	0.45	7.28	3.62	1.69			9.69	-24.79	6.58
SS-5	349	1	04/29/1991 02:00	5.55	10.84	0.60	2.41	0.13	5.25							
		2	05/12/1991 02:00	36.68	11.67	4.28	2.28	0.84	5.97	1.13	0.42	7.39	11.7			
		3	05/25/1991 02:00	30.95	10.26	3.18	2.01	0.62	5.95	0.79	0.24	2.64	31.0			
		4	06/07/1991 02:00	343.75	6.50	22.36	0.70	2.40	10.89	25.50	87.66	65.67	1338.8	7.47	-23.42	2.30
		5	06/20/1991 02:00	396.92	7.14	28.35	0.73	2.88	11.46	24.13	95.79	54.61	1499.8	7.25	-24.16	2.35
		6	07/03/1991 02:00	499.76	6.62	33.08	0.74	3.67	10.50	25.09	125.38	79.29	1913.2	7.57	-24.26	2.28
		7	07/16/1991 02:00	251.53	7.24	18.20	0.84	2.11	10.04	18.20	45.79	26.75	529.9	6.71	-24.79	3.91
		8	07/29/1991 02:00	126.06	6.94	8.75	0.87	1.10	9.30	7.98	10.06	6.07	90.8		-24.60	7.94
		9	08/11/1991 02:00	183.93	5.08	9.33	0.64	1.17	9.32	4.92	9.05	5.52	86.0	7.72	-24.13	7.80
		10	08/24/1991 02:00	158.24	5.00	7.90	0.65	1.02	9.03	4.40	6.96	3.65	61.1	7.41	-24.52	8.15
		11	03/07/1992 03:52	87.43	4.58	4.00	0.66	0.58	8.08	3.54	3.09	5.21	22.5	7.67	-24.58	7.29
SS-5	499	1	04/29/1991 02:00	6.02	8.03	0.48	1.34	0.08	6.99							
		2	05/12/1991 02:00	67.10	4.85	3.25	0.72	0.48	7.90	2.56	1.72	1.14	9.5	9.92	-23.77	
		3	05/25/1991 02:00	121.75	5.07	6.17	0.74	0.90	8.04	3.16	3.85	6.36	74.7	8.98	-23.40	8.41
		4	06/07/1991 02:00	488.67	5.20	25.39	0.55	2.69	11.02	21.75	106.26	67.77	1771.9	7.30	-22.90	3.55
		5	06/20/1991 02:00	533.60	6.80	36.30	0.72	3.86	10.97	23.61	125.97	73.72	1728.1	7.34	-24.03	2.83
		6	07/03/1991 02:00	621.79	6.26	38.94	0.68	4.23	10.74	23.24	144.53	67.58	1639.2	7.16	-24.49	3.08
		7	07/16/1991 02:00	436.84	6.83	29.82	0.79	3.44	10.12	16.60	72.52	40.96	738.4	6.52	-24.75	4.78
		8	07/29/1991 02:00	226.88	5.38	12.20	0.65	1.48	9.64	6.51	14.77	10.77	140.9	7.05	-24.30	8.46
		9	08/11/1991 02:00	166.55	4.48	7.45	0.54	0.90	9.66	4.46	7.43	4.57	79.8	7.54	-24.30	8.91
		10	08/24/1991 02:00	119.64	5.30	6.34	0.70	0.83	8.89	4.11	4.92	2.82	47.2	7.87	-23.97	7.54
		11	03/07/1992 03:52	123.68	3.61	4.47	0.50	0.62	8.36	3.14	3.88			7.47	-24.47	8.98
AM1-92	140	1	9/30/1992 23:36	43.52	10.25	4.46	1.67	0.73	7.16	3.29	1.43	1.32	25.6	10.01	-24.35	6.35
AM1-92	290	1	9/30/1992 23:36	157.04	6.26	9.84	0.93	1.47	7.83	3.63	5.71	1.17	41.0	8.93	-24.42	7.62
		2	11/4/1992 23:36	109.54	5.14	5.63	0.73	0.80	8.18	2.09	2.29	0.70	31.4	7.80	-24.58	8.20
		3	12/9/1992 23:36	152.09	3.90	5.94	0.54	0.82	8.46	1.24	1.88	0.52	19.0	8.07	-24.26	8.34
		4	1/13/1993 23:36	400.81	2.55	10.22	0.36	1.46	8.19	1.76	7.06	0.95	24.9	7.65	-23.70	8.03
		5	2/17/1993 23:36	356.96	2.83	10.09	0.42	1.49	7.91	1.91	6.82	1.30	27.2	8.46	-23.65	8.29
		6	3/24/1993 23:36	196.55	3.32	6.53	0.49	0.97	7.87	2.07	4.08	0.53	14.0	8.96	-23.59	8.25
		7	4/28/1993 23:36	145.85	4.30	6.28	0.63	0.92	7.99	2.63	3.84	1.09	16.0	10.31	-23.15	8.26
		8	6/2/1993 23:36	173.95	19.16	33.33	0.75	1.30	29.89	4.87	8.48	5.88	68.2	6.86	-12.19	5.14
		9	7/7/1993 23:36	67.31	9.15	6.16	0.80	0.54	13.30	7.17	4.83	18.40	130.0	6.46	-21.40	7.10
		10	8/10/1993 11:48	135.00	8.33	11.25	0.89	1.21	10.88	9.27	12.52	25.47	215.2	5.79	-25.39	5.81
AM1-92	490	1	9/30/1992 23:36	144.92	4.76	6.90	0.68	0.98	8.19	4.16	6.03	1.04	36.5	8.37	-24.19	8.02
		2	11/4/1992 23:36	100.85	5.17	5.21	0.64	0.65	9.35	2.95	2.98	0.76	31.0	7.83	-24.52	8.22
		3	12/9/1992 23:36	182.61	3.90	7.12	0.64	1.17	7.10	1.57	2.87	0.71	26.3	8.23	-24.18	8.83
		4	1/13/1993 23:36	478.67	2.47	11.82	0.37	1.77	7.80	1.71	8.18	1.23	40.9	7.64	-23.85	8.80
		5	2/17/1993 23:36	365.20	2.64	9.65	0.39	1.43	7.87	1.83	6.70	1.09	25.9	7.53	-23.94	8.62
		6	3/24/1993 23:36	195.31	2.88	5.62	0.37	0.71	9.18	2.26	4.42	0.67	12.8	7.57	-23.81	8.72
		7	4/28/1993 23:36	119.76	3.73	4.47	0.58	0.69	7.67	2.91	3.48	0.68	10.9	8.66	-23.73	8.30
		8	6/2/1993 23:36	351.73	5.02	17.66	0.56	1.97	10.46	6.72	23.65	40.31	418.4	6.91	-23.63	7.01
		9	7/7/1993 23:36	952.62	7.54	71.78	0.82	7.79	10.75	12.68	120.81	218.45	1503.6	5.61	-26.35	5.00
L144	412	1	10/8/1991 20:00	260.47	3.39	8.82	0.50	1.29	7.98	3.438	8.955	2.88	54.2	6.85	-24.46	8.23
		2	11/4/1991 20:00	103.99	4.48	4.66	0.63	0.65	8.36	4.252	4.422	1.10	35.8	7.32	-25.16	8.12
		3	12/1/1991 20:00	24.12	5.15	1.24	0.75	0.18	8.06	4.035	0.973	0.22	7.0	6.80	-24.77	7.72
		4	12/28/1991 20:00	28.30	5.54	1.57	0.97	0.27	6.66	3.139	0.888	0.19	5.8	8.13	-23.66	7.57
		5	1/24/1992 20:00	14.76	5.07	0.75	0.79	0.12	7.46	2.939	0.434	0.08	2.4	9.56	-24.12	7.48
		6	2/20/1992 20:00	12.36	5.05	0.63	0.72	0.09	8.22	2.978	0.368	0.06	2.1	9.35	-23.34	7.72
		7	3/18/1992 20:00	38.23	6.54	2.50	1.03	0.39	7.40	3.656	1.398	0.12	4.4	10.39	-22.34	7.28
		8	4/14/1992 20:00	6.03	7.85	0.47	1.48	0.09	6.19	4.326	0.261	0.02	0.6	11.81	-21.86	5.95
		9	5/11/1992 20:00	41.49	4.76	1.98	0.82	0.34	6.77	4.381	1.818	0.19	4.2	10.21	-22.37	7.44
		10	6/7/1992 20:00	57.79	3.92	2.27	0.61	0.35	7.50	5.042	2.914	0.88	11.0	7.26	-22.59	7.41
		11	7/4/1992 20:00	77.76	4.15	3.22	0.60	0.46	8.12	8.057	6.265	0.73	18.7	8.61	-22.82	6.75
		12	7/31/1992 20:00	55.16	4.87	2.69	0.58	0.32	9.85	7.067	3.898	0.84	14.7	7.29	-24.19	7.01
		13	8/27/1992 20:00	147.97	4.91	7.27	0.55	0.81	10.46	7.500	11.098	2.90	44.0	6.07	-24.51	7.24

Appendix 2. Analytical data continued (page 2 of 2)

Station	Trap depth m	Seq #	Mid-Date mm/dd/yy hh:mm	TDW flux mg/m^2/d	POC %	POC flux mg/m^2/d	TN %	TN flux mg/m^2/d	CN Ratio molar	BIOSI %	BIOSI flux mg/m^2/d	CHLA flux ug/m^2/d	PHAEO flux ug/m^2/d	$\delta^{15}N_{tot}$ ‰	$\delta^{13}C_{org}$ ‰	%Al
L144	1311	1	10/8/1991 20:00	179.37	2.88	5.17	0.36	0.65	9.34	4.984	8.940	1.08	22.1	6.54	-23.75	7.97
		2	11/4/1991 20:00	199.36	3.99	7.96	0.48	0.95	9.77	4.801	9.571	1.01	22.5	8.22	-23.47	7.89
		3	12/1/1991 20:00	122.48	3.02	3.70	0.38	0.47	9.20	5.491	6.725	0.37	6.6	7.19	-23.80	8.02
		4	12/28/1991 20:00	172.97	3.04	5.26	0.39	0.67	9.21	4.249	7.350	0.68	17.3	7.02	-23.56	7.89
		5	1/24/1992 20:00	76.71	2.99	2.29	0.40	0.31	8.72	4.335	3.325	0.32	7.4	7.48	-23.29	8.15
		6	2/20/1992 20:00	103.01	2.80	2.88	0.37	0.38	8.81	4.199	4.325	0.50	9.5	7.33	-23.15	7.97
		7	3/18/1992 20:00	84.01	3.03	2.55	0.42	0.35	8.41	4.390	3.688	0.26	5.3	8.03	-22.94	7.91
		8	4/14/1992 20:00	124.20	2.98	3.70	0.40	0.50	8.61	4.234	5.259	0.34	6.6	8.19	-22.62	7.81
		9	5/11/1992 20:00	96.18	2.73	2.62	0.37	0.35	8.71	3.849	3.702	0.39	6.7	8.00	-22.83	7.86
		10	6/7/1992 20:00	135.47	2.65	3.59	0.36	0.48	8.68	3.556	4.817	0.57	9.5	7.77	-22.79	7.49
		11	7/4/1992 20:00	99.45	3.38	3.36	0.53	0.52	7.48	4.200	4.177	0.45	7.9	10.55	-22.47	7.70
		12	7/31/1992 20:00	123.29	3.09	3.81	0.39	0.49	9.16	4.058	5.003	0.51	6.5	7.30	-23.55	7.91
		13	8/27/1992 20:00	406.94	3.08	12.53	0.37	1.49	9.80	4.696	19.108	1.95	26.0	6.41	-23.92	8.10
A01-90	615	1	09/20/1990 13:10	2.42	7.38	0.18	0.72	0.017	11.95							
A01-90	615	2	10/23/1990 05:41	3.39	6.30	0.21	0.86	0.029	8.54							
A01-90	615	3	11/24/1990 05:41	1.97	8.16	0.16	1.10	0.022	8.65							
A01-90	615	4	12/26/1990 05:41	3.96	6.32	0.25	0.69	0.027	10.68							
A01-90	615	5	01/27/1991 05:41	6.28	4.73	0.30	0.49	0.031	11.26							
A01-90	615	6	02/28/1991 05:41	1.82	7.95	0.14	1.29	0.023	7.19							
A01-90	615	7	04/01/1991 05:41	1.30	10.63	0.14	1.56	0.020	7.95							
A01-90	615	8	05/03/1991 05:41	2.97	9.84	0.29	1.66	0.049	6.91							
A01-90	615	9	06/04/1991 05:41	5.13	7.49	0.38	1.22	0.063	7.16							
A01-90	615	10	07/06/1991 05:41	59.64	6.17	3.68	1.04	0.620	6.91	2.70	1.61	0.091	2.0			
A01-90	1515	1	09/20/1990 12:06	2.58	6.59	0.17	0.49	0.013	15.68							
A01-90	1515	2	10/23/1990 05:32	1.55	8.23	0.13	1.03	0.016	9.32							
A01-90	1515	3	11/24/1990 05:32	4.25	5.68	0.24	0.68	0.029	9.74							
A01-90	1515	4	12/26/1990 05:32	30.92	4.46	1.38	0.60	0.184	8.74	3.20	0.99	0.067	1.6			
A01-90	1515	5	01/27/1991 05:32	42.01	3.71	1.56	0.45	0.189	9.60	3.17	1.33	-0.004	0.0			
A01-90	1515	6	02/28/1991 05:32	26.15	4.04	1.06	0.52	0.135	9.15	3.57	0.93	-0.004	0.0			
A01-92	600	1	10/08/1992 12:00	1.69	13.49	0.23	2.11	0.04	7.47	5.93	0.100	0.016	1.77			
A01-92	600	2	11/04/1992 12:00	1.27	12.41	0.16	1.96	0.02	7.39	5.65	0.072	0.007	0.90			
A01-92	600	3	12/01/1992 12:00	6.51	7.40	0.48	1.17	0.08	7.37	7.02	0.457	-0.159	3.63			
A01-92	600	4	12/28/1992 12:00	1.46	9.37	0.14	1.43	0.02	7.62	5.45	0.080	-0.004	0.54			
A01-92	600	5	01/24/1993 12:00	0.72	39.14	0.28	6.61	0.05	6.90	0.58	0.004	0.004	0.15			
A01-92	600	6	02/20/1993 12:00	0.58	27.97	0.16	5.35	0.03	6.10	1.94	0.011	0.004	0.14			
A01-92	600	7	03/19/1993 12:00	0.58	16.19	0.09	2.87	0.02	6.57	4.73	0.028	0.005	0.13			
A01-92	600	8	04/15/1993 12:00	0.53	13.69	0.07	2.55	0.01	6.25	3.53	0.019	0.002	0.11			
A01-92	600	9	05/12/1993 12:00	0.36	16.74	0.06	3.27	0.01	5.98	2.26	0.008	0.005	0.13			
A01-92	600	10	06/08/1993 12:00	2.59	10.43	0.27	1.25	0.03	9.72	4.00	0.103	0.182	1.82			
A01-92	600	11	07/05/1993 12:00	9.88	9.99	0.99	0.95	0.09	12.21	8.49	0.839	0.375	5.38			
A01-92	600	12	08/01/1993 12:00	43.51	7.70	3.35	0.77	0.33	11.67	5.27	2.291	1.824	59.69			
A01-92	600	13	08/22/1993 12:00	6.22	5.85	0.36	0.78	0.05	8.73	4.76	0.296	0.081	3.78			
A01-93	568	1	09/18/1993 00:00	35.32	7.01	2.48	1.00	0.35	8.21	5.70	2.015	0.273	11.43			
A01-93	568	2	10/18/1993 00:00	14.65	6.33	0.93	0.85	0.13	8.64	5.44	0.796	0.065	6.83			
A01-93	568	3	11/17/1993 00:00	21.56	5.93	1.28	0.86	0.18	8.07	7.51	1.619	**-0.116**	5.47			
A01-93	568	4	12/17/1993 00:00	16.24	6.61	1.07	0.90	0.15	8.54	9.80	1.591	0.186	6.92			
A01-93	568	5	01/16/1994 00:00	44.03	4.97	2.19	0.62	0.27	9.29	8.26	3.636	0.346	14.98			
A01-93	568	6	02/15/1994 00:00	65.11	4.66	3.03	0.69	0.45	7.92	6.03	3.929	0.444	13.14			
A01-93	568	7	03/17/1994 00:00	7.02	20.05	1.41	3.85	0.27	6.07	2.28	0.160	0.025	0.47			
A01-93	568	8	04/16/1994 00:00	8.75	16.03	1.40	2.73	0.24	6.86	3.17	0.277	0.011	0.55			
A01-93	568	9	05/16/1994 00:00	9.24	29.23	2.70	5.39	0.50	6.32	1.15	0.106	0.009	0.22			
A01-93	568	10	06/15/1994 00:00	18.91	29.44	5.57	3.69	0.70	9.31	4.17	0.789	0.037	1.32			
A01-93	568	11	07/15/1994 00:00	1.56	10.45	0.16	1.83	0.03	6.65	3.56	0.056	0.046	1.27			
A01-93	568	12	08/14/1994 00:00	28.69	4.41	1.26	0.59	0.17	8.65	4.42	1.269	0.023	5.29			

Appendix 3 A) Table of the average %$POC_{refractory}$ in the terrigenous fraction at each sediment trap depth. This average value was used to calculate the %$POM_{refractory}$ for samples where aluminum data was not possible due to small sample size. B) Table of the average % $BIOSI_{old}$ in the terrigenous fraction at each sediment trap depth. This average value at each trap depth was used to estimate the $OPAL_{old}$ in samples that were too small to allow for BIOSI analysis.

A)

Station	Trap depth (m)	%$POM_{refractory}$ in $TERR_{total}$ flux	standard deviation	number of samples	%$POC_{refractory}$ in $TERR_{total}$ flux	%$POM_{refractory}$ in $TERR_{total}$ MINIMUM	%$POM_{refractory}$ in $TERR_{total}$ MAXIMUM
SS-5	199	1.55	0.14	5	1.27	1.42	1.77
SS-5	349	1.78	0.22	8	1.46	1.56	2.21
SS-5	499	1.91	0.14	9	1.56	1.76	2.15
L144	412	1.79	0.07	9	1.47	1.75	1.89
L144	1311	1.82	0.13	13	1.49	1.65	1.87
AM1-92	140	1.66		1	1.36		
AM1-92	290	1.81	0.10	10	1.48	1.68	2.04
AM1-92	490	1.83	0.05	9	1.50	1.71	1.88
average % $POC_{refractory}$ in $TERR_{total}$ flux =					1.45		

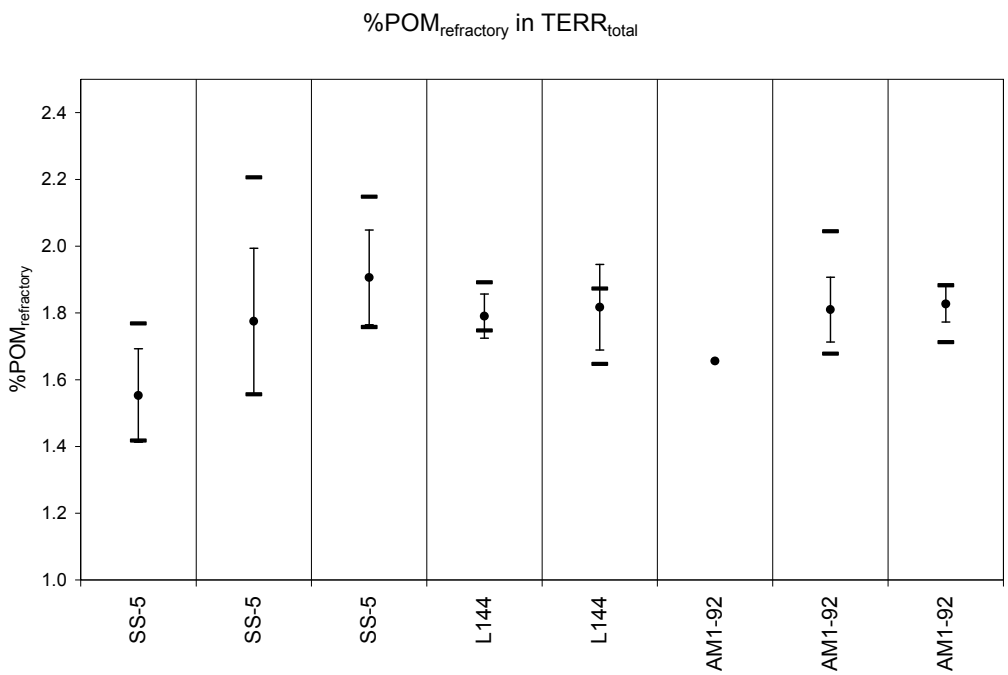

Appendix 3 continued (Appendix 3B)

B)

Station		average %$OPAL_{old}$ in $TERR_{total}$	standard deviation	number of samples	%$BIOSIol_d$ in $TERR_{total}$	%$OPAL_{old}$ in $TERR_{total}$ MINIMUM	%$OPALol_d$ in $TERR_{total}$ MAXIMUM
SS-5	199	2.25	0.20	5	0.94	2.06	2.56
SS-5	349	2.57	0.31	8	1.07	2.26	3.17
SS-5	499	2.75	0.20	9	1.15	2.54	3.09
L144	412	2.60	0.08	9	1.08	2.53	2.73
L144	1311	2.59	0.08	13	1.08	2.39	2.71
AM1-92	140	2.40		1			
AM1-92	290	2.62	0.14	10	1.09	2.43	2.95
AM1-92	490	2.64	0.08	9	1.10	2.48	2.72
average % BIOSI in $TERR_{total}$ flux =					1.07		

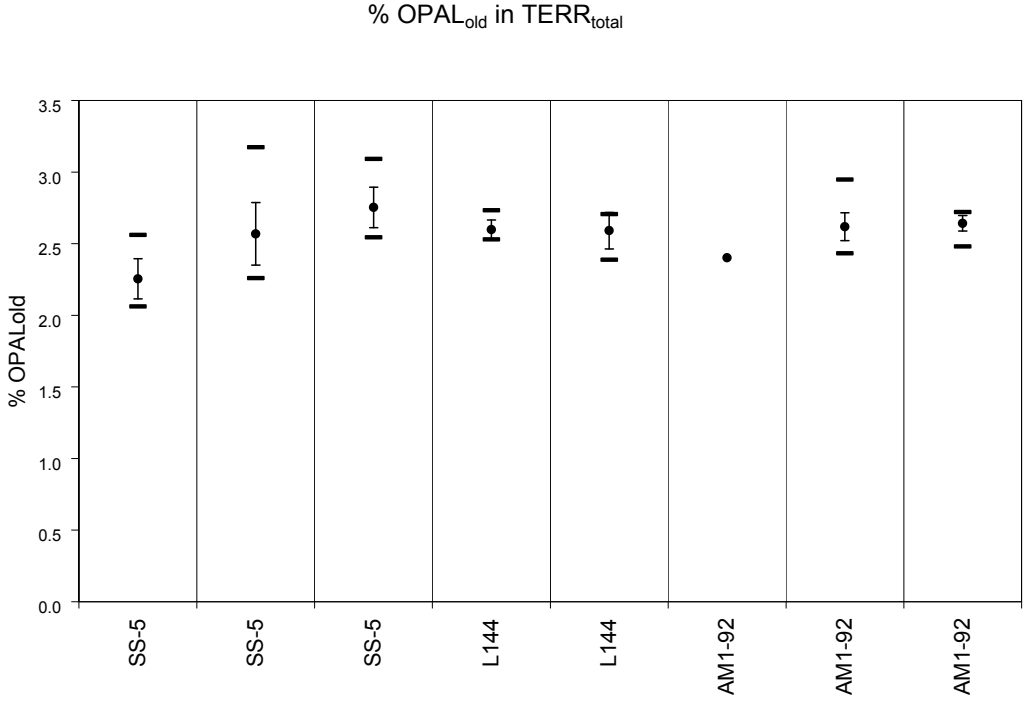

Appendix 4 Air temperatures at Tuktoyaktuk Airport and at Sachs Harbour during the 1991 spring/summer deployment at site SS-5.

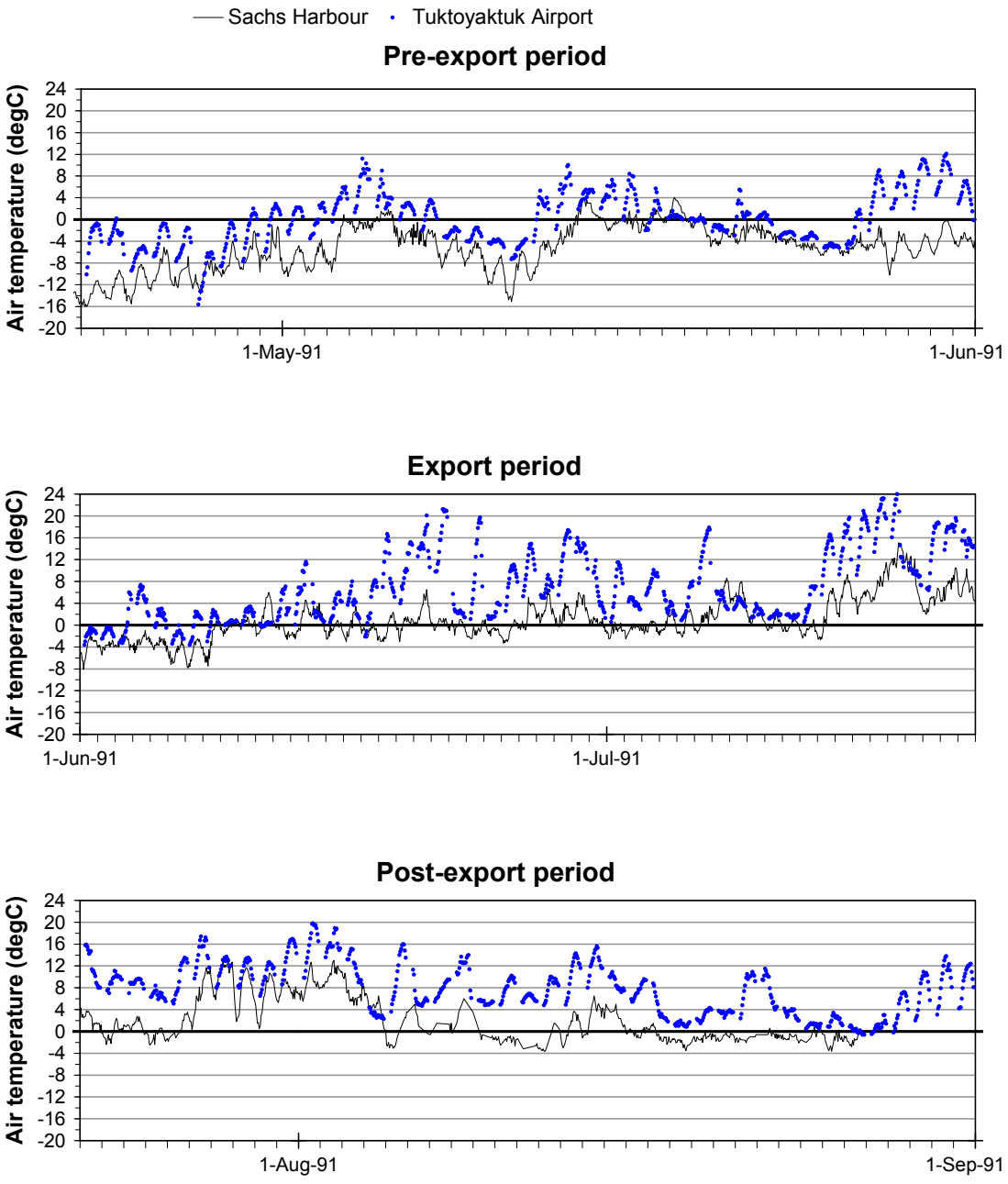

Appendix 5 Ocean currents at site AM1-92 for A) 59 m, B) 161 m, C) 512 m, and D) monthly average and maximum current speeds. Plots A to C are of current speed versus direction and histograms of current direction for each depth (4 pages).

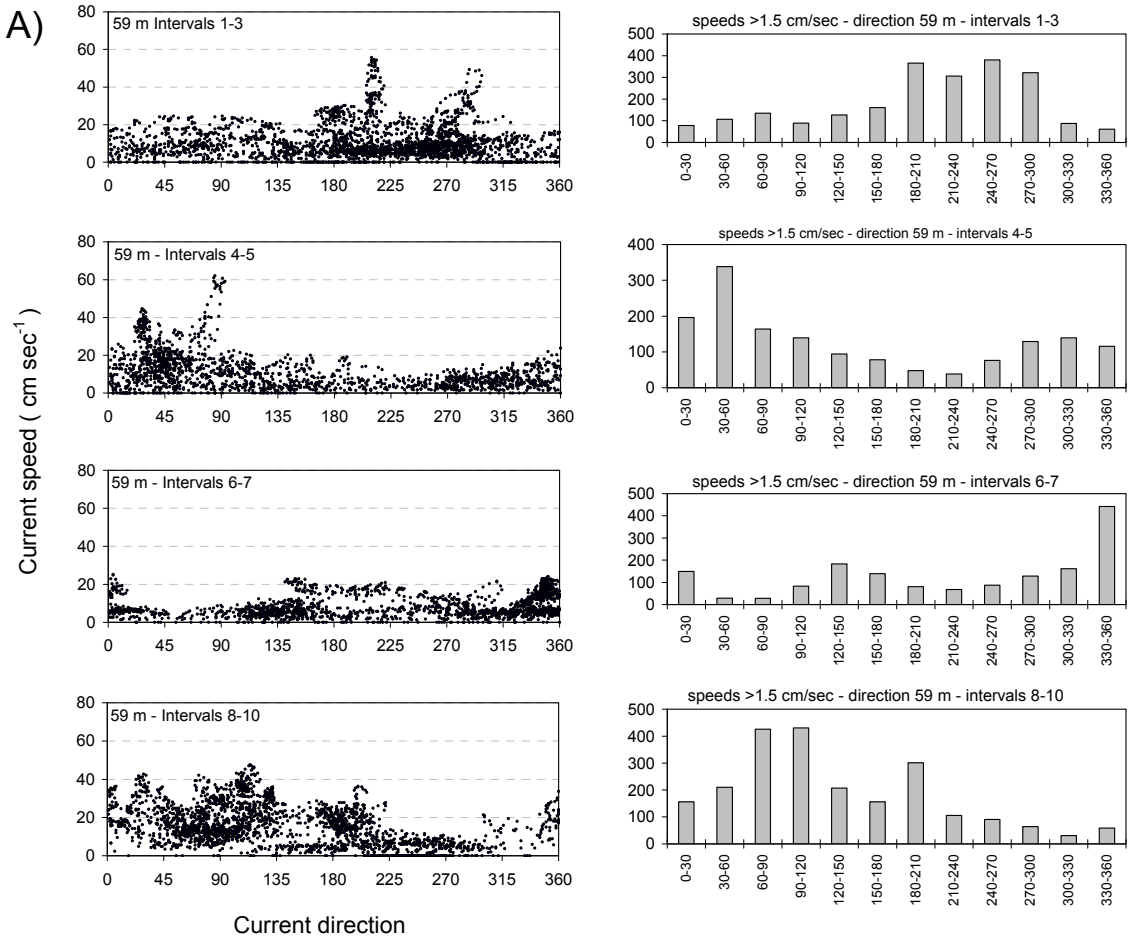

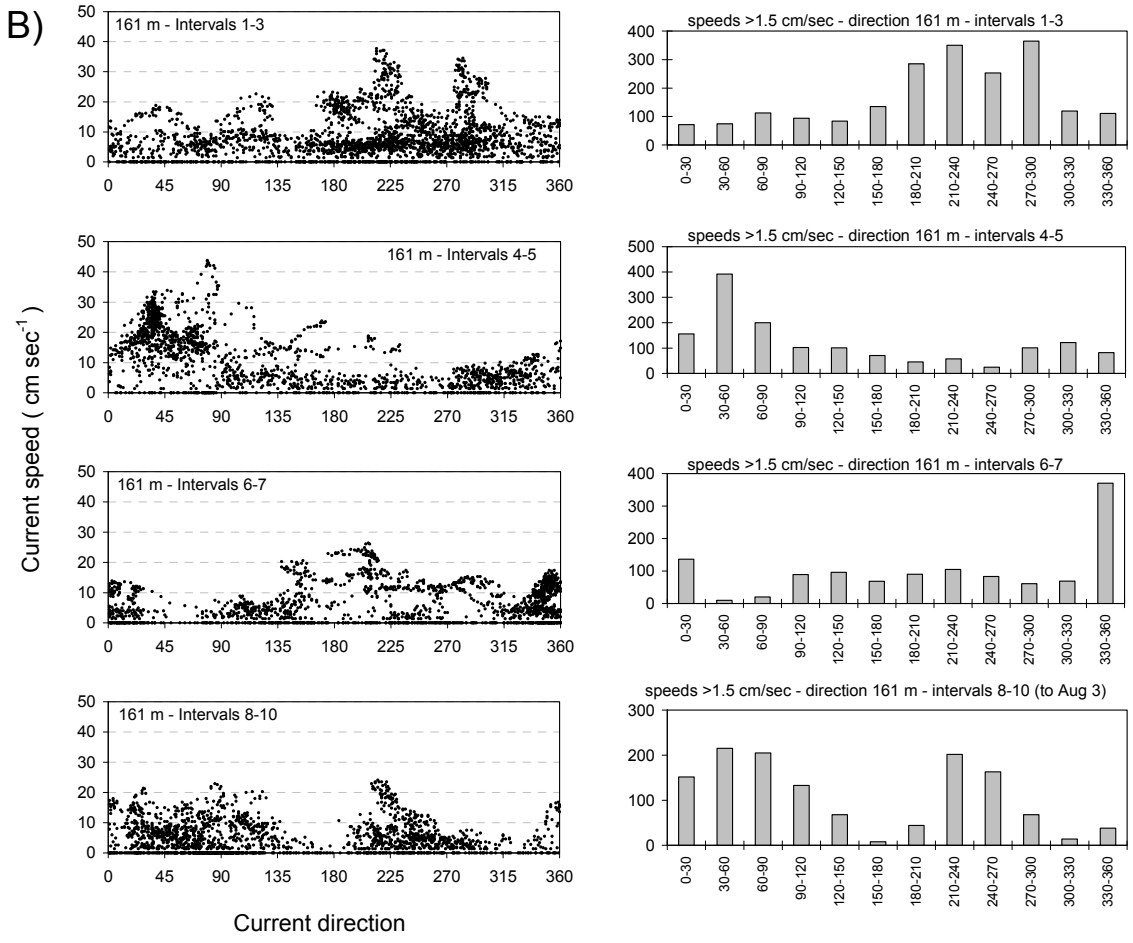
B)
161 m - Intervals 1-3
161 m - Intervals 4-5
161 m - Intervals 6-7
161 m - Intervals 8-10
Current speed (cm sec-1)
Current direction
speeds >1.5 cm/sec - direction 161 m - intervals 1-3
speeds >1.5 cm/sec - direction 161 m - intervals 4-5
speeds >1.5 cm/sec - direction 161 m - intervals 6-7
speeds >1.5 cm/sec - direction 161 m - intervals 8-10 (to Aug 3)
0-30
30-60
60-90
90-120
120-150
150-180
180-210
210-240
240-270
270-300
300-330
330-360

Appendix 5 continued (page 2 of 4).

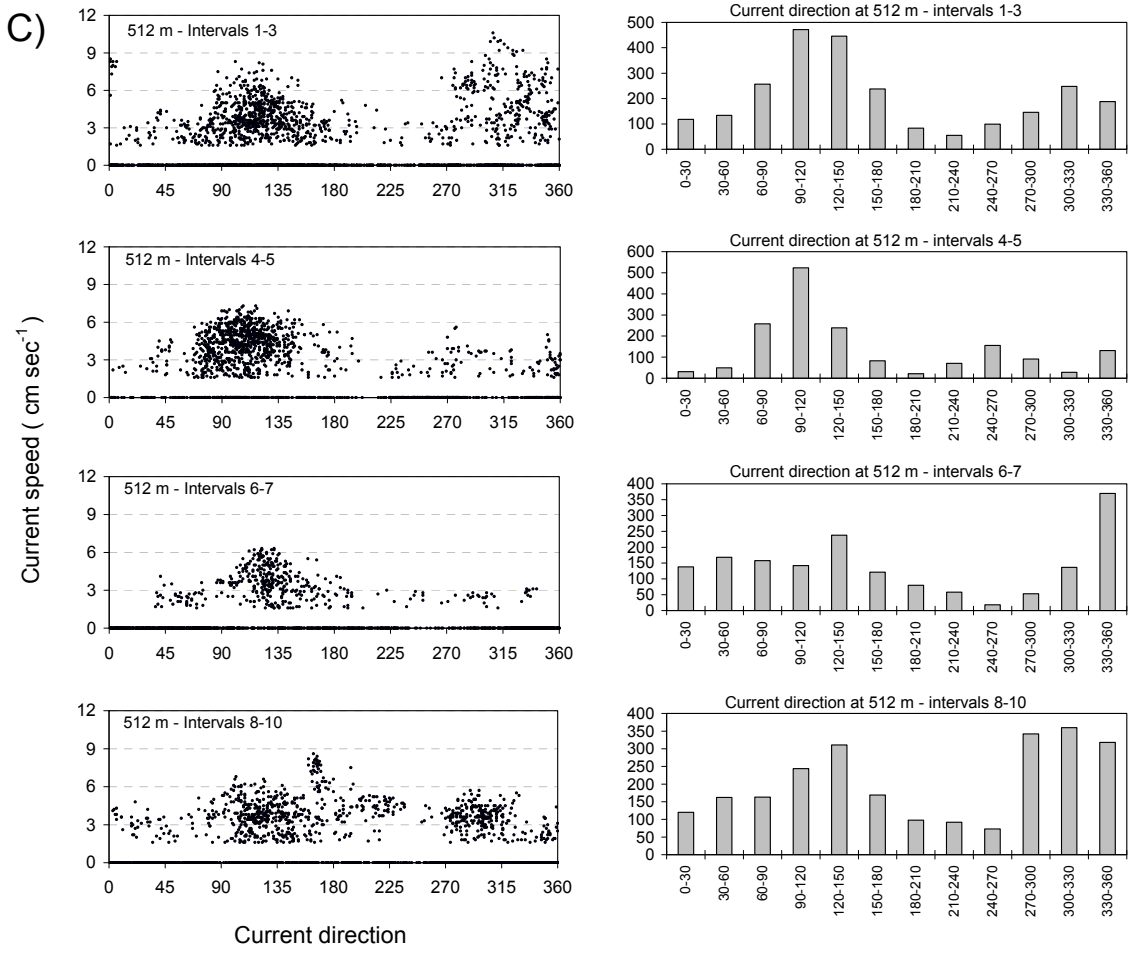

Appendix 5 continued (page 3 of 4).

D)

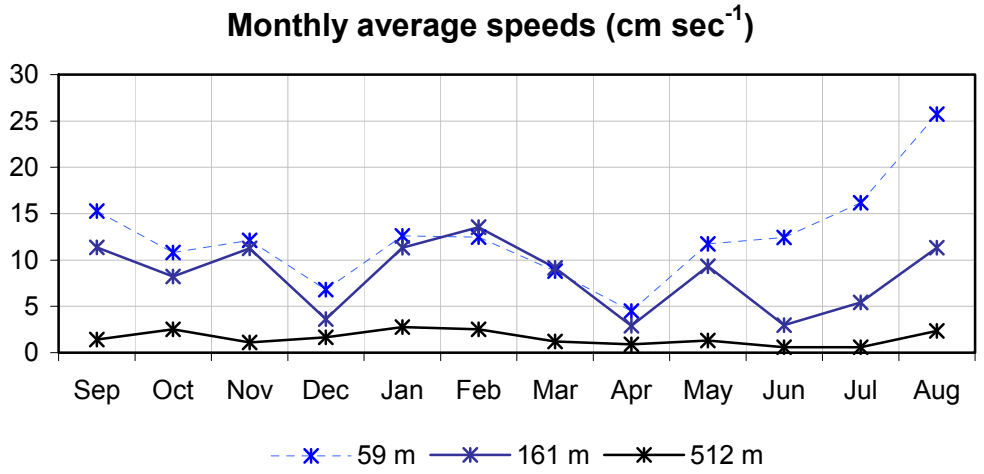
Monthly average speeds (cm sec-1)
30
25
20
15
10
5
0
Sep
Oct
Nov
Dec
Jan
Feb
Mar
Apr
May
Jun
Jul
Aug
59 m
161 m
512 m

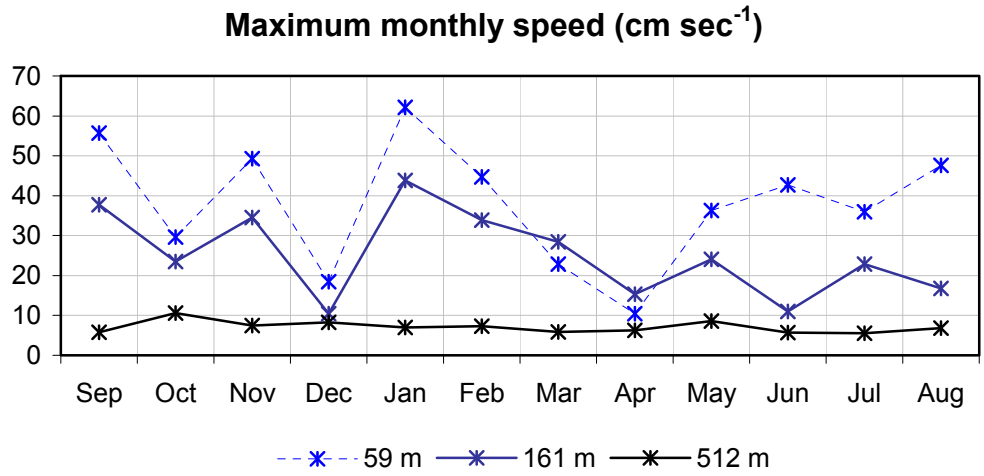
Maximum monthly speed (cm sec-1)
70
60
50
40
30
20
10
0
Sep
Oct
Nov
Dec
Jan
Feb
Mar
Apr
May
Jun
Jul
Aug
59 m
161 m
512 m